# Arthritis & Rheumatology

An Official Journal of the American College of Rheumatology
www.arthritisrheum.org and wileyonlinelibrary.com

**Editor**
Daniel H. Solomon, MD, MPH, *Boston*

**Deputy Editors**
Richard J. Bucala, MD, PhD, *New Haven*
Mariana J. Kaplan, MD, *Bethesda*
Peter A. Nigrovic, MD, *Boston*

**Co-Editors**
Karen H. Costenbader, MD, MPH, *Boston*
David T. Felson, MD, MPH, *Boston*
Richard F. Loeser Jr., MD, *Chapel Hill*

**Journal Publications Committee**
Betty Tsao, PhD, *Chair, Charleston*
Elana Bernstein, MD, MSc, *New York*
Krati Chauhan, MD, MPH, *Springfield*
Cynthia Crowson, PhD, *Stewartville*
Daniel B. Horton, MD, MS, *New Brunswick*
Victoria Menzies, ARNP, PhD, *Alachua*
Suraj Rajasimhan, PharmD, *Columbia*
Faria Sami, MD, *Birmingham*

**Editorial Staff**
Susan Case, *Vice President, Strategic Marketing, Communications and Publishing, Maryland*
Maggie Parry, *Director, Quality and Production, Georgia*
Brian T. Robinson, *Director, Digital Content, Pennsylvania*
Chris Reynolds, *Product Manager, Georgia*
Christy Austin, *Publishing Coordinator, Washington*
Laura Bolte, *Managing Editor, North Carolina*

**Associate Editors**
Marta Alarcón-Riquelme, MD, PhD, *Granada*
Neil Basu, MD, PhD, *Glasgow*
Edward M. Behrens, MD, *Philadelphia*
Bryce Binstadt, MD, PhD, *Minneapolis*
Nunzio Bottini, MD, PhD, *San Diego*
John Carrino, MD, MPH, *New York*
Andrew Cope, MD, PhD, *London*
Adam P. Croft, MBChB, PhD, MRCP, *Birmingham*
Nicola Dalbeth, MD, FRACP, *Auckland*
Chad Deal, MD, *Cleveland*
Brian M. Feldman, MD, FRCPC, MSc, *Toronto*
Richard A. Furie, MD, *Great Neck*
J. Michelle Kahlenberg, MD, PhD, *Ann Arbor*
Yvonne Lee, MD, MMSc, *Chicago*
Katherine Liao, MD, MPH, *Boston*
Bing Lu, MD, DrPH, *Boston*
Stephen P. Messier, PhD, *Winston-Salem*
Rachel E. Miller, PhD, *Chicago*
Janet E. Pope, MD, MPH, *FRCPC, London, Ontario*
Lisa G. Rider, MD, *Bethesda*
Christopher T. Ritchlin, MD, MPH, *Rochester*
William Robinson, MD, PhD, *Stanford*
Carla R. Scanzello, MD, PhD, *Philadelphia*
Georg Schett, MD, *Erlangen*
Ami A. Shah, MD, MHS, *Baltimore*
Sakae Tanaka, MD, PhD, *Tokyo*
Maria Trojanowska, PhD, *Boston*
Edith M. Williams, PhD, MS, *Rochester*

**Advisory Editors**
Ayaz Aghayev, MD, *Boston*
Joshua F. Baker, MD, MSCE, *Philadelphia*
Bonnie Bermas, MD, *Dallas*
Jamie Collins, PhD, *Boston*
Kristen Demoruelle, MD, PhD, *Denver*
Christopher Denton, PhD, FRCP, *London*
Anisha Dua, MD, MPH, *Chicago*
John FitzGerald, MD, *Los Angeles*
Lauren Henderson, MD, MMSc, *Boston*
Monique Hinchcliff, MD, MS, *New Haven*
Hui-Chen Hsu, PhD, *Birmingham*
Mohit Kapoor, PhD, *Toronto*
Seoyoung Kim, MD, ScD, MSCE, *Boston*
Vasileios Kyttaris, MD, *Boston*
Carl D. Langefeld, PhD, *Winston-Salem*
Christian Lood, PhD, *Seattle*
Dennis McGonagle, FRCPI, PhD, *Leeds*
Julie Paik, MD, MHS, *Baltimore*
Amr Sawalha, MD, *Pittsburgh*
Julie Zikherman, MD, *San Francisco*

**AMERICAN COLLEGE OF RHEUMATOLOGY**

Carol Langford, MD, MHS, *Cleveland,* **President**
William Harvey, MD, MSc, *Boston*, **President-Elect**
Anne Bass, MD, *New York,* **Treasurer**
Angus Worthing, MD, *Washington, DC,* **Secretary**
Steven Echard, IOM, CAE, *Atlanta*, **Executive Vice-President**

© 2025 American College of Rheumatology. All rights reserved. No part of this publication may be reproduced, stored or transmitted in any form or by any means without the prior permission in writing from the copyright holder. Authorization to copy items for internal and personal use is granted by the copyright holder for libraries and other users registered with their local Reproduction Rights Organization (RRO), e.g. Copyright Clearance Center (CCC), 222 Rosewood Drive, Danvers, MA 01923, USA (www.copyright.com), provided the appropriate fee is paid directly to the RRO. This consent does not extend to other kinds of copying or use such as copying for general distribution, for advertising or promotional purposes, for creating new collective works, for resale, or for artificial intelligence tools or technologies. Special requests should be addressed to: permissions@wiley.com.

Access Policy: Subject to restrictions on certain backfiles, access to the online version of this issue is available to all registered Wiley Online Library users 12 months after publication. Subscribers and eligible users at subscribing institutions have immediate access in accordance with the relevant subscription type. Please go to onlinelibrary.wiley.com for details.

The views and recommendations expressed in articles, letters, and other communications published in Arthritis & Rheumatology are those of the authors and do not necessarily reflect the opinions of the editors, publisher, or American College of Rheumatology. The publisher and the American College of Rheumatology do not investigate the information contained in the classified advertisements in this journal and assume no responsibility concerning them. Further, the publisher and the American College of Rheumatology do not guarantee, warrant, or endorse any product or service advertised in this journal.

Cover design: Todd Machen

♾This journal is printed on acid-free paper.

# Arthritis & Rheumatology

An Official Journal of the American College of Rheumatology
www.arthritisrheum.org and wileyonlinelibrary.com

**VOLUME 77 • February 2025 • NO. 2**

**Cover image:** The image on the cover (from Umeda et al; pages 180–189) shows hypoxic tubular epithelial cells from patients and mice with lupus that produce ADAM9, which activates transforming growth factor β1 to stimulate the production of α-smooth muscle actin (green) and type I collagen (red) by fibroblasts, leading to fibrosis.

# In this Issue

Highlights from this issue of *A&R* | By Lara C. Pullen, PhD

## Emapalumab for Rheumatologic Disease-Associated HLH

p. 226

To optimize treatment, rheumatologists must differentiate among sepsis, hemophagocytic lymphohistiocytosis (HLH), rheumatologic disease–associated HLH, and a flare-up of underlying rheumatologic disease. Unfortunately, once rheumatologic disease–associated HLH is diagnosed, there are no established recommendations for its management. In this issue, Chandrakasan et al (p. 226) report results from the REAL-HLH study, which indicate that emapalumab-containing regimens stabilized or normalized most key laboratory parameters in patients with rheumatologic disease-associated HLH. The regimens also reduced the glucocorticoid dose used by patients and were associated with low disease-related mortality.

The retrospective medical chart review included demographics, clinical characteristics, real-world treatment patterns, and outcomes in patients with HLH treated with emapalumab in the United States. The overall patient population was racially diverse; approximately 73% were female, and 66.7% had systemic juvenile idiopathic arthritis (sJIA)/adult-onset Still disease (AOSD). Although the population consisted of patients with refractory/recurrent disease at high risk of mortality, there were only two deaths (86.7% overall survival). The authors acknowledge that since theirs is a retrospective study, missing or incomplete chart data may limit their findings.

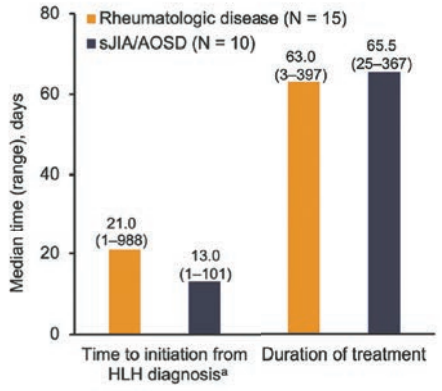


**Figure 1.** Time to emapalumab initiation from HLH diagnosis and duration of treatment with emapalumab.

The investigators found that rheumatologists most frequently initiated emapalumab to treat refractory and recurrent disease. The median emapalumab starting dose in the subset of patients with sJIA/AOSD was lower, and the treatment duration was longer than that documented in the open-label, prospective trial of emapalumab in patients with rheumatologic disease–associated HLH and underlying sJIA/AOSD. The researchers found that patients in their chart review also often had abnormal laboratory values at the time closest to or at the time of emapalumab initiation, a finding that is consistent with those reported for rheumatologic disease–associated HLH in other retrospective case series and that underscores macrophage activation syndrome severity in this population. Treated patients experienced reductions in glucocorticoid dose as early as week 4. Following treatment with emapalumab-containing regimens, two of seven patients (one of four patients with sJIA/AOSD) considered for hematopoietic stem cell transplantation received it. The authors concluded that real-world treatment patterns indicate that emapalumab-containing regimens have the potential to benefit patients with rheumatologic disease–associated HLH.

## Intravenous Secukinumab for Treatment of Active PsA

p. 171

While many patients with psoriatic arthritis (PsA) prefer oral and subcutaneous (SC) routes of drug administration, a recent study found that three-quarters of patients with inflammatory diseases such as PsA who received intravenous (IV) biologics reported being very satisfied with their current IV medication. In this issue, Kivitz et al (p. 171) report that IV secukinumab led to rapid and sustained clinical measures of PsA and had a safety profile consistent with that of SC secukinumab. The improvements in PsA disease control with IV secukinumab treatment were consistent with previous phase 3 studies investigating SC secukinumab treatment for patients with PsA, and the incidence of treatment discontinuation due to treatment-emergent adverse events with IV secukinumab over the entire 52-week treatment period was consistent with previous reports on SC secukinumab.

The results came from the phase 3 INVIGORATE-2 trial, a placebo-controlled trial of IV secukinumab, and not a head-to-head comparison between IV and SC routes of secukinumab administration. Of the 191 patients randomized to IV secukinumab and 190 to placebo and then IV secukinumab, 92.7% and 89.5%, respectively, completed the entire study period. Approximately one-third (31.4%) of patients who received IV secukinumab achieved 50% improvement in American College of Rheumatology response criteria (ACR50) at week 16, compared to 6.3% who received placebo. Patients who switched from placebo to secukinumab at week 16 showed rapid improvements in ACR50 rates such that by week 52, both treatment arms experienced similar improvements in efficacy outcomes. The authors concluded that administering IV secukinumab could provide rheumatologists with additional treatment options to help address the individual treatment needs of patients with PsA.

# Increased Risk for CV Events After Newly Diagnosed Gout

Previous studies have demonstrated increased cardiovascular (CV) morbidity following gout diagnosis; however, those studies have not focused on early gout or on the temporal association between first gout diagnosis and CV events.

p. 202

In this issue, Cipolletta et al (p. 202) report that individuals newly diagnosed with gout had an increased risk of CV events in the 30 days following the first consultation at which gout was diagnosed compared to baseline. The findings build on the group's previous report stating that gout flares were associated with a transient increase in CV events.

The investigators used a nationwide dataset of primary care, hospitalization, and mortality records of 76,440 individuals. They identified 4,398 patients with CV events up to 2 years before or up to 2 years after their first recorded diagnosis of gout. The team then used a self-controlled case series design to examine the association between a transient exposure and an outcome of interest while automatically accounting for fixed covariates.

Using a cohort study design, the researchers found that CV event incidence in the 30 days following the first gout diagnosis was comparable to that reported in other studies including different populations that examined the short-term risk of CV events following respiratory infections. Comparing the incidence of CV events in the 30 days after the first gout diagnosis (31.2 events per 1,000 person-years) to the incidence in days 31 to 730 after gout diagnosis (21.6 events per 1,000 person-years), researchers found a rate difference of –9.6 events per 1,000 person-years. Although the results did not reach statistical significance, the team also found that women had a higher incidence rate of CV events after the diagnosis of gout compared to men.

The authors acknowledge that their study's findings were limited by the uncertainty that surrounds the onset of gout symptoms and the risk of residual unmeasured time-varying confounding.

# Journal Club

*A monthly feature designed to facilitate discussion on research methods in rheumatology.*

## Unraveling the Genetics of Shared Clinical and Serological Manifestations in Patients with SIADs

Bianchi et al, *Arthritis Rheumatol.* 2025;77:212–225.

Systemic lupus erythematosus, primary Sjögren disease, and idiopathic inflammatory myopathies are rheumatic diseases collectively known as systemic inflammatory autoimmune diseases (SIADs). They share not only a type I interferon signature and identical circulating autoantibodies but also similar clinical characteristics. A better understanding of the genetics underlying SIAD disease mechanisms and associated phenotypes could inform patient stratification and treatment. To address this knowledge gap, Bianchi et al used a large and well-characterized Scandinavian SIAD cohort and performed targeted DNA next-generation sequencing (NGS) of coding and potentially regulatory regions of immune-related genes.

The researchers identified common molecular processes underlying overlapping features shared among different diseases, suggesting there may be additional risk factors linked to distinct features. Use of the largest NGS resource currently available for an inclusive collection of key SIADs allowed for comprehensive compiling of genetic variation covering the full spectrum of allele frequencies. Mammalian evolutionary constraint, a strong predictor of functionality in complex diseases, was leveraged to define key noncoding regulatory gene elements included in the targeted array. A genetic score-based method was implemented using aggregation, functional weighting, and analysis of genetic variants in regions of interest and per individual. This enabled comparison and interpretation of the differential genetic load among specific groups of individuals.

Case–control association analysis yielded both well-known and potentially novel SIADs loci. Subgroups defined by the presence of antinuclear antibodies and anti-double stranded DNA autoantibodies had unique genetic profiles reflecting the heterogeneous nature of such molecules. Further, in silico functional evaluation and in vitro reporter experiments showed that DUSP1 protective genetic variants lead to increased gene expression and potentially to anti-inflammatory effects on the SIAD-associated skin phenotype, consistent with findings in other skin disorders.

### Questions

1. **What is currently known about genetic determinants underlying shared and unique serological and clinical features in SIADs?**
2. **What are the strengths and limitations of the gene-based test used in this study, and how does it compare with other variant-aggregating methods?**
3. **What could be learned by whole-genome sequencing of this study cohort or inclusion of a different cohort?**
4. **What improvements could be made to this study's reporter experiments? What other approaches could be used?**

# Clinical Connections

## Hypoxia Promotes ADAM9 Expression by Tubular Epithelial Cells and Tissue Fibrosis in LN

Umeda et al, *Arthritis Rheumatol.* 2025;77:180–189

**CORRESPONDENCE**
**George C. Tsokos, MD**: gtsokos@bidmc.harvard.edu
**Masataka Umeda, MD, PhD**: masatakau0807@nagasaki-u.ac.jp

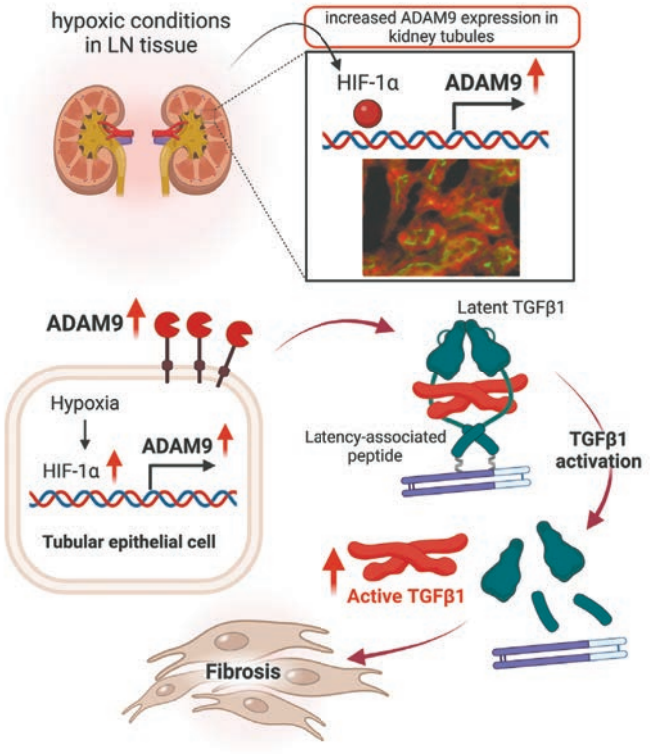


### KEY POINTS

- Hypoxic conditions in the kidney of patients with LN lead to the expression of HIF-1α, which enhances production of the metalloproteinase ADAM9.
- ADAM9 converts latent TGFβ1 to the profibrotic cytokine TGFβ1.
- TECs from mice and lupus patients express increased levels of ADAM9.
- Genetic absence of ADAM9 in lupus-prone mice limits kidney fibrosis and preserves renal function.

### SUMMARY

Despite recent advances, some patients with lupus nephritis (LN) still progress to end-stage renal disease. Fibrosis is a significant contributor to late-stage disease and kidney function decline. Once initiated, fibrosis progresses through the action of the profibrotic cytokine TGFβ1. In patients with LN, microvasculature injury leads to hypoxia and the production of hypoxia-inducible factor 1α (HIF-1α). The ADAM family of proteins are involved in the degradation of extracellular and cell surface molecules, with ADAM9 promoting Th17 cell differentiation through TGFβ1 activation.

Umeda et al showed that in LN, the transcription factor HIF-1α drives increased expression of ADAM9 by tubular epithelial cells (TECs) in both LN patients and MRL/*lpr* mice. ADAM9 converts the latent TGFβ1 to bioactive TGFβ1, thereby promoting tissue fibrosis. Chemical hypoxia of primary mouse TECs leads to increased *ADAM9* expression, and HIF-1α binds to and enhances ADAM9 promoter activity. TECs derived from ADAM9-deficient mice had reduced ability to degrade the latency-associated peptide, a component of latent TGFβ1. Fibroblasts co-cultured with ADAM9-deficient TECs and latent TGFβ1 under hypoxic conditions produced decreased amounts of collagen type I and α-smooth muscle actin. ADAM9-deficient MRL/*lpr* mice exhibited reduced interstitial fibrosis, decreased Th17 cell infiltration in the kidney, and reduced glomerulonephritis. Taken together, this study supports considering approaches to limit HIF-1α production or inhibit ADAM9 activity to prevent the development of kidney fibrosis in patients with LN.

# Role of TLR7/8 Activation in Immune Cells and Muscle by RNA-Containing Immune Complexes in Myositis

Wu et al, *Arthritis Rheumatol*. 2025;77:190–201

**CORRESPONDENCE**
**Yin Wu, BS**: yin.wu@emdserono.com

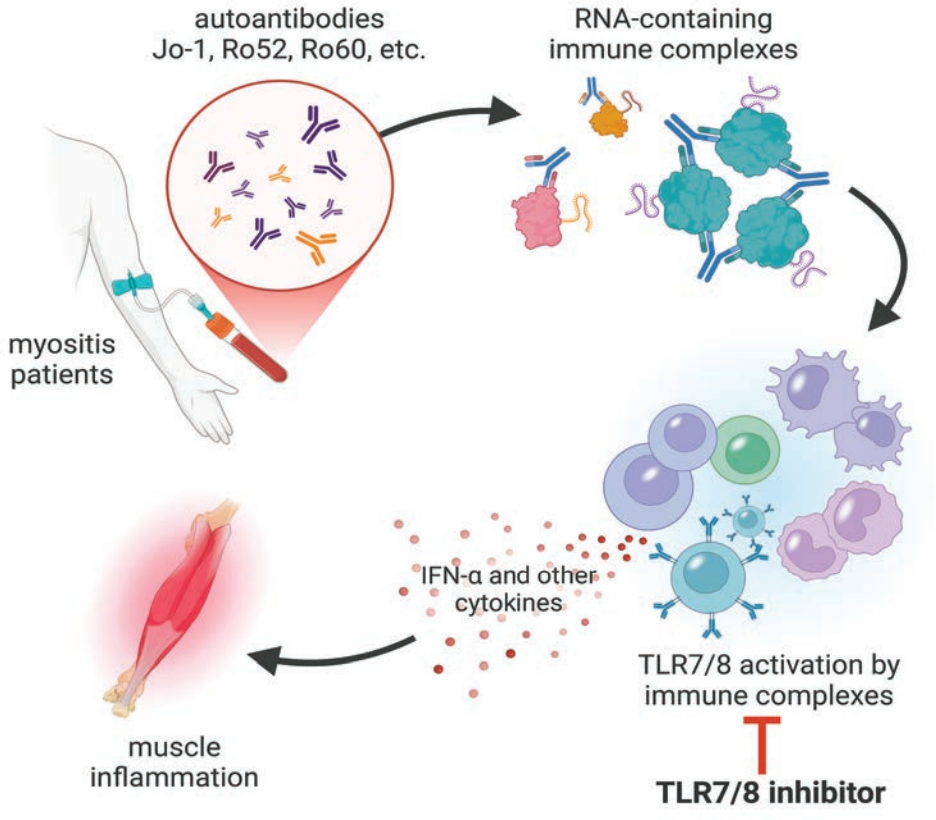


## KEY POINTS

- IIM is an autoimmune disease that commonly leads to muscle weakness.
- Patients with IIM develop autoantibodies that activate TLR7/8, which drives inflammation and adversely impacts muscle cells.
- TLR7/8 inhibitors may reduce both inflammation and the pathogenicity of autoantibodies that drive IIM and lead to tissue damage.

## SUMMARY

Idiopathic inflammatory myopathies (IIMs) are a heterogeneous group of autoimmune disorders commonly associated with muscle weakness. Inflammation is known to be a key driver of IIM, and evidence suggests that aberrant activation of toll-like receptors 7 and 8 (TLR7/8) may be involved in IIM pathogenesis.

Wu et al found that immune complexes generated using immunoglobulin from patients with IIM stimulate immune cells to produce IFN-α, which could be completely inhibited by the TLR7/8 inhibitor enpatoran. Enpatoran also blocked cytokine induction in response to RNAs associated with autoantibodies common to both lupus and IIM (e.g., anti-Ro60 and anti-Ro52), as well as IIM-specific autoantibodies (anti-Jo-1), providing strong evidence that RNA-containing immune complexes induce cytokine production via activation of TLR7/8. Furthermore, muscle stem cells were negatively impacted by supernatants from TLR7/8-activated immune cells in vitro, and endothelial cells and immune cells in mouse muscle exhibited an inflammatory phenotype in response to TLR7/8 activation. These findings highlight the key role of TLR7/8 in IIM pathogenesis and suggest that TLR7/8 inhibition may be an effective therapeutic strategy.

**Arthritis & Rheumatology**
Vol. 77, No. 2, February 2025, pp 121–123
DOI 10.1002/art.43015
© 2024 American College of Rheumatology

American College of Rheumatology
Empowering Rheumatology Professionals

EDITORIAL

# Gout Flares as Vascular Red Flags

Mariano Andrés

In the last two decades, extensive research has positioned gout as a significant risk factor for cardiovascular diseases. People with gout may develop all the different forms of cardiovascular events, from both atherosclerotic and nonatherosclerotic origin.[1] The often large comorbidity profile does not fully explain numbers, with residual cardiovascular morbidity and, notably, mortality after adjustment.[2] Persistent inflammation associated with monosodium urate (MSU) crystal deposition and hyperuricemia, which is also pro-oxidant, might explain the increased cardiovascular risk in patients with gout. However, whether direct causality exists and which mechanisms underlie it remain to be firmly established. Besides that, the risk level varies among patients with gout,[3] and efforts should also include pursuing an accurate cardiovascular risk stratification to tailor their management. In gout, we know that tophi, long-term disease, or the highest quartiles of hyperuricemia are associated with a higher risk of developing cardiovascular events. Additionally, all-cause and cardiovascular mortality were markedly more common in patients not reaching urate therapeutic targets using urate-lowering therapy (ULT) compared with those who successfully reached the targets.[4] However, the search to identify the high cardiovascular risk profile of gout is not complete.

In this issue of *Arthritis & Rheumatology*,[5] Cipolletta et al share new findings that align with their recent research.[6,7] Using the United Kingdom's Clinical Practice Research Datalink database, they showed a 1.4- to 2.3-times higher incidence of vascular events (including myocardial infarction, stroke, and venous thromboembolism) immediately following a gout flare. By comparing different time frames, they identified the high-risk period as the 30 days following the flare. The increased risk was observed in patients who either first consulted due to gout[5] or had long-standing disease.[6,7] The latter group's risk period for atherosclerotic events could last up to 120 days after the flare. Recent data from research in Australia, which focused on hospitalized gout flares, also indicated a heightened risk (1.7 times) of major vascular events within 30 days.[8] It is still unclear whether this phenomenon also occurs in in-hospital flares when patients are admitted for other reasons.

To interpret the data, it is crucial to be able to identify gout flares in a retrospective study using an existing database. More importantly, capture and separate gout flares and vascular events in time. It is possible that gout flares that do not require clinical attention may go unnoticed. Additionally, the initial diagnosis of gout in primary care may occur days or weeks after a gout flare (or several) has been managed at home. The authors made notable efforts to address this issue. They implemented a strict definition for the initial classification of gout, requiring the prescription of an anti-inflammatory drug at the time of coding, and obtained similar results. Furthermore, they considered the period before gout diagnosis to minimize the likelihood that vascular events may have preceded the gout flare, which could occur after the onset of a vascular issue.

From a mechanistic perspective, the acute inflammatory insult might explain the rise in vascular events. Distant sites of inflammation, such as the joint, would promote endothelial cell activation, plaque instability, impaired fibrinolysis, and atherothrombosis through soluble inflammatory mediators.[9] Moreover, an immediate vascular risk after a gout flare might also impact our clinical practice (Figure 1). Firstly, we may consider whether patients need special surveillance after the flare. However, there is no clue on how to perform it, and the number of patients would be considerable. The authors confirmed an increased event risk after excluding patients with established cardiovascular disease or thromboembolic risk factors,[5–7] indicating a general phenomenon. One option might be focusing on these high-risk patients, but the data set is mainly based on primary care, and possibly high-risk populations were not sufficiently captured. Suppose we accept that gout flares increase the risk of a vascular event. In that case, a therapeutic strategy for the flare should also consider preventing the vascular event (perhaps by

Supported by Carlos III Health Institute (Acción Estratégica en Salud 2021, PI21/00544; Contratos para Intensificación en el SNS 2022, INT22/00023), co-funded by the European Union.

Mariano Andrés, MD, PhD: Miguel Hernandez University, San Juan de Alicante, Spain, and Dr. Balmis General University Hospital and Alicante Institute for Health and Biomedical Research, Alicante, Spain.

Author disclosures are available at https://onlinelibrary.wiley.com/doi/10.1002/art.43015.

Address correspondence via email to Mariano Andrés, MD, PhD, at mariano.andresc@umh.es.

Submitted for publication August 23, 2024; accepted in revised form September 17, 2024.

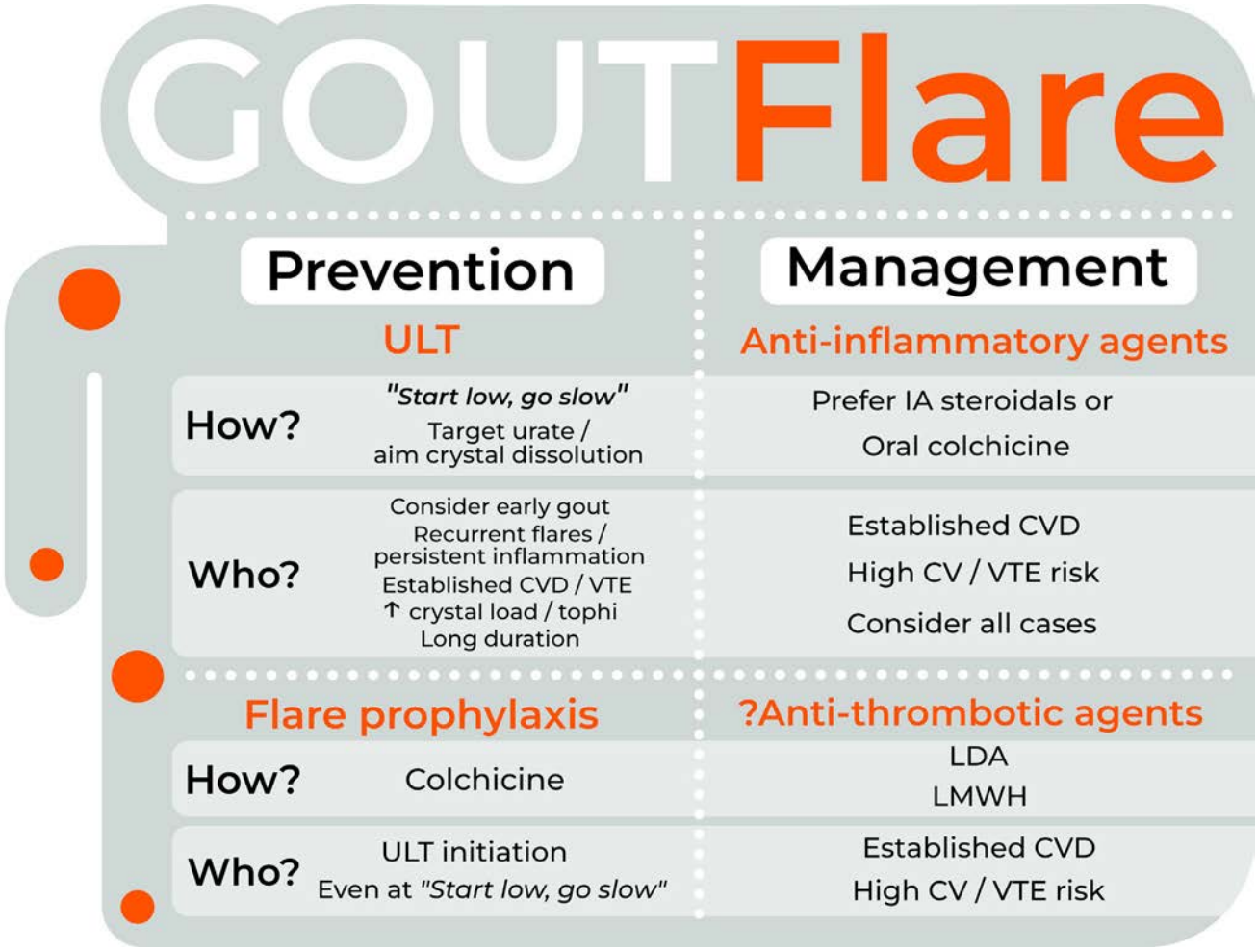


**Figure 1.** Potential implications to clinical practice if gout flares are confirmed as vascular red flags, according to current evidence and author's opinion. CV, cardiovascular; CVD, cardiovascular disease; IA, intra-articular; LDA, low-dose aspirin; LMWH, low molecular-weight heparins; ULT, urate-lowering therapy; VTE, venous thromboembolism.

using low-dose aspirin or fractionated heparin). This intervention must be appropriately evaluated in trials.

Secondly, we may reconsider the treatment choice to address the flare. Colchicine or glucocorticoids (especially intra-articular) may have a better cardiovascular profile than nonsteroidal anti-inflammatory drugs (NSAIDs) after the flare, but no trials have evaluated this endpoint.[10] Interestingly, when Cipolletta et al stratified the data based on the prescribed agent for the flare,[5] they observed that the increased risk appeared to be reduced or nonexistent in patients treated with colchicine. For patients prescribed glucocorticoids or NSAIDs, the data also did not meet significance, but there was a trend indicating a higher risk. Low numbers due to strict exposure definition and stratification hindered the analyses. Probably very few patients received intra-articular glucocorticoids. Additionally, information on the dosage and duration of agents, as well as treatment outcomes, is not available. Finally, we should not rule out prescription biases (eg, NSAIDs avoided in patients with established cardiovascular disease).

And thirdly, perhaps the most relevant consideration is how to approach the long-term management of patients with gout. Should patients be treated aiming for specific serum urate (SU) targets,[9–11] or should the focus be on managing symptomatic episodes such as flares?[12] Lowering SU levels below the saturation point (6.8 mg/dL or 0.40 mmol/L) favors MSU crystal dissolution at a rate that depends on the achieved levels.[9] The absence of MSU crystals would definitively cease gout flares. Additionally, SU levels likely determine the frequency of flares. In UK Biobank data, more than 95% of flares occurred in patients with gout with baseline SU levels above 6mg/dL.[11] The 10-year risk of flares showed a 58% increase per 1 mg/dL rise in SU levels. Therefore, reducing SU levels would also decrease the rate of flares. Considering data from trials,[12,13] this phenomenon likely begins before there is a significant reduction in MSU crystal load. Given its proinflammatory effects, soluble urate itself could also contribute to flares.[14] Lowering SU levels would help prevent subsequent flares and might have a vascular benefit, in line with

data from Cipolletta. Considering the transitory flare peak when starting ULT, flare prophylaxis such as colchicine appears to be then desirable. Even when a "start low, go slow" strategy for ULT is followed.[12] Long-term use of colchicine without a plan to control SU levels would eventually lead to severe, disabling tophaceous disease with a massive crystal load. On the other hand, anticipating ULT after the first gout flare, especially but not exclusively in those with very high SU levels or significant crystal load, could also be beneficial from a cardiovascular standpoint.

The United Kingdom[5–7] and Australia[8] data come from retrospective analyses. These findings need confirmation through prospective studies, with accurate identification of flares and the time span until vascular events. In the meantime, we should be especially aware that the 30 days after a gout flare pose a high vascular risk. *Red flags* are clinical characteristics commonly used to evaluate patients with back pain, helping to identify potentially severe or life-threatening cases. Although individual red flags may have low diagnostic accuracy,[15] they are helpful when used together to identify patients who need further diagnostic work-up. Based on compiled data, gout flares—especially if recent or very recurrent—along with tophi, long-term disease, and uncontrolled SU levels, should be considered our *vascular red flags* for patients with gout.

## ACKNOWLEDGMENTS

The author is very grateful to Enrique Sillero, MD, for the artwork accompanying this editorial.

## AUTHOR CONTRIBUTIONS

Dr Andrés drafted the article, revised it critically for important intellectual content, and approved the final version to be published.

## REFERENCES

1. Ferguson LD, Molenberghs G, Verbeke G, et al. Gout and incidence of 12 cardiovascular diseases: a case-control study including 152 663 individuals with gout and 709 981 matched controls. Lancet Rheumatol 2024;6(3):e156–e167.
2. Clarson LE, Chandratre P, Hider SL, et al. Increased cardiovascular mortality associated with gout: a systematic review and meta-analysis. Eur J Prev Cardiol 2015;22(3):335–343.
3. Andrés M, Bernal JA, Sivera F, et al. Cardiovascular risk of patients with gout seen at rheumatology clinics following a structured assessment. Ann Rheum Dis 2017;76(7):1263–1268.
4. Pérez Ruiz F, Richette P, Stack AG, et al. Failure to reach uric acid target of <0.36 mmol/L in hyperuricaemia of gout is associated with elevated total and cardiovascular mortality. RMD Open 2019;5(2):e001015.
5. Cipolletta E, Nakafero G, Richette P, et al. Short-term risk of cardiovascular events in people newly diagnosed with gout. Arthritis Rheumatol 2025;77(2):202–211.
6. Cipolletta E, Tata LJ, Nakafero G, et al. Association between gout flare and subsequent cardiovascular events among patients with gout. JAMA 2022;328(5):440–450.
7. Cipolletta E, Tata LJ, Nakafero G, et al. Risk of venous thromboembolism with gout flares. Arthritis Rheumatol 2023;75(9):1638–1647.
8. Lopez D, Dwivedi G, Nossent J, et al. Risk of major adverse cardiovascular event following incident hospitalization for acute gout: a Western Australian population-level linked data study. ACR Open Rheumatol 2023;5(6):298–304.
9. Libby P, Buring JE, Badimon L, et al. Atherosclerosis. Nat Rev Dis Primers 2019;5(1):56.
10. Khanna PP, Gladue HS, Singh MK, et al. Treatment of acute gout: a systematic review. Semin Arthritis Rheum 2014;44(1):31–38.
11. McCormick N, Yokose C, Challener GJ, et al. Serum urate and recurrent gout. JAMA 2024;331(5):417–424.
12. Stamp L, Horne A, Mihov B, et al. Is colchicine prophylaxis required with start-low go-slow allopurinol dose escalation in gout? A non-inferiority randomised double-blind placebo-controlled trial. Ann Rheum Dis 2023;82(12):1626–1634.
13. Tedeschi SK, Hayashi K, Zhang Y, et al. Identifying the association between serum urate levels and gout flares in patients taking urate-lowering therapy: a post hoc cohort analysis of the CARES trial with consideration of dropout. Ann Rheum Dis 2024;83(10):1375–1380.
14. Joosten LAB, Crişan TO, Bjornstad P, Johnson RJ. Asymptomatic hyperuricaemia: a silent activator of the innate immune system. Nat Rev Rheumatol 2020;16(2):75–86.
15. Underwood M, Buchbinder R. Red flags for back pain. BMJ 2013;347:f7432.

American College of Rheumatology
Empowering Rheumatology Professionals

**Arthritis & Rheumatology**
Vol. 77, No. 2, February 2025, pp 124–139
DOI 10.1002/art.42990
© 2024 American College of Rheumatology

# IκBζ as a Central Modulator of Inflammatory Arthritis Pathogenesis

Gaurav Swarnkar,[1] Musarrat Naaz,[1] Dorothy Mims,[1] Prashant Gupta,[2] Timothy Peterson,[3] Matthew J. Christopher,[1] Srikanth Singamaneni,[2] Gabriel Mbalaviele,[1] and Yousef Abu-Amer[4]

**Objective.** Current therapies targeting individual factors in inflammatory arthritis show variable efficacy, often requiring treatment with combinations of drugs, and are associated with undesirable side effects. NF-κB is critical for the production and function of most inflammatory cytokines. However, given its essential role in physiologic processes, targeting NF-κB is precarious. Hence, identifying pathways downstream of NF-κB that selectively govern the expression of inflammatory cytokines in inflammatory arthritis would be advantageous. We have previously identified IκBζ as a unique inflammatory signature of NF-κB that controls the transcription of inflammatory cytokines only under pathologic conditions while sparing physiologic NF-κB signals.

**Methods.** We generated mice harboring myeloid, lymphoid, and global deletion of *Nfkbiz* (the gene encoding IκBζ). These models were subjected to serum transfer-induced arthritis. Additionally, pharmacologic inhibitors of IκBζ were injected intraperitonially. Joint swelling, microcomputed tomography, immunohistochemistry, flow cytometry, and cytokine measurements were conducted using synovial tissue samples.

**Results.** Global deletion of *Nfkbiz* or depletion of neutrophils (vastly IκBζ$^+$ cells) reduced inflammatory synovial cells and increased anti-inflammatory and regenerative synovial cells, plummeted expression of inflammatory factors and ameliorated experimental mouse inflammatory arthritis. Further, expression of immune responsive gene-1, the enzyme responsible for itaconate production, was increased in synovial cells. Accordingly, the itaconate derivative dimethyl itaconate (DI) inhibited IκBζ-mediated inflammatory factors. Further, in silico screen identified 8-hydroxyquinoline (HQ) as a putative inhibitor of IκBζ not affecting physiologic NF-κB activity. Congruently, systemic administration of either DI or HQ inhibited joint swelling and damage.

**Conclusion.** Our study positions IκBζ as an inflammation-specific target for therapeutic consideration in rheumatoid arthritis because its inhibition spares the beneficial functions of NF-κB.

## INTRODUCTION

Rheumatoid arthritis (RA) is a chronic inflammatory autoimmune disease considered as one of the leading causes of disability worldwide, with a prevalence of approximately 1% of the world total population.[1–8] The disease is characterized by synovitis and joint swelling[9] affecting most of the small joints in the body.[10] RA symptoms include variable degree of joints pain; impaired physical ability; general sickness; and psychologic, social, and economic impact.[10–12]

Although the pathogenesis of RA is not completely understood, elevated levels of proinflammatory cytokines in the synovium is considered a hallmark of the disease.[5,13] These proinflammatory mediators, secreted by a variety of synovial cells, recruit immune cells to the joint space and contribute to amplification of the joint inflammatory load that ultimately damage articular cartilage and

Supported by the NIH and National Institute of Arthritis and Musculoskeletal and Skin Diseases (grants R01-AR072623, R01-AR082192, and R01-AR081270 to Dr Abu-Amer, grants R01-AR076758, R01-AG077732, and R01-AI161022 to Dr Mbalaviele), the Shriners Hospital for Children (grant 85109 to Dr Abu-Amer), and the NIH Core Center for Musculoskeletal Biology and Medicine (grant P30-AR074992 to Dr Abu-Amer) .

[1]Gaurav Swarnkar, PhD, Musarrat Naaz, PhD, Dorothy Mims, MS, Matthew J. Christopher, MD, PhD, Gabriel Mbalaviele, PhD: Washington University School of Medicine, St. Louis, Missouri; [2]Prashant Gupta, PhD, Srikanth Singamaneni, PhD: Washington University in St. Louis, Missouri; [3]Timothy Peterson, PhD: Washington University School of Medicine, HealthSpan Technologies, Inc., and Bioio, Inc., St. Louis, Missouri; [4]Yousef Abu-Amer, PhD: Washington University School of Medicine and Shriners Hospital for Children, St. Louis, Missouri.

Additional supplementary information cited in this article can be found online in the Supporting Information section (https://acrjournals.onlinelibrary.wiley.com/doi/10.1002/art.42990).

Author disclosures and graphical abstract are available at https://onlinelibrary.wiley.com/doi/10.1002/art.42990.

Address correspondence via email to Yousef Abu-Amer, PhD, at abuamery@wustl.edu.

Submitted for publication September 17, 2023; accepted in revised form September 10, 2024.

subchondral bone. Interleukin-1β (IL-1β), tumor necrosis factor α (TNFα), IL-17, IL-6, monocyte chemotactic protein 1, and other cytokines and chemokines are among the highly abundant factors in the synovium that promote activation of pathologic and inflammatory neutrophils, macrophage, chondrocyte, osteoclasts (OCs), Teff cells, and synovium fibroblast in human and murine RA joints.[14]

Despite significant progress in RA research, there is no cure available. Even with the best clinical management, patients with RA present with mild to severe limitation in mobility and pain. The current standard of care relies on combination of disease modifying antirheumatic drugs, nonsteroidal anti-inflammatory drugs (NSAIDs), steroids, and biologics, including anti–IL-1β and anti-TNF neutralization antibodies. These therapies are designed for reducing or neutralizing the inflammatory cytokines (biologics) and hence have limited efficacy owing to cytokine redundancies, instability of the biologics administered, and various adverse side effects altering normal physiology including infections and cancer.[2,14–16] Therefore, more research is warranted to identify novel therapeutic targets that can be administered across the spectrum of RA diseases with increased efficacy and minimal adverse effects. NF-κB signaling in immune and nonimmune cells plays a crucial role in the production and function of inflammatory cytokines and catabolic mediators that dominate RA.[17–21] These inflammatory cytokines and catabolic mediators rely on NF-κB signaling for their expression, function, or both. Hence, it's logical that selective and strategic targeting of NF-κB activation could be more effective to plummet the production and function of inflammatory culprits compared with the established therapies employing individual cytokine neutralization strategies. However, given the essential role of NF-κB in normal physiologic processes, systemic inhibition of NF-κB is deleterious. Thus, an alternative novel approach to target molecules and pathways downstream of NF-κB activation that exclusively regulate expression of these inflammatory cytokines under pathologic inflammatory conditions is likely to be more effective and safer.

In this regard, we have demonstrated recently in chondrocytes that IκBζ is a unique inflammatory signature of NF-κB, which is robustly expressed under pathologic inflammatory condition compared with negligible expression under physiologic conditions.[22,23] In addition, IκBζ has been shown to regulate IL-17 secretion from Th17 Teff cells.[24] Another study reported that silencing *Nfkbiz* in fibroblast resulted in reduced neutrophil recruitment to sites of inflammation.[25] In the current study, we aim to characterize the central role of IκBζ in RA progression. Our data show that, contrary to global inhibition of NF-κB, deletion of IκBζ does not impact normal skeletal physiology. Notably, we found that IκBζ selectively promotes the transcription of various inflammatory cytokines and catabolic enzymes in arthritic joints. Our research further identified the tricarboxylic acid cycle metabolite, itaconate, and the antibacterial compound 8-hydroxyquinoline (HQ) as potent IκBζ inhibitors that ameliorate RA. In summary, we have identified IκBζ as a potent inflammatory mediator of NF-κB signaling that can be selectively targeted to decrease the inflammation burden and joint pathology in RA animal models.

## MATERIAL AND METHODS

**Study design.** Mice were randomly assigned to experimental groups. Sample size was determined based on previous experience with penetrance of each mouse model. Outliers were included in the final calculations. K/BxN serum was collected, pooled, and tested for standardized use across all experiments. Safe and effective dosage of dimethyl itaconate (DI) and HQ was determined in pilot studies. Mouse genotype, gene, and protein deletions were routinely validated by quantitative polymerase chain reaction (qPCR) and Western blots. All reagents and cytokines were purchased from validated sources. Experiments reflect a minimum of three independent biologic replicates. Figure legends include detailed descriptions of experimental design, sample size and statistical analyses. YA, GM, and TP were masked to the experimental groups, and data were assessed by at least three independent investigators.

**Animals.** Approval for using different animal models was obtained from Washington University School of Medicine Institutional Animal Care and Use Committee. Mice were housed at the Washington University School of Medicine barrier facility with 12-hour light–dark cycles switching at 6:00 PM and 6:00 AM. *Lysozyme-Cre* (strain no. 004781), CAGG-Cre-ERT2 (*Actin*-Cre; strain no. 004682), *Lck-Cre* (strain no. 003802), wild type (WT) C57BL/6J CD45.1 (strain no. 002014), and WT C57BL/6J mice (strain no. 000664) were purchased from Jackson laboratory. *Ubc-Cre*-ERT2 (strain no. 007001) mice were kindly provided by Dr Matthew Silva (Washington University). *LysM-Cre*, *Lck-Cre*, and CAGG-Cre-ERT2 and *Ubc-Cre*-ERT2 mice were bred with *Nfkbiz*-flox mice to generate littermate WT control (*Nfkbiz*-flox only) and experimental *LysM-Cre*$^{+/-}$:*Nfkbiz*$^{-/-}$ KO (*Nfkbiz*$^{\Delta LysM}$), *Lck-Cre*$^{+/-}$:*Nfkbiz*$^{-/-}$ KO (*Nfkbiz*$^{\Delta Lck}$), *CAGG*-Cre$^{+/-}$-*ERT2*:*Nfkbiz*$^{-/-}$ KO (*Nfkbiz*$^{\Delta CAGG}$), and *Ubc*-Cre$^{+/-}$-*ERT2*:*Nfkbiz*$^{-/-}$ KO (*Nfkbiz*$^{\Delta Ubc}$) mice.

**Mouse model and interventions.** *Serum transfer-induced arthritis.* K/BxN arthritic mice were generated by crossing the KRN mice with the B6.I-Ag7 mice. Arthritic serum was collected and pooled from 6- to 10-week-old male and female K/BxN mice. To study the effect of global deletion of *Nfkbiz* on serum transfer-induced arthritis (STIA), eight-week-old male and female *Nfkbiz*$^{\Delta CAGG}$, *Nfkbiz*$^{\Delta Ubc}$, and littermate control (*Nfkbiz* floxed) mice were fed with tamoxifen diet for 15 days (day −14 to day 1). K/BxN serum was administered on day 0 (200 μL intraperitoneally [IP]) and day 2 (100 μL IP). To study the effect of myeloid and lymphoid specific *Nfkbiz* deletion, *Nfkbiz*$^{\Delta LysM}$, *Nfkbiz*$^{\Delta Lck}$, and littermate (eight-week-old male and female) mice were used, respectively. K/BxN serum was administered on day 0 (200 μL

IP) and day 2 (100 μL IP). For pharmacologic IκBζ inhibition, 10-week-old WT male C57BL/6J mice were divided into four groups (control, STIA, STIA + DI, and STIA + HQ). DI (at 800 mg/kg body weight) or HQ (at 10 mg/kg body weight) was administered IP. DI (category no. 592498) and HQ (category no. H6878) were purchased form Millipore-Sigma. Paw and ankle thicknesses were measured with a digital caliper. At the end of the experiment, tissue samples were harvested for further analyses.

***In vivo* cell depletion.** To investigate the role of T cells and neutrophils in mouse STIA, eight-week-old male WT C57BL/6J mice were divided into three groups (STIA control mice, $STIA^{+}TCR\beta$ T cell–depleted mice, and $STIA^{+}Ly6G$ neutrophil-depleted mice). Two days before STIA induction (day −2), phostphate buffer saline (PBS) was administered (IP) to the control group, T cells depleted group was treated (IP) with 100 μg per mouse TCRβ neutralizing antibody (Bioxcell, category no. BE0102), and neutrophils depleted group received 400 μg per mouse Ly6G neutralization antibody (Bioxcell, category no. BE0075-1). Neutralizing antibodies were again administered on day 1 and day 4 after STIA induction. T cells and neutrophil neutralization efficiency was measured using fluorescence-activated cell sorting (FACS) analysis in blood. Paw and ankle thicknesses were measured with a digital caliper.

**Bone marrow transplantation.** On day 0, eight-week-old male CD45.1 mice (n =10, Jackson Laboratories strain number 002014) were irradiated using 1,000 cGy radiation. On the same day, total bone marrow cells were isolated from Donor CD45.2 $Nfkbiz^{\Delta CAGG}$ mouse. After red blood cell lysis, $5 \times 10^6$ $CD45.2^{+}$ *Nfkbiz* null cells were transplanted to irradiated host (CD45.1). After bone marrow transplantation (BMT), the host chimera mice were kept on antibiotic (enrofloxacin 1 mL per 250 mL of water) for two weeks. BMT or chimerism efficiency was analyzed using FACS (antibodies for CD45.1 and CD45.2) after four and six weeks in blood. For controls in FACS analysis, we used bone marrow cells from CD45.1 and CD45.2 mice. STIA was induced seven weeks after BMT as described previously under STIA model. Paw and ankle thicknesses were measured with a digital caliper. At the end of the experiment, tissue samples were harvested for further analyses.

**Microcomputed tomography and histology.** At the end of the experimental timeline, mice were euthanized and long bones with intact ankle joints and paw were collected. The skin was removed from the ankle and paw followed by fixation in 10% formalin for 24 hours at room temperature. After fixation, bones were washed in PBS and to 70% ethanol (volume/volume [v/v]) for storage until further processing. Paw–ankle joints were scanned using Scanco Medical microcomputed tomography (μCT) system (Scanco) at a resolution of 20 μm, slice increment of 20 μm, voltage 55 of kV, current of 145 μA, and exposure time of 200 ms. After scanning, three-dimensional images were constructed. μCT was done at the Musculoskeletal Center Research Core at Washington University in St. Louis. For histologic analysis, bones were decalcified in 14% acid free EDTA solution for two weeks. After decalcification, the bones were dehydrated in graded ethanol (30–70%), cleared through xylene and embedded in paraffin block for further sectioning. Paraffin embedded bone sections were stained with tartare resistant acid phosphatase (TRAP) and hematoxylin and eosin stain to visualize osteoclast and inflammatory burden, respectively.

**Isolation of synovial cells.** For real-time PCR and flow cytometry analysis, synovial cells were isolated from paw and ankle joints. At the end of the experiment, paw and ankle joints were dissected and skin was removed. The tissue samples were dissected further without cutting the bone in the joints to avoid any contamination from the bones. Dissected tissues were digested in PBS containing 2 mg/mL of collagenase D and 2 mg/mL of DNase I for 60 minutes at 37°C in shaking water bath (250 revolutions per minute). After every 15 minutes, tubes with the tissues were vortexed briefly. The supernatant containing the synovial cells was passed through a 100-μ strainer, centrifuged, and suspended in appropriate buffer and processed for further analysis.

**Cell culture.** Total mouse bone marrow cells (BMCs) from long bones were used for macrophage (bone marrow–derived macrophages [BMMs]) and OC culture. BMCs were differentiated to BMM by culturing them in a-minimum essential medium (α-MEM) containing 100 units/mL of penicillin/streptomycin and 10% fetal bovine serum (FBS) (v/v) with 20 ng/mL of macrophage colony-stimulating factor (M-CSF), for four days.

For OC culture, BMCs were first plated overnight in a petri dish to separate adherent cells from nonadherent cells. Next day, nonadherent cells were collected and replated in as per experimental conditions in the presence of M-CSF (20 ng/mL) and receptor activator of NF-κB ligand (RANKL) (50 ng/mL) for three to four days. Differentiated OCs were observed under a microscope, followed by fixation and TRAP staining using TRAP-Leukocyte kit (Sigma).

Primary calvarial osteoblast (cOB) culture was done, as described earlier.[26] Briefly, mouse calvaria from newborn one- to two-day-old *Nfkbiz* floxed mice were digested in serum free α-MEM containing 0.1% dispase and 0.1% collagenase (15 minutes per digestion). First digestion (heterogeneous population) was discarded. Cells from the next four digestions were collected and cultured in ascorbic acid free-α-MEM containing 10% FBS. To delete *Nfkbiz*, *Nfkbiz* floxed cOB were transfected with Adeno-GFP (as a control) and Adeno-Cre (multiplicity of infection 1:20). Six hours after transfection, the media was changed, and cOB were cultured in osteogenic differentiation media (α-MEM containing 10% FBS, 10 m*M* β glycerophosphate, and 50 μg/mL of ascorbic acid) for an additional three days.

To isolate WT and *Nfkbiz*-null neutrophils, WT and *Nfkbiz*$^{\Delta CAGG}$ mice were fed a tamoxifen diet for 14 days. On day 15, neutrophils were isolated from bone marrow using a neutrophil isolation kit (no. 130-097-658, Miltenyi Biotec). Isolated neutrophils were cultured in RPMI 1640 media containing 10% FBS and treated with or without lipopolysaccharide (LPS) (100 ng/mL) for three hours and were processed for further analysis.

**Flow-cytometry analysis.** Synovial cells from the WT and *Nfkbiz*$^{\Delta CAGG}$ arthritic ankle and paws were isolated, washed, and resuspended in PBS containing Fixable Viability Dye eFluor 780 (no. 65-0865-14, eBiosciences) for 30 minutes at 4°C to stain dead cells. Additionally, 20 μL of cells were kept aside before live/dead staining to be used as unstained controls in flow analysis. After live/dead cells staining, the cells were washed with FACS cell staining buffer (no. 420201, Bio legend) and resuspended in 200 μL of FACS cell staining buffer. To block nonspecific Fc-mediated interactions, the remaining cells were incubated with 1 μg of anti-mouse CD16/CD32 (no. 101302, Biolegend) per 100 μL of cells for 20 min at room temperature. Based on flow analysis, the fluorochrome-labeled antibodies were combined in a master mix (1:200 dilution) and added to the cells. Fluorescence minus one samples were also prepared for flow analysis. The cells were incubated with antibodies for 30 minutes at 2–8°C, followed by two times washing cell staining buffer. After staining, the cells were fixed, washed, and resuspended in flow staining buffer. For intracellular staining (IL-1β and IκBζ), the cells were fixed and stained using a True-Nuclear Transcription Factor kit (Biolegend, category no. 424401). The next day, the flow acquisition was done using Attune-Nxt Flow-cytometer (ThermoFisher Scientific). The analysis was done using Flowjo-V10. The gating strategies are shown in Fig S1.

**Behavioral analysis.** Grip strength analysis was performed on day 7 after STIA induction. Mice were acclimatized to the behavioral testing room (Animal Models of Joint Injury Core at the Musculoskeletal Center Research Core at Washington University in St. Louis) for two hours before the assessment. Grip strength was performed using Bioseb Grip Strength apparatus (Bioseb). Briefly, the grip strength meter is positioned horizontally, and the mice were held by the tail and lowered toward the apparatus. Mice were allowed to grab the metal grid and then pulled backward in the horizontal plane. The force applied to the grid or to the bar just before it loses grip is recorded as the peak force or grip strength. Each animal was subjected to test three times. The values were averaged for each mouse for further analysis. Thermal sensitivity was measured using Hot Plate Test (Bioseb). Briefly, the mice were placed on the surface of plate set at 55°C, which has a built-in timer. The timer was stopped at the instant the mouse licked or lifted its paw from the hot plate. Each animal was subjected to test three times with 15 minutes interval between each trial. The values were averaged for each mouse for analysis.

**Real-time PCR.** At the end of experiment, BMMs, osteoclasts, osteoblasts, neutrophils, and synovial cells were used for qPCR analysis. CD11b$^{+}$ cells from WT and *Nfkbiz*$^{\Delta LysM}$ mice were isolated ankle-paw joints using MACS (CD11b microbeads ultrapure, mouse, Miltenyi biotech). RNA isolation was done using a PureLink RNA mini kit (no. 12183025, Invitrogen), and complementary DNA were prepared using a high-capacity reverse transcription kit (no. 4374967, Applied Biosystems). Quantitative real-time PCRs were done on a BioRad CFX96 real-time system using iTaq Universal SYBR Green Supermix (no. 1725124, BioRad). Messenger RNA (mRNA) expressions were normalized using *β-actin* as a housekeeping gene. The following primers were used for qPCR analysis: *Il1α-F*, GAAGAAGAGACGGCTGAGTTT; *Il1α-R*, TCACTCTGGTAGGTGTAAGGT; *Il1β-F*, TGTAATGAAAGACGGCACACC; *Il1β-R*, TCTTCTTTGGGTATTGCTTGG; *Tnfα-F*, CTGTAGCCCACGTCGTAGC; *Tnfα-R*, TTGAGATCCATGCCGTTG; *Irg1-F*, GGTATCATTCGGAGGAGAA; *Irg1-R*, ACAGAGGGAGGGTGGAATCT; *Lcn2-F*, CCATCTATGAGCTACAAGAGAACAAT; *Lcn2-R*, TCTGATCCAGTAGCGACAGC; *Mmp3-F*, TGCAGCTCTACTTTGTTCTTTGA; *Mmp3-R*, AGAGATTTGCGCCAAAAGTG; *Mmp9-F*, ACTGGGCTTAGATCATTCCAGCGT; *Mmp9-R*, ACACCCACATTTGACGTCCAGAGA; *Rankl-F*, TGAAGACACACTACCTGACTCCTG; *Rankl-R*, CCCACAATGTGTTGCAGTTC; *S100A8-F*, CATGCCCTCTACAAGAATGACT; *S100A8-R*, TATCACCATCGCAAGGAACTC; *Nfkbiz-F*, GGAAGCCCGATGAATACCA; *Nfkbiz-R*, TTCCTGCTCTACCTGCCACT; *Nlrp3-F*, CCCTTGGAGACACAGGACTC; *Nlrp3-R*, GAGGCTGCAGTTGTCTAATTCC; *Il6-F*, GCTACCAAACTGGATATAATCAGGA; *Il6-R*, CCAGGTAGCTATGGTACTCCAGAA; *Trap-F*, CACTCCCACCCTGAGATTTGT; *Trap-R*, CATCGTCTGCACGGTTCTG; *Nfatc1-F*, TCCAAAGTCATTTTCGTGGA; *Nfatc1-R*, CTTTGCTTCCATCTCCCAGA; *Actb-F*, CTAAGGCCAACCGTGAAAAG; and *Actb-R*, ACCAGAGGCATACAGGGACA.

**Western blot and enzyme-linked immunosorbent assay.** At the end of the experiment, BMMs were lysed in Mammalian Cell Lysis Buffer (Cell Signaling Technology) containing protease/phosphatase inhibitor (Halt Protease Phosphatase Inhibitor Cocktail; Thermo Fisher Scientific). Protein concentration was determined by Rapid Gold bicinchoninic acid assay (no. A53227, Pierce, ThermoFisher), and equal amounts of protein were loaded onto sodium dodecyl sulfate–polyacrylamide gel electrophoresis gel. Premade 4% to 12% of Bolt Bis-Tris gels were used to run the protein. The transfer was done using an iBlot transfer unit (ThermoFisher). After transfer the membranes were blocked in 5% bovine serum albumin (BSA) in PBS-Tween (PBST) (0.1% v/v) for one hour at room temperature and probed overnight at 4°C with specific primary antibodies diluted in 5% BSA in PBST. The following

primary antibodies were used: IκBζ (no. 14-16801-82, Thermo Fisher/Invitrogen), Nlrp3 (no. AG-20B-0014-C100 Adipogen Life Sciences), IL1β (no. AB9722, Abcam), Irg1 (no. ab222411, Abcam), and actin (category no. A2228, Sigma). The next day, the membranes were washed three times with PBST and probed with secondary antibodies from LI-COR (Odyssey Imager; donkey anti-rabbit/IRDye, anti-mouse IRDye 680RD, Donkey anti-rat/IRDye 800CW, 1:10,000 dilution) for one hour at room temperature. Membranes were then washed three times with PBST and scanned using LI-COR Odyssey Imager (LI-COR Biosciences) at low resolution using Licor Image Studio software. Serum was isolated on day 3 after STIA induction. Serum IL-1β enzyme-linked immunosorbent assay (ELISA) was performed using an IL-1β mouse uncoated ELISA kit (no. 88-7012-22, ThermoFisher, Invitrogen), as per the kit protocol.

***In silico* analysis.** Two different machine learning methods were used to identify pharmacological inhibitors that could phenocopy *Nfkbiz* inhibition: (1) a cell fitness–based prediction, and (2) a human curated "-omic" prediction. Both approaches used the PRISM dataset as the source of pharmacologics.[27] In brief, method 1 relies on mapping the fitness profiles of drug treatment with those of *Nfkbiz* genetic inhibition. Method 2 relies on mapping various -omic analyses, such as transcriptomics, text mining, and proteomics with *Nfkbiz* genetic inhibition. It is human curated in the sense that humans determined the weightings that each different type of -omics contribute to the *Nfkbiz* genetic inhibition mapping.

**Statistical analysis.** All experiments represent biologic replicates and were repeated at least three times, unless otherwise stated (in figure legends). Statistical analyses were performed using appropriate statistical test using GraphPad Prism. Multiple treatments were analyzed by one-way or two-way analysis of variance followed by Tukey's test multiple comparisons test. Student's *t*-test was used for comparing two groups. *P* values are indicated when applicable (*$P < 0.05$, **$P < 0.01$, ***$P < 0.001$, and ****$P < 0.0001$).

## RESULTS

**IκBζ regulation of inflammatory and physiologic functions of NF-κB activation in bone cells.** NF-κB activation is crucial for OC differentiation, survival, and inflammatory osteolysis.[28–34] IκBζ is a downstream component of NF-κB mediating a subset of target genes, yet its role in osteoclastogenesis and inflammatory osteolysis is unclear. Therefore, we first tested if IκBζ inhibition regulates osteoclastogenesis and physiologic skeletal homeostasis. Because RANKL is a well-established activator of NF-κB during physiologic OC differentiation, we characterized the bone phenotype and OC function *in LysM-Cre*$^{+/-}$: *Nfkbiz*$^{-/-}$ knockout (*Nfkbiz*$^{\Delta LysM}$) mice compared to WT littermate controls under normal physiologic conditions. μCT analysis showed no difference in basal bone structure between WT control and *Nfkbiz*$^{\Delta LysM}$ mice (Figure 1A). Bone parameters such as bone volume/total volume (Figure 1B), trabecular number (Figure 1C), trabecular thickness (Figure 1D), and trabecular separation (Figure 1E) were comparable between WT and *Nfkbiz*$^{\Delta LysM}$ mice. qPCR data indicated that RANKL, which induces OC differentiation via NF-κB activation, failed to increase *Nfkbiz* expression (Figure 1G). In addition, deletion of *Nfkbiz* did not affect OC differentiation (Figure 1F), as observed by no significant changes in *Trap* and *Nfatc1* gene expression (Figure 1H and 1I). We also investigated the physiologic role of IκBζ in primary calvarial osteoblast (OB) cells. Consistent with OC data, *Nfkbiz* deletion in calvarial OB (Fig S2A and B) did not affect expression of OB genes, such as alkaline phosphatase (*Alp*) and collagen type 1 (*Col1*) (Figure 1J) under physiologic OB differentiation conditions.

**IκBζ regulation of pathologic functions of NF-κB activation in myeloid cells.** We demonstrated recently that IκBζ is a distinctive inflammatory signature of NF-κB activation in chondrocyte cells, controlling expression of *Il1β*, *Il6*, and *Tnfsf11* (*Rankl*).[22] These cytokines act in a paracrine and autocrine manner to amplify inflammatory signaling and catabolic enzymes, ultimately leading to joint swelling followed by cartilage and bone destruction. Based on this observation, we next investigated if IκBζ controls expression of inflammatory genes in response to specific pathologic stimulation in cell types implicated in RA progression. To this end, we treated WT and *Nfkbiz*-null macrophages with vehicle or LPS. *Nfkbiz* mRNA expression was extremely low and IκBζ protein expression was undetectable in all cells we tested under physiologic conditions (Figure 2). On the other hand, LPS treatment resulted in a significant increase in the expression of *Nfkbiz* and other inflammatory genes in WT macrophages (Figure 2A–E). Conversely, expression of inflammatory genes, such as *Il1β*, *Il6*, and *Il18* in LPS-treated *Nfkbiz*-null macrophages (Figure 2A) was significantly reduced (Figure 2B–D). There was no statistically significant change in expression of *Nlrp3* expression (Figure 2E), indicating that downstream to NF-κB, IκBζ regulates very specific subsets of inflammatory genes. Concurrently, immunoblotting (Figure 2F) and ELISA (Figure 2G) showed decreased pro-IL-1β expression and IL-1β secretion in *Nfkbiz*-null macrophages. Note undetectable IκBζ protein expression (Figure 2F) and extremely low *Nfkbiz* mRNA expression in untreated WT and knockout cells (Figure 2A, H, K).

Our initial data (Figure 1) showed that IκBζ does not mediate RANKL-induced physiologic OC differentiation and function. However, it has been shown that in the presence of inflammatory signals such as LPS and IL-1β, preosteoclast (pre-OC) differentiate to pathologically activated osteoclasts (PAOCs),[35] which are not only hyperactive in resorbing bone but also secrete various inflammatory cytokines (such as IL-1β) to further amplify inflammatory cascade in skeletal inflammatory diseases such as RA. Our results show that *Nfkbiz* deletion (Figure 2H) hindered

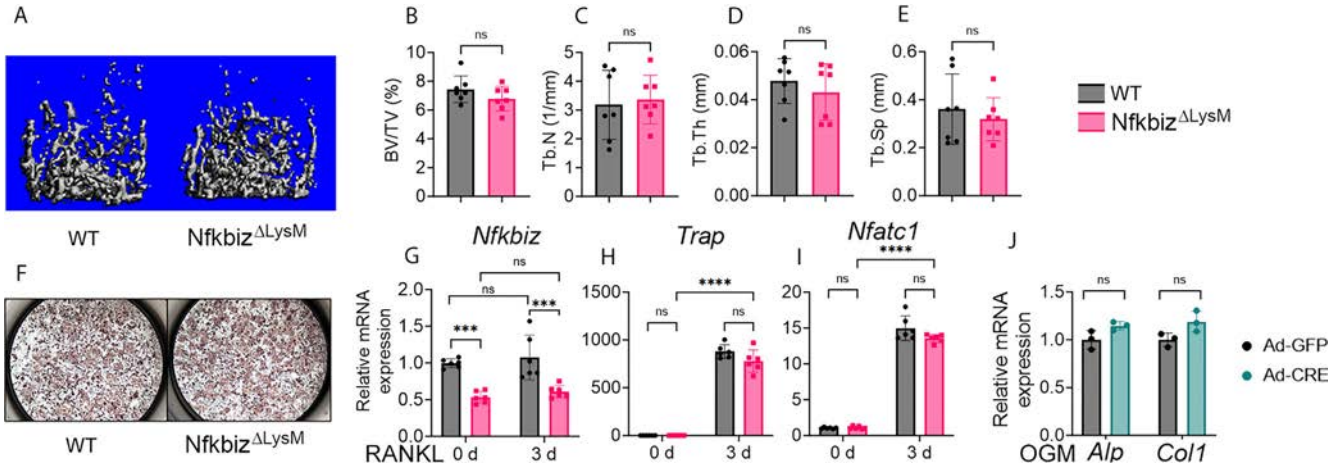


**Figure 1.** IκBζ does not regulate physiologic functions of NF-κB activation in bone cells, and the deletion of IκBζ does not affect bone mass. Seven-week-old *LysM-Cre*$^{+/-}$:*Nfkbiz*$^{-/-}$ knockout (*Nfkbiz*$^{\Delta LysM}$) and littermate WT control animals were killed, and long bones were isolated. (A) Microcomputed tomography images, (B) BV/TV, (C) connective density, (D) Tb.Th., and (E) Tb.Sp. Bone marrow cells were isolated from *Nfkbiz*$^{\Delta LysM}$ and littermate WT control animals and cultured in RANKL and macrophage colony-stimulating factor for four days. (F) TRAP staining and quantitative polymerase chain reaction for (G) *Nfkbiz*, (H) *Trap*, and (I) *Nfatc1* show no differences in osteoclast differentiation between WT and *Nfkbiz*$^{\Delta LysM}$ bone marrow–derived macrophages. Calvarial osteoblast expressing Ad-GFP (control) and Ad-Cre (*Nfkbiz* null calvarial osteoblast) were cultured in osteoblast OGM for three days. (J) Quantitative polymerase chain reaction showing expression of osteoblast genes *Alp* and *Col1* (representative of three independent experiments). Data are presented as means ± SDs. **P* < 0.05, ***P* < 0.01, ****P* < 0.001, and *****P* < 0.0001. Student's *t*-test was used for two groups, and two-way analysis of variance was used for more than two variables. (G and H) Quantitative polymerase chain reaction reflects biologic replicates. *Alp*, alkaline phosphatase; Ad-CRE, Adeno-Cre; Ad-GFP, Adeno-GFP; BV/TV, bone volume/total volume; *Col1*, collagen type 1; mRNA, messenger RNA; ns, not significant; OGM, osteogenic differentiated media; RANKL, receptor activator of NF-κB ligand; Tb.N, trabecular number; Tb.Sp, trabecular separation; Tb.Th, trabecular thickness; *Trap*, tartare resistant acid phosphatase; WT, wild type.

differentiation of PAOC as observed by significantly low expression of *Il1β* (Figure 2I) and *Il6* (Figure 2J) in LPS-treated pre-OC. Neutrophils plays a major role in RA initiation and progression, especially in mouse model of RA, such as STIA. In this regard, the data show that, similar to macrophages, LPS treatment significantly increased *Nfkbiz* expression in WT neutrophils (Figure 2K), whereas *Nfkbiz* deletion significantly hindered LPS induction of *Il1β* expression in neutrophils (Figure 2L).

Collectively, these findings suggest that *Nfkbiz* is not activated in physiologic conditions as well as in response to noninflammatory NF-κB activation (such as RANKL) and therefore, contrary to inhibition of NF-κB, the deletion of IκBζ does not appear to impact normal skeletal physiology. These data are consistent with our previous report in which we showed that *Nfkbiz* deletion in chondrocytes had no adverse effect on articular cartilage at basal level.[22] More importantly, the data show that IκBζ controls expression of inflammatory genes in response to pathologic stimulation in various cell types.

**Attenuation of experimental STIA in global conditional ablation of *Nfkbiz*.** Our findings clearly demonstrate that in response to specific inflammatory stimuli, IκBζ regulates expression of various inflammatory genes such as *Il1β*, *Il6*, and so on. Based on this observation, we surmised that under inflammatory joint diseases such as RA, IκBζ is essential for expression of inflammatory signals and therefore inhibiting IκBζ holds promise to attenuate inflammatory RA. In RA synovium, inflammatory and catabolic cytokines are secreted from different immune and nonimmune cell types (T cells, monocyte, macrophage, pathologic OC, fibroblast, neutrophils, chondrocytes, etc). Therefore, to effectively diminish the expression of inflammatory cues from various cell types involved in RA progression, we induced STIA in WT and in inducible global-*Nfkbiz* null mouse. Specifically, *CAGG*-ERT2-cre$^{+/-}$: *Nfkbiz*$^{-/-}$ KO (*Nfkbiz*$^{\Delta CAGG}$), *Ubc*-ERT2-cre$^{+/-}$:*Nfkbiz*$^{-/-}$ KO (*Nfkbiz*$^{\Delta Ubc}$), and their respective littermate WT (*Nfkbiz* flox) mice were subjected to STIA two weeks after tamoxifen-induced activation of Cre recombinases (Figure 3A). Paw and ankle thickness measurement (Figure 3B and 3C) and μCT analysis (Figure 3D) clearly displayed that global ablation of *Nfkbiz* attenuates experimental mouse STIA.

Further, histologic analysis showed diminished inflammatory burden (Figure 3E; asterisks) and reduced TRAP-positive OCs (Figure 3F; arrows) in the paw–ankle joint in global *Nfkbiz* null mice subjected to STIA. Consistently, qPCR analysis from synovium cells isolated from arthritic paw and ankle joint showed significant reduction in the expression of inflammatory and catabolic genes, including *Nfkbiz*, *Lcn2*, *Mmp9*, *Mmp3*, *Rankl*, *S100A8* (*Mrp8*), *Tnfα*, *Il1α*, and *Il1β* in global *Nfkbiz* knockout mice compared to WT control mice (Figure 3G and H). STIA-induced WT and global *Nfkbiz* null mice were also used to perform behavioral analysis to functionally correlate with RA pathology. Grip strength and thermal analgesia tests confirmed that *Nfkbiz* deletion inhibited RA progress

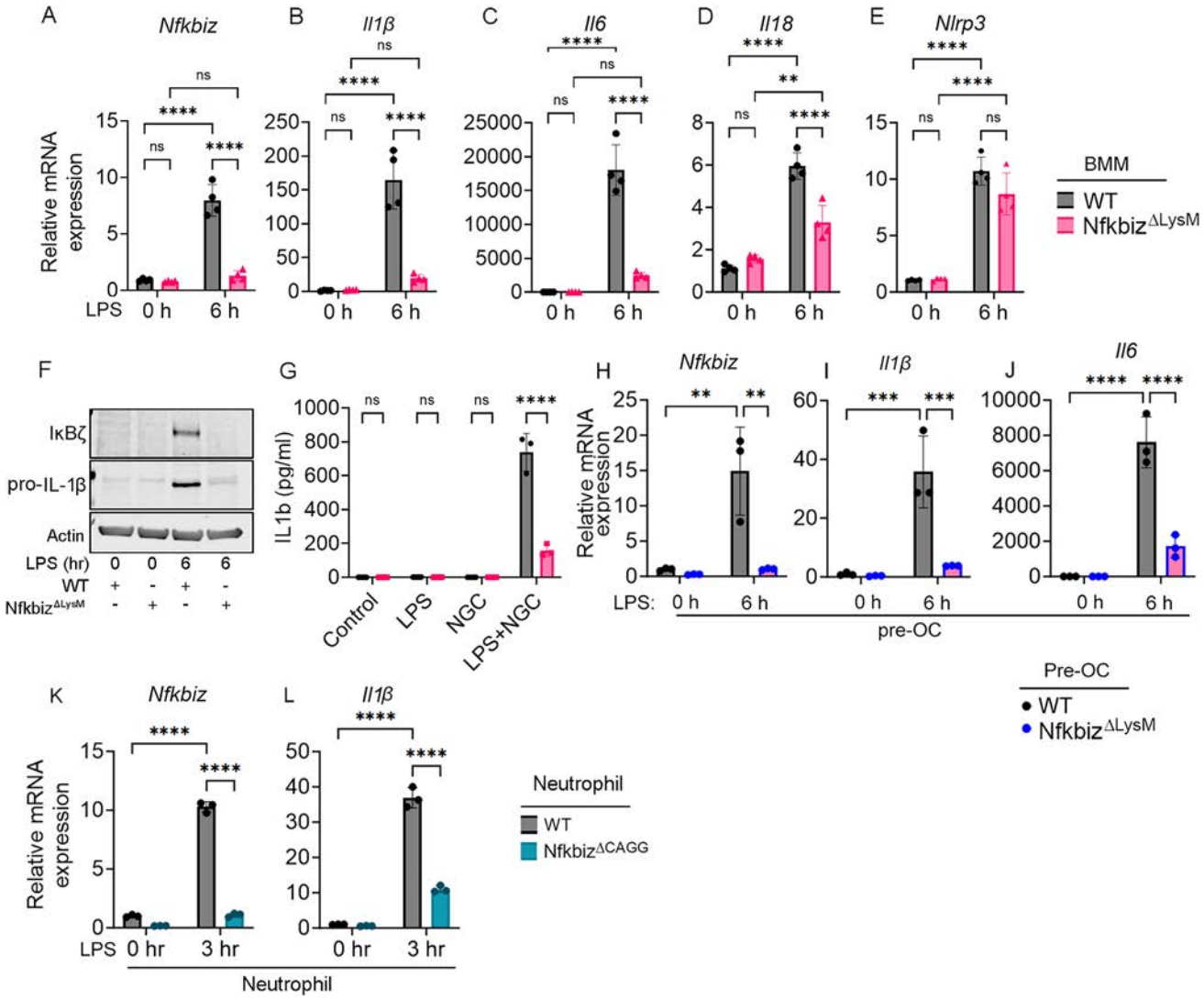


**Figure 2.** IκBζ regulates pathologic functions of NF-κB activation in myeloid cells: bone marrow cells isolated from *Nfkbiz*$^{\Delta LysM}$ and littermate WT mice were differentiated to macrophage (BMM) with macrophage colony-stimulating factor for four days. On day 4, BMMs were treated with LPS (100 ng/mL) for six hours. Quantitative polymerase chain reaction analysis for the expression of (A) *Nfkbiz*, (B) *Il1β*, (C) *Il6*, (D) *Il18*, and (E) *Nlrp3*. Western blot analysis showing (F) expression of IκBζ and pro-IL-1β in WT and *Nfkbiz*$^{\Delta LysM}$ BMM. (G) Enzyme-linked immunosorbent assay showing IL-1β secretion from BMM treated with LPS (100 ng/mL) for 3 hours followed by NGC (15 μ*M*) for 30 minutes. BMMs cultured with RANKL (50 ng/mL) for two days to differentiate them to pre-OCs. Pre-OCs were treated with LPS for six hours. Quantitative polymerase chain reaction in pre-OC showing expression of (H) *Nfkbiz*, (I) *Il1β*, and (J) *Il6*. Neutrophils were isolated from WT and *Nfkbiz*$^{\Delta CAGG}$ mice two weeks after Cre induction. Quantitative polymerase chain reaction showing expression of (K) *Nfkbiz* and (L) *Il1β* in neutrophils. Data are represented as means ± SDs. **P* < 0.05, ***P* < 0.01, ****P* < 0.001, and *****P* < 0.0001. Student's *t*-test was used for two groups, and two-way analysis of variance was used for more than two variables. Quantitative polymerase chain reaction and Western blots are representative of three independent experiments. BMM, bone marrow–derived macrophage; IL-1β, interleukin-1β; LPS, lipopolysaccharide; mRNA, messenger RNA; NGC, Nigericin; ns, not significant; pre-OC, preosteoclast; WT, wild type.

in STIA mice (Figure 3I and J). Notably, global deletion of IκBζ had no significant effect on gross basal phenotype, albeit IκBζ deficient mice displayed susceptibility to infections and incremental effect on T cell stability (reviewed in the study by Gautam et al[36]).

**Global conditional ablation of *Nfkbiz* and the frequency of synovial cells.** Because RA pathologic progression is dominated by hyperproliferation of various immune and nonimmune cells, we quantified the frequency of different myeloid lineage cells (including neutrophils) and synovial fibroblast in the arthritic synovium in WT and *Nfkbiz*$^{\Delta CAGG}$ mice after STIA induction. Compared to WT mice, we observed significantly low numbers of total synovium cells (Figure 4A and P) in the *Nfkbiz*$^{\Delta CAGG}$ mice, indicating decreased STIA progression. Further, FACS analysis using CD11b$^{+}$ cells (Figure 4B) confirmed decreased expression of Ly6G$^{+}$ neutrophil cells (Figure 4C), Ly6C$^{+}$

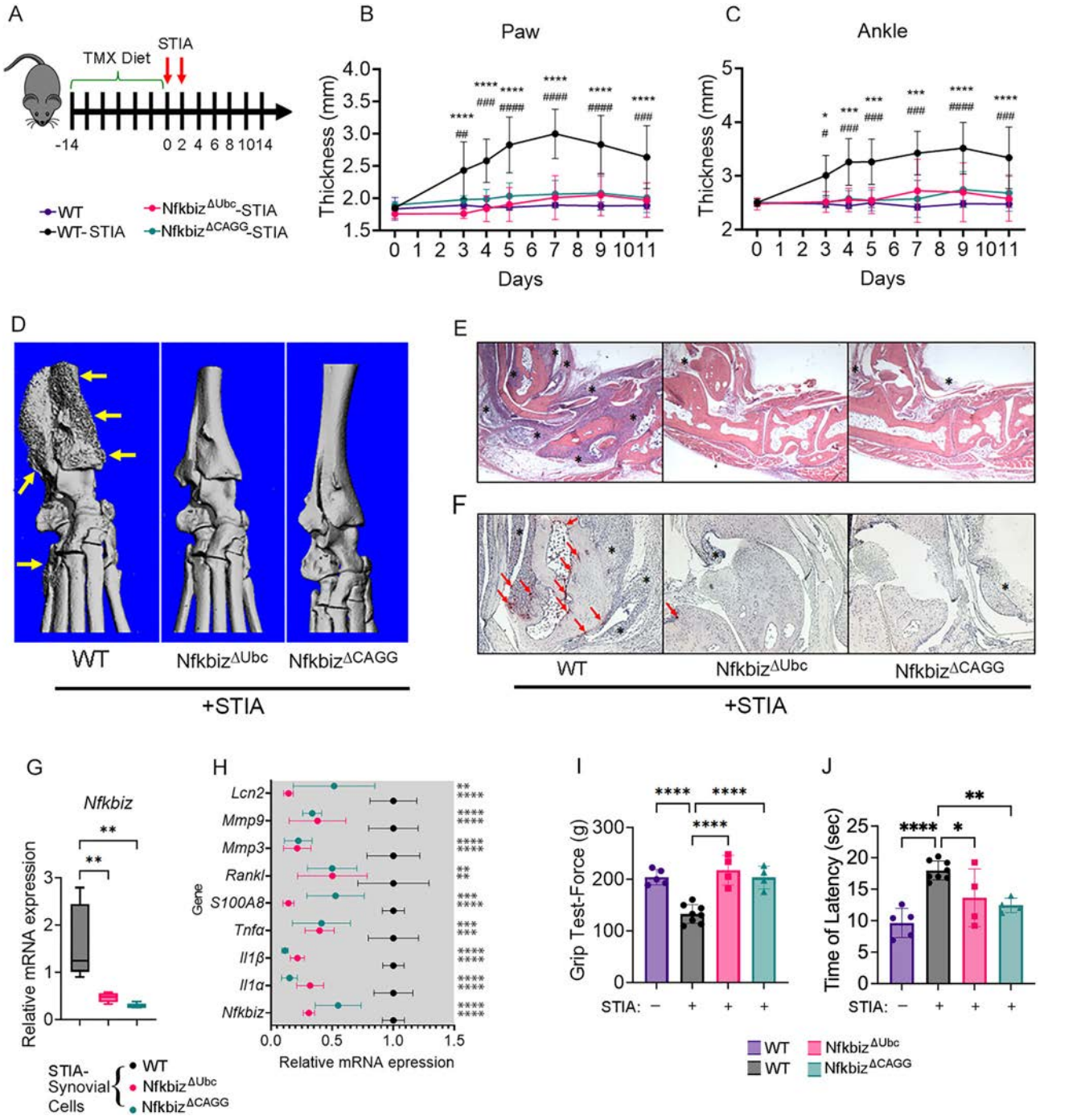


**Figure 3.** Global ablation of *Nfkbiz* attenuates experimental STIA. (A) Eight-week-old *Nfkbiz*$^{\Delta CAGG}$, *Nfkbiz*$^{\Delta Ubc}$, and littermate (*Nfkbiz-fl*) mice after two weeks of Tamoxifen administration were subjected to STIA (n = 7–11 per group). *Nfkbiz* floxed mice were used as non-STIA control. Rheumatoid arthritis progression was monitored by (B) paw and (C) ankle thickness measurement. (D) Representative microcomputed tomography (n = 8) showing no osteolysis in global *Nfkbiz* null mice. Arrows indicate bone erosion. (E) Representative hematoxylin and eosin (E) and tartare resistant acid phosphatase (F) staining in WT, *Nfkbiz*$^{\Delta Ubc}$, and *Nfkbiz*$^{\Delta CAGG}$ arthritic paw–ankle joint (n = 4). Asterisks and arrows in (E) and (F) point to inflammation and osteolysis, respectively. (G and H) Quantitative polymerase chain reaction analysis from total synovial cells (n = 3–9 for G and n = 6 biologic replicates for H) showing expression of different genes. (I and J) WT (control), WT+STIA, *Nfkbiz*$^{\Delta Ubc}$+STIA, and *Nfkbiz*$^{\Delta CAGG}$+STIA animals subjected to grip strength and hot plate analgesia tests on day 7 after STIA. Data are represented as means ± SDs. $^{*}P < 0.05$, $^{**}P < 0.01$, $^{***}P < 0.001$, $^{****}P < 0.0001$, $\#P < 0.05$, $\#\#P < 0.01$, $\#\#\#P < 0.001$, and $\#\#\#\#P < 0.0001$. Asterisks and hashtags in (B) and (C) represent *P* values of WT-STIA compared with *Nfkbiz*$^{\Delta CAGG}$ and *Nfkbiz*$^{\Delta Ubc}$, respectively. Student's *t*-test was used for two groups, and two-way analysis of variance was done for more than two variables. STIA, serum transfer-induced arthritis; TMX, tamoxifen; WT, wild type.

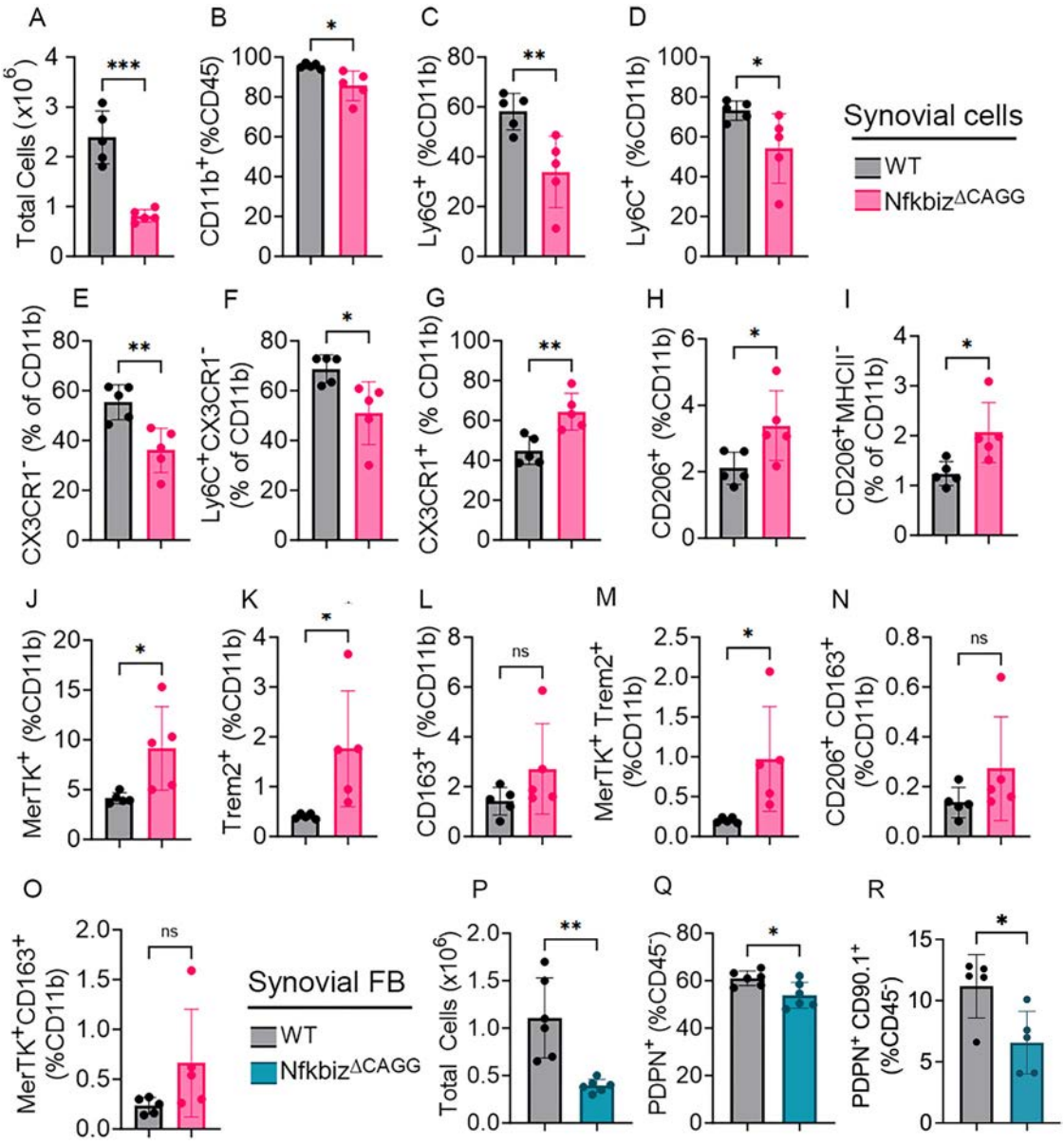


**Figure 4.** Deletion of IκBζ protects phenotypes of synovial cells against inflammatory arthritis. Fluorescence-activated cell sorting analysis from WT–serum transfer-induced arthritis and *Nfkbiz*$^{\Delta CAGG}$–serum transfer-induced arthritis arthritic paw and ankle joint synovium cells (n = 5–6), biologic replicates, per group) showing (A) total cells, (B) CD11b$^+$ cell (% CD45$^+$cells), (C) Ly6G$^+$ cells (% CD11b$^+$ cells), (D) Ly6C$^+$ cells (% CD11b$^+$ cells), (E) CX3CR1$^+$ cells (% CD11b$^+$ cells), (F) CX3CR1$^-$ cells (% CD11b$^+$ cells), (G) Ly6C$^+$ CX3CR1$^-$ (% CD11b$^+$ cells), (H) CD206$^+$ (% CD11b$^+$ cells), (I) CD206$^+$MHCII$^-$ (% CD11b$^+$ cells), (J) MerTK$^+$ cells (% CD11b$^+$ cells), (K) Trem2$^+$ cells (% CD11b$^+$ cells), (L) CD163$^+$ cells (% CD11b$^+$ cells), (M) MerTK$^+$Trem2$^+$ (% CD11b$^+$ cells), (N) CD206$^+$CD163$^+$ (% CD11b$^+$ cells), and (O) MerTK$^+$CD163$^+$ cells (% CD11b$^+$ cells). A separate experiment showing (P) total synovial cell counts, (Q) PDPN$^+$ (% of CD45$^-$ cells), and (R) PDPN$^+$CD90.1$^+$ cells (% of CD45$^-$ cells). Data are represented as means ± SDs. *$P < 0.05$, **$P < 0.01$, and ***$P < 0.001$. Student's *t*-test was used for two groups, and two-way analysis of variance was done for more than two variables. quantitative polymerase chain reaction data are representative of three or more independent experiments. FB, Fibroblast; PDPN$^+$, podoplanin-positive; WT, wild type.

monocytes (Figure 4D), CX3CR1$^-$ (Figure 4E), and Ly6C$^+$CX3CR1$^-$ proinflammatory macrophage cells (Figure 4F). Concomitantly frequency of anti-inflammatory and repair associated CX3CR1$^+$ cells[37] (Figure 4G), M2-like CD206$^+$ (Figure 4H and I), and tissue resident synovial macrophage cells expressing MerTK$^+$, Trem2$^+$, CD163$^+$ were higher or trending higher in STIA *Nfkbiz*$^{\Delta CAGG}$ mice compared to STIA WT mice synovium (Figure 4J–O). Similarly, analysis of the CD45$^-$ population (nonmyeloid or stromal cells) revealed a significant decrease in podoplanin-positive (PDPN$^+$) synovial fibroblasts in STIA-*Nfkbiz*$^{\Delta CAGG}$ mice joint synovium (Figure 4Q). Further gating showed a decrease in number of PDPN$^+$CD90.1$^+$ cells (Figure 4R), which are typically associated with severe and destructive RA. Given the significantly low number of total synovial cells (Figure 4P), the absolute number of these

inflammatory synovial fibroblasts was significantly low in arthritic synovium of *Nfkbiz*$^{\Delta CAGG}$ compared to WT mice indicating amelioration of arthritis.

Considering the key role of IL-1β in RA pathology, the relative frequency of IL-1β$^+$ cells were also compared. The data show a significant decrease in the IL-1β$^+$ cells in total synovium and IκBζ$^+$ total synovial cells (Fig S3A and B), total hematopoietic cells, IκBζ$^+$ hematopoietic cells (Fig S3C and D), total T cells (CD3$^+$), IκBζ$^+$ T cells (Fig S3E and F), total myeloid cells (CD11b$^+$), IκBζ$^+$ myeloid cells (Fig S3G and H), macrophages (F480$^+$), IκBζ$^+$ macrophages (Fig S3I and J), neutrophils (Ly6G$^+$) and IκBζ$^+$ neutrophils (Fig S3K and L). This flow analysis shows that global *Nfkbiz* deletion significantly decreases the inflammatory cells in arthritic joints. In summary, the data from global *Nfkbiz*-deficient STIA mice demonstrates that IκBζ plays a crucial role in various cells involved in RA and elicits an inflammatory phenotype, whereas its deletion restores an anti-inflammatory protective phenotype by immune and fibroblast cells in the synovial joint.

**Divergent effect of IκBζ in different cellular compartments in RA.** Because RA pathogenesis involves both hematopoietic and nonhematopoietic cells, we further explored whether expression of *Nfkbiz* in any specific cellular compartments drives the STIA pathogenesis and whether deleting *Nfkbiz* from specific cellular compartments is sufficient to alleviate STIA in mice. To this end, we generated chimeric mice harboring *Nfkbiz*-null hematopoietic and WT nonhematopoietic cells and subjected them to STIA along with WT control mice. The chimerism was confirmed using flow analysis in blood before the start of STIA induction (Fig S4A) and bone marrow at the end of the STIA experiment (Fig S4B). Compared to WT mice, we did not observe any significant difference in paw and ankle swelling (Fig S4C and D) in the chimeric mice. Furthermore, unlike global deletion of *Nfkbiz*, we observed no significant differences in total synovial cells, CD45$^+$, CD11b$^+$ myeloid cells, Ly6G$^+$ neutrophils, Ly6C$^+$ monocytes, CD45$^-$ nonhematopoietic cells, PDPN$^+$, and PDPNN$^+$CD90.1$^+$ fibroblast cells in chimeric mice when compared to WT mice (Fig S4E–K).

These results suggest that the reduction of *Nfkbiz* expression in hematopoietic cells is not sufficient to ameliorate STIA in mice. Despite successful chimerism, it remains possible that remnant WT hematopoietic cells that persisted in the chimeric mice may have contributed to the pathology. To further scrutinize the role of IκBζ in hematopoietic cells in RA, *Nfkbiz* deletion was conducted in myeloid and lymphoid cells, and the effect on STIA was examined. To this end, using WT and *Nfkbiz*$^{\Delta Lck}$ mice (lacking *Nfkbiz* in T cells), we show that the deletion of *Nfkbiz* in T cells failed to alleviate STIA (Fig S5A and B). Next, to determine the contribution of IκBζ in myeloid cells, WT and *Nfkbiz*$^{\Delta LysM}$ mice were subjected to STIA (Fig S6). Paw and ankle thickness measurement (Fig S6A and B) and μCT analysis (Fig S6C) showed that *Nfkbiz*$^{\Delta LysM}$ mice were not protected from STIA. Even though we did not observe any significant protection in the *Nfkbiz*$^{\Delta LysM}$ mice, CD11b$^+$ isolated from arthritic paw from *Nfkbiz*$^{\Delta LysM}$ mice showed significant decrease in *Nfkbiz* expression compared to CD11b$^+$ cells from WT mice (Fig S6D). As expected CD11b$^-$ cells did not show any decrease in *Nfkbiz* expression in KO mice compared to WT (Fig S6D). However, surprisingly the total CD11b$^+$ cells failed to show any decreases in expression of *Il1β*, *Il1α*, *Lcn2*, *Tnfα*, and *S100a8* gene expression (Fig S6E–I), suggesting that Lysozyme-Cre does not target all myeloid cells involved in STIA pathogenesis. This was further validated by measuring the expression of different inflammatory genes in total synovial cells isolated from WT and *Nfkbiz*$^{\Delta LysM}$ mice.

Unlike global *Nfkbiz* deletion (Figure 3H), we did not observe any significant decreases in the expression of *Lcn2*, *Mmp9*, *Mmp3*, *Rankl*, *S100a8* (*Mrp8*), *Tnfα*, *Il1α*, and *Il1β* (Fig S6J). Similarly, unlike the global deletion of *Nfkbiz* (Fig S3), flow analysis in total synovial cells isolated form arthritic paw from WT and *Nfkbiz*$^{\Delta LysM}$ mice did not show significant difference in the IL1β$^+$ cells and IκBζ$^+$ total synovial cells (Fig S6K), total hematopoietic cells, IκBζ$^+$ hematopoietic cells (Fig S6L), total T cells (CD3$^+$) and IκBζ$^+$ T cells (Fig S6M), total myeloid cells (CD11b$^+$) and IκBζ$^+$ myeloid cells (Fig S6M), macrophages (F480$^+$) and IκBζ$^+$ macrophages (Fig S6O), and neutrophils (Ly6G$^+$) (Fig S6P, left panel). However, there was a significant increase in the IL1β$^+$IκBζ$^+$ neutrophils (Fig S6P, right panel), suggesting that not all neutrophils are targeted by Lysozyme-cre, and these cells may be sufficient to propagate the inflammation in other synovial cells.

Based on these observations, we further explored the contribution of T cells and neutrophils in STIA pathogenesis. In this regard, we induced STIA in T cells (Figure 5A) and neutrophil-depleted (Figure 5B) mice. The data show that compared to control-STIA group, whereas T cell depletion failed to alter or modify STIA, neutrophil depletion significantly alleviated the STIA-induced paw and ankle swelling compared to control-STIA group (Fig 5C and D). FACS analysis further showed that neutrophil-depleted mice, but not T cell–depleted mice, had decreased number of total arthritic synovial cells (Figure 5E), CD45$^+$ cells (Figure 5F), CD11b$^+$ cells (Figure 5G), and Ly6G$^+$ cells (Figure 5H) when compared to control-STIA groups. Flow analysis also confirmed negligible presence of T cells in the arthritic synovium (Figure 5I) in all the groups. Failure of T cells depletion and *Nfkbiz-null* T cells (Fig S5) to modify STIA, along with negligible presence of T cells in the arthritic knee and paw joints of STIA mice, suggest that T cells are not major contributors of STIA pathogenesis. However, the significant inhibition of STIA-induced increase in paw and ankle swelling in neutrophil-depleted mouse and failure of Lysozyme-M Cre to deplete IκBζ in neutrophils (Fig S6P) suggest that IκBζ-sufficient neutrophils are potential drivers of STIA. In summary, the data show that even though IκBζ regulates inflammation in various hematopoietic and nonhematopoietic cells, IκBζ$^+$ neutrophils are the critical culprit cells in STIA.

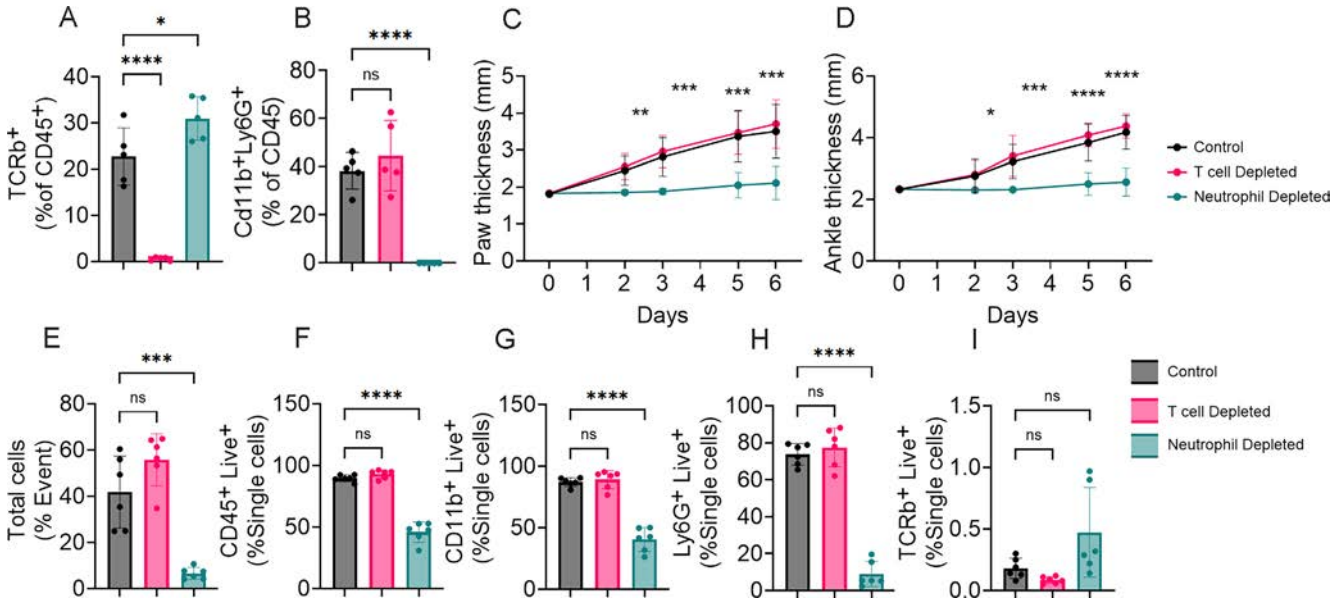


**Figure 5.** Neutrophil depletion significantly attenuates experimental mouse RA (serum transfer-induced arthritis). Eight-week-old male wildtype C57BL/6J mice (control), T cell–depleted (administration of 100 μg per mouse TCRβ neutralizing antibody) mice, and neutrophil-depleted mice (depleted administration of 400 μg Ly6G neutralizing antibody) were subjected to serum transfer-induced arthritis (n = 6–7 per group). Depletion efficiency was analyzed by flow analysis (n = 5 per group) of blood cells on day 1 (A) TCRβ$^+$ cells (percentage of CD45$^+$ cells) and (B) Cd11b$^+$Ly6G$^+$ cells (percentage of CD45$^+$ cells). RA progression was monitored by (C) paw and (D) ankle thickness measurement. Asterisks represent *P* values of serum transfer-induced arthritis–control compared serum transfer-induced arthritis–neutrophil–depleted group. There were no significant differences between the serum transfer-induced arthritis–control group and the serum transfer-induced arthritis–T cell–depleted group. Data are represented as means ± SDs. $^*P < 0.05$, $^{**}P < 0.01$, $^{***}P < 0.001$, and $^{****}P < 0.0001$. One-way analysis of variance was done for three groups. RA, rheumatoid arthritis.

**Immune responsive gene-1–itaconate axis and the mediated inhibition of IκBζ and alleviation of mouse RA.** It has been reported that inflammatory agents, primarily LPS, robustly induce metabolic regulation of myeloid cells, and immune responsive gene-1 (Irg1) has emerged as a potent anti-inflammatory mediator giving rise to intracellular accumulation of itaconate.[38] Further, Irg1-null cells exhibited higher and prolonged secretion[38,39] of IL-1b. First, qPCR analysis form CD11b$^+$ cells form arthritis paws showed increased expression of *Acod1* (Irg1) (Figure 6A). More interestingly, Western blot analysis (Figure 6B) showed that LPS treatment of macrophages for 3 and 6 hours resulted in increased expression of IκBζ and IL-1β, which was abrogated after 24 hours treatment with LPS coinciding with robust expression of Irg1 (Figure 6B). Because neutrophils are the major population among the arthritic synovial cells and key driver of STIA, we also confirmed the expression of Irg1 in LPS-treated neutrophils. Similar to macrophages, LPS-treated neutrophils showed increased expression of Irg1 along with decreased expression of IL-1β (Fig S7). Increased expression of Irg1 typically leads to the synthesis and accumulation of intracellular itaconate.[38,39] Taken together, these findings suggest that Irg1 signaling inhibits the IκBζ-mediated IL-1β inflammatory cascade and led us to consider the Irg1 anti-inflammatory metabolite itaconate as a potential IκBζ inhibitor candidate.

*In vitro* analysis using myeloid cells showed that the cell-permeable DI metabolite specifically inhibited inflammatory signals downstream to IκBζ activity without affecting physiologic NF-κB activity. *In vitro* qPCR (Figure 6C and D) and Western blot analysis (Figure 6G and Fig S8) showed that DI did not inhibit expression of *Nfkbiz*, *Nlrp3*, and phosphorylation of p65, which are induced in response to NF-κB activation, but only inhibited genes downstream to IκBζ, such as *Il1β* and *Il6* (Figure 6E and F). Next, we sought to identify small molecule drugs that could phenocopy DI and genetic IκBζ inhibition. We used two different in silico methods, one leveraging cell fitness as the screening phenotype[40] and the other leveraging diverse other -omic phenotypes (including protein–protein interactions, text mining, and gene expression) that were human curated in terms of their weighting.[41] HQ was identified as the top candidate IκBζ inhibitor using the cell fitness method, whereas arglabin was identified as the top candidate using the human curated method.

In *in vivo* testing, HQ mimicked DI effect as a potential inhibitor of IκBζ-mediated inflammation (Figure 6C–G), whereas arglabin was not considered further because it failed to validate *in vitro* (Fig S9). Mechanistically, DI and HQ appear to inhibit IκBζ function rather than *Nfkbiz* transcription and translation. Next, we used the STIA model to investigate the therapeutic efficacy of DI and HQ (Figure 6H). Paw and ankle thickness measurements (Figure 6I and J), clearly demonstrated that similar to genetic

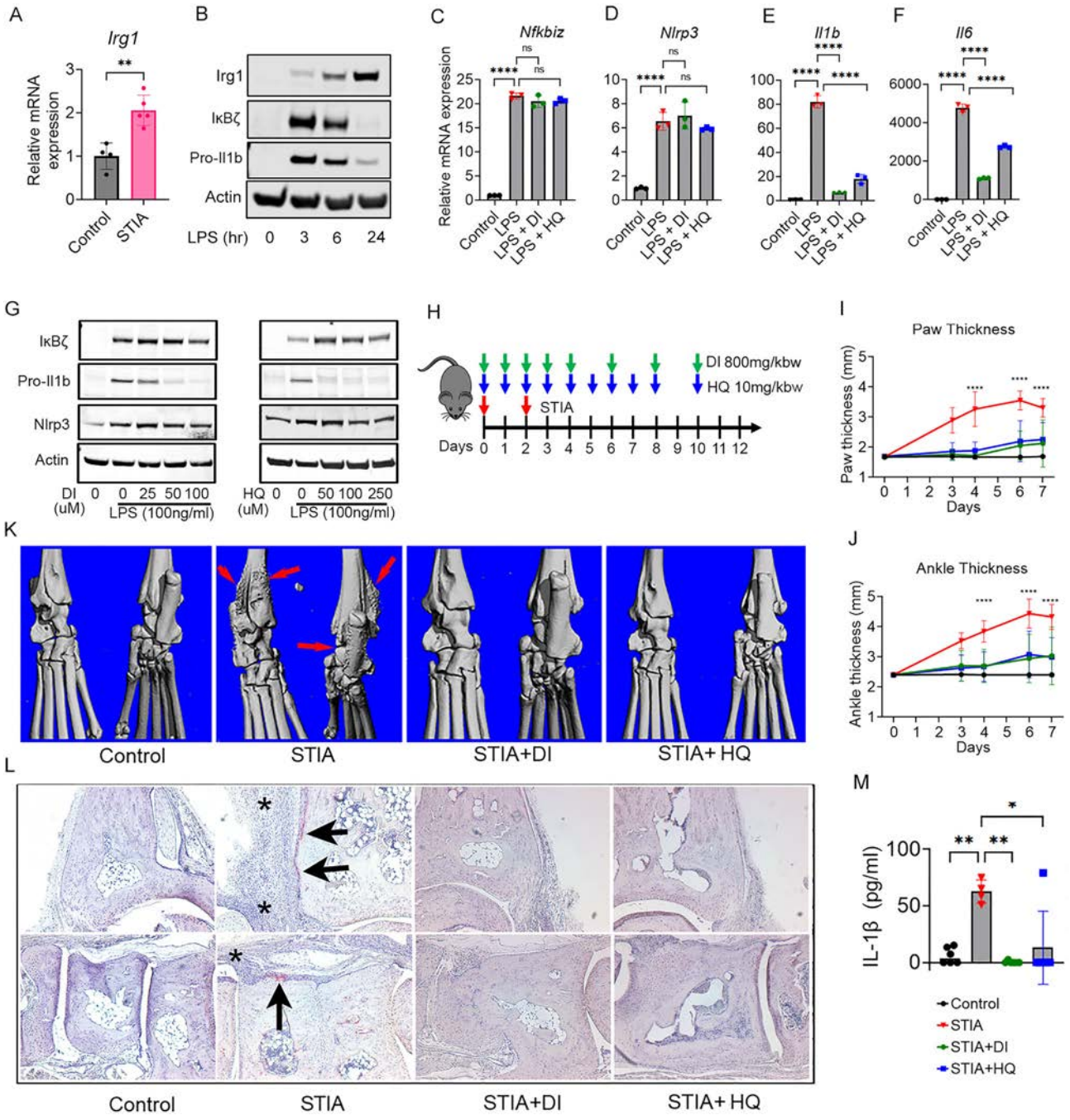


**Figure 6.** Pharmacologic inhibition of IκBζ attenuates experimental mouse rheumatoid arthritis (STIA). (A) Quantitative polymerase chain reaction for *Irg1* in synovium CD11b$^+$ cells from Control and STIA arthritic paw–ankle joint. (B) Western blot for Irg1, IκBζ, and IL-1β from wild type bone marrow–derived macrophages treated with LPS, as shown. Bone marrow–derived macrophages were treated with LPS (100 ng/mL) with or without DI or HQ for three hours followed by qPCR for (C) *Nfkbiz*, (D) *Nlrp3*, (E) *Il1β*, and (F) *Il6*. (G) Western blot, showing expression of IκBζ, pro-IL1β, and Nlrp3. (H) Wild type mice subjected to STIA were treated with DI or HQ, as indicated (n = 5 per group). (I) Paw and (J) ankle thickness measurement (n = 10, each paw from the 5 mice per group was used for analysis), (K) Microcomputed tomography images; frontal and dorsal views (arrows point to bone erosion). (L) tartare resistant acid phosphatase staining (arrows point to osteoclasts/bone resorption) in arthritic joint (upper panel is ankle joint, lower panel is talonavicular-carpal joints, ×10 magnification). (M) serum levels of IL-1β. Data are represented as means ± SDs. $^*P < 0.05$, $^{**}P < 0.01$, $^{***}P < 0.001$, and $^{****}P < 0.0001$ (Student's *t*-test was used for two groups, and two-way analysis of variance was done for more than two variables). Quantitative polymerase chain reaction and Western blot are representative of three or more independent experiments. DI, dimethyl itaconate; HQ, 8-hydroxyquinoline; IL-1β, Interleukin-1β; Irg1, immune responsive gene-1; LPS, lipopolysaccharide; qPCR, quantitative polymerase chain reaction; STIA, serum transfer-induced arthritis.

deletion of *Nfkbiz*, pharmacologic inhibition of IκBζ using DI and HQ attenuated STIA progression in mice. Examples of μCT (Figure 6K) and histologic analysis (Figure 6L) are shown. Plummeted serum levels of IL-1β further validated that DI and HQ inhibit IκBζ-induced inflammatory gene and protein expression (Figure 6M). In summary, we identified DI and HQ as potential pharmacologic inhibitors of IκBζ function, which can be further considered as candidate for developing therapeutic strategies to treat RA.

## DISCUSSION

Major strides have been made using NSAIDs and biologics targeting TNFα, IL-6, IL-17, IL-1β, and several other signaling molecules to treat RA.[2,15,42] However, despite their disease-modifying effect, no interventions have made remarkable and lasting effect, and some approaches displayed severe adverse effects limiting their utility. Among the primary challenges are the multicellular and multifactorial pathogenicity of various subtypes of RA, rendering targeting individual cells or factors ineffective. Although the inflammatory response is orchestrated by the transcription factor NF-κB, targeting NF-κB genetically or with inhibitors is also futile because it hinders its physiologic function, which is essential for cell survival.[43]

In this study, we aimed to identify an inflammatory signature amenable for effective therapeutic intervention in RA that transcend limitations of approaches targeting individual inflammatory cytokines or factors in RA. Our study identified IκBζ, an NF-κB downstream transcription factor, as an inflammation mediator and amplifier, which when disabled genetically or pharmacologically resulted with significant attenuation of murine RA. Equally important, inducible global ablation of IκBζ in mature mice appears to have negligible effect on normal physiology. In fact, we show that physiologic levels of RANKL, a prominent NF-κB activator, do not induce expression of IκBζ. Gleaning from our previously published work[22,23] and from work by others in the field,[24,44] we suggest that IκBζ is a key component of the inflammatory vicious cycle downstream of NF-κB directly contributing to and propagating cytokine storm response by several cell types.

At the cellular level, our findings demonstrate that genetic deletion of *Nfkbiz* attenuates the expression of a group of prominent inflammatory, senescence, catabolic, and osteoclastogenic factors in synovial cell extracts. Consistently, frequency of inflammatory macrophages and neutrophils plumets whereas that of anti-inflammatory macrophages ($CD206^+$ and $CD163^+$) and resident synovial macrophages ($CX3CR1^+$, $MerTK^+$, and $Trem2^+$) rises in mice lacking IκBζ subjected to experimental arthritis. We also show that deletion of IκBζ diminishes infiltrating neutrophils ($Ly6G^+$) and restricts the inflammatory phenotype of synovial fibroblasts. The significance of these observations is buttressed by recent findings highlighting the crucial role of joint protective resident macrophages[45–47] and synovial lining fibroblasts,[48] and assign a novel role of IκBζ in destabilizing and derailing the phenotype of these cells into an inflammatory one, whereas its deletion fortifies the anti-inflammatory phenotype of these cells.

However, the contribution of IκBζ to the inflammatory phenotype of different cell types remains poorly understood. In STIA, we demonstrate that depletion of neutrophils (vastly $I\kappa B\zeta^+$) significantly abrogates STIA joint swelling. Surprisingly, depletion of IκBζ in macrophages (using lysozyme-cre mediated deletion) or T cells (using Lck-Cre mediated deletion) failed to significantly alter disease pathology. Despite these observations, we show that in immune cells (macrophages and neutrophils) IκBζ is absolutely required for proper expression of IL-1β, an inflammatory cytokine that has been abundantly shown to function as a major culprit of RA and osteoarthritis (OA). This dichotomy requires further investigation in future studies. IL-1β, which is also secreted by other synovial cells including activated "destructive" fibroblasts,[49] activates the NF-κB–IκBζ axis in articular chondrocytes leading, as we have published,[22,23] to their demise through pyroptosis and further secretion of inflammatory mediators that fuel the vicious cycle. Interestingly, conditional deletion of IκBζ in chondrocytes protected against posttraumatic OA in mice despite presence of intact IκBζ-sufficient macrophages without negatively affecting the integrity of the physiologic joint.[22,23,50] Collectively, these observations imply that IκBζ-mediated inflammatory response in neutrophils and chondrocytes elicits a joint inflammatory response impacting other cellular constituents in the joint.

In other disease models, a central role of IκBζ in the inflammatory response has been also shown in inflammatory Th17 cells, wherein it regulates expression of IL-17, another potent proinflammatory cytokine dominating psoriatic arthritis.[24,44,51] In fact, mice harboring deletion of IκBζ in Th17 were resistant to experimental autoimmune encephalomyelitis.[24] These findings suggest that contribution of IκBζ to T cell pathology differs in different inflammatory diseases perhaps owing to their reliance on different inflammatory cytokines and regulatory machinery. Regardless, global *Nfkbiz* deletion or systemic pharmacologic inhibition of IκBζ robustly attenuates RA more effectively compared with limited targeting of certain cellular compartments.

The mechanisms governing expression and stability of IκBζ remain enigmatic. We have shown previously in chondrocytes that inflammation induces metabolic changes, giving rise to reactive oxygen species that stabilize IκBζ protein expression and its inflammatory function. Accordingly, limiting the glycolytic response genetically by deleting lactate dehydrogenase and pharmacologically by quenching reactive oxygen species with N-acetyl-L-cysteine, were sufficient to plummet IκBζ expression, inhibit expression of IκBζ-induced inflammatory factors, and alleviate posttraumatic OA. However, recent advances suggest that other modes of IκBζ regulation may exist.[52] In this regard, we report that levels of Irg1, also known as cis-aconitate decarboxylase, are elevated in STIA cells and following LPS stimulation coinciding with reduced expression of IκBζ and IL-1β. More

importantly, previous studies demonstrated that levels of IL-1β are elevated in Irg1-null macrophages,[38,39] suggesting that metabolites downstream of Irg1 are likely involved in regulating the IκBζ–IL-1β inflammatory axis. Itaconate is the predominant immune metabolite of Irg1 with widely described anti-inflammatory properties.[52–55] Our finding that the cell-permeable derivative DI inhibits IκBζ-induced IL-1β expression and protects against joint inflammation and destruction, positions DI as a potential therapeutic target for RA and sheds light on a potential novel IκBζ regulatory mechanism, yet to be detailed. Using in silico analysis, we also identified the antibacterial compound HQ that potently mimics DI function: inhibiting IκBζ and inflammatory arthritis. HQ is an organic compound derived from quinoline. In the past, HQ and its derivative has also been studied as an anti-cancer drug, antineurodegenerative, antioxidant, antimicrobial, and anti-inflammatory drug with poorly defined molecular mechanism.[56–58] This is a novel application of this drug, the underlying mechanism of which in RA remains to be elucidated. In summary, this work identifies IκBζ as an attractive RA therapeutic target sparing essential NF-κB physiologic machinery. This study also highlights Irg1-itaconate immune-modulation of the IκBζ induced inflammation and demonstrates remarkable mitigation of murine RA by DI and HQ.

Unlike global deletion, deletion of IκBζ in myeloid cells using lysozyme-cre, deletion in T cells, or in hematopoietic cells (WT nonhematopoietic cells) did not alleviate STIA in mice. There are few possible reasons to explain this outcome. First, deletion of *Nfkbiz* using cell specific Cre may not be optimal to completely delete *Nfkbiz* in these cells. Specifically, *Nfkbiz* gene deletion using LysM-cre may not be optimal, allowing for the remaining IκBζ sufficient myeloid cells to mount an inflammatory response. LysM-cre targets monocytes, macrophages, and a subset of granulocytes of neutrophils, suggesting insufficient deletion of *Nfkbiz* in neutrophils. Hence inflammatory signals during initial neutrophil activation in STIA are sufficient to propagate the inflammation in other cells involved with normal IκBζ expression. Second, a multitude of other nonmyeloid cells including activated synovial fibroblasts,[44] activated articular chondrocytes,[22] and Th17 lymphocytes[24] express IκBζ and are prone to mount an inflammatory response. Similarly, irradiation followed by BMT to generate chimera does not completely remove the host WT hematopoietic cells having normal expression of *Nfkbiz* along with WT nonhematopoietic cells. These WT cells can initiate and amplify the inflammatory STIA in mouse. Hence, our approach to globally delete *Nfkbiz* demonstrated superior attenuation of RA.

Our study does not elucidate the precise mechanism by which itaconate inhibits IκBζ function. In this regard, recent advances suggest that itaconate promotes protein expression of activating transcription factor-3, which has been suggested as a negative regulator of IκBζ.[59] However, it remains unknown if itaconate inhibits IκBζ directly as it does with other proteins, such as binding to and modifying stimulator of interferon genes[60] or gasdermin D,[39] a key component of the inflammasome-pyroptosis pathway. Therefore, we cannot claim that DI and HQ are very selective inhibitors of IκBζ function. Even though under our experimental conditions these agents are inhibiting IκBζ function without affecting NF-κB activation, future studies are warranted to designate DI and HQ as specific pharmacologic inhibitors of IκBζ.

## AUTHOR CONTRIBUTIONS

All authors contributed to at least one of the following manuscript preparation roles: conceptualization AND/OR methodology, software, investigation, formal analysis, data curation, visualization, and validation AND drafting or reviewing/editing the final draft. As corresponding author, Dr Abu-Amer confirms that all authors have provided the final approval of the version to be published, and takes responsibility for the affirmations regarding article submission (eg, not under consideration by another journal), the integrity of the data presented, and the statements regarding compliance with institutional review board/Helsinki Declaration requirements.

## REFERENCES


1. Guo Q, Wang Y, Xu D, et al. Rheumatoid arthritis: pathological mechanisms and modern pharmacologic therapies. Bone Res 2018; 6(1):15.
2. Shams S, Martinez JM, Dawson JRD, et al. The therapeutic landscape of rheumatoid arthritis: current state and future directions. Front Pharmacol 2021;12:680043.
3. Helmick CG, Felson DT, Lawrence RC, et al. Estimates of the prevalence of arthritis and other rheumatic conditions in the United States. Part I. Arthritis Rheum 2008;58(1):15–25.
4. Silman AJ, Pearson JE. Epidemiology and genetics of rheumatoid arthritis. Arthritis Res 2002;4(Suppl 3)(suppl 3):S265–S272.
5. Aletaha D, Smolen JS. Diagnosis and management of rheumatoid arthritis: a review. JAMA 2018;320(13):1360–1372.
6. Smolen JS, Aletaha D, Barton A, et al. Rheumatoid arthritis. Nat Rev Dis Primers 2018;4(1):18001.
7. Chopra A, Abdel-Nasser A. Epidemiology of rheumatic musculoskeletal disorders in the developing world. Best Pract Res Clin Rheumatol 2008;22(4):583–604.
8. Cross M, Smith E, Hoy D, et al. The global burden of rheumatoid arthritis: estimates from the global burden of disease 2010 study. Ann Rheum Dis 2014;73(7):1316–1322.
9. Aletaha D, Funovits J, Smolen JS. Physical disability in rheumatoid arthritis is associated with cartilage damage rather than bone destruction. Ann Rheum Dis 2011;70(5):733–739.
10. Mohammed RHA, Goyal A, Bansal P. *Hand and Wrist Rheumatoid Arthritis*. In: StatPearls. Treasure Island (FL): StatPearls Publishing; 2024. https://www.ncbi.nlm.nih.gov/books/NBK560890/
11. Hastings DE, Evans JA. Rheumatoid wrist deformities and their relation to ulnar drift. J Bone Joint Surg Am 1975;57(7):930–934.
12. Marrelli K, Cheng AJ, Brophy JD, et al. Perceived versus performance fatigability in patients with rheumatoid arthritis. Front Physiol 2018;9: 1395.
13. Redlich K, Smolen JS. Inflammatory bone loss: pathogenesis and therapeutic intervention. Nat Rev Drug Discov 2012;11(3):234–250.
14. Yap HY, Tee SZ, Wong MM, et al. Pathogenic role of immune cells in rheumatoid arthritis: implications in clinical treatment and biomarker development. Cells 2018;7(10):7.

15. Huang J, Fu X, Chen X, et al. Promising therapeutic targets for treatment of rheumatoid arthritis. Front Immunol 2021;12:686155.
16. McInnes IB, Liew FY. Cytokine networks–towards new therapies for rheumatoid arthritis. Nat Clin Pract Rheumatol 2005;1(1):31–39.
17. Gasparini C, Feldmann M. NF-kappaB as a target for modulating inflammatory responses. Curr Pharm Des 2012;18(35):5735–5745.
18. Liu T, Zhang L, Joo D, et al. NF-kappaB signaling in inflammation. Signal Transduct Target Ther 2017;2(1):17023.
19. Tak PP. Is early rheumatoid arthritis the same disease process as late rheumatoid arthritis? Best Pract Res Clin Rheumatol 2001;15(1):17–26.
20. Tak PP, Firestein GS. NF-kappaB: a key role in inflammatory diseases. J Clin Invest 2001;107(1):7–11.
21. Tak PP, Gerlag DM, Aupperle KR, et al. Inhibitor of nuclear factor kappaB kinase beta is a key regulator of synovial inflammation. Arthritis Rheum 2001;44(8):1897–1907.
22. Arra M, Swarnkar G, Alippe Y, et al. IκB-ζ signaling promotes chondrocyte inflammatory phenotype, senescence, and erosive joint pathology. Bone Res 2022;10(1):12.
23. Arra M, Swarnkar G, Ke K, et al. LDHA-mediated ROS generation in chondrocytes is a potential therapeutic target for osteoarthritis. Nat Commun 2020;11(1):3427.
24. Okamoto K, Iwai Y, Oh-Hora M, et al. IkappaBzeta regulates T(H)17 development by cooperating with ROR nuclear receptors. Nature 2010;464(7293):1381–1385.
25. Slowikowski K, Nguyen HN, Noss EH, et al. CUX1 and IkappaBzeta (NFKBIZ) mediate the synergistic inflammatory response to TNF and IL-17A in stromal fibroblasts. Proc Natl Acad Sci USA 2020;117(10):5532–5541.
26. Bakker AD, Klein-Nulend, J. Osteoblast isolation from murine calvaria and long bones. Methods Mol Biol 2012;816:19–29.
27. Corsello SM, Nagari RT, Spangler RD, et al. Discovering the anticancer potential of non-oncology drugs by systematic viability profiling. Nat Cancer 2020;1(2):235–248.
28. Abu-Amer Y. NF-kappaB signaling and bone resorption. Osteoporos Int 2013;24(9):2377–2386.
29. Abu-Amer Y, Darwech I, Otero J. Role of the NF-kappaB axis in immune modulation of osteoclasts and bone loss. Autoimmunity 2008;41(3):204–211.
30. Clohisy JC, Roy BC, Biondo C, et al. Direct inhibition of NF-kappa B blocks bone erosion associated with inflammatory arthritis. J Immunol 2003;171(10):5547–5553.
31. Ke K, Chen TH, Arra M, et al. Attenuation of NF-kappaB in intestinal epithelial cells is sufficient to mitigate the bone loss comorbidity of experimental mouse colitis. J Bone Miner Res 2019;34(10):1880–1893.
32. Otero JE, Chen T, Zhang K, et al. Constitutively active canonical NF-kappaB pathway induces severe bone loss in mice. PLoS One 2012;7(6):e38694.
33. Swarnkar G, Shim K, Nasir AM, et al. Myeloid deletion of nemo causes osteopetrosis in mice owing to upregulation of transcriptional repressors. Sci Rep 2016;6(1):29896.
34. Swarnkar G, Zhang K, Mbalaviele G, et al. Constitutive activation of IKK2/NF-κB impairs osteogenesis and skeletal development. PLoS One 2014;9(3):e91421.
35. Shiratori T, Kyumoto-Nakamura Y, Kukita A, et al. IL-1β Induces pathologically activated osteoclasts bearing extremely high levels of resorbing activity: a possible pathological subpopulation of osteoclasts, accompanied by suppressed expression of kindlin-3 and talin-1. J Immunology 2018;200(1):218–228.
36. Gautam P, Maenner S, Cailotto F, et al. Emerging role of IκBζ in inflammation: emphasis on psoriasis. Clin Transl Med 2022;12(10):e1032.
37. Culemann S, Grüneboom A, Nicolas-Avila JA, et al. Locally renewing resident synovial macrophages provide a protective barrier for the joint. Nature 2019;572(7771):670–675.
38. Hooftman A, Angiari S, Hester S, et al. The immunomodulatory metabolite itaconate modifies NLRP3 and inhibits inflammasome activation. Cell Metab 2020;32(3):468–478.e7.
39. Bambouskova M, Potuckova L, Paulenda T, et al. Itaconate confers tolerance to late NLRP3 inflammasome activation. Cell Rep 2021;34(10):108756.
40. Jacobs NC, Park J, Saccone NJ, et al. Cell fitness is an omniphenotype. bioRxiv Preprint posted online April 5, 2023. https://doi.org/10.1101/487157
41. Szklarczyk D, Gable AL, Nastou KC, et al. The STRING database in 2021: customizable protein-protein networks, and functional characterization of user-uploaded gene/measurement sets. Nucleic Acids Res 2021;49(D1):D605–D612.
42. Palominos PE, Lineburger IB, Xavier RM. Emerging protein kinase inhibitors for the treatment of rheumatoid arthritis. Expert Opin Emerg Drugs 2021;26(3):303–321.
43. Pasparakis, M. Regulation of tissue homeostasis by NF-B signalling: implications for inflammatory diseases. Nat Rev Immunol 2009;9(11):778–788.
44. Slowikowski K, Nguyen HN, Noss EH, et al. CUX1 and IκBζ (NFKBIZ) mediate the synergistic inflammatory response to TNF and IL-17A in stromal fibroblasts. Proc Natl Acad Sci USA 2020;117(10):5532–5541.
45. Culemann S, Grüneboom A, Nicolás-Ávila JÁ, et al. Locally renewing resident synovial macrophages provide a protective barrier for the joint. Nature 2019;572(7771):670–675.
46. Alivernini S, MacDonald L, Elmesmari A, et al. Distinct synovial tissue macrophage subsets regulate inflammation and remission in rheumatoid arthritis. Nat Med 2020;26(8):1295–1306.
47. Waterborg CEJ, Beermann S, Broeren MGA, et al. Protective role of the MER tyrosine kinase via efferocytosis in rheumatoid arthritis models. Front Immunol 2018;9:742.
48. Croft AP, Campos J, Jansen K, et al. Distinct fibroblast subsets drive inflammation and damage in arthritis. Nature 2019;570(7760):246–251.
49. Yan M, Komatsu N, Muro R, et al. ETS1 governs pathological tissue-remodeling programs in disease-associated fibroblasts. Nat Immunol 2022;23(9):1330–1341.
50. Choi MC, MaruYama T, Chun CH, et al. Alleviation of murine osteoarthritis by cartilage-specific deletion of IκBζ. Arthritis Rheumatol 2018;70:1440–1449.
51. Mandal A, Kumbhojkar N, Reilly C, et al. Treatment of psoriasis with NFKBIZ siRNA using topical ionic liquid formulations. Sci Adv 2020;6(30):eabb6049.
52. Li ZY, Zheng WB, Kong W, et al. Itaconate: a potent macrophage immunomodulator. Inflammation 2023;46(4):1177–1191.
53. Peace CG, O'Neill LA. The role of itaconate in host defense and inflammation. J Clin Invest 2022;132(2):132.
54. Yu XH, Zhang DW, Zheng XL, et al. Itaconate: an emerging determinant of inflammation in activated macrophages. Immunol Cell Biol 2019;97(2):134–141.
55. Murphy MP, O'Neill LAJ. Krebs cycle reimagined: the emerging roles of succinate and itaconate as signal transducers. Cell 2018;174(4):780–784.
56. Cherdtrakulkiat R, Worachartcheewan A, Tantimavanich S, et al. Discovery of novel halogenated 8-hydroxyquinoline-based anti-MRSA agents: In vitro and QSAR studies. Drug Dev Res 2020;81(1):127–135.

57. Chen C, Yang X, Fang H, et al. Design, synthesis and preliminary bioactivity evaluations of 8-hydroxyquinoline derivatives as matrix metalloproteinase (MMP) inhibitors. Eur J Med Chem 2019;181:111563.
58. Oliveri V, Attanasio F, Puglisi A, et al. Multifunctional 8-hydroxyquinoline-appended cyclodextrins as new inhibitors of metal-induced protein aggregation. Chemistry 2014;20(29):8954–8964.
59. Bambouskova M, Gorvel L, Lampropoulou V, et al. Electrophilic properties of itaconate and derivatives regulate the IκBζ-ATF3 inflammatory axis. Nature 2018;556(7702):501–504.
60. Li W, Li Y, Kang J, et al. 4-octyl itaconate as a metabolite derivative inhibits inflammation via alkylation of STING. Cell Rep 2023;42(3):112145.

**Arthritis & Rheumatology**
Vol. 77, No. 2, February 2025, pp 140–150
DOI 10.1002/art.42982
© 2024 The Author(s). *Arthritis & Rheumatology* published by Wiley Periodicals LLC on behalf of American College of Rheumatology. This is an open access article under the terms of the Creative Commons Attribution-NonCommercial-NoDerivs License, which permits use and distribution in any medium, provided the original work is properly cited, the use is non-commercial and no modifications or adaptations are made.

American College of Rheumatology
Empowering Rheumatology Professionals

# Do Existing Magnetic Resonance Imaging Definitions of Knee Osteoarthritis Identify Knees That Will Develop Clinically Significant Disease Over Up To 11 Years of Follow-Up?

Alison H. Chang,[1] Frank W. Roemer,[2] Ali Guermazi,[3] Orit Almagor,[1] Jungwha (Julia) Lee,[1] Joan S. Chmiel,[1] Lutfiyya N. Muhammad,[1] Jing Song,[1] and Leena Sharma[1]

**Objective.** In individuals without radiographic knee osteoarthritis (OA), we investigated whether magnetic resonance imaging (MRI)–defined knee OA at baseline was associated with incident radiographic and symptomatic disease during up to 11 years of follow-up.

**Methods.** Osteoarthritis Initiative participants without tibiofemoral radiographic knee OA at baseline were assessed for MRI-based tibiofemoral cartilage damage, osteophyte presence, bone marrow lesions, and meniscal damage/extrusion. We defined MRI knee OA using alternative, reported definitions (Def A and Def B). Kellgren–Lawrence (KL) grade, joint space narrowing (JSN), and frequent knee symptoms (Sx) were assessed at baseline, 1-, 2-, 3-, 4-, 6-, 8-, and 10/11-year follow-up visits. Incident tibiofemoral radiographic knee OA (outcome) was defined as (1) KL ≥2, (2) KL ≥2 and JSN, or (3) KL ≥2 and Sx. Adjusted Cox proportional hazards regression models examined associations of baseline MRI-defined knee OA (Def A and Def B) with incident outcomes during up to 11 years of follow-up.

**Results.** Among 1,621 participants (mean ± SD age 58.8 ± 9.0 years, mean ± SD body mass index 27.2 ± 4.5 kg/m$^2$, 59.5% women), 17% had MRI-defined knee OA by Def A and 24% by Def B. Baseline MRI-defined knee OA was associated with incident KL ≥2 (odds ratio 2.94 [95% confidence interval (95% CI) 2.34–3.68] for Def A and 2.44 [95% CI 1.97–3.03] for Def B). However, a substantial proportion of individuals with baseline MRI-defined knee OA did not develop incident KL ≥2 during follow-up (59% for Def A and 64% for Def B). Findings were similar for the other two outcomes.

**Conclusion.** Current MRI definitions of knee OA do not adequately identify knees that will develop radiographic and symptomatic disease.

## INTRODUCTION

Current pharmacologic approaches do not modify disease course in persons with knee osteoarthritis (OA). Guidelines[1–3] advocate weight management and exercise to relieve symptoms and maintain function in individuals with established disease. Knee OA typically develops over many years. Early identification could provide a window of opportunity for timely efforts to prevent disease development and early progression, minimize symptoms, and preserve function.

A recent scoping review[4] revealed that 72% of studies of early-stage knee OA incorporated radiography in defining the condition. However, using radiography to identify early knee OA is limited by its poor sensitivity in detecting early structural changes.[5] In contrast, magnetic resonance imaging (MRI) allows for comprehensive multiplanar visualization of various joint tissues known to be affected by knee OA before the established signs of radiographic OA—osteophyte presence and joint space narrowing—are present.[5,6] MRI classification criteria for preradiographic knee OA can provide a uniform approach to identify

This article was prepared using an Osteoarthritis Initiative (OAI) public-use data set, and its contents do not necessarily reflect the opinions or views of the OAI Study Investigators, the NIH, or the private funding partners of the OAI. The OAI is a public–private partnership between the NIH (contracts N01-AR-2-2258, N01-AR-2-2259, N01-AR-2-2260, N01-AR-2-2261, and N01-AR-2-2262) and private funding partners (Merck Research Laboratories, Novartis Pharmaceuticals, GlaxoSmithKline, and Pfizer, Inc.) and is conducted by the OAI Study Investigators. Private sector funding for the OAI is managed by the Foundation for the NIH. Supported by the National Institute of Arthritis and Musculoskeletal and Skin Diseases, NIH (grant P30-AR-072579).

[1]Alison H. Chang, PT, DPT, MS, Orit Almagor, MA, Jungwha (Julia) Lee, PhD, Joan S. Chmiel, PhD, Lutfiyya N. Muhammad, PhD, Jing Song, MS, Leena Sharma, MD: Northwestern University Feinberg School of Medicine, Chicago, Illinois; [2]Frank W. Roemer, MD: University of Erlangen-Nuremberg, Erlangen, Germany, and Boston University School of Medicine, Boston, Massachusetts; [3]Ali Guermazi, MD, PhD: Boston University School of Medicine, Boston, Massachusetts.

Additional supplementary information cited in this article can be found online in the Supporting Information section (http//acrjournals.onlinelibrary.wiley.com/doi/10.1002/art.42982).

Author disclosures are available at http//onlinelibrary.wiley.com/doi/10.1002/art.42982.

Address correspondence via email to Alison H. Chang, PT, DPT, MS, at hsini@northwestern.edu.

Submitted for publication May 1, 2024; accepted in revised form August 20, 2024.

individuals who are more likely to develop radiographic and symptomatic knee OA and who may be candidates for studies of interventions to delay or prevent disease development or early progression.

To date, two MRI-based definitions of tibiofemoral (TF) OA have been proposed (Figure 1). Hunter and colleagues developed an MRI definition of knee OA [referred as definition (Def) A in our study] through a Delphi process and recommended future testing of the validity of this definition in a cohort with early, preradiographic disease.[7] As shown in Figure 1, this definition requires assessment of cartilage damage, osteophyte, subchondral bone marrow lesion, meniscal damage or extrusion, and bone attrition. Using data from the Multicenter Osteoarthritis Study (MOST), Liew and colleagues evaluated the performance metrics of nine candidate MRI definitions against concurrent radiographic OA and symptomatic OA. They proposed an alternative, simpler definition (referred as Def B in our study)[8] that only requires assessment of cartilage damage and osteophyte presence.

Identifying knees likely to develop clinically significant disease is crucial for initiating early intervention before substantial structural changes occur. The Osteoarthritis Research Society International (OARSI) has launched an initiative to establish classification criteria for early-stage knee OA to identify such individuals.[4,9] Imaging, particularly MRI, is among the seven domains to consider for accurately identifying those with a high probability of early-stage knee OA.[9,10] To our knowledge, the implications of having MRI-defined knee OA and potential association with an increased risk of subsequent, incident radiographic and symptomatic disease have not been examined. In individuals without TF radiographic knee OA, we aimed to 1) determine the prevalence of MRI-defined knee OA using Def A and Def B and 2) for each definition, examine whether the baseline presence of MRI-defined knee OA was associated with subsequent incident TF radiographic and symptomatic disease during up to 11 years of follow-up.

## MATERIALS AND METHODS

**Study sample.** The Osteoarthritis Initiative (OAI) is a multicenter, prospective, longitudinal observational cohort study of men and women aged 45 to 79 years at enrollment, all with or at increased risk of developing symptomatic, radiographic knee OA.[11] OAI participants from Projects 22, 46, 47, and 48 (see Supplementary Material S1) without TF radiographic disease (Kellgren–Lawrence [KL] grade 0 or 1) in both knees and who had complete MRI readings in at least one knee at the baseline visit constituted our analysis sample. Each participant contributed one knee (right knee, or left knee if right knee MRI data were unavailable) for analysis.

OAI eligibility criteria for increased risk of symptomatic, radiographic knee OA[11] were knee symptoms in the past 12 months, overweight, knee injury causing difficulty walking for ≥1 week, history of any knee surgery, family history of total knee replacement for OA in a biologic parent or sibling, Heberden's nodes, repetitive knee bending at or outside of work, and being 70 to 79 years of age. OAI exclusion criteria[11] were rheumatoid or inflammatory

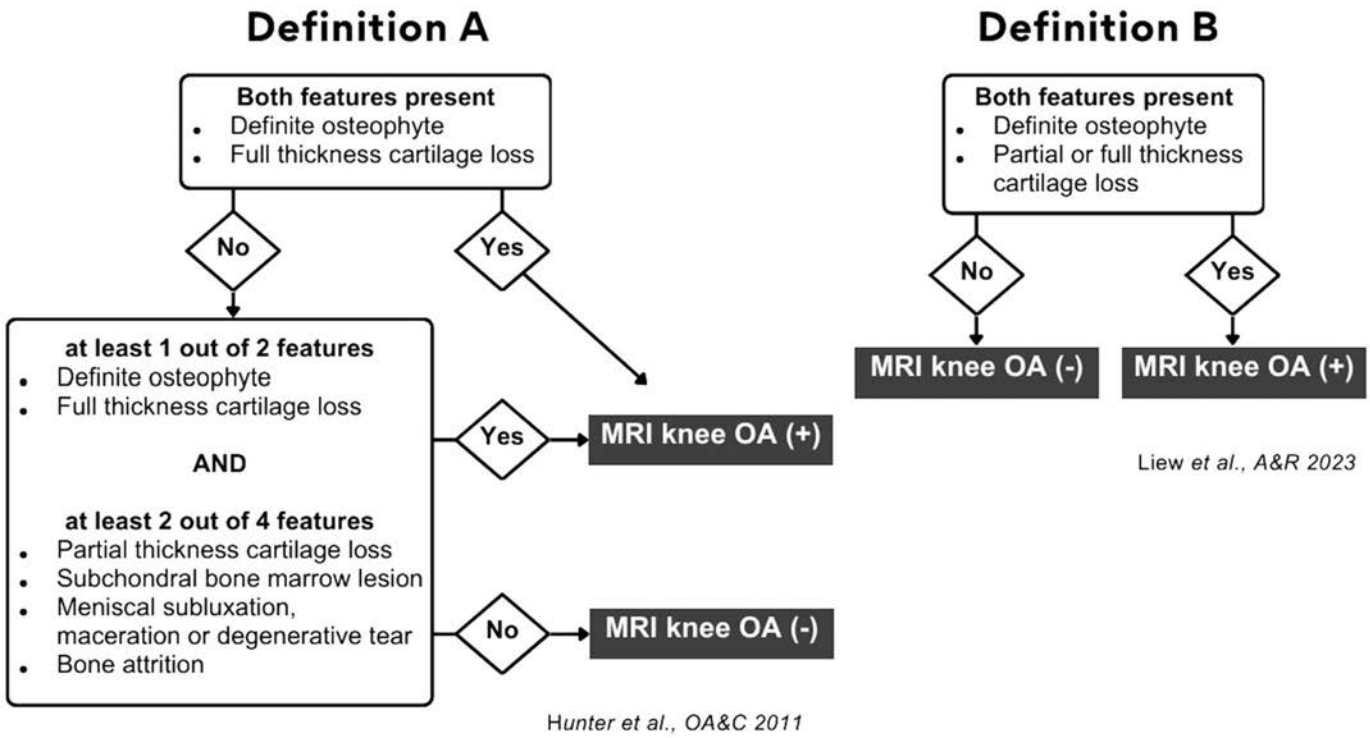


**Figure 1.** MRI criteria for knee (tibiofemoral) OA by definition A and definition B. MRI, magnetic resonance imaging; OA, osteoarthritis.

arthritis, severe bilateral joint space narrowing, unilateral total knee replacement and severe contralateral joint space narrowing, bilateral total knee replacement or plan for it in the next three years, contraindications to MRI, positive pregnancy test, inability to provide a blood sample, use of walking aids other than a single straight cane for >50% of the time during ambulation, severe comorbidity, or current participation in a double-blind randomized trial. The institutional review board at each site approved the study, and all participants gave written informed consent. OAI data are publicly available at https://nda.nih.gov/oai/.

**Assessment of MRI-based knee lesions.** MRI data were acquired using 3T Siemens Trio scanners at each site, including sequences of coronal intermediate-weighted (IW) turbo spin echo (TSE), sagittal IW TSE with fat-suppression, and 3D dual-echo steady-state water excitation, obtained in the sagittal plane with coronal and axial multiplanar reconstructions. MRI assessments were performed on the right knee, or left knee if the images of the right knee were technically unacceptable. Three expert musculoskeletal radiologists (FWR and AG), anonymized to all other study data, scored the extent of tissue lesions using the MRI OA Knee Score (MOAKS).[12] Reading reliability demonstrated very good (0.61–0.80) or excellent (0.81–1.00) agreement.[12] Paired images were read with known chronology.[13]

Osteophyte presence was scored in six TF locations (0, none; 1, small; 2, medium; 3, large) (Figure 2A and B). Articular cartilage was scored for lesion size and degree of full-thickness loss in 10 TF subregions (0, normal; 1.0, 1%–10% area damaged, no full thickness; 1.1, 1%–10% area, 1%–10% full thickness; 2.0, 10%–75% area, no full thickness; 2.1, 10%–75% area, 1%–10% full thickness; 2.2, 10%–75% area, 10%–75% full thickness; 3.0, >75% area, no full thickness; 3.1, >75% area, 1%–10% full thickness; 3.2, >75% area, 10%–75% full thickness; 3.3, >75% area, >75% full thickness) (Figure 2C). Bone marrow lesions (BMLs) were scored in 10 TF subregions (0, none; 1, <25% of subregion; 2, 25%–50%; 3, >50%) (Figure 2D). Meniscal damage was scored in six locations (0, normal; 1, signal abnormality; 2, radial tear; 3, horizontal tear; 4, vertical tear; 5, complex tear; 6, partial maceration; 7, progressive partial maceration; 8, complete maceration) (Figure 2D). Meniscal extrusion was scored in two locations (0, <2 mm; 1, 2–2.9 mm; 2, 3–4.9 mm; 3, >5 mm). Figure 2E and F illustrate the 10 subregions for cartilage and BML assessment.

**Predictor baseline MRI-defined knee OA by Def A and Def B.** Figure 1 shows the algorithm for determining MRI-defined knee OA (TF compartment) by Def A[7] and by Def B[8] at baseline. Definite osteophyte was defined as a score ≥1 in any of the six TF locations. Full-thickness cartilage damage was defined as a score 1.1, 2.1, 2.2, 3.1, 3.2, or 3.3 and partial-thickness cartilage damage as any other score that is >0 in any of the 10 TF subregions. Subchondral BML was defined as a size score ≥1 in any of the 10 TF subregions. Meniscal subluxation, maceration, or degenerative tear was defined as either a meniscal damage score 2, 3, 5, 6, 7, or 8 in any of the six locations or a meniscal extrusion score ≥2 in any of the two locations. Bone attrition was not assessed in the OAI data set.

**Assessment of baseline sociodemographic, knee-specific, and health-related characteristics.** Participants self-reported educational level, race, marital status, and employment status. Comorbidity was assessed by the Self-Administered Comorbidity Questionnaire (range: 0–10, higher scores indicating a greater number of comorbidities).[14] Depressive symptoms were evaluated using the Center for Epidemiologic Studies Depression Scale (CES-D) (range: 0–60, ≥16 defined as having high depressive symptoms).[15,16] Knee pain, symptoms, sport and recreation function, and quality of life were measured using the Knee Injury and Osteoarthritis Outcome Score (KOOS) (range for each: 0–100, with higher scores indicating better status).[17] Western Ontario and McMaster Universities Arthritis Index (WOMAC) evaluated knee pain (range: 0–20), knee stiffness (range: 0–8), and function (range: 0–68). Gait speed (m/s) was quantified during a 20-meter walk. Chair stand rate (number per minute) was calculated based on the time required for five repetitions of rising from a chair and sitting down.

**Outcome incident radiographic knee OA during up to 11 years of follow-up.** At baseline, 1-, 2-, 3-, 4-, 6-, 8-, and 10- or 11-year follow-up visits, knee radiographs were obtained using the posteroanterior fixed-flexion weight-bearing protocol,[18] using a plexiglass positioning frame (SynaFlexer). KL grade[19] and joint space narrowing (JSN) in the TF compartment were centrally evaluated by two experts who were masked to each other's readings and all other data. Frequent knee symptoms, defined as pain, aching, or stiffness for more than half of the days of a month in the past year, were assessed at the same follow-up visits. Incident radiographic knee OA of the index knee was defined alternatively as 1) KL grade ≥2, 2) KL grade ≥2 and JSN (ie, OARSI grade ≥1), and 3) KL grade ≥2 and the presence of frequent knee symptoms during up to 11 years of follow-up.

**Statistical analyses.** The analysis sample included OAI participants without radiographic evidence of knee OA (ie, KL grade 0 and 1) in both knees at baseline and who had complete baseline MRI readings of either knee. Each participant contributed one knee for the analysis. Descriptive statistics for baseline sociodemographic, knee-specific, and health-related characteristics were computed. Continuous variables are reported as means with standard deviations and median with interquartile ranges; categorical variables are reported as counts with percentages.

The prevalence of MRI-defined knee OA at baseline was analyzed separately using Def A and Def B. For each of these definitions, the rate of incident radiographic knee OA during up to 11 years of follow-up (outcome) was separately calculated for 1)

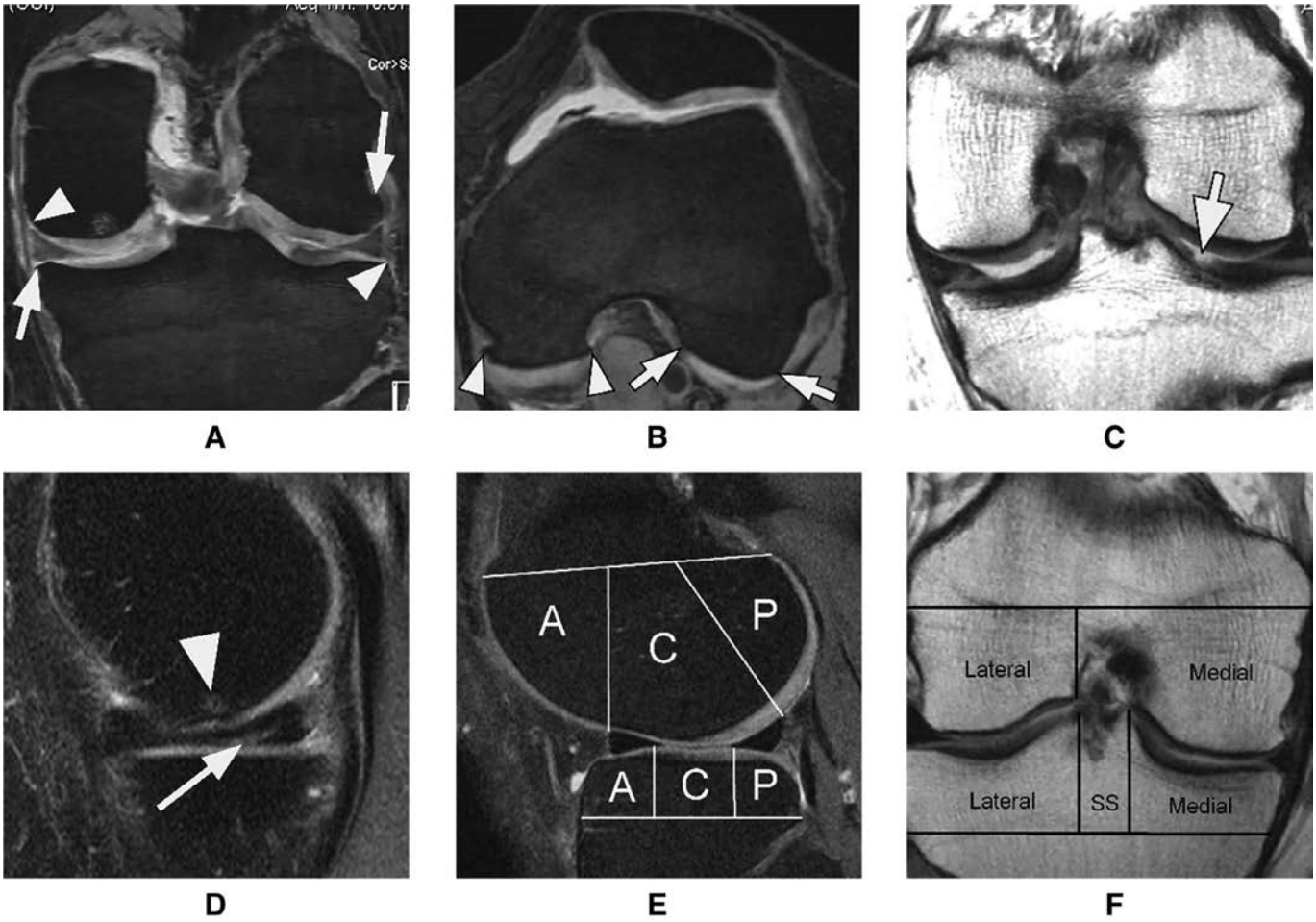


**Figure 2.** MRI assessment. (A) Osteophytes were considered in this study in six locations based on the MOAKS scoring instrument. Arrows point to small grade 1 osteophytes at the medial tibia and the lateral femur, while arrowheads demarcate the additional two locations that are considered on coronal images (here, coronal reformation of the DESS sequence). (B) Additional two locations considered for the tibiofemoral joint are at the posterior medial (arrowheads) and lateral (arrows) femur. The larger osteophyte at the two possible locations for the medial and lateral posterior femur is considered and recorded. (C) Cartilage damage is scored considering all available sequences. This coronal intermediate-weighted image shows a focal (grade 1.1 in the MOAKS system) full-thickness lesion in the central subregion of the lateral tibia (arrow). Focal lesions do not contribute to joint space narrowing on the anterior-posterior radiograph but are an early feature of OA. (D) Sagittal intermediate-weighted fat suppressed image shows a small subchondral bone marrow lesion (arrowhead) and a posterior horizontal meniscal tear (arrow). (E) MOAKS system subdivides the tibiofemoral joint into 10 distinct subregions. Sagittal image shows the anterior (A), central (C), and posterior (P) subregions for the femur and tibia. Although, for the tibia, all three subregions are considered to be part of the tibiofemoral joint, for the femur only, the central and posterior subregions are considered tibiofemoral, whereas the anterior femoral subregion is considered being part of the patellofemoral joint. (F) Coronal image shows the subdivision into the medial and lateral tibiofemoral compartment, while the SS (subspinous) region is not considered part of the articular tibiofemoral joint but assessed separately as the attachment site for the cruciate ligaments. DESS, dual echo steady state; MOAKS, MRI OA Knee Score; MRI, magnetic resonance imaging; OA, osteoarthritis.

KL grade ≥2, 2) KL grade ≥2 and JSN, and 3) KL grade ≥2 and the presence of frequent knee symptoms. For each follow-up time point, the numbers of participants at risk of developing the outcome (ie, those who did not yet have the outcome at this visit and therefore were at risk of developing it subsequent to that visit), experiencing the outcome (ie, those newly documented to have the outcome at this visit), and who were censored (ie, follow-up without the outcome) were quantified. Cox proportional hazards regression models with interval-censored survival,[20,21] adjusted for age, sex, body mass index (BMI), and KOOS pain, examined associations of baseline MRI-defined knee OA (Def A) with incident radiographic knee OA (respectively, defined as KL grade ≥2, KL grade ≥2 and JSN, and KL grade ≥2 and frequent knee symptoms). Similarly, adjusted Cox regression models examined associations of baseline MRI-defined knee OA (Def B) with incident radiographic knee OA. For each of the six regression models, we summarized results using adjusted risk ratios and associated 95% confidence intervals (95% CIs) and plotted interval-censored Cox regression survival curves.

We performed sensitivity analyses stratified by baseline sex (female vs male), BMI (obese vs overweight vs healthy weight), and the presence of frequent knee symptoms (yes vs no). We conducted additional sensitivity analyses, restricting the analysis to knees with KL grade 0. All analyses were performed using SAS Version 9.4 (SAS Institute Inc, Cary, NC).

## RESULTS

In the OAI cohort, 1,936 participants had no radiographic evidence of TF OA (ie, KL grade 0 or 1 in both knees) at baseline. After excluding 315 participants who did not have complete baseline MRI readings of either knee, the final analysis sample consisted of 1,621 participants (mean ± SD age 58.8 ± 9.0 years, mean ± SD BMI 27.2 ± 4.5 kg/m$^2$, 59.5% women). Each participant contributed one index knee (right knee, or left knee if right knee MRI data unavailable) for analysis; 81.4% of index knees were KL grade 0, and 18.6% were KL grade 1. Table 1 summarizes the baseline demographic, knee-specific, and health-related variables for the study sample.

**Prevalence of MRI-defined knee OA at baseline.** Among 1,621 OAI participants without TF radiographic knee OA, the prevalence of MRI-defined knee OA was 17% according to Def A and 24% according to Def B. Fifteen percent had OA by both definitions, 11% by one but not the other definition, and 74% did not have MRI OA by either definition (Supplementary Table 1).

**Associations of baseline MRI-defined knee OA with incident radiographic knee OA during up to 11 years of follow-up.** The rate of incident radiographic knee OA defined as KL ≥2 was 22%, 16% defined by KL ≥2 and JSN, and 14% defined by KL ≥2 and frequent knee symptoms. Figure 3 shows the frequencies of incident radiographic knee OA in knees with and without baseline MRI-defined knee OA. For example, among those with baseline MRI OA by Def A (n = 283), 41% developed

**Table 1.** Baseline demographic, knee-specific, and health-related variables for participants, N = 1,621*

| Variable | n (%) | Mean ± SD | Median (IQR) |
|---|---|---|---|
| Age, y | – | 58.8 ± 9.0 | 57 (15) |
| Women | 964 (59.5) | – | – |
| BMI (kg/m$^2$) | – | 27.2 ± 4.5 | 26.6 (6.3) |
| Education (≥college graduate)[a] | 1,032 (64.2) | – | – |
| Race[b] | | | |
| White/Caucasian | 1,363 (84.2) | – | – |
| Black or African American | 218 (13.5) | – | – |
| Asian | 13 (0.8) | – | – |
| Other non-White | 24 (1.5) | – | – |
| Marital status (married)[a] | 1,127 (70.1) | – | – |
| Employment (employed)[c] | 1,121 (69.2) | – | – |
| Comorbidities (Comorbidity Questionnaire ≥2)[d] | 116 (7.3) | – | – |
| High depressive symptoms (CES-D ≥16)[e] | 140 (8.7) | – | – |
| KL grade (index knee) | | | |
| 0 | 1,320 (81.4) | – | – |
| 1 | 301 (18.6) | – | – |
| KOOS pain (0–100, index knee) | – | 88.4 ± 14.4 | 94.4 (16.7) |
| KOOS symptoms (0–100, index knee) | – | 90.4 ± 10.8 | 92.9 (14.3) |
| KOOS sport and recreation function (0–100)[f] | – | 80.4 ± 21.3 | 85.0 (33.3) |
| KOOS quality of life (0–100) | – | 74.5 ± 20.2 | 75.0 (31.3) |
| WOMAC pain (0–20) | – | 1.8 ± 2.6 | 1.0 (3.0) |
| WOMAC stiffness (0–8) | – | 1.2 ± 1.4 | 1.0 (2.0) |
| WOMAC function (0–68)[g] | – | 5.3 ± 8.2 | 1.1 (7.2) |
| Gait speed (m/s) | – | 1.4 ± 0.2 | 1.4 (0.3) |
| Chair stand rate (#/min)[h] | – | 30.8 ± 10.6 | 30.0 (11.4) |

*BMI, body mass index; CES-D, Center for Epidemiological Studies Depression Scale; IQR, interquartile range; KL, Kellgren–Lawrence; KOOS, Knee Injury and Osteoarthritis Outcome Score; WOMAC, Western Ontario and McMaster Universities Arthritis Index. Higher KOOS scores indicate better status; higher WOMAC scores indicate worse status. Because the 17-item KOOS Activity of Daily Living subscale is identical to the 17-item WOMAC function subscale, the KOOS Activitiy of Daily Living subscale was not separately assessed in the Osteoarthritis Initiative.
[a] n = 1,608.
[b] n = 1,618.
[c] n = 1,619.
[d] n = 1,596.
[e] n = 1,605.
[f] n = 1,341.
[g] n = 1,616.
[h] n = 1,620.

knee OA (defined as KL ≥2) during follow-up, and 59% did not. Among those without baseline MRI OA by Def A (n = 1,338), 82% did not develop knee OA, and 18% did. Among those with baseline MRI OA by Def B (n = 389), 36% developed knee OA (by KL ≥2), and 64% did not. Among those without baseline MRI OA by Def B (n = 1,232), 83% did not develop knee OA, and 17% did.

As shown in Figure 4, MRI-defined knee OA by Def A at baseline was associated with a 2.94 (95% CI 2.34–3.68) times increased risk of incident KL ≥2; MRI-defined knee OA by Def B was associated with a 2.44 (95% CI 1.97–3.03) times increased risk over up to 11 years of follow-up. Similar associations were observed for outcomes of incident KL ≥2 and JSN and of incident KL ≥2 and frequent knee symptoms. Repeating the analyses only in knees with KL grade 0 (n = 1,230) or in knees with KL grade 1 (n = 301) yielded similar findings (see Supplementary Figure 1). Subgroup analyses stratified by sex, BMI categories, and frequent knee symptoms are shown in Supplementary Figures 2 to 4. The results were comparable across these subgroup analyses. Lastly, Figure 5 shows the interval-censored Cox regression survival curves by Def A and by Def B, adjusted for baseline age, sex, BMI, and KOOS pain.

## DISCUSSION

We investigated the prevalence and long-term implications of MRI-defined knee OA using two definitions (Def A and Def B) in 1,621 OAI participants without TF radiographic knee OA at baseline. The prevalence of MRI-defined knee OA was 17% according to Def A and 24% according to Def B, confirming that structural joint changes were present in the absence of radiographic signs in persons at higher risk for knee OA.[22] We identified an association between baseline MRI-defined knee OA and the development of incident radiographic and symptomatic disease during up to 11 years of follow-up. However, a substantial proportion of individuals with baseline MRI-defined knee OA did not develop radiographic knee OA during follow-up (59% for Def A and 64% for Def B, using KL ≥2 as the outcome). Similar findings were observed for the outcomes of KL ≥2 and JSN and of KL ≥2 and frequent knee symptoms.

To our knowledge, this is the first study applying MRI definitions of knee OA to examine the association between baseline MRI-defined knee OA and subsequent incident radiographic and symptomatic disease. Our findings inform the ongoing effort to define early-stage knee OA and raise the question of whether MRI-defined OA (at least based on the two evaluated definitions) represents a precursor state for early OA. If MRI-defined knee OA is indeed a precursor state, an additional event(s) or exposure(s) may need to occur for the transition to OA. Future research should develop alternative algorithms that integrate MRI data, symptoms, and physical examination findings. Machine learning and artificial intelligence could enhance the precision and predictive power of these criteria.

MRI-based definitions of knee OA have been examined in several cross-sectional studies. The associations of Def A and Def B with concurrent radiographic knee OA (defined as KL grade ≥2) and symptomatic knee OA (defined as self-reported physician-diagnosed knee OA, frequent knee pain, and pain while walking during the clinic visit) were examined in 1,185 MOST participants.[8] 40% of the study sample had KL grade ≥2; 36% had frequent knee pain. Both definitions performed similarly, with high sensitivity (87%–96%) and low specificity (26%–37%). In another study of 113 young adults who were 5 years post–anterior cruciate ligament tear, Def A and Def B were compared with concurrent radiographic knee OA (defined by OARSI scoring of osteophytes and joint space narrowing).[23] Surprisingly, both definitions exhibited low sensitivity (48%–52%) and moderate specificity (76%–77%). The authors speculated that the high false negative rate (ie, knees with radiographic JSN but without MRI OA) may be attributed to positioning errors during radiograph acquisition and meniscal extrusion in the absence of cartilage damage. These cross-sectional studies suggest that MRI-defined knee OA may be associated with radiographic and symptomatic disease at the same time point.

Two longitudinal studies[24,25] have examined the association of MRI-defined knee OA based on Def A with other outcomes. In a population-based sample of 888 middle-aged women from the Rotterdam Study, MRI-defined TF OA, with or without radiographic TF OA, was associated with an increased likelihood of prevalent knee pain and persistent knee pain two years later.[24] Another study investigated the association between baseline MRI-defined TF OA and tibial cartilage loss 2.6 and 10.7 years later in a population-based sample from the Tasmania Older Adult Cohort (n = 574).[25] Compared with participants with neither radiographic nor MRI OA, those with MRI OA only were more likely to experience concurrent knee pain and exhibited greater annual tibial cartilage loss over 2.6 years, but not over 10.7 years. Different methods used for measuring tibial cartilage volume at the two time points and potential floor effects may have contributed to the discrepant findings. Neither study explored whether baseline MRI-defined knee OA was a precursor of clinically significant knee OA.

In the present study of participants without radiographic TF OA at baseline, the presence of MRI OA, according to both Def A and Def B, was associated with increased risk of incident radiographic knee OA during up to 11 years of follow-up. As illustrated in Figure 3, Def A may slightly outperform Def B in identifying risk for future radiographic OA. However, significant overlap in the 95% CIs suggests that these differences were not statistically significant. Notably, for both Def A and Def B, more than half of those with baseline MRI OA did not develop radiographic OA. In other words, MRI OA by these definitions was not a strong indicator of future radiographic disease. Findings were similar in strata defined by the presence of baseline frequent knee symptoms (see Supplementary Figure 4). Conversely, >82% of those without baseline

**Incident radiographic knee OA defined as KL ≥ 2**

| Baseline MRI definition | Incident knee OA (yes) | Incident knee OA (no) | |
|---|---|---|---|
| A (yes) | 116 (41%) | 167 (59%) | 283 |
| A (no) | 239 (18%) | 1099 (82%) | 1338 |
| | 355 (22%) | 1266 (78%) | 1621 |
| B (yes) | 141 (36%) | 248 (64%) | 389 |
| B (no) | 214 (17%) | 1018 (83%) | 1232 |
| | 355 (22%) | 1266 (78%) | 1621 |

**Incident radiographic knee OA defined as KL ≥ 2 and joint space narrowing**

| Baseline MRI definition | Incident knee OA (yes) | Incident knee OA (no) | |
|---|---|---|---|
| A (yes) | 92 (33%) | 191 (67%) | 283 |
| A (no) | 173 (13%) | 1165 (87%) | 1338 |
| | 265 (16%) | 1356 (84%) | 1621 |
| B (yes) | 107 (28%) | 282 (72%) | 389 |
| B (no) | 158 (13%) | 1074 (87%) | 1232 |
| | 265 (16%) | 1356 (84%) | 1621 |

**Incident radiographic knee OA defined as KL ≥ 2 and frequent knee symptoms**

| Baseline MRI definition | Incident knee OA (yes) | Incident knee OA (no) | |
|---|---|---|---|
| A (yes) | 76 (27%) | 207 (73%) | 283 |
| A (no) | 152 (11%) | 1186 (89%) | 1338 |
| | 228 (14%) | 1393 (86%) | 1621 |
| B (yes) | 89 (23%) | 300 (77%) | 389 |
| B (no) | 139 (11%) | 1093 (89%) | 1232 |
| | 228 (14%) | 1393 (86%) | 1621 |

**Figure 3.** Frequency of incident radiographic knee OA over up to 11 years of follow-up in knees with and without baseline MRI-defined knee OA by definitions A and B. *Each cell contains the number (row %) of participants*. Color figure can be viewed in the online issue, which is available at http://onlinelibrary.wiley.com/doi/10.1002/art.42982/abstract.

MRI OA did not develop radiographic OA over the 11-year follow-up period, suggesting that the absence of MRI OA may serve as an indicator for a more favorable outcome.

In our analysis sample, the prevalence of MRI OA was 17% by Def A and 24% by Def B. Additionally, 9% had MRI OA by Def B but not A, whereas 2% had MRI OA by Def A but not

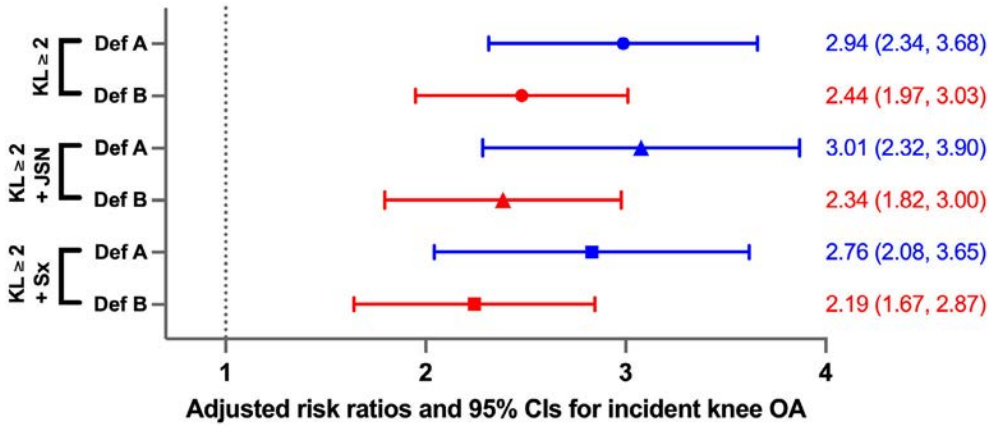


**Figure 4.** Associations of baseline MRI-defined knee OA with incident radiographic knee OA during up to 11 years of follow-up. Cox proportional hazards regression models were adjusted for baseline age, sex, BMI, and KOOS pain (n = 1,621). Baseline MRI-defined knee OA was defined as Def A or Def B. Incident radiographic knee OA was defined as (1) KL grade ≥2, (2) KL grade ≥2 and JSN, or (3) KL grade ≥2 and Sx. For example, the top two lines show the adjusted risk ratios and 95% CIs for Def A (blue line) and Def B (red line) using KL ≥2 as the outcome. The middle two lines show results for Def A and Def B using KL ≥2 and JSN as the outcome. The bottom two lines show results for Def A and Def B using KL ≥2 and Sx as the outcome. BMI, body mass index; Def, definition; JSN, joint space narrowing; KL, Kellgren–Lawrence; KOOS, Knee Injury and Osteoarthritis Outcome Score; MRI, magnetic resonance imaging; OA, osteoarthritis; Sx, frequent knee symptoms; 95% CI, 95% confidence interval.

B. Whether these MRI pathologies represent early-stage disease is an ongoing debate. A systematic review and meta-analysis of 63 studies concluded that cartilage defects, meniscal tears, BMLs, and osteophytes are common incidental MRI findings in injury-free, asymptomatic knees not at higher risk for knee OA.[26] The pooled prevalence was 4% to 14% in adults under 40 years of age, rising to 19% to 43% in adults at or over 40. In asymptomatic individuals not at higher risk for knee OA, these MRI-detected lesions may be a manifestation of aging.

On the contrary, in persons at higher risk for knee OA and without radiographic disease, MRI tissue lesions were associated with adverse structural and symptomatic outcomes in longitudinal studies. In OAI participants with normal knee radiographs at baseline, adding each of several MRI-detected tissue lesions as a predictor to a base model improved the prediction of incident radiographic OA over 7 years[27]; worsening MRI lesions were associated with concurrent incident radiographic OA and subsequent persistent symptoms.[28] Another OAI-based study showed that having multiple MRI-detected tissue lesions simultaneously increased the risk of radiographic knee OA two years later.[29] Similarly, in MOST participants without radiographic knee OA, severity of MRI-based tissue lesions was associated with an increased likelihood of incident radiographic OA within seven years.[30] In a sample from the Cohort Hip and Cohort Knee Study without baseline radiographic knee OA (n = 148), cartilage damage, osteophytes, BMLs, meniscal pathology, and effusion were each linked to radiographic knee OA development five years later.[31] These studies focused on the association between MRI-detected tissue lesions and incident disease but did not seek to develop or evaluate an MRI definition of disease. Our study demonstrates that the existing MRI definitions of knee OA may not adequately identify knees that will develop radiographic and symptomatic disease.

The current study has several notable strengths. To our knowledge, this is the first longitudinal study examining whether meeting the current MRI definitions of knee OA is associated with an elevated risk of future radiographic and symptomatic disease. It addresses a critical knowledge gap in the literature and has important implications for optimal early-OA clinical trial recruitment. Furthermore, it leverages data from the OAI, a large-scale, prospective, longitudinal observational cohort study that employed standardized, rigorous methodologies in MRI and radiograph image acquisitions and readings. The extended follow-up period of up to 11 years facilitates the examination of the long-term prognostic implications of MRI-defined knee OA.

Although the study presents valuable insights, it has limitations. The OAI was deliberately designed to study persons who are at higher risk for knee OA; results cannot be generalized to the population at large. However, it is the high-risk population who will be the focus of prevention and early intervention studies. It is important to acknowledge the difference in scoring systems used. Although the Whole Organ MRI Score was used in both Def A and Def B criteria, our study employed the MOAKS scoring system. MOAKS provides a more comprehensive assessment of tissue lesions, including additional subregional assessment, and enhanced characterization of cartilage lesions and meniscal pathology.[32] Specifically, the lack of MRI-measured bone attrition assessment in the OAI limits the full consideration of each tissue lesion when applying Def A criteria. However, attrition usually represents late-disease bone remodeling. We were able to include MRI data for all KL 0 knees. However, to date, MRI data have been publicly released for a subset of KL1 knees, limiting generalizability of findings for these knees. Lastly, a longer follow-up period may more clearly elucidate the very long-term outcomes of MRI-defined knee OA. Our study sample consisted of

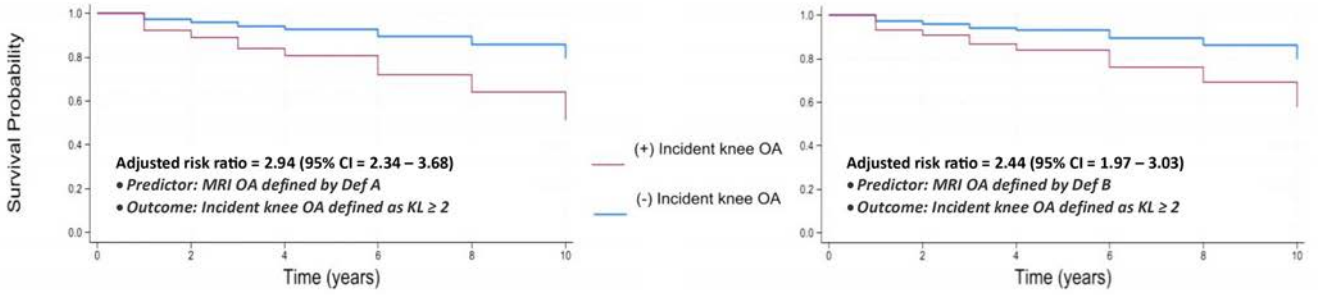


| Frequency of outcome (KL ≥ 2) and censoring at each timepoint | | | | | | | | |
|---|---|---|---|---|---|---|---|---|
| **Status** | **Baseline** | **1 yr.** | **2 yr.** | **3 yr.** | **4 yr.** | **6 yr.** | **8 yr.** | **10/11 yr.** |
| At risk | 1621 | 1621 | 1493 | 1413 | 1317 | 1180 | 1056 | 815 |
| Outcome at this visit | 0 | 69 | 26 | 40 | 25 | 64 | 54 | 77 |
| Outcome, time of last follow-up | 0 | 59 | 54 | 56 | 112 | 60 | 187 | 738 |

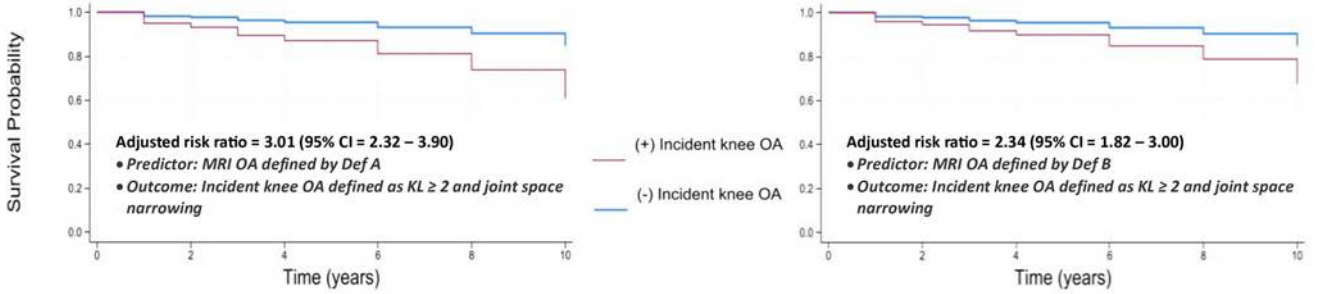


| Frequency of outcome (KL ≥ 2 and joint space narrowing) and censoring at each timepoint | | | | | | | | |
|---|---|---|---|---|---|---|---|---|
| **Status** | **Baseline** | **1 yr.** | **2 yr.** | **3 yr.** | **4 yr.** | **6 yr.** | **8 yr.** | **10/11 yr.** |
| At risk | 1621 | 1621 | 1519 | 1449 | 1364 | 1223 | 1118 | 860 |
| Outcome at this visit | 0 | 43 | 16 | 27 | 19 | 42 | 47 | 71 |
| Outcome, time of last follow-up | 0 | 59 | 54 | 58 | 122 | 63 | 211 | 789 |

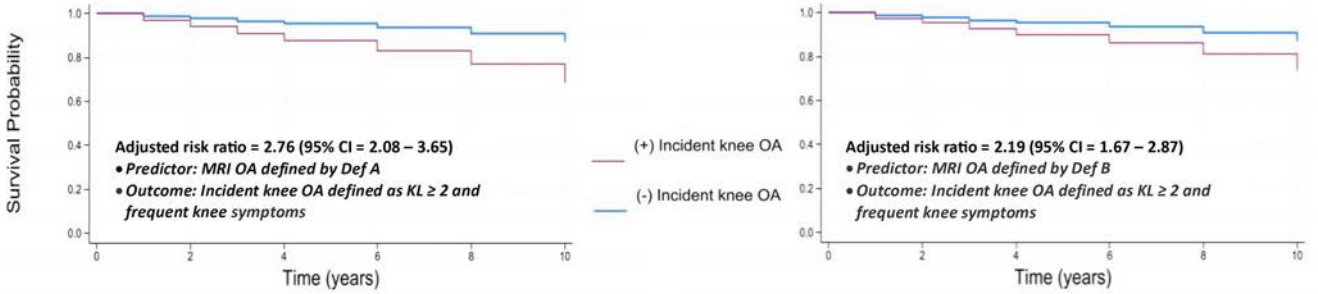


| Frequency of outcome (KL ≥ 2 and frequent knee symptoms) and censoring at each timepoint | | | | | | | | |
|---|---|---|---|---|---|---|---|---|
| **Status** | **Baseline** | **1 yr.** | **2 yr.** | **3 yr.** | **4 yr.** | **6 yr.** | **8 yr.** | **10/11 yr.** |
| At risk | 1621 | 1621 | 1534 | 1456 | 1370 | 1226 | 1128 | 876 |
| Outcome at this visit | 0 | 28 | 24 | 28 | 24 | 35 | 40 | 49 |
| Outcome, time of last follow-up | 0 | 59 | 54 | 58 | 120 | 63 | 212 | 827 |

**Figure 5.** Interval-censored Cox regression survival curves by Def A and Def B, adjusted for age, sex, BMI, and KOOS pain, during up to 11 years of follow-up. The predictors were baseline MRI-defined knee OA by Def A (left plots) or Def B (right plots). The outcomes were incident radiographic knee OA defined as (1) KL grade ≥2 (top row), (2) KL grade ≥2 and joint space narrowing (middle row), or (3) KL grade ≥2 and frequent knee symptoms (bottom row). For example, the top table shows the frequency of outcome (defined as KL grade ≥2) and censoring at each time point. The top left figure shows the survival curves of those with (red line) versus without (blue line) the outcome for Def A. The top right figure shows the survival curves for Def B. BMI, body mass index; Def, definition; KL, Kellgren–Lawrence; KOOS, Knee Injury and Osteoarthritis Outcome Score; MRI, magnetic resonance imaging; OA, osteoarthritis; 95% CI, 95% confidence interval. Color figure can be viewed in the online issue, which is available at http://onlinelibrary.wiley.com/doi/10.1002/art.42982/abstract.

individuals at an increased risk for symptomatic, radiographic knee OA, based on symptoms, BMI, history of knee injury/surgery, family history, and/or repetitive knee bending. The relatively low incidence of radiographic knee OA within up to 11 years (14%–22%) underscores the challenge of tracking a disease that may be slow to progress.[33]

In conclusion, the two current MRI definitions of knee OA may not adequately identify knees that will go on to develop radiographic and symptomatic disease. Future efforts should focus on exploring alternative imaging-based algorithms or algorithms that incorporate MRI features, symptoms, and physical examination findings. Leveraging machine learning and artificial intelligence may enhance the precision and predictive power of these classification criteria.

## ACKNOWLEDGMENTS

The authors would like to thank OAI participants and study site investigators and coordinators for their contribution to the study. We acknowledge the minimal use of large language models in the preparation of this manuscript, such as checking spelling and grammar and assistance with literature search. This use was employed to enhance clarity without influencing the scientific content or conclusions of this work.

## AUTHOR CONTRIBUTIONS

All authors contributed to at least one of the following manuscript preparation role conceptualization AND/OR methodology, software, investigation, formal analysis, data curation, visualization, and validation AND drafting or reviewing/editing the final draft. As corresponding author, Dr Chang confirms that all authors have provided the final approval of the version to be published, and takes responsibility for the affirmations regarding article submission (eg, not under consideration by another journal), the integrity of the data presented, and the statements regarding compliance with institutional review board/Helsinki Declaration requirements.

## REFERENCES

1. Kolasinski SL, Neogi T, Hochberg MC, et al. 2019 American College of Rheumatology/Arthritis Foundation guideline for the management of osteoarthritis of the hand, hip, and knee. Arthritis Care Res (Hoboken) 2020;72(2):149–162.
2. Bannuru RR, Osani MC, Vaysbrot EE, et al. OARSI guidelines for the non-surgical management of knee, hip, and polyarticular osteoarthritis. Osteoarthritis Cartilage 2019;27(11):1578–1589.
3. Moseng T, Vliet Vlieland TPM, Battista S, et al. EULAR recommendations for the non-pharmacological core management of hip and knee osteoarthriti 2023 update. Ann Rheum Dis 2024;83:730–740.
4. Liew JW, King LK, Mahmoudian A, et al; OARSI Early Osteoarthritis Classification Criteria Task Force. A scoping review of how early-stage knee osteoarthritis has been defined. Osteoarthritis Cartilage 2023;31(9):1234–1241.
5. Roemer FW, Guermazi A, Demehri S, et al. Imaging in osteoarthritis. Osteoarthritis Cartilage 2022;30(7):913–934.
6. Roemer FW, Demehri S, Omoumi P, et al. State of the art: imaging of osteoarthritis-revisited 2020. Radiology 2020;296(1):5–21.
7. Hunter DJ, Arden N, Conaghan PG, et al; OARSI OA Imaging Working Group. Definition of osteoarthritis on MRI: results of a Delphi exercise. Osteoarthritis Cartilage 2011;19(8):963–969.
8. Liew JW, Rabasa G, LaValley M, et al. Development of an MRI-based definition of knee osteoarthriti data from the Multicenter Osteoarthritis Study. Arthritis Rheumatol 2023;75:1132–1138.
9. Mahmoudian A, King LK, Liew JW, et al; OARSI Early-stage Symptomatic Knee Osteoarthritis Initiative. Timing is everything: towards classification criteria for early-stage symptomatic knee osteoarthritis. Osteoarthritis Cartilage 2024;32(6):649–653.
10. Driban JB, Harkey MS, McAlindon TE, et al. The importance of context and intent when defining early-stage knee osteoarthritis. Osteoarthritis Cartilage 2023;31(9):1145–1147.
11. Nevitt MC, Felson DT, Lester G. The Osteoarthritis Initiative: protocol for the cohort study. Osteoarthritis Initiative. 2006. Accessed [January 15, 2024]. https://nda.nih.gov/static/docs/StudyDesignProtocolAndAppendices.pdf
12. Hunter DJ, Guermazi A, Lo GH, et al. Evolution of semi-quantitative whole joint assessment of knee OA: MOAKS (MRI Osteoarthritis Knee Score). Osteoarthritis Cartilage 2011;19(8):990–1002.
13. Felson DT, Nevitt MC. Blinding images to sequence in osteoarthriti evidence from other diseases. Osteoarthritis Cartilage 2009;17(3):281–283.
14. Katz JN, Chang LC, Sangha O, et al. Can comorbidity be measured by questionnaire rather than medical record review? Med Care 1996;34(1):73–84.
15. Radloff LS. The CES-D scale: a self-report depression scale for research in the general population. Appl Psychol Meas 1977;1(3):385–401.
16. Vilagut G, Forero CG, Barbaglia G, et al. Screening for depression in the general population with the Center for Epidemiologic Studies Depression (CES-D): a systematic review with meta-analysis. PLoS ONE 2016;11(5):e0155431.
17. Roos EM, Lohmander LS. The Knee injury and Osteoarthritis Outcome Score (KOOS): from joint injury to osteoarthritis. Health Qual Life Outcomes 2003;1:64.
18. Overview and description of central image assessments. Osteoarthritis Initiative. 2016. Accessed [January 15, 2024]. https://nda.nih.gov/static/docs/ImageAssessmentDataOverview.pdf
19. Kellgren JH, Lawrence JS. Radiological assessment of osteo-arthrosis. Ann Rheum Dis 1957;16(4):494–502.
20. Cox DR. Regression models and life-tables. J R Stat Soc Ser B Methodol 1972;34(2):187–202.
21. Turnbull BW. The empirical distribution function with arbitrarily grouped, censored and truncated data. J R Stat Soc Ser B Methodol 1976;38(3):290–295.
22. Guermazi A, Niu J, Hayashi D, et al. Prevalence of abnormalities in knees detected by MRI in adults without knee osteoarthriti population based observational study (Framingham Osteoarthritis Study). BMJ 2012;345:e5339.
23. Liew JW, Turkiewicz A, Roemer FW, et al. Diagnostic accuracy of candidate magnetic resonance imaging knee osteoarthritis definitions versus radiograph in an acute anterior cruciate ligament injury cohort. Arthritis Care Res (Hoboken) 2024;76:409–414.
24. Schiphof D, Oei EHG, Hofman A, et al. Sensitivity and associations with pain and body weight of an MRI definition of knee osteoarthritis compared with radiographic Kellgren and Lawrence criteria: a population-based study in middle-aged females. Osteoarthritis Cartilage 2014;22(3):440–446.
25. Cai G, Cicuttini F, Aitken D, et al. Comparison of radiographic and MRI osteoarthritis definitions and their combination for prediction of tibial cartilage loss, knee symptoms and total knee replacement: a longitudinal study. Osteoarthritis Cartilage 2020;28(8):1062–1070.

26. Culvenor AG, Øiestad BE, Hart HF, et al. Prevalence of knee osteoarthritis features on magnetic resonance imaging in asymptomatic uninjured adult a systematic review and meta-analysis. Br J Sports Med 2019;53(20):1268–1278.
27. Sharma L, Hochberg M, Nevitt M, et al. Knee tissue lesions and prediction of incident knee osteoarthritis over 7 years in a cohort of persons at higher risk. Osteoarthritis Cartilage 2017;25(7):1068–1075.
28. Sharma L, Nevitt M, Hochberg M, et al. Clinical significance of worsening versus stable preradiographic MRI lesions in a cohort study of persons at higher risk for knee osteoarthritis. Ann Rheum Dis 2016; 75(9):1630–1636.
29. Roemer FW, Kwoh CK, Hannon MJ, et al. What comes first? Multitissue involvement leading to radiographic osteoarthriti magnetic resonance imaging–based trajectory analysis over four years in the Osteoarthritis Initiative. Arthritis Rheumatol 2015;67(8):2085–2096.
30. Niu J, Felson DT, Neogi T, et al. Patterns of coexisting lesions detected on magnetic resonance imaging and relationship to incident knee osteoarthriti the Multicenter Osteoarthritis Study. Arthritis Rheumatol 2015;67(12):3158–3165.
31. van Oudenaarde K, Jobke B, Oostveen ACM, et al. Predictive value of MRI features for development of radiographic osteoarthritis in a cohort of participants with pre-radiographic knee osteoarthritis-the CHECK study. Rheumatology (Oxford) 2017;56(1):113–120.
32. Roemer FW, Hunter DJ, Crema MD, et al. An illustrative overview of semi-quantitative MRI scoring of knee osteoarthriti lessons learned from longitudinal observational studies. Osteoarthritis Cartilage 2016;24(2):274–289.
33. Felson D, Niu J, Sack B, et al. Progression of osteoarthritis as a state of inertia. Ann Rheum Dis 2013;72(6):924–929.

**Arthritis & Rheumatology**
Vol. 77, No. 2, February 2025, pp 151–162
DOI 10.1002/art.42984
© 2024 The Author(s). *Arthritis & Rheumatology* published by Wiley Periodicals LLC on behalf of American College of Rheumatology. This is an open access article under the terms of the Creative Commons Attribution-NonCommercial-NoDerivs License, which permits use and distribution in any medium, provided the original work is properly cited, the use is non-commercial and no modifications or adaptations are made.

American College of Rheumatology
Empowering Rheumatology Professionals

# Enhancement of Intracellular Cholesterol Efflux in Chondrocytes Leading to Alleviation of Osteoarthritis Progression

Gyuseok Lee,[1] Jiye Yang,[2] Su-Jin Kim,[1] Thanh-Tam Tran,[1] Sun Young Lee,[1] Ka Hyon Park,[1] Seung-Hee Kwon,[1] Ki-Ho Chung,[1] Jeong-Tae Koh,[1] Yun Hyun Huh,[2] Jong-Keun Seon,[3] Hyun Ah Kim,[4] Jang-Soo Chun,[2] and Je-Hwang Ryu[1]

**Objective.** Osteoarthritis (OA) is the most common degenerative disease worldwide, with no practical means of prevention and limited treatment options. Recently, our group unveiled a novel mechanism contributing to OA pathogenesis in association with abnormal cholesterol metabolism in chondrocytes. In this study, we aimed to establish a clinical link between lipid profiles and OA in humans, assess the effectiveness of cholesterol-lowering drugs in suppressing OA development in mice, and uncover the cholesterol-lowering mechanisms that effectively impede OA progression.

**Methods.** Five clinically approved cholesterol-lowering drugs (fenofibrate, atorvastatin, ezetimibe, niacin, and lomitapide) were injected into the knee joints or administered with diet to mice with OA who underwent destabilization of the medial meniscus induction and were fed a 2% high-cholesterol diet. Gene expression linked to cholesterol metabolism was determined using microarray analysis. Furthermore, the in vivo functions of these genes were explored through intra-articular injection of either its inhibitor or adenovirus.

**Results.** Logistic regression analysis confirmed a close relationship between the diagnostic criteria of hyperlipidemia based on serum lipid levels and OA incidence. Among the cholesterol-lowering drugs examined, fenofibrate exerted the most significant protective effect against cartilage destruction, which was attributed to elevated levels of high-density lipoprotein cholesterol that are crucial for cholesterol efflux. Notably, cholesterol efflux was suppressed during OA progression via down-regulation of apolipoprotein A1–binding protein (AIBP) expression. Overexpression of AIBP effectively inhibits OA progression.

**Conclusion.** Our results suggest that restoration of cholesterol homeostasis to a normal state through administration of fenofibrate or AIBP overexpression, both of which induce cholesterol efflux, offers an effective therapeutic option for patients with OA.

## INTRODUCTION

Osteoarthritis (OA), the most common type of arthritis that causes chronic disability and poses a significant socioeconomic burden, affects 7% of the world population.[1] Cartilage destruction, triggered by an imbalance in the expression of anabolic/catabolic factors in chondrocytes, are major symptoms of OA.[2] No effective disease-modifying drugs are currently available, necessitating a treatment approach that predominantly involves artificial joint replacement surgery. OA has long been regarded as a degenerative disease that results from repetitive use and excessive mechanical loading on joints.[3] However, recent studies indicate that OA is closely related to metabolic diseases such as hypertension, hyperglycemia, and obesity rather than being solely

Supported by the National Research Foundation of Korea (grants 2019R1A5A2027521, 2021R1A2C3005727, and 2021R1I1A1A01061246) and the Korean Fund for Regenerative Medicine, both funded by the Korean government (the Ministry of Science and ICT, the Ministry of Health and Welfare; grant 22A0104L1).

[1]Gyuseok Lee, PhD, Su-Jin Kim, PhD, Thanh-Tam Tran, PhD, Sun Young Lee, PhD, Ka Hyon Park, PhD, Seung-Hee Kwon, MS, Ki-Ho Chung, PhD, Jeong-Tae Koh, PhD, Je-Hwang Ryu, PhD: Chonnam National University, Gwangju, Republic of Korea; [2]Jiye Yang, MS, Yun Hyun Huh, PhD, Jang-Soo Chun, PhD: Gwangju Institute of Science and Technology, Gwangju, Republic of Korea; [3]Jong-Keun Seon, MD: Chonnam National University Hwasun Hospital and Medical School, Hwasun, Republic of Korea; [4]Hyun Ah Kim, MD: Hallym University, Sacred Heart Hospital, Anyang, Republic of Korea.

Additional supplementary information cited in this article can be found online in the Supporting Information section (http://onlinelibrary.wiley.com/doi/10.1002/art.42984).

Author disclosures are available at https://onlinelibrary.wiley.com/doi/10.1002/art.42984.

Address correspondence via email to Je-Hwang Ryu, PhD, at jesryu@jnu.ac.kr.

Submitted for publication December 10, 2023; accepted in revised form August 20, 2024.

attributed to wear and tear.[4,5] For instance, the prevalence of OA in joints not subjected to load by body mass is reported to increase with obesity, highlighting the significance of systemic factors in disease development.[6] Indeed, studies have been published demonstrating that OA can be influenced by systemic factors such as adipokines, glucose, cholesterol, triglycerides (TGs), and various metabolic derivatives.[4,5,7,8]

Recent investigations by our group and others have uncovered regulatory mechanisms underlying OA progression involving abnormal cholesterol metabolism.[9] Cholesterol accumulates in chondrocytes during OA progression, and accumulated cholesterol leads to deterioration of mitochondrial activity or transformation into oxysterols that activate nuclear receptor Rora.[10,11] Activated Rora induces cartilage-degrading enzymes, in turn promoting OA development.[11] Accordingly, novel therapeutic strategies involving modulation of serum cholesterol or intracellular cholesterol levels in chondrocytes may have potential clinical efficacy against OA. The serum cholesterol level is increased via biosynthesis in the liver and dietary cholesterol absorption from the intestine. Cholesterol accumulating in the liver combines with very low–density lipoprotein (VLDL)-containing TGs to form low-density lipoprotein (LDL) and is transported to peripheral tissues. LDL interacts with peripheral cells via lipoprotein receptors, resulting in cholesterol influx into cells. Intracellular cholesterol homeostasis is regulated by conversion to other molecules or efflux. Cholesterol efflux from the cell is mediated by high-density lipoprotein (HDL), which interacts with efflux mediators, including Abca1, Abcg1, and Scarb1. HDL delivers cholesterol to the liver for conversion to bile acid and is excreted from the body.[12]

Hypercholesterolemia, characterized by elevated LDL cholesterol in serum, is a major risk factor for atherosclerosis and is linked to complications such as coronary artery disease, stroke, peripheral vascular disease, and kidney issues, as well as metabolic disorders like hypertension and diabetes.[13] Elevated serum cholesterol also affects intracellular cholesterol levels in various tissues, especially adipose tissue, leading to abnormal adipocyte hypertrophy and macrophage differentiation.[14] Therefore, cholesterol-lowering drugs may be effectively employed to manage diverse atherosclerotic complications, metabolic disorders, and intracellular alterations in various tissues through regulation of serum lipid levels. Numerous studies to date have explored the potential of cholesterol-lowering drugs in the management of OA.[15–19] However, their efficacy remains a subject of considerable debate, and no definitive conclusions have been reached.

In the current study, our first objective was to investigate the effects of cholesterol-lowering drugs on cartilage degeneration in patients with OA. To this end, five drugs with distinct mechanisms of action were selected. Statins are well-known cholesterol-lowering drugs that suppress cholesterol synthesis by inhibiting the hydroxymethylglutaryl-coenzyme A reductase activity, the rate-limiting step of cholesterol biosynthesis. Ezetimibe is a commonly used drug often combined with statins that can reduce serum cholesterol levels by inhibiting cholesterol absorption from the small intestine through Npc1l1 blockade in enterocytes. Fenofibrate promotes HDL production via Ppara activation, thereby inducing cholesterol efflux. Niacin inhibits the Dgat2 activity, leading to reduced synthesis of TGs and, consequently, a decrease in the serum VLDL and LDL levels. Lomitapide inhibits the microsomal TG transfer protein activity, thereby blocking VLDL synthesis and reducing serum LDL levels.[20,21]

By comparing the effects of these drugs on cartilage degeneration, we sought to determine which mechanism of cholesterol regulation could be an effective target for OA treatment. Additionally, we aimed to investigate whether conditions mimicking OA could induce abnormal accumulation of intracellular cholesterol in chondrocytes, not only as a result of increased cholesterol uptake but also due to blockage of cholesterol efflux. We also determined whether the cholesterol efflux dysfunction during OA pathogenesis relies on down-regulation of apolipoprotein A1–binding protein (AIBP), a factor that boosts cholesterol efflux by facilitating interactions between Abca1 and apolipoprotein A1 (Apoa1), a major component of HDL.[22] Finally, we sought to demonstrate whether AIBP-mediated cholesterol efflux effectively reversed the cartilage destruction. In summary, our objective is to verify the potential of inhibiting OA by regulating serum cholesterol levels through cholesterol-lowering drugs or by controlling intracellular cholesterol levels through the induction of cholesterol efflux.

## PATIENTS AND METHODS

**Human participants.** Human data from the Korea National Health and Nutrition Examination Survey (KNHNES) VII (2017–2020) were analyzed. Data were obtained after approval from the Institutional Review Board of the Korea Disease Control and Prevention Agency (2018-01-03-2C-A). Further details can be found in the Supplementary Materials and Methods. Human sera were obtained from the Hallym Aging Study.[23,24] Samples were obtained after approval from the Institutional Review Board of Hallym University (HIRB-2007-001). Written informed consent was obtained from all study participants. The sera of individuals with Kellgren–Lawrence (KL) grade 0 and patients with OA with KL grade 3 or 4 were analyzed as previously described[25] to measure the serum cholesterol levels. Details are provided in the Supplementary Materials and Methods.

**Animal studies.** C57BL/6 male and female mice (5 weeks old) were purchased from Damool Science. Experimental OA was induced by destabilization of the medial meniscus (DMM) surgery on the right knee joints during feeding a 2% cholesterol-containing diet (high-cholesterol diet [HCD]) with or without cholesterol-lowering drug administration or intra-articular (IA) injection of adenovirus overexpressing *Aibp* or

BI0115. Mice were housed at a constant temperature and relative air humidity with a 12-hour light/dark cycle in pathogen-free barrier facilities at Chonnam National University. For each experiment, sex- and age-matched mice were used and randomly allocated to each experimental group. All experiments using mice were approved by the Animal Care and Ethics Committees of Chonnam National University (IACUC-YB-R-2019-92). Details are provided in the Supplementary Materials and Methods.

**Statistical analysis.** All experiments were performed independently at least three times. Appropriate statistical methods are selected based on the number of comparisons and type of variables. Briefly, Osteoarthritis Research Society International (OARSI)/osteophyte/synovitis scores, being ordinal variables, were analyzed using Mann–Whitney U test or Kruskal–Wallis test. For continuous variables such as subchondral bone plate (SBP) thickness, cholesterol assay, oxidized HDL enzyme-linked immunosorbent assay, efflux assay, and quantitative reverse transcriptase–polymerase chain reaction results, *t*-test or one-way analysis of variance (ANOVA) was employed. In one-way ANOVA, the type of post hoc test was determined based on the homogeneity of variances. Significance was accepted at $P$ less than 0.05. Details are provided in the Supplementary Materials and Methods.

**Data availability.** Microarray data have been deposited at the GEO under accession codes GSE104793 (interleukin [IL]-1β), GSE104794 (*Epas1*), and GSE104795 (*Zip8*). All other data that support the findings of this study are available on reasonable request from the corresponding author. Additional methods are included in the Supplemental Material and Methods.

## RESULTS

**Close correlation between abnormal cholesterol metabolism and OA pathogenesis.** To establish the clinical association between hyperlipidemia and OA pathogenesis, logistic regression analysis was conducted on the relationship between diagnostic criteria of hyperlipidemia according to serum lipid levels and OA incidence based on health surveys and a questionnaire survey targeting 34,598 participants aged 19 to 75 years (KNHNES 2007–2020). Our results demonstrated a positive correlation between hyperlipidemia, specifically hyper-TG levels ≥200 mg/dL, and hypo-HDL levels ≤40 mg/dL and the incidence of OA (Table 1).

Further stratification of patients revealed a stronger association between low serum HDL levels and OA in female patients compared to male patients as well as in both elderly male and female patients older than 50 years of age (Supplementary Tables 1–3). These trends are similar to the reported prevalence of OA, which is higher in women and more common with advanced age.[26] To further validate these findings, we analyzed the serum lipid profiles of healthy controls and patients with OA diagnosed with KL grades 3 to 4 presenting with severe symptoms. Consistent with data from logistic regression analysis, serum HDL levels were significantly lower in both male and female patients with OA. Total cholesterol (TC) and LDL levels displayed a tendency of increase in patients with OA but were not statistically significant (Figure 1A).

**Table 1.** Distribution of dyslipidemia components in subjects with and without osteoarthritis and results of logistic regression analysis of data based on health surveys and questionnaire survey targeting of participants aged 19 to 75 years (n = 34,598 participants; Korea National Health and Nutrition Examination Survey 2007–2020)*

| | | | Model 1 | | Model 2 | |
|---|---|---|---|---|---|---|
| Component | No OA, n (%) | OA, n (%) | OR (95% CI) | *P* value | OR (95% CI) | *P* value |
| Hyper-TC | | | | | | |
| No | 23,146 (82.53) | 3,955 (68.55) | 1 | <0.0001 | 1 | 0.2260 |
| Yes | 5,631 (17.47) | 1,866 (31.55) | 2.17 (2.02–2.33) | <0.0001 | 0.94 (0.85–1.04) | 0.2260 |
| Hyper-TG | | | | | | |
| No | 24,619 (84.89) | 4,908 (84.11) | 1 | 0.2181 | 1 | 0.0036 |
| Yes | 4,158 (15.11) | 913 (15.89) | 1.06 (0.97–1.17) | 0.2181 | 1.20 (1.06–1.35) | 0.0036 |
| Hypo-HDL | | | | | | |
| No | 24,141 (84.07) | 4,606 (80.28) | 1 | <0.0001 | 1 | <0.0001 |
| Yes | 4,636 (15.93) | 1,215 (19.72) | 1.30 (1.19–1.42) | <0.0001 | 1.32 (1.17–1.48) | <0.0001 |
| Hyper-LDL | | | | | | |
| No | 26,220 (91.45) | 5,190 (89.20) | 1 | <0.0001 | 1 | 0.9934 |
| Yes | 2,557 (8.55) | 631 (10.80) | 1.30 (1.16–1.45) | <0.0001 | 1.00 (0.87–1.15) | 0.9934 |
| Dyslipidemia | | | | | | |
| No | 19,756 (68.88) | 3,619 (62.82) | 1 | <0.0001 | 1 | <0.0001 |
| Yes | 9,021 (31.12) | 2,202 (37.18) | 1.31 (1.22–1.41) | <0.0001 | 1.22 (1.12–1.34) | <0.0001 |

* OR and 95% CI were estimated using logistic regression analysis. Model 1 was unadjusted model. Model 2 was adjusted for age, sex, body mass index, hypertension and diabetes. CI, confidence interval; HDL, high-density lipoprotein; LDL, low-density lipoprotein; OA, osteoarthritis; OR, odds ratio; TC, total cholesterol; TG, triglyceride.

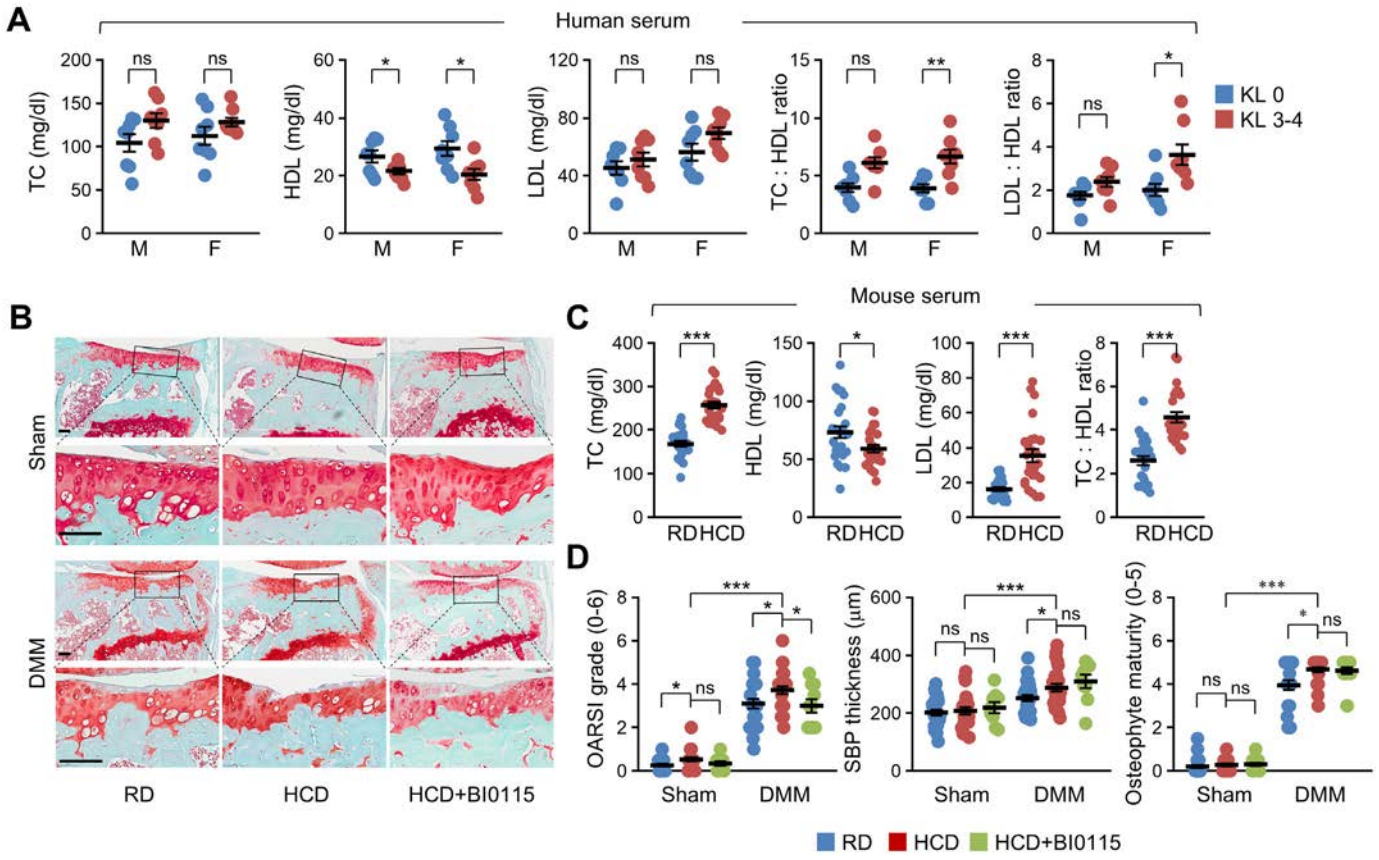


**Figure 1.** Hypercholesterolemia is closely associated with OA pathogenesis, and regulation of cholesterol transport modulates OA progression. (A) Serum TC, HDL, LDL, TC to HDL ratio, and LDL to HDL ratio of human male and female patients with OA diagnosed with KL grades 0 and 3 to 4, respectively (n = 8 per group). *$P < 0.05$, **$P < 0.01$. (B) Representative safranin O staining images of knee joint (scale, 100 μm), (C) serum cholesterol profiling, and (D) scoring of OARSI grade, SBP thickness, and osteophyte maturity in male mice fed an RD or HCD with or without BI0115 intra-articular injection and subjected to DMM surgery (RD, HCD n = 26, HCD+BI0115 n = 18, total 70 mice). Circles represent individual samples; lines with whiskers show the mean ± SEM. *$P < 0.05$, ***$P < 0.005$. Significant differences were detected by (A and C) two-tailed *t*-test for serum cholesterol profiling and (D) SBP thickness between sham and DMM and one-way analysis of variance with Bonferroni post hoc test for SBP thickness among RD, HCD, and HCD+BI0115 or Mann–Whitney U test for OARSI, osteophyte, and synovitis score between sham and DMM and Kruskal–Wallis test for OARSI, osteophyte, and synovitis score among RD, HCD, and HCD+BI0115. DMM, destabilization of the medial meniscus; F, female; HCD, high-cholesterol diet; HCD+BI0115, HCD with BI0115; HDL, high-density lipoprotein; KL, Kellgren–Lawrence; LDL, low-density lipoprotein; M, male; ns, not significant; OA, osteoarthritis; OARSI, Osteoarthritis Research Society International; RD, regular diet; SBP, subchondral bone plate; TC, total cholesterol.

Associations of serum cholesterol levels with OA pathogenesis were further evaluated in a mouse model with OA administered with an HCD. In the joints of mice with OA induced through DMM surgery, an HCD significantly exacerbated cartilage degradation (evaluated as OARSI grade), thickening of SBP, and osteophyte formation accompanied by elevated TC and LDL levels and decreased HDL levels (Figure 1B–D). In a previous study, we demonstrated increased cholesterol influx into chondrocytes under conditions mimicking OA due to up-regulation of Olr1, an oxidized LDL receptor.[11] To evaluate the significance of abnormal intracellular cholesterol accumulation resulting from increased exogenous cholesterol supply in OA pathogenesis, Olr1 function was suppressed through IA injection of BI0115, a selective Olr1 inhibitor. Administration of BI0115 resulted in attenuation of cartilage degradation (Figure 1D), confirming an association between OA pathogenesis and hyperlipidemia. Synovial inflammation was not regulated by an HCD or IA injection of BI0115 (Supplementary Figure 1A). These results suggest that cholesterol-lowering drugs that reduce serum cholesterol levels or strategies promoting cholesterol efflux to lower intracellular cholesterol levels have potential utility in modulation of OA progression.

**Alleviation of OA through regulation of serum cholesterol levels via cholesterol-lowering drugs.** To ascertain whether the reduction of serum cholesterol levels by cholesterol-lowering drugs plays a regulatory role on OA progression, we selected five clinically approved cholesterol-lowering drugs for treatment to mice fed an HCD with DMM surgery. The selected drugs used in this experiment have been shown to regulate serum cholesterol levels through distinct mechanisms.

Fenofibrate promotes cholesterol efflux by stimulating HDL production in the liver, atorvastatin inhibits cholesterol biosynthesis in the liver, ezetimibe blocks the absorption of dietary cholesterol in the intestine, and niacin and lomitapide reduce VLDL production in the liver and down-regulate LDL formation (Supplementary Figure 2A). Four weeks after HCD feeding, all cholesterol-lowering drugs were administered for nine weeks. DMM surgery was performed three weeks after the start of treatment with cholesterol-lowering drugs (Figure 2A; Supplementary Figure 2B).

Dietary administration of all drugs led to reduction of the serum TC level, which was elevated by the HCD. As their reported mechanisms of action, fenofibrate increased serum HDL, whereas ezetimibe and lomitapide suppressed serum LDL levels (Figures 2B and 3A). Among these drugs, fenofibrate clearly exerted protective effects against cartilage destruction and subchondral bone sclerosis in male mice. Although atorvastatin and ezetimibe showed a tendency to reduce cartilage destruction, the effects were not statistically significant. In contrast, niacin and lomitapide exerted no protective effects against OA progression (Figure 2C and D). Female mice exhibited slightly different responses to cholesterol-lowering drugs compared to male mice. In female mice, ezetimibe exerted the most effective inhibition of cartilage destruction. Fenofibrate also reduced cartilage destruction. Atorvastatin, niacin, and lomitapide had no significant effect on OA progression in male mice. In contrast to in male mice, subchondral bone sclerosis was not regulated by cholesterol-lowering drugs in female mice (Figure 2B and C). None of the drugs influenced osteophyte formation and synovial inflammation in both male and female mice (Figures 2D and 3C; Supplementary Figure 1B). We conducted an experiment to test if fenofibrate could restore cartilage after OA onset. Fenofibrate mixed with an HCD was given to mice who underwent DMM operation. Results showed a trend toward reduced cartilage damage, but it was not statistically significant (Supplementary Figure 3).

To establish whether the inhibitory effects of the cholesterol-lowering drugs on osteoarthritic cartilage destruction are attributable to their actions on serum cholesterol levels and not influenced by locally expressed cholesterol or regulation of other factors (for example, Ppara targeting by fenofibrate) in chondrocytes, drugs were directly injected into the knee region of mice with OA induced with DMM fed an HCD. In contrast to the above findings (Figures 2 and 3), IA injection of the cholesterol-lowering drugs did not have an impact on cartilage degradation and serum lipid levels in mice (Supplementary Figure 4). Additionally, direct treatment of these drugs to osteoarthritic chondrocytes did not induce suppression of cartilage-degrading enzymes, such as *Mmp3*, *Mmp9*, *Adamts4*, and *Adamts5*, that are up-regulated during OA pathogenesis (Supplementary Figure 5). Our data indicate that protective effects of fenofibrate and ezetimibe against OA progression are mediated through regulation of serum cholesterol levels rather than direct interactions with chondrocytes. Accordingly, we propose that cholesterol-lowering drugs, particularly fenofibrate, may serve as therapeutic agents for both male and female patients with OA. Furthermore, these results highlight the effectiveness of HDL-mediated cholesterol efflux, the mechanism of action of fenofibrate, in OA therapy.

**Decreased cholesterol efflux ability in chondrocytes during OA pathogenesis, leading to impaired removal of excess cholesterol.** To further clarify the association between OA pathogenesis and cholesterol efflux, we investigated the potential alterations in HDL-mediated cholesterol efflux in chondrocytes during disease progression. Osteoarthritic chondrocytes treated with proinflammatory cytokines (IL-1β) or infected with adenovirus overexpressing OA regulators (Hif2a,[27] Zip8[28]) displayed accumulation of cholesterol-containing oxidized LDL (Figure 4A). The increase in intracellular cholesterol levels in osteoarthritic chondrocytes could be attributed to increased cholesterol influx, as suggested previously.[11] Additionally, this increase could be due to the inhibition of cholesterol efflux, the process through which excess cholesterol within cells is removed by HDL. Microarray analysis of osteoarthritic chondrocytes revealed significant alterations in the expression patterns of genes related to cholesterol metabolic process, including intracellular cholesterol sensing factors (*Insig2*), oxysterol synthases (*Ch25h*, *Cyp7b1*), and HDL receptors (*Abca1*, *Abca2*, *Scarb1*; Figure 4B). These gene expression patterns appear to represent adaptive responses to reduce intracellular cholesterol levels in osteoarthritic chondrocytes. Microarray analysis additionally revealed significant increases in the expression of HDL-associated proteins, including the serum amyloid A (SAA) family, and haptoglobin (Hp), known for their roles in inducing the formation of dysfunctional HDL and disrupting cholesterol efflux from cells (Figure 4B).[29–31]

Consistent with this finding, the production of oxidized HDL, a type of dysfunctional HDL,[32,33] increased in the culture medium of osteoarthritic chondrocytes along with HDL (Figure 4C). Moreover, the expression levels of genes involved in cholesterol efflux, including HDL receptors (*Abca5*,[34] *Abca8*[35]), cholesterol ester–forming enzyme (*Soat1*[36]), and HDL-binding proteins (*Aibp*[22]), except canonical efflux mediators such as *Abca1* and *Scarb1*, were decreased in osteoarthritic chondrocytes (Figure 4D; Supplementary Figure 6). These results suggest that the cholesterol efflux from OA chondrocytes is inhibited by the production of dysfunctional HDL and decrease in noncanonical cholesterol efflux mediators. Indeed, HDL-mediated cholesterol efflux from cholesterol-loaded chondrocytes was suppressed following treatment with proinflammatory cytokines, such as IL-1β, leading to elevated intracellular cholesterol concentrations (Figure 4E). Based on the collective findings, we conclude that inefficient cholesterol efflux is a significant factor to abnormal accumulation of cholesterol observed in patients with osteoarthritic chondrocytes.

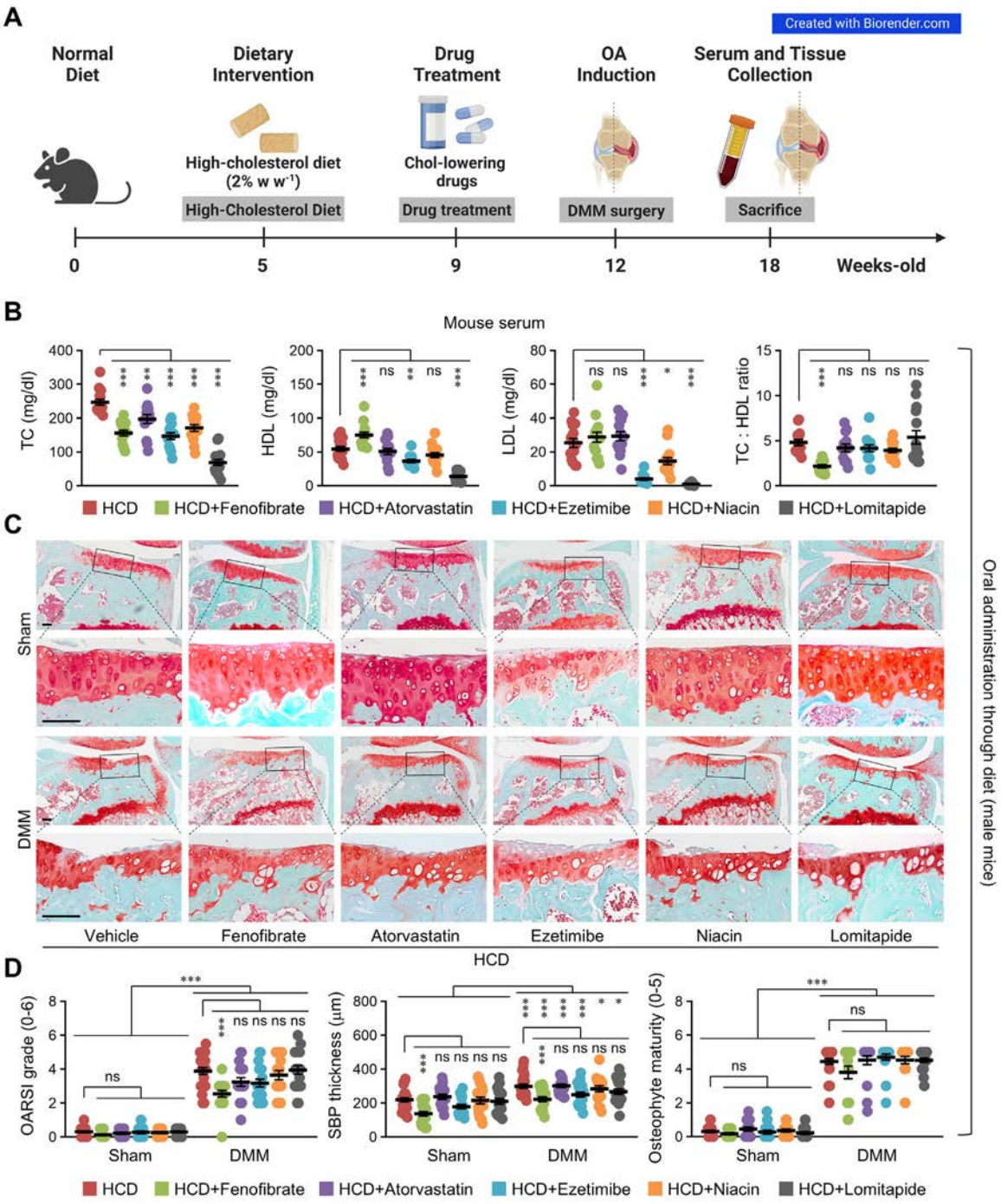


**Figure 2.** Dietary administration of Chol-lowering drugs regulates serum Chol levels and fenofibrate inhibits cartilage destruction in male mice with OA who were fed an HCD. (A) Timeline of animal experiment with OA for Chol-lowering drug administration. (B) Serum Chol profiling (n ≥ 13 per group). *$P < 0.05$, **$P < 0.01$, ***$P < 0.005$. (C) Representative safranin O staining images of knee joint (scale, 100 μm) and scoring of OARSI grade, SBP thickness, and osteophyte maturity in male mice fed an HCD with Chol-lowering drugs and subjected to DMM surgery (HCD n = 29, HCD with drug administration n = 20, total 129 mice). Circles represent individual samples; lines with whiskers show the mean ± SEM. *$P <$ 0.05, ***$P <$ 0.005. Significant differences were detected by (D) two-tailed *t*-test for SBP thickness between sham and DMM groups and (B) one-way ANOVA with Bonferroni or Dunnett T3 post hoc test for serum Chol profiling and (D) SBP thickness between groups with HCD and HCD with drug administration or Mann–Whitney U test for OARSI grade and osteophyte maturity between sham and DMM group and Kruskal–Wallis test for OARSI grade and osteophyte maturity between groups HCD and HCD with drug administration. Chol, cholesterol; DMM, destabilization of the medial meniscus; HCD, high-Chol diet; HCD+Atorvastatin, HCD with atorvastatin; HCD+Ezetimibe, HCD with ezetimibe; HCD +Fenofibrate, HCD with fenofibrate; HCD+Lomitapide, HCD with lomitapide; HCD+Niacin, HCD with niacin; HDL, high-density lipoprotein; LDL, low-density lipoprotein; ns, not significant; OA, osteoarthritis; OARSI, Osteoarthritis Research Society International; SBP, subchondral bone plate; TC, total Chol; w $w^{-1}$, weight in weight.

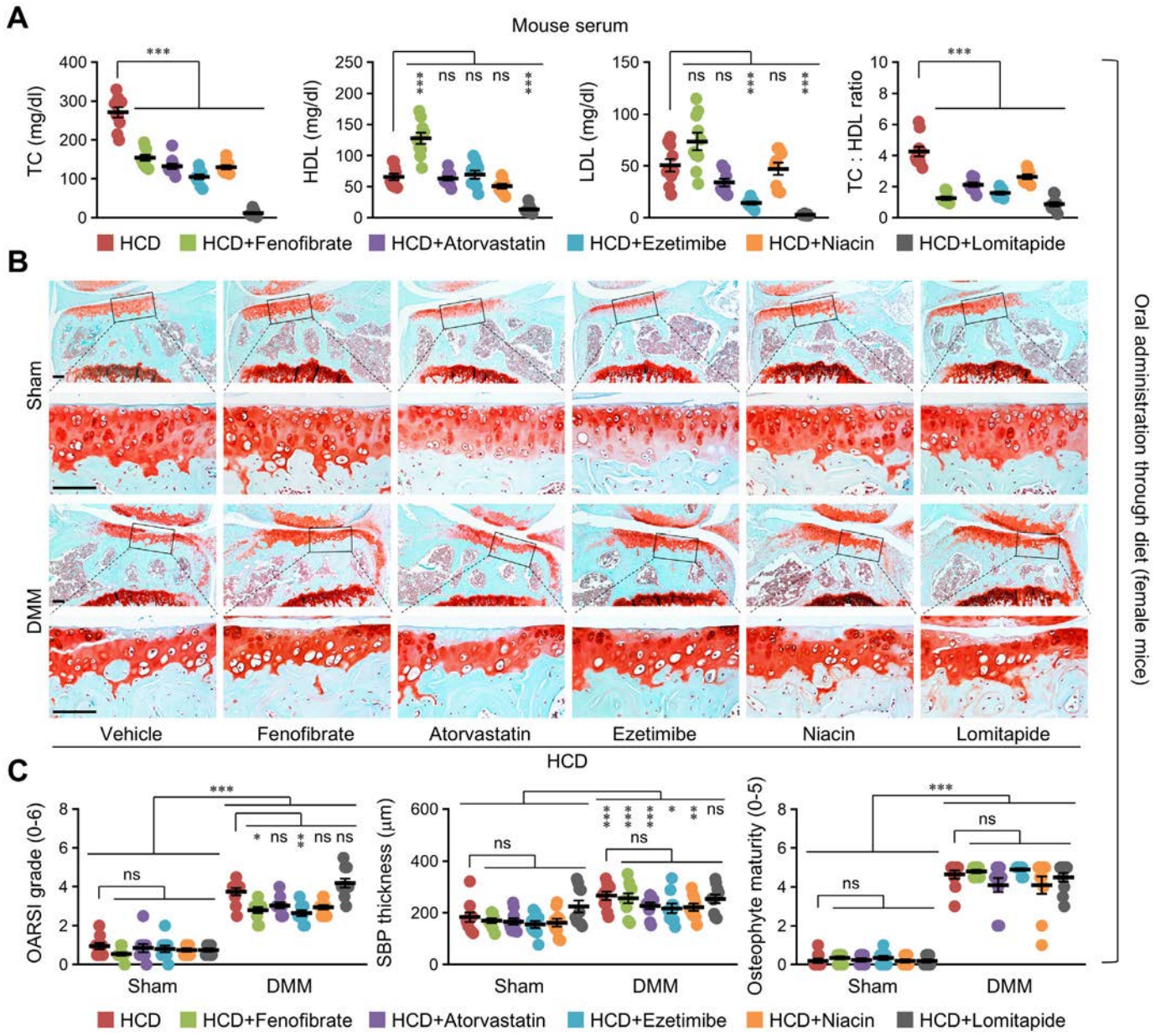


**Figure 3.** Dietary administration of cholesterol-lowering drugs regulates serum cholesterol levels, and fenofibrate and ezetimibe inhibit cartilage destruction in female mice with OA fed an HCD. (A) Serum cholesterol profiling (n = 10 per group). ***$P < 0.005$. (B) Representative safranin O staining images of the knee joint (scale, 100 μm) and scoring of OA parameters including OARSI grade, SBP thickness, and osteophyte maturity in female mice fed an HCD with cholesterol-lowering drugs and subjected to DMM surgery (n = 10 mice per group, total 60 mice). Circles represent individual samples; lines with whiskers show the mean ± SEM. *$P < 0.05$, **$P < 0.01$, ***$P < 0.005$. Significant differences were detected by (C) two-tailed t-test for SBP thickness between sham and DMM groups and (A) one-way ANOVA with Dunnett T3 post hoc test for serum cholesterol profiling and (C) SBP thickness between groups with HCD and HCD with drug administration or Mann–Whitney U test for OARSI grade and osteophyte maturity between groups with sham and DMM and Kruskal–Wallis test for OARSI grade and osteophyte maturity between groups with HCD and HCD with drug administration. DMM, destabilization of the medial meniscus; HCD, high-cholesterol diet; HCD+Atorvastatin, HCD with atorvastatin; HCD+Ezetimibe, HCD with ezetimibe; HCD+Fenofibrate, HCD with fenofibrate; HCD+Lomitapide, HCD with lomitapide; HCD+Niacin, HCD with niacin; HDL, high-density lipoprotein; LDL, low-density lipoprotein; ns, not significantly different; OA, osteoarthritis; OARSI, Osteoarthritis Research Society International; SBP, subchondral bone plate; TC, total cholesterol.

**Prevention of OA through promotion of AIBP-mediated cholesterol efflux from osteoarthritic chondrocytes.** The above results suggest that stimulation of HDL-mediated intracellular cholesterol efflux offers a novel approach for management of OA. Direct treatment of cholesterol-preloaded osteoarthritic chondrocytes with HDL resulted in decreased expression of matrix-degrading genes, including *Mmp3*, *Mmp9*, *Mmp12*, *Mmp13*, *Adamts4*, and

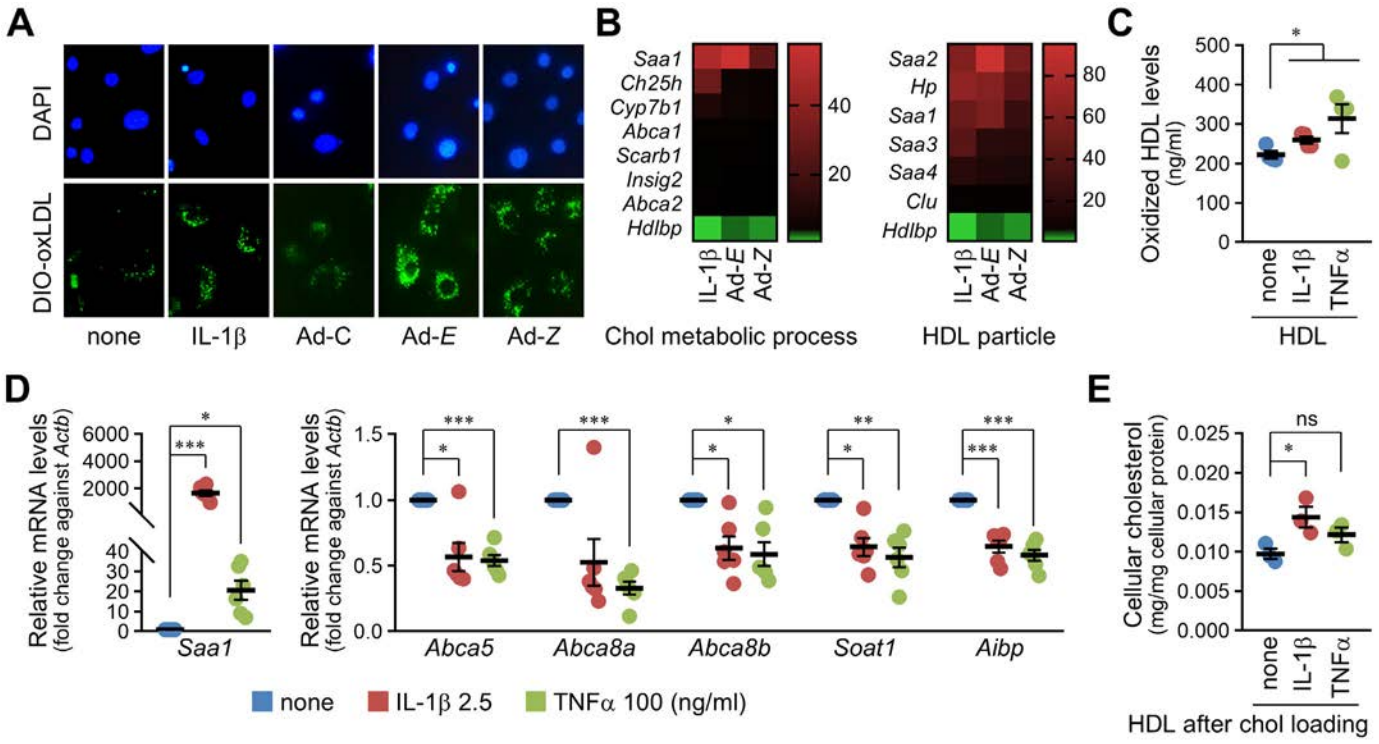


**Figure 4.** Chol efflux is suppressed in osteoarthritis chondrocytes via HDL oxidization and expression of efflux mediators is reduced. (A) Representative immunofluorescence image of DIO-oxLDL uptake (n = 4) and (B) heatmap of microarray showing genes of Chol metabolic process (GO 0008203) and HDL particle (GO 0034364) (n = 3) in chondrocytes treated with IL-1β (2.5 ng/mL) or infected with adenovirus overexpressing *Epas1* (Ad-*E*) and *Zip8* (Ad-*Z*). (C) Oxidized HDL levels in culture media incubated with chondrocytes treated with IL-1β (5 ng/mL) or TNFα (100 ng/mL) in the presence of HDL (10 μg/mL; n = 4). **P* < 0.05. (D) mRNA levels of *Saa1* and indicated Chol efflux mediators in chondrocytes treated with IL-1β or TNFα (n = 6). **P* < 0.05, ***P* < 0.01, ****P* < 0.005. (E) Cellular Chol levels in Chol-preloaded chondrocytes (800 μM) treated with IL-1β (2.5 ng/mL) or TNFα (50 ng/mL) in the presence of HDL (50 μg/mL; n = 3). Circles represent individual samples; lines with whiskers show mean ± SEM. **P* < 0.05. Significant differences were detected by (C) two-tailed *t*-test for oxidized HDL enzyme-linked immunosorbent assay and (E) Chol assay or (D) one-way analysis of variance with Dunnett T3 post hoc test for mRNA levels. Ad-C, control adenovirus; Chol, cholesterol; DIO-oxLDL, 3,3'-dioctadecyloxacarbocyanine-lebelled oxidized LDL; GO, Gene Ontology; HDL, high-density lipoprotein; IL, interleukin; mRNA, messenger RNA; ns, not significant; TNF, tumor necrosis factor.

*Adamts5*, supporting the theory that stimulation of intracellular cholesterol efflux plays a regulatory role in OA pathogenesis (Supplementary Figure 7A and B). During the search for factors that regulate the expression of cartilage-degrading enzymes by promoting intracellular cholesterol efflux, we observed a notable decrease in the expression of AIBP in osteoarthritic chondrocytes (Figure 4D; Supplementary Figure 6). Because AIBP is known to be involved in various biologic processes through the promotion of cholesterol efflux,[37–39] we examined the hypothesis that the AIBP acts as a potential regulatory factor in OA development by promoting cholesterol efflux in chondrocytes and mice with OA. In the cartilage of mice with OA, AIBP was down-regulated similar to data obtained with osteoarthritic chondrocytes (Figure 5A). Adenoviral overexpression of *Aibp* promoted cholesterol efflux from chondrocytes (25.8%–40.3%; Figure 5B). Concomitant with induction of cholesterol efflux, matrix-degrading gene expression including *Mmp3*, *Mmp12*, *Mmp13*, and *Adamts5* in IL-1β–treated chondrocytes was suppressed (Figure 5C).

In addition, IA injection of *Aibp*-encoding adenovirus in mouse cartilage reduced cartilage destruction and subchondral sclerosis induced by DMM surgery alone (Figure 5D and E) and in combination with an HCD (Figure 5F and G). These findings suggest that AIBP-mediated cholesterol efflux effectively counteracts cartilage destruction resulting from abnormal intracellular cholesterol accumulation. In summary, we propose that normalization of cholesterol levels using fenofibrate or promotion of cholesterol efflux through *Aibp* overexpression may potentially provide a promising therapeutic approach for OA.

## DISCUSSION

As a common degenerative disease, OA is historically considered a disease caused by accumulating mechanical stress in cartilage due to aging. Recently, several studies have revealed the association between OA and cholesterol levels in serum or cartilage tissue, indicating the potential impact of dyslipidemia on OA progression.[9–11,17,40–42] These findings

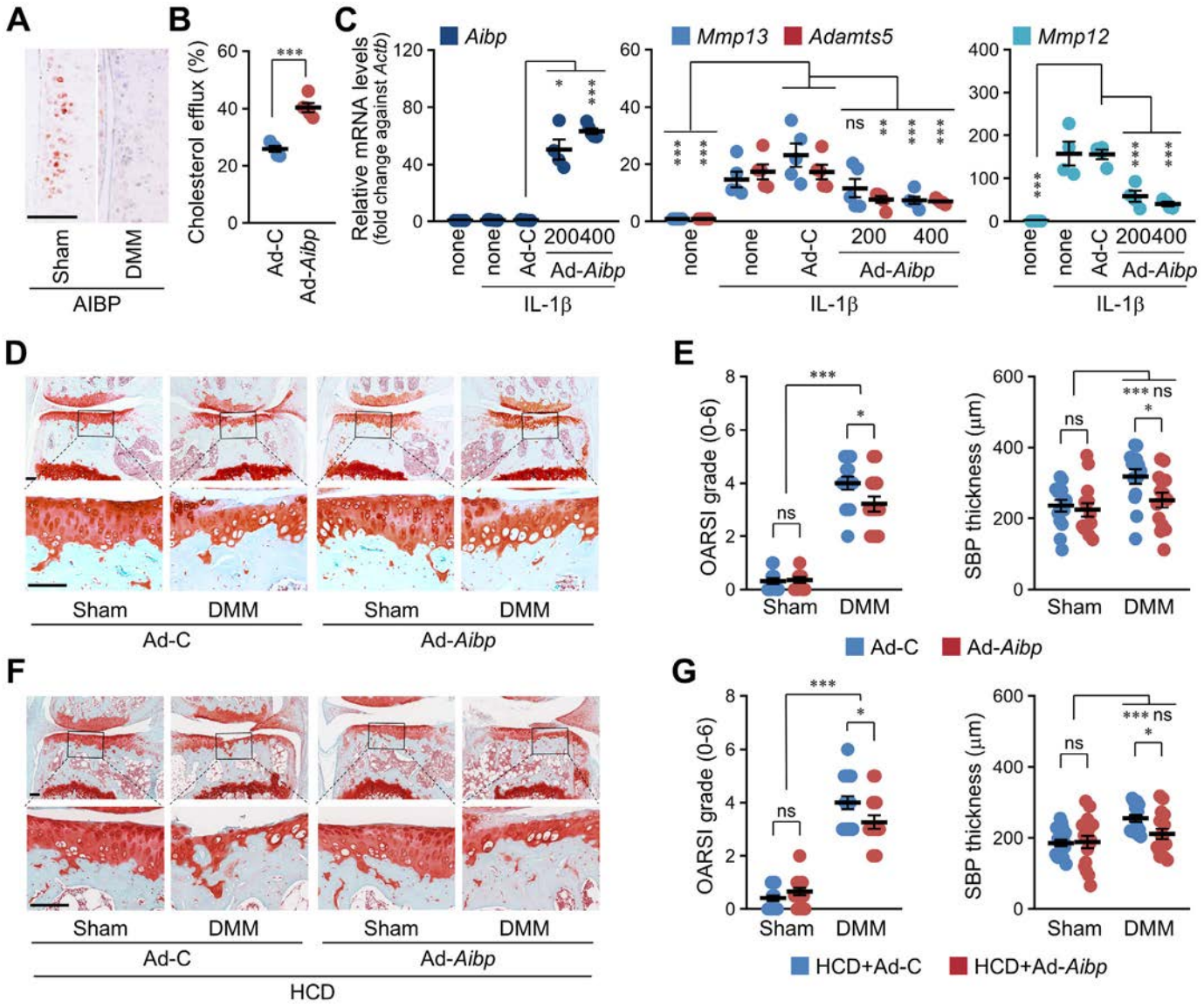


**Figure 5.** AIBP is down-regulated in OA cartilage, and its overexpression promotes cholesterol efflux from OA chondrocytes and inhibits disease progression. (A) Representative AIBP immunostaining images of cartilage from mice with DMM surgery. Scale, 100 μm (n = 4). (B) Cholesterol efflux from chondrocytes infected with a multiplicity of infection of 400 of Ad-*Aibp* (n = 5). ***$P < 0.005$. (C) mRNA levels of indicated genes (n ≥ 4) in chondrocytes infected with Ad-*Aibp* in the presence of IL-1β (2.5 ng/mL). *$P < 0.05$, **$P < 0.01$, ***$P < 0.005$. (D and F) Representative safranin O staining images of knee joint (scale, 100 μm) and (E and G) OARSI grade and SBP thickness in male mice fed a (D and E) regular diet (n = 14 mice per group, total 28 mice) or (F and G) HCD (n = 17 mice per group, total 34 mice) with Ad-*Aibp* intra-articular injection and subjected to DMM surgery. Circles represent individual samples; lines with whiskers show mean ± SEM. *$P < 0.05$, ***$P < 0.005$. Significant differences were detected by two-tailed *t*-test for (B) cholesterol efflux and (E and G) SBP thickness or (C) one-way analysis of variance with Dunnett T3 post hoc test for mRNA levels or (E and G) Mann–Whitney U test for OARSI grade. Ad-*Aibp*, adenovirus overexpressing *Aibp*; Ad-C, control adenovirus; AIBP, apolipoprotein A1–binding protein; DMM, destabilization of the medial meniscus; HCD, high-cholesterol diet; HCD+Ad-*Aibp*, HCD with Ad-*Aibp*; HCD+Ad-C, HCD with Ad-C; IL, interleukin; mRNA, messenger RNA; ns, not significant; OA, osteoarthritis; OARSI, Osteoarthritis Research Society International; SBP, subchondral bone plate.

suggest that elevated cholesterol exacerbates cartilage degradation and OA progression. In addition, several studies have examined the role of cholesterol-lowering drugs in OA progression.[18,43–45] However, there has been no research directly investigating the mechanisms by which cholesterol-lowering drugs may influence OA progression or comparing the inhibitory effects of various cholesterol-lowering drugs on OA progression. In this study, our aim was to identify the most effective cholesterol-lowering mechanisms and administration routes for OA treatment and to propose new OA regulatory targets based on these findings. By extending beyond the clinical potential suggested by previous studies, we have

demonstrated the efficacy of cholesterol-lowering drugs through the elucidation of their molecular mechanisms.

Data from serum lipid profiling of patients with OA and logistic regression analysis (Table 1) confirm that decreased HDL and increased TG in serum are positively correlated with OA pathogenesis. Previous studies have demonstrated a link between serum HDL and TG levels and development of OA but no significant positive correlation of pathogenesis with TC and LDL levels.[40,46] This lack of correlation could be attributed to the widespread use of statin-type cholesterol-lowering medications among patients who were hyperlipidemic in the surveyed population. For accurate assessment of the relationship between serum TC and LDL levels and OA development, future analyses should exclude patients who receive cholesterol-lowering drugs.

In our study, administration of all cholesterol-lowering drugs led to the reduction of serum TC levels. However, only fenofibrate and ezetimibe showed protective activity against cartilage destruction, as shown in Figures 2 and 3. The results suggest that enhancing cholesterol efflux from cartilage tissue (fenofibrate) or inhibition of the external cholesterol uptake (ezetimibe) may be more effective than other cholesterol-lowering drugs that inhibit biosynthesis (atorvastatin) or transport (niacin, lomitapide). Although treatment with both ezetimibe and lomitapide led to similar reductions in serum TC and LDL, it is important to note that lomitapide did not exert a protective effect against OA progression in mice. Administration of lomitapide led to a reduction in serum HDL levels compared to ezetimibe, further supporting the theory that decreased serum HDL levels are closely associated with the development of OA.

Our additional data revealed that fenofibrate or ezetimibe administration can reduce cholesterol-induced cartilage destruction, but the correlation between cartilage integrity and liver health remains unclear. Histologic analysis of liver tissue indicates that cholesterol accumulation in cartilage tissue is more closely associated with cartilage destruction than cholesterol accumulation in liver tissue (data not shown). However, the effect of long-term steatosis or other liver diseases on OA pathogenesis remains unclear and requires further study.

Although systemic administration of cholesterol-lowering drugs inhibited cartilage damage, IA injection did not show an inhibitory effect on cartilage damage. We suggested that protective effects of these drugs are not due to their direct impact on chondrocytes but rather may be attributed to their systemic action targeting the synthesis, absorption, transport, and excretion of cholesterol, which in turn reduces cholesterol levels in cartilage tissue. Our suggestion can be supported by subsequent experiments showing that direct treatment of chondrocytes with cholesterol-lowering drugs did not regulate the cartilage-degrading enzyme expression. Conversely, treating the HDL or inducing the overexpression of AIBP in chondrocytes reduced matrix-degrading enzyme expression in chondrocytes, thereby supporting our suggestion. These experiments were conducted to mimic the systemic alteration of cholesterol transport, particularly cholesterol efflux.

Some previous studies revealed that direct statin treatment could inhibit matrix-degrading enzyme expression and that statins are effective in preventing OA progression.[45] However, meta-analysis of observational studies found no significant association between statin reception and OA development.[16] In other studies, ezetimibe treatment to chondrocytes showed protective effects against IL-1β–induced extracellular matrix degradation.[44] However, administration of ezetimibe to mice who were hyperlipidemic and fed an HCD did not inhibit the OA progression.[17] Unlike these previous studies, our data showed that direct treatment of atorvastatin or ezetimibe did not inhibit matrix-degrading enzyme expression, and dietary administration of atorvastatin tends to protect OA progression but is not statistically significant. Additionally, dietary administration of ezetimibe showed a protective effect against cartilage destruction in only female mice. This difference between previous studies and our data appears to be due to differences in animal models and doses of drug received.

Fenofibrate, an agonist of Ppara, activates lipolysis and eliminates TG-rich particles from the plasma. Earlier studies have shown that fenofibrate has the potential to attenuate OA progression regardless of HDL up-regulation. Nogueira-Recalde et al[18] suggested that fenofibrate inhibits OA progression by inducing apoptosis and autophagy in senescent chondrocytes through regulation of Ppara activity. Therefore, the theory that the protective effect of fenofibrate against cartilage destruction may be due to removal of senescent chondrocytes rather than regulation of serum cholesterol levels could not be ruled out. However, in contrast to this study, we showed that direct treatment of chondrocytes or IA injection of fenofibrate had no effect on the expression of cartilage-degrading enzymes and cartilage destruction. In addition, the down-regulation of cartilage-degrading enzymes with HDL treatment in chondrocytes indicates that fenofibrate-induced HDL up-regulation could suppress the progression of OA. The close association between reduced serum HDL levels and severity of OA, coupled with the inhibitory effect of fenofibrate on OA progression through elevation of HDL, highlights the potential significance of HDL-mediated cholesterol efflux in maintenance of cartilage homeostasis.

Considering that HDL performs various functions beyond cholesterol efflux, such as antithrombotic, antioxidant, and anti-inflammatory activities, the possibility that inhibition of cartilage-degrading enzyme expression by HDL may be attributed to its anti-inflammatory properties rather than its role in cholesterol efflux should not be overlooked. However, the association between cholesterol efflux and OA pathogenesis is strongly supported by previous studies that report a decrease in the expression of genes regulating cholesterol efflux, such as Apoa1, Abca1, and liver X receptor, in OA cartilage.[42,47] Moreover, our

experiments revealed intracellular cholesterol accumulation and inhibition of cholesterol efflux in osteoarthritic chondrocytes with dysfunctional HDL formation in addition to down-regulation of cholesterol efflux mediators, in particular AIBP. These results clearly indicate a definitive association between HDL-mediated cholesterol efflux and OA progression.

In our study, microarray analysis revealed a notable increase in the expression of HDL particles, including the SAA family,[29,48] and Hp,[30,31] which are known to impair the function of HDL and disrupt cholesterol efflux from cells. SAA family and Hp have also been identified as acute-phase proteins involved in the acute inflammatory response.[49] According to previous studies, the acute-phase protein SAA promotes the production of IL-6 and cartilage-degrading enzymes, such as Mmp1 and Mmp3, in chondrocytes and fibroblast-like synoviocytes.[41,49] Moreover, OA is regarded as a local inflammatory disease, and many factors involved in chronic- and acute-phase inflammation are up-regulated.[50] Therefore, the theory that up-regulated SAA family and Hp may act as acute-phase proteins induced by OA cannot be eliminated. To conclusively confirm the formation of dysfunctional HDL by SAA and Hp, we attempted to quantify dysfunctional HDL levels in synovial fluid from mice with OA. However, it was a challenge to obtain sufficient synovial fluid from mouse joint tissues. Assessment of dysfunctional HDL levels in the synovial fluid of human patients with OA would be ideal, but this is significantly hindered by difficulties in collecting synovial fluid from healthy individuals. Future studies should focus on precise analysis using synovial fluid samples.

Our collective results demonstrate that fenofibrate protects against cartilage destruction by regulating serum cholesterol levels, in particular enhancing HDL-mediated cholesterol efflux. Furthermore, AIBP, a factor that promotes cholesterol efflux, may serve as a novel therapeutic target for OA treatment. In summary, our findings highlight the potential applicability of existing cholesterol-lowering medications in mitigating OA progression. We anticipate the emergence of effective novel therapeutic avenues for OA treatment based on enhancement of HDL-mediated cellular cholesterol efflux.

We administered five different cholesterol-lowering drugs to experimental mice with OA who were fed an HCD and verified their protective role against cartilage destruction. Future research should observe the efficacy of cholesterol-lowering drugs in mice with OA according to skeletal maturity, investigate their effects in mice with aging-induced OA (as opposed to posttraumatic OA), and explore their therapeutic or regenerative effects after the onset of OA. Additionally, it is important to acknowledge that external factors such as drug concentration, experimental duration and conditions, and potential disparities in translating these findings to human applications warrant further comprehensive investigation. Moreover, comparative experiments with other drugs that were not examined in this study are essential. Future research should also explore the statistical differences between male and female patients under conditions in which body weight and serum lipid levels are controlled to ensure a more comprehensive understanding of the drug effects. This broader approach could provide deeper insights into how different medications and their distinct mechanisms of action affect OA progression, which may lead to potential new treatment options.

## ACKNOWLEDGMENTS

We thank Boehringer Ingelheim for providing the Lox-1 specific inhibitor BI0115 through the open innovation platform opnMe (https://opnme.com). The graphical abstract was created with BioRender.com. During the writing of this manuscript, a large language model (ChatGPT 3.5, OpenAI) was used for spelling and grammar checking and sentence correction.

## AUTHOR CONTRIBUTIONS

All authors contributed to at least one of the following manuscript preparation roles: conceptualization AND/OR methodology, software, investigation, formal analysis, data curation, visualization, and validation AND drafting or reviewing/editing the final draft. As corresponding author, Dr Ryu confirms that all authors have provided the final approval of the version to be published, and takes responsibility for the affirmations regarding article submission (eg, not under consideration by another journal), the integrity of the data presented, and the statements regarding compliance with institutional review board/Helsinki Declaration requirements.

## REFERENCES

1. Hunter DJ, March L, Chew M. Osteoarthritis in 2020 and beyond: a Lancet Commission. Lancet 2020;396:1711–1712.
2. Mobasheri A, Saarakkala S, Finnilä M, et al. Recent advances in understanding the phenotypes of osteoarthritis. F1000Res 2019;8:2091.
3. Coaccioli S, Sarzi-Puttini P, Zis P, et al. Osteoarthritis: new insight on its pathophysiology. J Clin Med 2022;11:6013.
4. Sobieh BH, El-Mesallamy HO, Kassem DH. Beyond mechanical loading: the metabolic contribution of obesity in osteoarthritis unveils novel therapeutic targets. Heliyon 2023;9:e15700.
5. Wei G, Lu K, Umar M, et al. Risk of metabolic abnormalities in osteoarthritis: a new perspective to understand its pathological mechanisms. Bone Res 2023;11:1–16.
6. Marshall M, Watt FE, Vincent TL, et al. Hand osteoarthritis: clinical phenotypes, molecular mechanisms and disease management. Nat Rev Rheumatol 2018;14:641–656.
7. Datta P, Zhang Y, Parousis A, et al. High-fat diet-induced acceleration of osteoarthritis is associated with a distinct and sustained plasma metabolite signature. Sci Rep 2017;7:8205.
8. Gkretsi V, Simopoulou T, Tsezou A. Lipid metabolism and osteoarthritis: lessons from atherosclerosis. Prog Lipid Res 2011;50:133–140.
9. Farnaghi S, Crawford R, Xiao Y, et al. Cholesterol metabolism in pathogenesis of osteoarthritis disease. Int J Rheum Dis 2017;20:131–140.
10. Farnaghi S, Prasadam I, Cai G, et al. Protective effects of mitochondria-targeted antioxidants and statins on cholesterol-induced osteoarthritis. FASEB J 2016;31:356–367.
11. Choi WS, Lee G, Song WH, et al. The CH25H–CYP7B1–RORα axis of cholesterol metabolism regulates osteoarthritis. Nature 2019;566:254–258.

12. Duan Y, Gong K, Xu S, et al. Regulation of cholesterol homeostasis in health and diseases: from mechanisms to targeted therapeutics. Sig Transduct Target Ther 2022;7:1–29.
13. Libby P, Buring JE, Badimon L, et al. Atherosclerosis. Nat Rev Dis Primers 2019;5:1–18.
14. Su X, Chen X, Wang B. Pathology of metabolically-related dyslipidemia. Clinica Chimica Acta 2021;521:107–115.
15. Zhang Z, Deng C, Ma X, et al. The association between statin use and osteoarthritis-related outcomes: an updated systematic review and meta-analysis. Front Pharmacol 2022;13:1003370.
16. Wang J, Dong J, Yang J, et al. Association between statin use and incidence or progression of osteoarthritis: meta-analysis of observational studies. Osteoarthritis Cartilage 2020;28:1170–1179.
17. Gierman LM, Kühnast S, Koudijs A, et al. Osteoarthritis development is induced by increased dietary cholesterol and can be inhibited by atorvastatin in APOE*3Leiden.CETP mice—a translational model for atherosclerosis. Ann Rheum Dis 2014;73:921–927.
18. Nogueira-Recalde U, Lorenzo-Gómez I, Blanco FJ, et al. Fibrates as drugs with senolytic and autophagic activity for osteoarthritis therapy. EBioMedicine 2019;45:588–605.
19. Sahin K, Kucuk O, Orhan C, et al. Niacinamide and undenatured type II collagen modulates the inflammatory response in rats with monoiodoacetate-induced osteoarthritis. Sci Rep 2021;11:14724.
20. Barter PJ, Rye KA. New era of lipid-lowering drugs. Pharmacol Rev 2016;68:458–475.
21. Michaeli DT, Michaeli JC, Albers S, et al. Established and emerging lipid-lowering drugs for primary and secondary cardiovascular prevention. Am J Cardiovasc Drugs 2023;23:477–495.
22. Zhang M, Li L, Xie W, et al. Apolipoprotein A-1 binding protein promotes macrophage cholesterol efflux by facilitating apolipoprotein A-1 binding to ABCA1 and preventing ABCA1 degradation. Atherosclerosis 2016;248:149–159.
23. Kim HA, Kim I, Song YW, et al. The association between meniscal and cruciate ligament damage and knee pain in community residents. Osteoarthritis Cartilage 2011;19:1422–1428.
24. Kim IJ, Kim DH, Jung JY, et al. Association between bone marrow lesions detected by magnetic resonance imaging and knee pain in community residents in Korea. Osteoarthritis Cartilage 2013;21:1207–1213.
25. Kim HE, Shin Y, Jung IJ, et al. Overexpression of secretory leukocyte peptidase inhibitor (SLPI) does not modulate experimental osteoarthritis but may be a biomarker for the disease. Osteoarthritis Cartilage 2021;29:558–567.
26. Theis KA, Murphy LB, Guglielmo D, et al. Prevalence of arthritis and arthritis-attributable activity limitation - United States, 2016-2018. MMWR Morb Mortal Wkly Rep 2021;70:1401–1407.
27. Yang S, Kim J, Ryu JH, et al. Hypoxia-inducible factor-2α is a catabolic regulator of osteoarthritic cartilage destruction. Nat Med 2010;16:687–693.
28. Kim JH, Jeon J, Shin M, et al. Regulation of the catabolic cascade in osteoarthritis by the zinc-ZIP8-MTF1 axis. Cell 2014;156:730–743.
29. Han CY, Tang C, Guevara ME, et al. Serum amyloid A impairs the antiinflammatory properties of HDL. J Clin Invest 2016;126:266–281.
30. Watanabe J, Grijalva V, Hama S, et al. Hemoglobin and its scavenger protein haptoglobin associate with apoA-1-containing particles and influence the inflammatory properties and function of high density lipoprotein. J Biol Chem 2009;284:18292–18301.
31. Vaisar T, Tang C, Babenko I, et al. Inflammatory remodeling of the HDL proteome impairs cholesterol efflux capacity. J Lipid Res 2015;56:1519–1530.
32. Shao B, Tang C, Sinha A, et al. Humans with atherosclerosis have impaired ABCA1 cholesterol efflux and enhanced high-density lipoprotein oxidation by myeloperoxidase. Circ Res 2014;114:1733–1742.
33. Rosenson RS, Brewer HB, Ansell BJ, et al. Dysfunctional HDL and atherosclerotic cardiovascular disease. Nat Rev Cardiol 2016;13:48–60.
34. Ray AG, Choudhury KR, Chakraborty S, et al. Novel mechanism of cholesterol transport by ABCA5 in macrophages and its role in dyslipidemia. J Mol Biol 2020;432:4922–4941.
35. Trigueros-Motos L, van Capelleveen JC, Torta F, et al. ABCA8 regulates cholesterol efflux and high-density lipoprotein cholesterol levels. Arterioscler Thromb Vasc Biol 2017;37:2147–2155.
36. Liu X, Ducasa GM, Mallela SK, et al. Sterol-O-acyltransferase-1 has a role in kidney disease associated with diabetes and Alport syndrome. Kidney Int 2020;98:1275–1285.
37. Fang L, Choi SH, Baek JS, et al. Control of angiogenesis by AIBP-mediated cholesterol efflux. Nature 2013;498:118–122.
38. Gu Q, Yang X, Lv J, et al. AIBP-mediated cholesterol efflux instructs hematopoietic stem and progenitor cell fate. Science 2019;363:1085–1088.
39. Choi SH, Wallace AM, Schneider DA, et al. AIBP augments cholesterol efflux from alveolar macrophages to surfactant and reduces acute lung inflammation. JCI Insight 2018;3:e120519.
40. Papathanasiou I, Anastasopoulou L, Tsezou A. Cholesterol metabolism related genes in osteoarthritis. Bone 2021;152:116076.
41. de Seny D, Cobraiville G, Charlier E, et al. Apolipoprotein-A1 as a damage-associated molecular patterns protein in osteoarthritis: ex vivo and in vitro pro-inflammatory properties. PLoS One 2015;10:e0122904.
42. Tsezou A, Iliopoulos D, Malizos KN, et al. Impaired expression of genes regulating cholesterol efflux in human osteoarthritic chondrocytes. J Orthop Res 2010;28:1033–1039.
43. Heidari B, Babaei M, Yosefghahri B. Prevention of osteoarthritis progression by statins, targeting metabolic and inflammatory aspects: a review. Mediterr J Rheumatol 2021;32:227–236.
44. Weng Q, Hu T, Shen X, et al. Ezetimibe prevents IL-1β-induced inflammatory reaction in mouse chondrocytes via modulating NF-κB and Nrf2/HO-1 signaling crosstalk. Curr Pharm Biotechnol 2022;23:1772–1780.
45. Saberianpour S, Abolbashari S, Modaghegh MH, et al. Therapeutic effects of statins on osteoarthritis: a review. J Cell Biochem 2022;123:1285–1297.
46. Garcia-Gil M, Reyes C, Ramos R, et al. Serum lipid levels and risk of hand osteoarthritis: the Chingford Prospective Cohort Study. Sci Rep 2017;7:3147.
47. Collins-Racie LA, Yang Z, Arai M, et al. Global analysis of nuclear receptor expression and dysregulation in human osteoarthritic articular cartilage: reduced LXR signaling contributes to catabolic metabolism typical of osteoarthritis. Osteoarthritis Cartilage 2009;17:832–842.
48. Smith JD. Dysfunctional HDL as a diagnostic and therapeutic target. Arterioscler Thromb Vasc Biol 2010;30:151–155.
49. de Seny D, Cobraiville G, Charlier E, et al. Acute-phase serum amyloid a in osteoarthritis: regulatory mechanism and proinflammatory properties. PLoS One 2013;8:e66769.
50. Knights AJ, Redding SJ, Maerz T. Inflammation in osteoarthritis: the latest progress and ongoing challenges. Curr Opin Rheumatol 2023;35:128–134.

**Arthritis & Rheumatology**
Vol. 77, No. 2, February 2025, pp 163–170
DOI 10.1002/art.42993
© 2024 The Author(s). *Arthritis & Rheumatology* published by Wiley Periodicals LLC on behalf of American College of Rheumatology. This is an open access article under the terms of the Creative Commons Attribution-NonCommercial-NoDerivs License, which permits use and distribution in any medium, provided the original work is properly cited, the use is non-commercial and no modifications or adaptations are made.

American College of Rheumatology
Empowering Rheumatology Professionals

# Efficacy and Safety of Intravenous Secukinumab in Patients With Active Axial Spondyloarthritis: Results From a Randomized, Placebo-Controlled, Phase 3 Study

Atul Deodhar,[1] Jerzy Supronik,[2] Alan Kivitz,[3] Guillermo Valenzuela,[4] Karen Kapur,[5] Susanne Rohrer,[5] Eva Dokoupilová,[6] Hanno B. Richards,[5] and Karel Pavelka[7]

**Objective.** Our goal was to assess the efficacy and safety of intravenous (IV) secukinumab for the treatment of adults with active axial spondyloarthritis (axSpA) in INVIGORATE-1.

**Methods.** INVIGORATE-1 (NCT04156620) was a randomized, double-blind, parallel-group, phase 3 trial in patients with active axSpA (either radiographic or nonradiographic). Patients were randomized one to one to receive IV secukinumab (6 mg/kg at baseline followed by 3 mg/kg every four weeks) or IV placebo for 16 weeks. After week 16, patients randomized to placebo were switched to IV secukinumab (3 mg/kg every four weeks), and patients randomized to secukinumab continued treatment through week 52. The primary endpoint was the Assessment of SpondyloArthritis International Society (ASAS40) response at week 16. Safety was evaluated through week 60.

**Results.** Among patients initially randomized to IV secukinumab (n = 264) or placebo (n = 262), 86.0% and 88.9% completed the entire 60-week study period, respectively. A higher proportion of patients receiving secukinumab versus placebo met the primary endpoint (ASAS40 response) at week 16 (40.9% vs 22.9%; $P < 0.0001$). By week 24, patients who switched from placebo to secukinumab at week 16 achieved ASAS40 response rates comparable to those in patients originally randomized to secukinumab. All secondary efficacy endpoints were met at week 16, and responses were sustained through week 52. No new or unexpected safety signals were observed with IV secukinumab.

**Conclusion.** IV secukinumab was effective for the treatment of adults with active axSpA over 52 weeks. The safety profile was consistent with that in previous reports on subcutaneous secukinumab.

## INTRODUCTION

Axial spondyloarthritis (axSpA) is a chronic immune-mediated disease marked by axial skeletal inflammation and subsequent pain, stiffness, functional impairment, and reduced quality of life.[1] AxSpA disease manifestations exist on a spectrum including radiographic (r)-axSpA and nonradiographic (nr)-axSpA, characterized by the presence or absence of definitive radiographic damage to the sacroiliac joints, respectively.[2–5] Biologic treatments, including tumor necrosis factor inhibitors (TNFi) and interleukin-17 inhibitors, along with small-molecule JAK inhibitors, are recommended for patients with axSpA that is inadequately controlled with nonsteroidal anti-inflammatory drugs and physiotherapy.[6]

Secukinumab is a fully human monoclonal antibody inhibitor of interleukin-17A that has been shown to be an effective and well tolerated treatment for patients with r-axSpA, nr-axSpA, and axial psoriatic arthritis when administered subcutaneously.[7–12] In the MEASURE-1 and MEASURE-3 phase 3 trials, which investigated the efficacy and safety of secukinumab for the treatment of patients with axSpA, patients received an intravenous (IV) loading dose of secukinumab at baseline and at weeks 2 and 4 before switching to subcutaneous (SC) secukinumab every four weeks.[9,13] However, the safety and efficacy of an all-IV regimen

ClinicalTrials.gov identifier: NCT04156620.
Supported by Novartis Pharmaceuticals Corporation.
[1]Atul Deodhar, MD: Oregon Health and Science University, Portland, Oregon; [2]Jerzy Supronik, MD, PhD: NZOZ Centrum Medyczne Artur Racewicz, Bialystok, Poland; [3]Alan Kivitz, MD: Altoona Center for Clinical Research, Duncansville, Pennsylvania; [4]Guillermo Valenzuela, MD: Integral Rheumatology and Immunology Specialists, Plantation, Florida; [5]Karen Kapur, PhD, Susanne Rohrer, PhD, Hanno B. Richards, MD, PhD: Novartis Pharma AG, Basel, Switzerland; [6]Eva Dokoupilova, MD: Medical Plus, s.r.o., Uherske Hradiste, Czech Republic, and Masaryk University, Brno, Czech Republic; [7]Karel Pavelka, MD, PhD: Charles University, Prague, Czech Republic.

Additional supplementary information cited in this article can be found online in the Supporting Information section (https://acrjournals.onlinelibrary.wiley.com/doi/10.1002/art.42993).

Author disclosures are available at https://onlinelibrary.wiley.com/doi/10.1002/art.42993.

Address correspondence via email to Atul Deodhar, MD, at deodhara@ohsu.edu.

Submitted for publication March 11, 2024; accepted in revised form August 22, 2024.

of secukinumab for the treatment of axSpA has not been previously studied. An IV-only administration was explored in the present study because it potentially offers flexibility in treatment decision-making for patients and health care providers. The purpose of INVIGORATE-1 was to investigate the long-term efficacy and safety of IV secukinumab (6 mg/kg loading dose, 3 mg/kg every four weeks thereafter) in patients with active axSpA through 52 weeks.

## PATIENTS AND METHODS

**Study design and patient population.** INVIGORATE-1 (NCT04156620) was a multicenter, randomized, double-blind, placebo-controlled, phase 3 study of the safety, efficacy, and tolerability of IV secukinumab in patients with active axSpA. Enrolled patients were ≥18 years old with a documented diagnosis of axSpA and fulfilled the Assessment of SpondyloArthritis international Society (ASAS) axSpA classification criteria.[14] They were also required to have had disease onset at <45 years of age and inflammatory back pain (IBP) according to ASAS IBP criteria for at least six months.[14] All patients were required to have a Bath Ankylosing Spondylitis Disease Activity Index (BASDAI) score of greater than four and total back pain visual analog scale rating of >40 mm (scale range, 0–100 mm).[15] Patients with prior documented radiological evidence of r-axSpA fulfilling the 1984 modified New York criteria for ankylosing spondylitis were included in the r-axSpA stratum.[16] Patients with suspected nr-axSpA were administered a sacroiliac joint x-ray (central reading). Those patients with radiological evidence meeting the 1984 Modified New York criteria for ankylosing spondylitis as confirmed by the central imaging facility were also included in the r-axSpA stratum. Patients with nr-axSpA did not meet the modified New York criteria for ankylosing spondylitis based on sacroiliac joint x-ray (central reading) but fulfilled the ASAS classification criteria for axSpA. In addition, all patients with nr-axSpA had objective signs of inflammation at screening by magnetic resonance imaging of sacroiliac joints (central reading) and/or elevated high-sensitivity C-reactive protein (hsCRP; ≥5 mg/L for nr-axSpA; ≥10 mg/L for r-axSpA).[17,18] Key exclusion criteria were total ankylosis of the spine, active ongoing inflammatory disease other than axSpA, use of high-potency opioid analgesics, and evidence of ongoing infections or malignant processes within three months of screening.

After a 10-week screening period, patients were stratified by radiographic disease status (r-axSpA or nr-axSpA) and randomized one to one to receive IV secukinumab (6 mg/kg at baseline and 3 mg/kg every four weeks thereafter) or IV placebo for 16 weeks (treatment period 1) (Supplementary Figure 1). Randomization was done via Interactive Response Technology. Patients who were intolerant of or had inadequate response to a TNFi were allowed to enter the study and represented ≤20% of the study population. At week 16, patients randomized to placebo

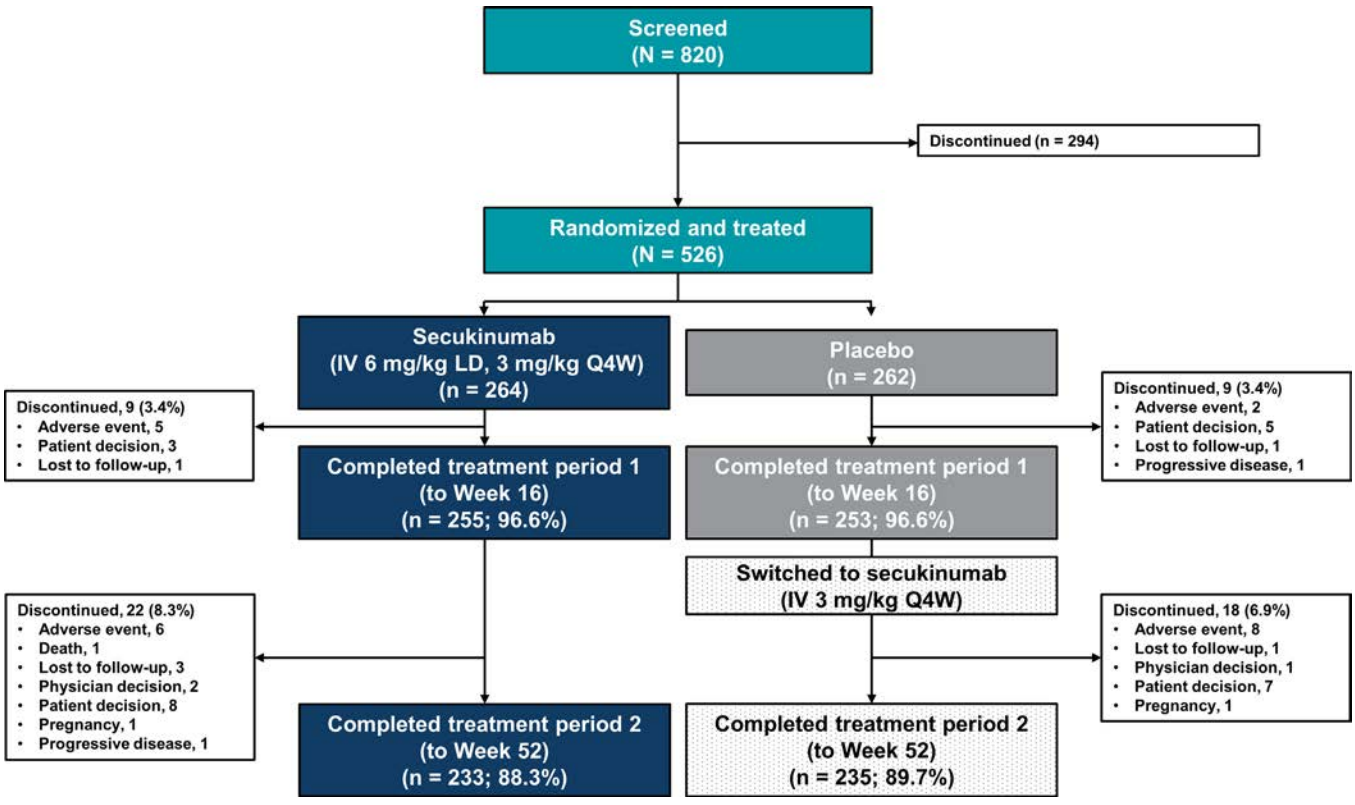


**Figure 1.** Patient disposition through week 52. IV, intravenous; LD, loading dose; Q4W, every 4 weeks.

were switched to IV secukinumab (3 mg/kg every four weeks), and patients originally randomized to IV secukinumab continued receiving IV secukinumab every four weeks through week 52 (treatment period 2). A posttreatment follow-up visit occurred at week 60 (safety follow-up period). Patients, investigator staff, and physicians performing the assessments remained blinded to treatment from randomization until the week 60 database lock.

The study was conducted according to the International Conference on Harmonization E6 (R2) Guideline for Good Clinical Practice, which has its origin in the Declaration of Helsinki. The study protocol, all amendments, the informed consent form, consent form updates, and any other written information provided to patients were reviewed and approved by the independent ethics committee or institutional review board for each participating center. Written informed consent was obtained from each patient at screening before any study-specific procedure was performed.

**Assessments and outcomes.** The primary endpoint was ASAS40 response (improvement of ≥40% and absolute improvement of ≥2 units [on a 10-unit scale] in at least three of the four main ASAS domains, with no worsening in the remaining domain) at week 16 (Supplementary Figure 2). Secondary endpoints included the following efficacy outcomes at week 16, in hierarchical order: achievement of Ankylosing Spondylitis Disease Activity Score–C-reactive protein (ASDAS-CRP) major improvement; change from baseline in the BASDAI;[15] ASAS5/6 response, defined as ≥20% improvement in at least five of six domains; change from baseline in the Bath Ankylosing Spondylitis Functional Index (BASFI);[19] change from baseline in the 36-Item Short Form Health Survey Physical Component Summary Score (SF-36 PCS);[20] change from baseline in Ankylosing Spondylitis Quality of Life (ASQoL);[21] change from baseline in hsCRP; ASAS20 response (improvement of ≥20% and ≥1 unit on a scale of 10 in at least three of the four main ASAS domains); achievement of ASDAS-CRP inactive disease (ASDAS-CRP <1.3); ASAS partial remission; and change from baseline in the Pittsburgh Sleep Quality Index (PSQI).[22] Exploratory efficacy outcomes included assessment of spinal mobility by the Bath Ankylosing Spondylitis Metrology Index (BASMI)[23] and of enthesitis using the Spondyloarthritis Research Consortium of Canada enthesitis index (SPARCC)[24] and Maastricht Ankylosing Spondylitis Enthesitis Score (MASES).[25] Efficacy was further assessed through week 52 using the same outcome measures. Subgroup analyses of efficacy variables at week 16 compared radiographic strata (r-axSpA vs nr-axSpA) and previous TNFi exposure (TNFi naive vs inadequate response).

Safety was assessed by the incidence of treatment-emergent adverse events (TEAEs), serious adverse events (AEs), and treatment discontinuation due to TEAEs through week 16 and over the entire treatment and follow-up periods (up to week 60).

**Table 1.** Patient demographics and baseline disease characteristics*

| Characteristic | Secukinumab (n = 264) | Placebo–secukinumab (n = 262) |
|---|---|---|
| Age, mean (SD), y | 39.8 (12.4) | 39.1 (11.7) |
| Male, n (%) | 165 (62.5) | 178 (67.9) |
| Race, n (%) | | |
| White | 180 (68.2) | 179 (68.3) |
| Asian | 59 (22.3) | 47 (17.9) |
| American Indian or Alaska Native | 17 (6.4) | 25 (9.5) |
| Black or African American | 7 (2.7) | 6 (2.3) |
| Ethnicity, n (%) | | |
| Hispanic or Latino | 35 (13.3) | 44 (16.8) |
| Not Hispanic or Latino | 225 (85.2) | 214 (81.7) |
| BMI, mean (SD), kg/m$^2$ | 26.8 (5.7) | 27.0 (5.9) |
| Disease, n (%) | | |
| r-axSpA | 208 (78.8) | 205 (78.2) |
| nr-axSpA | 56 (21.2) | 57 (21.8) |
| No previous TNFi exposure, n (%) | 233 (88.3) | 216 (82.4) |
| Methotrexate use at randomization, n (%) | 34 (12.9) | 35 (13.4) |
| Sulfasalazine use at randomization, n (%) | 54 (20.5) | 56 (21.4) |
| Time since axSpA diagnosis, mean (SD), y | 5.5 (7.7) | 4.6 (6.1) |
| Time since onset of back pain, mean (SD), y | 11.8 (10.4) | 10.7 (9.3) |
| Sacroiliac joint inflammation on MRI, n (%)[a] | 42/56 (75.0) | 36/57 (63.2) |
| MASES, mean (SD) | 3.2 (3.5) | 3.3 (3.8) |
| hsCRP, mean (SD), mg/L | 15.6 (24.9) | 15.7 (24.4) |
| Abnormal hsCRP, n (%)[b] | 125 (47.3) | 129 (49.2) |
| HLA-B27 positive, n (%) | 210 (79.5) | 215 (82.1) |
| Total back pain on VAS (0–100 mm), mean (SD), mm | 73.9 (13.9) | 74.1 (13.9) |

* axSpA, axial spondyloarthritis; BMI, body mass index; hsCRP, high-sensitivity C-reactive protein; MASES, Maastricht Ankylosing Spondylitis Enthesitis Score; MRI, magnetic resonance imaging; nr-axSpA, nonradiographic axial spondyloarthritis; r-axSpA, radiographic axial spondyloarthritis; TNFi, tumor necrosis factor inhibitor; VAS, visual analog scale.
[a] Among patients with nr-axSpA.
[b] hsCRP ≥5 mg/L in patients with nr-axSpA or ≥10 mg/L in patients with r-axSpA.

**Statistical analyses.** A sample size of 250 patients for each treatment arm was deemed appropriate to achieve adequate power for the primary and secondary endpoints. An overall error (two-sided) of 5% was used to control for Type I error. A predefined hierarchical hypothesis-testing procedure was used to assess primary and secondary efficacy endpoints at week 16 (Supplementary Figure 2). Differences between treatment groups were assessed in marginal response proportions using logistic regression for binary variables. Between-treatment differences in change from baseline were assessed using a mixed-effects model for repeated measures for continuous variables. The proportion of responders is reported for binary outcomes, and mean (SD) change from baseline is reported for continuous

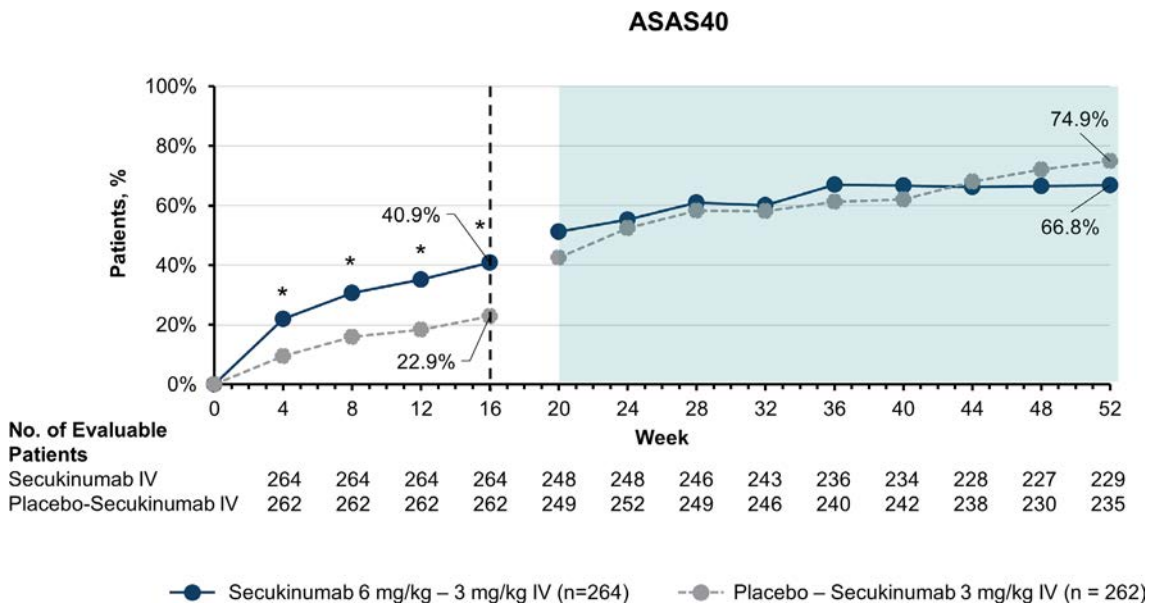


**Figure 2.** Proportions of patients with axSpA who achieved ASAS40 through week 16 (nonresponder imputation) and through week 52 (observed data). Unshaded area represents data reported using nonresponder imputation; shaded area represents time points when data are reported as observed. *$P < 0.0001$ vs placebo. ASAS, Assessment of SpondyloArthritis international Society; axSpA, axial spondyloarthritis; IV, intravenous.

outcomes. Data are reported through week 16 using nonresponder imputation for binary variables and mixed-effects model for repeated measures for continuous variables and from week 20 through week 52 as observed.

## RESULTS

**Patients.** A total of 820 patients were screened for participation in the study, of whom 526 eligible patients were randomized to receive either IV secukinumab (n = 264) or placebo (n = 262). Of the patients randomized, 96.6% from each group completed the 16-week treatment period 1 (Figure 1). Demographics and baseline characteristics were balanced across treatment groups (Table 1). A total of 413 patients had r-axSpA, and 113 patients had nr-axSpA. The majority of randomized patients were naive to TNFi therapy (85.4%). Nine patients from each treatment group discontinued before week 16, with similar reasons for discontinuation between groups. The most frequent reasons for discontinuation were AEs and patient decision. In total, 88.3% of patients randomized to IV secukinumab and 89.7% of patients randomized to IV placebo–secukinumab completed the 52-week treatment period; additionally, 86.0% of patients randomized to IV secukinumab and 88.9% of patients randomized to IV placebo–secukinumab completed the entire 60-week study period. The reasons for discontinuation during treatment period 2 were similar between treatment groups, with the most frequent being AEs, patient decision, and loss to follow-up.

**Efficacy.** The primary endpoint was met as patients receiving IV secukinumab achieved a significantly greater week 16 ASAS40 response rate of 40.9% compared with 22.9% ($P < 0.0001$) among patients receiving placebo (Figure 2). IV secukinumab resulted in rapid increases in ASAS40 response, observed as early as week 4.

All secondary efficacy endpoints within the predefined testing hierarchy were also met at week 16 (Figure 3). At week 16, significantly higher proportions of patients receiving IV secukinumab versus placebo achieved ASDAS-CRP major improvement (27.7% vs 7.6%; $P < 0.0001$), ASAS5/6 (43.9% vs 21.8%; $P < 0.0001$), ASAS20 (64.0% vs 40.5%; $P < 0.0001$), ASDAS-CRP inactive disease (15.9% vs 3.4%; $P < 0.0001$), and ASAS partial remission (14.8% vs 4.2%; $P < 0.0001$). Patients receiving IV secukinumab experienced greater improvements from baseline compared with those who received placebo in BASDAI (–2.70 vs –1.69; $P < 0.0001$), BASFI (–2.33 vs –1.39; $P < 0.0001$), SF-36 PCS (7.70 vs 4.69; $P < 0.0001$), ASQoL (–4.65 vs –2.88; $P < 0.0001$), hsCRP (0.39 vs 0.89; $P < 0.0001$), and PSQI (–2.42 vs –1.76; $P < 0.05$) measures.

By week 24, patients who switched from placebo to IV secukinumab achieved ASAS40 response rates comparable to those in patients originally randomized to IV secukinumab (Figure 2). ASAS40 response rates were maintained in both treatment groups through week 52 (IV secukinumab, 66.8%; IV placebo-secukinumab, 74.9%, observed data). Improvements achieved at week 16 in patients originally randomized to IV secukinumab either further improved or were sustained for all secondary outcomes through week 52 (Figure 4). Patients who switched from

placebo to secukinumab also demonstrated disease improvement across all outcome measures by week 52 and had results comparable to those in patients originally randomized to IV secukinumab.

Compared with patients receiving placebo, patients receiving IV secukinumab experienced numerical improvements in spinal mobility and enthesitis (among patients with enthesitis at baseline) as determined by mean change from baseline to week 16 in BASMI (secukinumab, –0.404; placebo, –0.246), MASES (secukinumab, –1.5; placebo, –1.0), and SPARCC (secukinumab, –1.2; placebo, –1.1) measures. These improvements extended through week 52 in patients originally randomized to IV secukinumab, and similar improvements were also observed in patients who switched to IV secukinumab after week 16 in BASMI (secukinumab, –0.746; placebo–secukinumab, –0.688), MASES (secukinumab, –2.2; placebo–secukinumab, –2.1), and SPARCC (secukinumab, –3.3; placebo–secukinumab, –3.2) measures.

Exploratory subgroup analyses by previous TNFi exposure (TNFi naive vs inadequate response; Supplementary Table 1) and radiographic status strata (r-axSpA vs nr-axSpA; Supplementary Table 2) showed numerically higher efficacy for IV

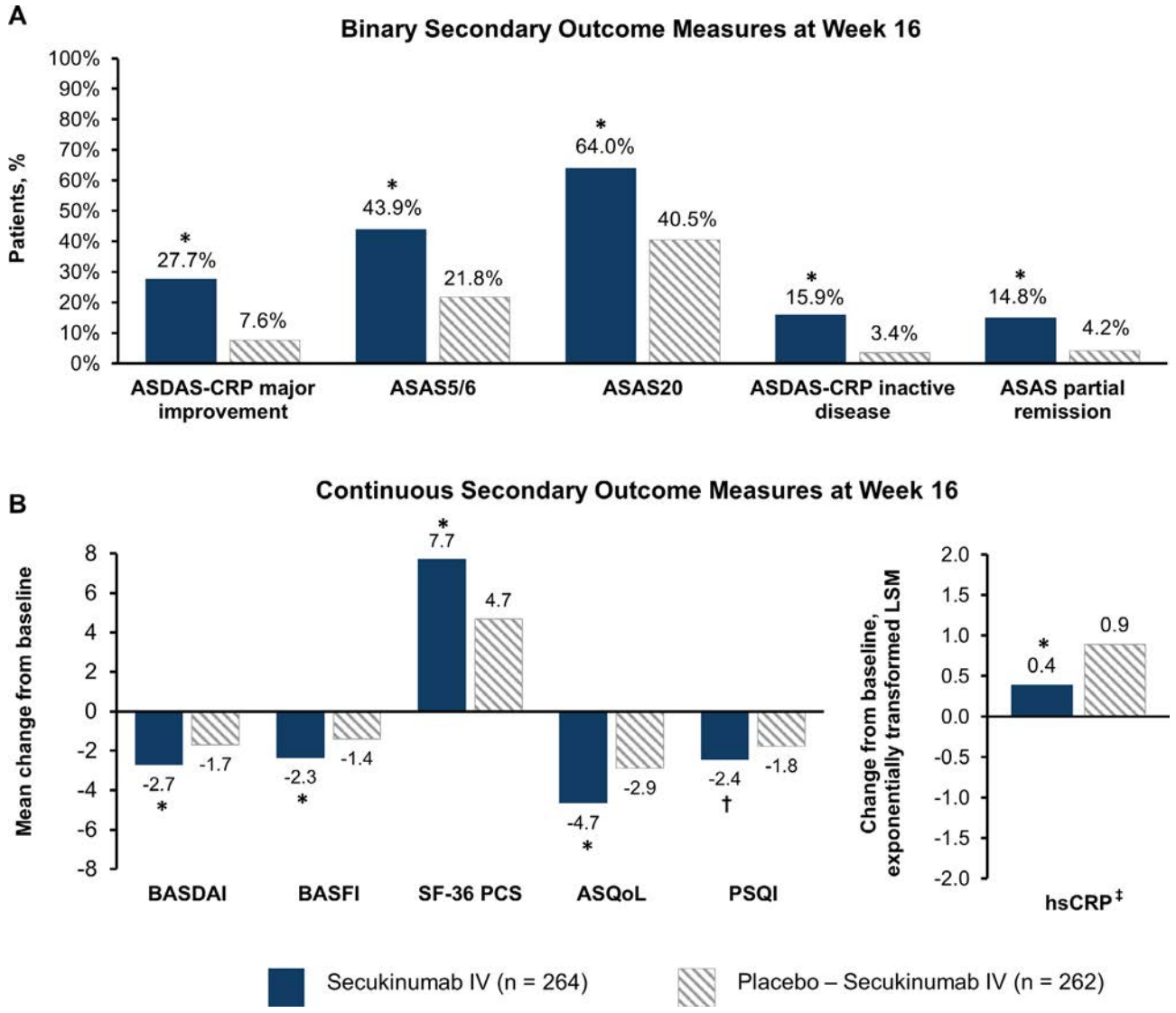


**Figure 3.** Achievement of efficacy responses and improvements in disease measures from baseline to week 16 using (A) nonresponder imputation for binary outcomes and (B) mixed-effects model for repeated measures for continuous measures. *$P < 0.0001$. †$P < 0.05$. ‡ Change in hsCRP from baseline was calculated as the log(e) ratio of the week 16 value versus the baseline value to normalize the distribution of hsCRP at each visit. A value of <1 indicates a reduction in hsCRP. ASAS, Assessment of SpondyloArthritis international Society; ASDAS-CRP, Ankylosing Spondylitis Disease Activity Score with C-reactive protein; ASQoL, Ankylosing Spondylitis Quality of Life Questionnaire; BASDAI, Bath Ankylosing Spondylitis Disease Activity Score; BASFI, Bath Ankylosing Spondylitis Functional Index; hsCRP, high-sensitivity C-reactive protein; IV, intravenous; LSM, least-squares mean; PSQI, Pittsburgh Sleep Quality Index; SF-36 PCS, Short Form 36 Physical Component Summary.

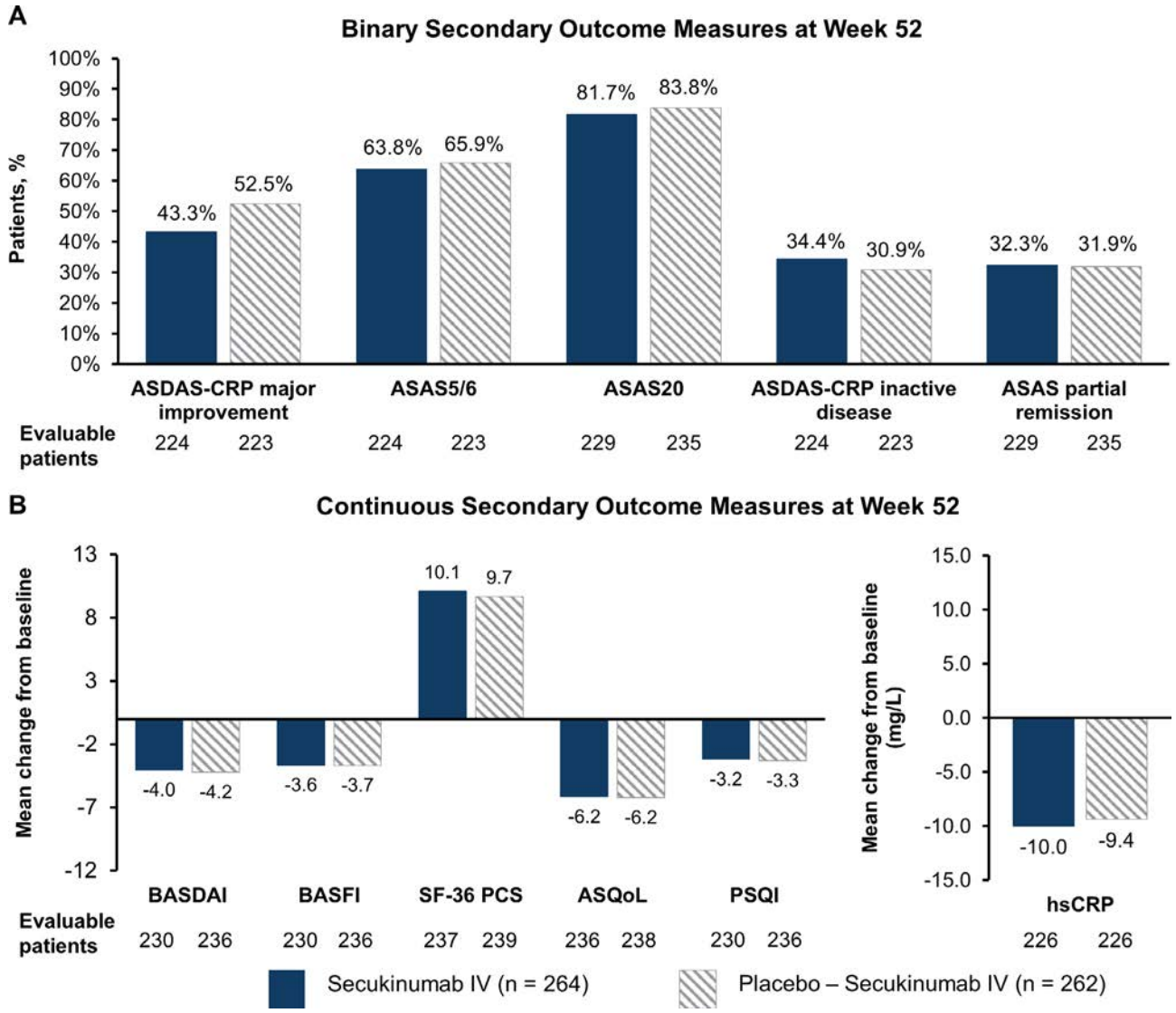


**Figure 4.** Achievement of (A) binary efficacy responses at week 52 (observed) and (B) improvements in continuous disease measures from baseline to week 52 (observed). ASAS, Assessment of SpondyloArthritis international Society; ASDAS-CRP, Ankylosing Spondylitis Disease Activity Score with C-reactive protein; ASQoL, Ankylosing Spondylitis Quality of Life Questionnaire; BASDAI, Bath Ankylosing Spondylitis Disease Activity Score; BASFI, Bath Ankylosing Spondylitis Functional Index; hsCRP, high-sensitivity C-reactive protein; IV, intravenous; PSQI, Pittsburgh Sleep Quality Index; SF-36 PCS, Short Form 36 Physical Component Summary.

secukinumab compared with placebo across all primary and secondary endpoints at week 16.

**Safety.** Up to week 16, TEAEs were reported in 38.6% and 39.1% of patients receiving IV secukinumab and placebo, respectively (Table 2). The most frequent TEAEs up to week 16 were COVID-19, diarrhea, nasopharyngitis, upper respiratory tract infection, and headache. Five patients (1.9%) receiving IV secukinumab discontinued treatment due to a TEAE compared with one patient (0.4%) receiving placebo. The exposure-adjusted incidence rate (EAIR) per 100 patient-years was 116.4 in patients

**Table 2.** Safety through week 16 (placebo-controlled period)*

| Parameter | Secukinumab (n = 264) | Placebo (n = 262) |
|---|---|---|
| TEAE, n (%) | 102 (38.6) | 102 (39.1) |
| Nonfatal SAE, n (%) | 7 (2.7) | 3 (1.1) |
| Most frequent TEAEs, n (%) | | |
| COVID-19 | 11 (4.2) | 9 (3.4) |
| Diarrhea | 8 (3.0) | 5 (1.9) |
| Nasopharyngitis | 6 (2.3) | 7 (2.7) |
| Upper respiratory tract infection | 6 (2.3) | 6 (2.3) |
| Headache | 4 (1.5) | 7 (2.7) |

* SAE, serious adverse event; TEAE, treatment-emergent adverse event.

who received any secukinumab during the entire 60-week safety period. Similar to findings in treatment period 1, the most commonly reported TEAEs were COVID-19 (EAIR = 14.1), nasopharyngitis (EAIR = 6.7), upper respiratory tract infection (EAIR = 4.6), arthralgia (EAIR = 4.2), diarrhea (EAIR = 3.7), and headache (EAIR = 3.5) in treatment period 2 (Supplementary Table 3).

In patients receiving IV secukinumab over the 52-week treatment period, the EAIRs for AEs of interest were low for uveitis (1.8), Crohn disease (0.8), and ulcerative colitis (0.4). One death due to suspected myocardial infarction was reported in the any-secukinumab group and was not suspected to be related to the study treatment.

## DISCUSSION

INVIGORATE-1 is the first randomized, placebo-controlled, phase 3 study to evaluate the long-term efficacy and tolerability of an all-IV regimen of secukinumab for the treatment of adults with active axSpA. The primary and secondary efficacy outcomes were met because IV secukinumab (6 mg/kg loading dose followed by a maintenance dose of 3 mg/kg every four weeks thereafter) demonstrated statistically significant and clinically meaningful efficacy compared with placebo at week 16. Patients experienced improvements across all measures of disease activity, physical function, quality of life, and sleep. These clinical improvements were either sustained or increased through week 52. Similar improvements were observed at week 16 across radiographic strata and in patients with or without previous TNFi exposure. The efficacy outcomes observed in this study are consistent with those in previous phase 3 studies that evaluated SC secukinumab for the treatment of patients with axSpA.[9,12,13,26,27] IV secukinumab was generally well tolerated through the entire 60-week safety period. Safety data were consistent with those in previous reports on SC secukinumab, and no new safety signals were observed.

IV secukinumab is now approved by the US Food and Drug Administration for the treatment of patients with axSpA. The approved dosing regimen was selected based on a model-informed drug discovery approach together with a pharmacokinetic (PK) bridging strategy using data from the known PK profile of SC secukinumab. The approved dosing regimen of IV secukinumab 1.75 mg/kg every four weeks with or without a 6-mg/kg loading dose was estimated to have PK properties similar to SC secukinumab 300 mg and 150 mg and was estimated to provide efficacy and safety similar to the approved SC doses.

An important decision for rheumatologists and their patients with axSpA when considering biologic therapy is the preferred route of administration. The increasing availability of biologics has greatly improved the treatment landscape of axSpA, and IV treatment options are emerging. Among the biologics currently approved by the US Food and Drug Administration for the treatment of r-axSpA, secukinumab and golimumab are the only therapies that offer both SC and IV dosing.[28–30] Moreover, infliximab is the only other biologic therapy that is indicated for IV use to treat patients with r-axSpA.[31] Neither golimumab nor infliximab is indicated for treating patients with nr-axSpA.

Recent studies have begun to highlight the importance of patient preference in treatment with biologics, particularly the desired route of administration. A systematic literature review by Overton et al reported that 16 of 18 relevant studies found that patients prefer SC over IV administration of monoclonal antibody–based therapy for chronic immune diseases.[32] The same analysis found that, among 31 studies in patients receiving non–monoclonal antibody–based therapy, 20 reported patient preference for SC administration. However, Bolge et al reported that among a population of patients receiving biologic therapy for r-axSpA, Crohn disease, psoriatic arthritis, psoriasis, rheumatoid arthritis, or ulcerative colitis, 82% preferred IV medication over SC injection.[33] Several considerations may influence whether a patient prefers IV over SC administration. Patients preferring SC therapy may favor the convenience of at-home treatment and the ease of self-administration, whereas patients preferring IV treatment may desire administration by a health care professional.

Several limitations should be considered when evaluating the findings of this study. INVIGORATE-1 was a confirmatory phase 3 study of the use of IV secukinumab to treat patients with axSpA and did not include a direct head-to-head comparison of the efficacy of IV and SC secukinumab. Therefore, comparisons between this study and others evaluating SC secukinumab for the treatment of patients with axSpA should be made with caution.

In conclusion, IV secukinumab demonstrated rapid and sustained improvement in the signs and symptoms of active axSpA through 52 weeks, consistent with the findings of previous reports on SC secukinumab. IV treatment was well tolerated, with a safety profile consistent with that reported in previous studies of SC secukinumab. The addition of an IV administration route for secukinumab could provide increased flexibility in disease management for rheumatologists and their patients with axSpA.

## AUTHOR CONTRIBUTIONS

All authors contributed to at least one of the following manuscript preparation roles: conceptualization AND/OR methodology, software, investigation, formal analysis, data curation, visualization, and validation AND drafting or reviewing/editing the final draft. As corresponding author, Dr Deodhar confirms that all authors have provided the final approval of the version to be published, and takes responsibility for the affirmations regarding article submission (eg, not under consideration by another journal), the integrity of the data presented, and the statements regarding compliance with institutional review board/Helsinki Declaration requirements.

## ROLE OF THE STUDY SPONSOR

This work was supported by Novartis Pharmaceuticals Corporation, East Hanover, NJ, USA. Novartis Pharmaceuticals Corporation

had a role in the study design and in the collection, analysis, or interpretation of the data and the decision to submit the manuscript for publication. Medical writing support was provided by Coles Keeter, PhD, of Nucleus Global, an Inizio Company, and was funded by Novartis Pharmaceuticals Corporation.

## REFERENCES

1. Navarro-Compán V, Sepriano A, El-Zorkany B, et al. Axial spondyloarthritis. Ann Rheum Dis 2021;80(12):1511–1521.
2. Michelena X, López-Medina C, Marzo-Ortega H. Non-radiographic versus radiographic axSpA: what's in a name? Rheumatology (Oxford) 2020;59(suppl 4):iv18–iv24.
3. Robinson PC, van der Linden S, Khan MA, et al. Axial spondyloarthritis: concept, construct, classification and implications for therapy. Nat Rev Rheumatol 2021;17(2):109–118.
4. Rudwaleit M, van der Heijde D, Landewé R, et al. The development of Assessment of SpondyloArthritis international Society classification criteria for axial spondyloarthritis (part II): validation and final selection. Ann Rheum Dis 2009;68(6):777–783.
5. Schwartzman S, Ruderman EM. A road map of the axial spondyloarthritis continuum. Mayo Clin Proc 2022;97(1):134–145.
6. Ramiro S, Nikiphorou E, Sepriano A, et al. ASAS-EULAR recommendations for the management of axial spondyloarthritis: 2022 update. Ann Rheum Dis 2023;82(1):19–34.
7. Braun J, Kiltz U, Buhring B, et al. Secukinumab in axial spondyloarthritis: a narrative review of clinical evidence. Ther Adv Musculoskelet Dis 2021;13:1759720X211041854.
8. Baraliakos X, Gossec L, Pournara E, et al. Secukinumab in patients with psoriatic arthritis and axial manifestations: results from the double-blind, randomised, phase 3 MAXIMISE trial. Ann Rheum Dis 2021;80(5):582–590.
9. Baeten D, Sieper J, Braun J, et al; MEASURE 1 Study Group; MEASURE 2 Study Group. Secukinumab, an interleukin-17A inhibitor, in ankylosing spondylitis. N Engl J Med 2015;373(26):2534–2548.
10. Marzo-Ortega H, Sieper J, Kivitz A, et al. Secukinumab provides sustained improvements in the signs and symptoms of active ankylosing spondylitis with high retention rate: 3-year results from the phase III trial, MEASURE 2. RMD Open 2017;3(2):e000592.
11. Pavelka K, Kivitz AJ, Dokoupilova E, et al; MEASURE 3 study group. Secukinumab 150/300 mg provides sustained improvements in the signs and symptoms of active ankylosing spondylitis: 3-year results from the phase 3 MEASURE 3 study. ACR Open Rheumatol 2020; 2(2):119–127.
12. Deodhar A, Blanco R, Dokoupilová E, et al. Improvement of signs and symptoms of nonradiographic axial spondyloarthritis in patients treated with secukinumab: primary results of a randomized, placebo-controlled phase III study. Arthritis Rheumatol 2021;73(1): 110–120.
13. Pavelka K, Kivitz A, Dokoupilova E, et al. Efficacy, safety, and tolerability of secukinumab in patients with active ankylosing spondylitis: a randomized, double-blind phase 3 study, MEASURE 3. Arthritis Res Ther 2017;19(1):285.
14. Sieper J, Rudwaleit M, Baraliakos X, et al. The Assessment of SpondyloArthritis international Society (ASAS) handbook: a guide to assess spondyloarthritis. Ann Rheum Dis 2009;68(suppl 2):ii1–ii44.
15. Garrett S, Jenkinson T, Kennedy LG, et al. A new approach to defining disease status in ankylosing spondylitis: the Bath Ankylosing Spondylitis Disease Activity Index. J Rheumatol 1994;21(12):2286–2291.
16. van der Linden S, Valkenburg HA, Cats A. Evaluation of diagnostic criteria for ankylosing spondylitis. A proposal for modification of the New York criteria. Arthritis Rheum 1984;27(4):361–368.
17. Wallman JK, Kapetanovic MC, Petersson IF, et al. Comparison of non-radiographic axial spondyloarthritis and ankylosing spondylitis patients–baseline characteristics, treatment adherence, and development of clinical variables during three years of anti-TNF therapy in clinical practice. Arthritis Res Ther 2015;17:378.
18. Poddubnyy D, Haibel H, Braun J, et al. Brief report: clinical course over two years in patients with early nonradiographic axial spondyloarthritis and patients with ankylosing spondylitis not treated with tumor necrosis factor blockers: results from the German Spondyloarthritis Inception Cohort. Arthritis Rheumatol 2015;67(9):2369–2375.
19. Calin A, Garrett S, Whitelock H, et al. A new approach to defining functional ability in ankylosing spondylitis: the development of the Bath Ankylosing Spondylitis Functional Index. J Rheumatol 1994; 21(12):2281–2285.
20. Ware JE Jr, Sherbourne CD. The MOS 36-item short-form health survey (SF-36). I. Conceptual framework and item selection. Med Care 1992;30(6):473–483.
21. Doward LC, Spoorenberg A, Cook SA, et al. Development of the ASQoL: a quality of life instrument specific to ankylosing spondylitis. Ann Rheum Dis 2003;62(1):20–26.
22. Buysse DJ, Reynolds CF III, Monk TH, et al. The Pittsburgh Sleep Quality Index: a new instrument for psychiatric practice and research. Psychiatry Res 1989;28(2):193–213.
23. Jones SD, Porter J, Garrett SL, et al. A new scoring system for the Bath Ankylosing Spondylitis Metrology Index (BASMI). J Rheumatol 1995;22(8):1609.
24. Maksymowych WP, Mallon C, Morrow S, et al. Development and validation of the Spondyloarthritis Research Consortium of Canada (SPARCC) Enthesitis Index. Ann Rheum Dis 2009;68(6):948–953.
25. Heuft-Dorenbosch L, Spoorenberg A, van Tubergen A, et al. Assessment of enthesitis in ankylosing spondylitis. Ann Rheum Dis 2003; 62(2):127–132.
26. Kivitz AJ, Wagner U, Dokoupilova E, et al. Efficacy and safety of secukinumab 150 mg with and without loading regimen in ankylosing spondylitis: 104-week results from MEASURE 4 study. Rheumatol Ther 2018;5(2):447–462.
27. Huang F, Sun F, Wan WG, et al. Secukinumab provided significant and sustained improvement in the signs and symptoms of ankylosing spondylitis: results from the 52-week, phase III China-centric study, MEASURE 5. Chin Med J (Engl) 2020;133(21):2521–2531.
28. Deodhar AA, Shiff NJ, Gong C, et al. Efficacy and safety of intravenous golimumab in ankylosing spondylitis patients with early and late disease through one year of the GO-ALIVE study. J Clin Rheumatol 2022;28(5):270–277.
29. Braun J, Deodhar A, Inman RD, et al. Golimumab administered subcutaneously every 4 weeks in ankylosing spondylitis: 104-week results of the GO-RAISE study. Ann Rheum Dis 2012;71(5):661–667.
30. Cosentyx® (secukinumab) [prescribing information]. East Hanover, NJ: Novartis Pharmaceuticals Corporation, October 2023.
31. van der Heijde D, Dijkmans B, Geusens P, et al; Ankylosing Spondylitis Study for the Evaluation of Recombinant Infliximab Therapy Study Group. Efficacy and safety of infliximab in patients with ankylosing spondylitis: results of a randomized, placebo-controlled trial (ASSERT). Arthritis Rheum 2005;52(2):582–591.
32. Overton PM, Shalet N, Somers F, et al. Patient preferences for subcutaneous versus intravenous administration of treatment for chronic immune system disorders: a systematic review. Patient Prefer Adherence 2021;15:811–834.
33. Bolge SC, Eldridge HM, Lofland JH, et al. Patient experience with intravenous biologic therapies for ankylosing spondylitis, Crohn's disease, psoriatic arthritis, psoriasis, rheumatoid arthritis, and ulcerative colitis. Patient Prefer Adherence 2017;11:661–669.

**Arthritis & Rheumatology**
Vol. 77, No. 2, February 2025, pp 171–179
DOI 10.1002/art.42997
© 2024 The Author(s). *Arthritis & Rheumatology* published by Wiley Periodicals LLC on behalf of American College of Rheumatology. This is an open access article under the terms of the Creative Commons Attribution-NonCommercial-NoDerivs License, which permits use and distribution in any medium, provided the original work is properly cited, the use is non-commercial and no modifications or adaptations are made.

American College of Rheumatology
Empowering Rheumatology Professionals

# Efficacy and Safety of Intravenous Secukinumab for the Treatment of Active Psoriatic Arthritis: Results From a Randomized, Placebo-Controlled Phase 3 Study

Alan Kivitz,[1] Liliana Sedova,[2] Melvin Churchill,[3] Roshan Kotha,[4] Atul Singhal,[5] Alexander Torres,[6] Guillermo Valenzuela,[7] Sarah Whelan,[8] Thomas Dumortier,[9] Xuan Zhu,[10] Ruvie Martin,[10] and Luminita Pricop[10]

**Objective.** The aim of this study was to evaluate the efficacy and safety of intravenous (IV) secukinumab in patients with active psoriatic arthritis (PsA).

**Methods.** INVIGORATE-2 (NCT04209205) was a randomized, placebo-controlled, phase 3 trial. Patients with active PsA were randomized 1:1 to receive IV secukinumab (6 mg/kg at baseline followed by 3 mg/kg every four weeks [q4w]) or placebo. At week 16, patients randomized to placebo were switched to IV secukinumab (3 mg/kg q4w), and patients who received IV secukinumab continued treatment through week 52. The primary efficacy endpoint was achievement of 50% improvement in American College of Rheumatology response criteria (ACR50) at week 16. Efficacy and safety were evaluated through weeks 52 and 60, respectively.

**Results.** Among 191 patients randomized to IV secukinumab and 190 to placebo/IV secukinumab, 177 (92.7%) and 170 (89.5%) completed the entire study period, respectively. A significantly higher proportion of patients who received IV secukinumab versus placebo achieved ACR50 at week 16 (31.4% vs 6.3%; adjusted $P < 0.0001$). All secondary efficacy endpoints were met at week 16 (all adjusted $P < 0.05$ using the predefined hypothesis-testing hierarchy). Patients who switched from placebo to secukinumab at week 16 showed rapid improvements in ACR50 rates; by week 52, both treatment arms experienced similar improvements in efficacy outcomes. No new or unexpected safety signals were observed with receiving IV secukinumab. One death was reported in the placebo group before week 16.

**Conclusion.** IV secukinumab led to rapid and sustained improvements in clinical measures of PsA, and the safety profile was consistent with that of secukinumab administered subcutaneously.

## INTRODUCTION

Psoriatic arthritis (PsA) is a chronic inflammatory musculoskeletal disease with a heterogenous presentation involving the peripheral and axial joints, entheses, skin, and nails.[1,2] Patients with PsA often experience reduced quality of life (QoL) due to chronic pain, reduced physical function and work capacity, extreme fatigue, and emotional and social impairment.[3] In addition to QoL burdens, patients with PsA face high economic burdens and have higher health care costs and resource use than those without PsA.[4]

Secukinumab is a fully human monoclonal antibody that selectively inhibits the proinflammatory cytokine interleukin-17A.[5] Subcutaneous (SC) secukinumab is approved in the United States and Europe for the treatment of several inflammatory diseases, including psoriasis, axial spondyloarthritis, and PsA.[6,7] In the phase 3 FUTURE 2 to 5 trials, SC secukinumab was effective at improving the signs and symptoms of psoriatic disease in adult patients with active PsA.[8–11] Secukinumab also improved key clinical disease domains in patients with PsA in the FUTURE 1 trial when delivered as an intravenous (IV) treatment

ClinicalTrials.gov identifier: NCT04209205.
Supported by Novartis Pharmaceuticals Corporation.
[1]Alan Kivitz, MD: Altoona Center for Clinical Research, Duncansville, Pennsylvania; [2]Liliana Sedova, MD: Institute of Rheumatology and Charles University in Prague, Prague, Czech Republic; [3]Melvin Churchill, MD: Arthritis Center of Nebraska, Lincoln; [4]Roshan Kotha, MD: Sharp Community Medical Group, La Mesa, California; [5]Atul Singhal, MD: SouthWest Arthritis Research Group, Mesquite, Texas; [6]Alexander Torres, MD: Highlands Advanced Rheumatology and Arthritis Center, Avon Park, Florida; [7]Guillermo Valenzuela, MD: Integral Rheumatology & Immunology Specialists, Plantation, Florida; [8]Sarah Whelan, MSc: Novartis Ireland Ltd, Dublin, Ireland; [9]Thomas Dumortier, MStat: Novartis Pharma AG, Basel, Switzerland; [10]Xuan Zhu, PhD, Ruvie Martin, PhD, Luminita Pricop, MD: Novartis Pharmaceuticals Corporation, East Hanover, New Jersey.

Additional supplementary information cited in this article can be found online in the Supporting Information section (https://acrjournals.onlinelibrary.wiley.com/doi/10.1002/art.42997).

Author disclosures are available at https://onlinelibrary.wiley.com/doi/10.1002/art.42997.

Address correspondence via email to Alan Kivitz, MD, at ajkivitz@yahoo.com.

Submitted for publication March 11, 2024; accepted in revised form September 6, 2024.

at weeks 0, 2, and 4, followed by SC treatment every four weeks thereafter[12]; however, no study has evaluated the efficacy and safety of long-term treatment with IV secukinumab. Because the majority of treatments approved for PsA are administered SC or orally,[13] alternate routes of delivery for biologics with established efficacy in patients with PsA, such as secukinumab, could provide additional flexibility to accommodate individualize patient and physician options in managing signs and symptoms of PsA. The purpose of INVIGORATE-2 is to investigate the long-term efficacy, safety, and tolerability of IV secukinumab in patients with active PsA through 52 weeks.

## PATIENTS AND METHODS

**Study design and patient population.** INVIGORATE-2 (NCT04209205) is a multicenter, randomized, double-blind, placebo-controlled, phase 3 study of the safety, efficacy, and tolerability of IV secukinumab in patients with active PsA.[14] Patients aged ≥18 years who fulfilled the Classification Criteria for Psoriatic Arthritis, had a diagnosis of PsA for six months or longer, and had active PsA (defined by three or more swollen and three or more tender joints despite current or past treatment with nonsteroidal anti-inflammatory drugs, disease-modifying antirheumatic drugs, or tumor necrosis factor [TNF] inhibitors) were enrolled in the study. Enrolled patients were required to have either signs of skin manifestations of plaque psoriasis or nail changes consistent with psoriasis or to have a documented history of plaque psoriasis. Concomitant use of methotrexate (≤25 mg/week) or glucocorticoids (≤10 mg/day) was allowed up to week 16 if the dose was stable for four weeks or two weeks, respectively, before randomization. Patients with previous exposure to interleukin-17 inhibitors or who had active ongoing inflammatory diseases other than PsA (such as inflammatory bowel disease) were excluded.

Patients were randomized 1:1 at baseline to receive IV secukinumab (6 mg/kg at baseline followed by 3 mg/kg every four weeks thereafter) or placebo every four weeks to week 16 (treatment period 1; Supplementary Figure 1). The IV secukinumab dose was chosen based on extensive pharmacokinetic analyses and modeling of data from the phase 2 and 3 studies of secukinumab in patients with PsA. Based on pharmacokinetic modeling, the minimum steady-state serum concentration ($C_{min}$) and maximum steady-state serum concentration ($C_{max}$) with 3 mg/kg IV secukinumab are predicted to be approximately 75% and 150% higher, respectively, than the $C_{min}$ and $C_{max}$ with 150 mg SC secukinumab every four weeks and approximately 14% lower and 75% higher, respectively, than the $C_{min}$ and $C_{max}$ with 300 mg SC secukinumab every four weeks. The higher loading dose was administered to achieve therapeutic steady-state concentrations by week 4. Randomization was done via Interactive Response Technology and was stratified by TNF inhibitor (TNFi) status (TNFi-naive or -inadequate responder). At week 16, patients randomized to placebo began receiving IV secukinumab (3 mg/kg) every four weeks, and patients randomized to IV secukinumab continued their dosing regimen to week 52 (treatment period 2). A posttreatment follow-up visit occurred at week 60 (safety follow-up period). Patients, investigator staff, and physicians performing the assessments remained blinded to treatment from randomization until the week 60 database lock.

The study adhered to the International Council for Harmonization E6 Guideline for Good Clinical Practice, which has its origin in the Declaration of Helsinki. The study protocol, informed consent form, consent form updates, and any other written information provided to patients were reviewed by the independent ethics committee or institutional review board for each participating center. Written informed consent was obtained from each patient before any study procedure was performed.

**Assessments and outcomes.** Primary and secondary efficacy endpoints were assessed through week 16 (placebo-controlled period [treatment period 1]), and efficacy was further assessed through week 52 using the same measures.[15,16] The primary efficacy outcome was 50% improvement in American College of Rheumatology response criteria (ACR50), and the primary efficacy time point was week 16. Categorical secondary efficacy endpoints included the proportions of patients achieving the following outcomes: 20% improvement in American College of Rheumatology response criteria (ACR20), resolution of enthesitis as assessed by the Leeds Enthesitis Index in patients with enthesitis at baseline, resolution of dactylitis as assessed by the Leeds Dactylitis Index in patients with dactylitis at baseline, 90% improvement in Psoriasis Area and Severity Index score (PASI90), and minimal disease activity (MDA). The proportion of patients achieving MDA was assessed as those achieving five or more of the following seven criteria: tender joint count ≤1, swollen joint count ≤1, PASI ≤1 or affected body surface area (BSA) ≤3%, patient pain (visual analog scale [VAS]) ≤15, patient global assessment of disease activity (VAS) ≤20, Health Assessment Questionnaire–Disability Index (HAQ-DI) ≤0.5, and tender entheseal points ≤1.[17] Additional continuous secondary efficacy endpoints were changed from baseline in the following measures: disease activity as assessed by the Psoriatic Arthritis Disease Activity Score (PASDAS); nail involvement as assessed by the modified Nail Psoriasis Severity Index (mNAPSI); and health-related QoL and functional ability as assessed by the HAQ-DI, Functional Assessment of Chronic Illness Therapy – Fatigue (FACIT-Fatigue), and 36-Item Short Form Health Survey physical component score (SF-36 PCS). Exploratory efficacy outcomes included achievement of 70% improvement in American College of Rheumatology response criteria (ACR70) and PASDAS low disease activity (PASDAS-LDA) and change from baseline in the patient's assessment of PsA pain (VAS). A subgroup analysis was conducted of primary and secondary efficacy variables at weeks 16 and 52 in patients grouped by previous TNFi exposure (TNFi-naive vs TNFi-inadequate responders). Safety was

assessed by the incidence of treatment-emergent adverse events (TEAEs), serious adverse events (SAEs), and treatment discontinuation due to TEAEs through week 16 and over the entire treatment period (week 60 safety analysis).

**Statistical analyses.** A sample size of 190 patients for each treatment arm was estimated to achieve adequate power for the primary and secondary endpoints. Closed testing procedures were used to maintain a familywise error rate of 5% across the endpoints.[18] A predefined statistical hypothesis-testing hierarchy strategy was used to assess primary and secondary efficacy endpoints at week 16 (Supplementary Figure 2). For binary variables through week 16, means and *P* values for marginal differences between treatment groups were assessed using logistic regression with nonresponder imputation for missing values; data from week 20 through week 52 are reported as observed. For continuous variables through week 16, least-squares (LS) mean change from baseline and *P* values for between-treatment differences in change from baseline were assessed using a mixed-effects model with repeated measures; data from week 20 through week 52 are reported as observed.

## RESULTS

**Patient characteristics.** A total of 381 patients were randomized to receive IV secukinumab (n = 191) or placebo (n = 190). Patient demographics and baseline disease characteristics were balanced between treatment arms (Table 1). The majority of patients randomized to receive IV secukinumab (86.4%) and placebo (85.3%) were naive to TNFi. Most patients who received IV secukinumab or placebo had baseline enthesitis (66.0% and 57.9%, respectively), nail psoriasis (68.1% and 63.7%, respectively), and psoriasis affecting ≥3% of the BSA (53.4% and 57.4%, respectively). Of the 381 patients randomized to treatment, 186 patients (97.4%) who received IV secukinumab and 183 patients (96.3%) who received placebo completed treatment period 1 (Figure 1). A total of 177 patients (92.7%) who received IV secukinumab and 170 patients (89.5%) who received placebo/IV secukinumab completed treatment period 2. The most common reasons for treatment discontinuation in both treatment periods were patient decision (2.9% of all patients) and adverse events (1.8% of all patients).

**Efficacy.** All primary and secondary efficacy endpoints for patients who received secukinumab versus placebo at week 16 achieved statistical significance (all adjusted $P < 0.05$) under the predefined hypothesis-testing hierarchy procedure (Supplementary Figure 2). Patients who received IV secukinumab achieved significantly higher ACR50 rates at week 16 (primary endpoint) than patients who received placebo (31.4% vs 6.3%; adjusted $P < 0.0001$; Table 2). Significantly higher ACR50 rates were observed with receiving IV secukinumab as early as week

**Table 1.** Patient demographics and baseline disease characteristics*

| Characteristic | IV secukinumab (n = 191) | Placebo/IV secukinumab (n = 190) |
|---|---|---|
| Age, mean (±SD), y | 47.5 (±13.5) | 48.1 (±13.7) |
| Sex, n (%) | | |
| Male | 87 (45.5) | 85 (44.7) |
| Female | 104 (54.5) | 105 (55.3) |
| Race, n (%) | | |
| White | 148 (77.5) | 153 (80.5) |
| Asian | 15 (13.1) | 26 (13.7) |
| Indian | 1 (0.5) | 3 (1.6) |
| American Indian or Alaska Native | 10 (5.2) | 9 (4.7) |
| Black or African American | 5 (2.6) | 1 (0.5) |
| Multiracial, n (%) | | |
| White and American Indian or Alaska Native | 3 (1.6) | 0 |
| Asian and Native Hawaiian or other Pacific Islander | 0 | 1 (0.5) |
| Ethnicity, n (%) | | |
| Hispanic or Latino | 34 (17.8) | 25 (13.2) |
| Not Hispanic or Latino | 155 (81.2) | 163 (85.8) |
| Not reported | 2 (1.0) | 2 (1.1) |
| Weight, mean (±SD), kg | 84.6 (±22.9) | 85.1 (±22.7) |
| Previous TNFi exposure, n (%) | | |
| Naive | 165 (86.4) | 162 (85.3) |
| Inadequate responder | 26 (13.6) | 28 (14.7) |
| Received MTX or other csDMARD at baseline, n (%) | 113 (59.2) | 110 (57.9) |
| Time since PsA diagnosis, mean (±SD), y | 6.0 (±7.3) | 5.8 (±7.1) |
| Patients with specific disease characteristics, n (%) | | |
| Enthesitis (LEI) | 126 (66.0) | 110 (57.9) |
| Dactylitis | 81 (42.4) | 71 (37.4) |
| Nail psoriasis | 130 (68.1) | 121 (63.7) |
| Psoriasis ≥3% of BSA | 102 (53.4) | 109 (57.4) |
| Disease and quality of life scores, mean (±SD) | | |
| TJC78 | 22.8 (±17.1) | 22.3 (±17.3) |
| SJC76 | 13.8 (±13.5) | 14.1 (±13.3) |
| DAS28-CRP | 4.4 (±1.0) | 4.5 (±1.0) |
| Physician's global assessment (VAS) | 56.3 (±20.8) | 56.7 (±20.2) |
| Patient's global assessment (VAS) | 55.8 (±21.6) | 57.3 (±21.5) |
| PsA Pain (VAS) | 55.5 (±23.6) | 57.3 (±22.9) |
| HAQ-DI | 1.3 (±0.5) | 1.3 (±0.6) |
| SF-36 PCS | 36.4 (±7.5) | 36.8 (±7.9) |
| FACIT-Fatigue | 27.9 (±11.3) | 28.2 (±11.1) |

* BSA, body surface area; csDMARD, conventional synthetic disease-modifying antirheumatic drug; DAS28-CRP, Disease Activity Score-28 for Rheumatoid Arthritis With C-Reactive Protein; FACIT-Fatigue, Functional Assessment of Chronic Illness Therapy – Fatigue; HAQ-DI, Health Assessment Questionnaire–Disability Index; IV, intravenous; LEI, Leeds Enthesitis Index; MTX, methotrexate; PsA, psoriatic arthritis; SF-36 PCS, 36-Item Short Form Health Survey physical component score; SJC76, swollen joint count of 76 joints; TJC78, tender joint count of 78 joints; TNFi, tumor necrosis factor inhibitor; VAS, visual analog scale.

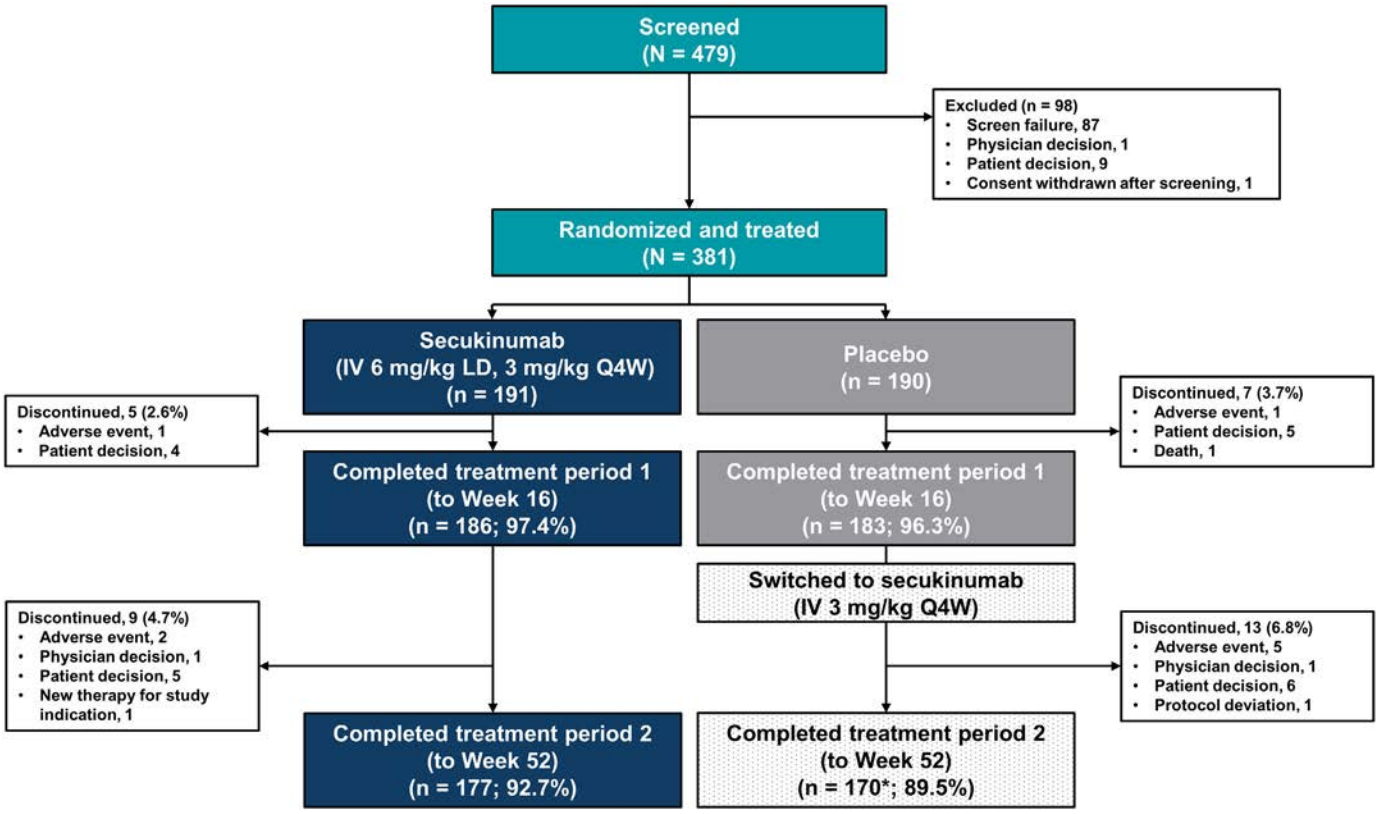


**Figure 1.** Patient disposition through week 52. IV, intravenous; LD, loading dose; Q4W, every four weeks. *One patient completed their last physician visit within the week 52 analysis window but discontinued the study before week 52.

**Table 2.** Efficacy of receiving secukinumab versus placebo at week 16 across prespecified primary and secondary endpoints*

| Efficacy measure[a] | IV secukinumab (n = 191) | Placebo/IV secukinumab (n = 190) | Adjusted *P* value |
|---|---|---|---|
| ACR50, n (%) | 60 (31.4) | 12 (6.3) | <0.0001 |
| ACR20, n (%) | 114 (59.7) | 55 (29.0) | <0.0001 |
| Minimal disease activity, n (%) | 43 (22.5) | 10 (5.3) | <0.0001 |
| PASI90, n (%)[b] | 49 (48.0) | 7 (6.4) | <0.0001 |
| PASDAS, LS mean change from baseline (±SE) | −2.2 (±0.1) | −1.1 (±0.1) | <0.0001 |
| HAQ-DI, LS mean change from baseline (±SE) | −0.39 (±0.04) | −0.15 (±0.04) | <0.0001 |
| SF-36 PCS, LS mean change from baseline (±SE) | 6.5 (±0.6) | 2.3 (±0.6) | <0.0001 |
| FACIT-Fatigue, LS mean change from baseline (±SE) | 6.2 (±0.8) | 3.3 (±0.8) | 0.0024 |
| mNAPSI, LS mean change from baseline (±SE)[c] | −9.3 (±1.1) | −3.1 (±1.1) | 0.0024 |
| Resolution of dactylitis, n (%)[d] | 48 (59.3) | 23 (32.4) | 0.0024 |
| Resolution of enthesitis, n (%)[e] | 70 (55.6) | 43 (39.1) | 0.01 |

* ACR20, 20% improvement in American College of Rheumatology response criteria; ACR50, 50% improvement in American College of Rheumatology response criteria; FACIT-Fatigue, Functional Assessment of Chronic Illness Therapy – Fatigue; HAQ-DI, Health Assessment Questionnaire–Disability Index; IV, intravenous; LS, least-squares; mNAPSI, modified Nail Psoriasis Severity Index; PASDAS, Psoriatic Arthritis Disease Activity Score; PASI90, 90% improvement in Psoriasis Area and Severity Index score; SF-36 PCS, 36-Item Short Form Health Survey physical component score.
[a] Efficacy measures are arranged according to the predefined hypothesis-testing hierarchy shown in Supplementary Figure 2. Binary outcomes used nonresponder imputation for missing data; continuous measures used mixed model for repeated measures.
[b] Patients with psoriasis at baseline were evaluated.
[c] Patients with nail psoriasis at baseline were evaluated.
[d] Patients with dactylitis at baseline were evaluated.
[e] Patients with enthesitis at baseline were evaluated.

4 compared with receiving placebo, and responses were maintained through week 16 ($P < 0.0005$; Figure 2). At week 16, patients who received IV secukinumab had greater achievement of all secondary binary outcomes than those who received placebo (Table 2). Significantly higher proportions of patients who received IV secukinumab versus placebo achieved ACR20 (59.7% vs 29.0%, respectively; adjusted $P < 0.0001$), MDA (22.5% vs 5.3%; adjusted $P < 0.0001$), PASI90 (48.0% vs 6.4%; adjusted $P < 0.0001$), and resolution of dactylitis (59.3% vs 32.4%; adjusted $P = 0.0024$) and enthesitis (55.6% vs 39.1%; adjusted $P = 0.01$). Similarly, patients who received IV secukinumab had greater improvements across all continuous secondary endpoints at week 16 than those who received placebo (Table 2). Significantly greater mean (±SD) changes from baseline in PASDAS (–2.2 [±0.1] vs –1.1 [±0.1]; adjusted $P < 0.0001$), HAQ-DI (–0.4 [±0] vs –0.2 [±0]; adjusted $P < 0.0001$), SF-36 PCS (6.5 [±0.6] vs 2.3 [±0.6]; adjusted $P < 0.0001$), FACIT-Fatigue (6.2 [±0.8] vs 3.3 [±0.8]; adjusted $P = 0.0024$), and mNAPSI (–9.3 [±1.1] vs –3.1 [±1.1]; adjusted $P < 0.0024$) scores were observed in patients who received IV secukinumab versus placebo. After patients switched from placebo to IV secukinumab at week 16, ACR50 rates increased rapidly (Figure 2). ACR50 rates were maintained or improved through week 52 among patients in both treatment groups (observed data; IV secukinumab 58.0%; placebo/IV secukinumab 64.0%). At week 52, high proportions of patients who received IV secukinumab as well as placebo/IV secukinumab achieved each of the binary efficacy measures (Table 3). Patients who received IV secukinumab and

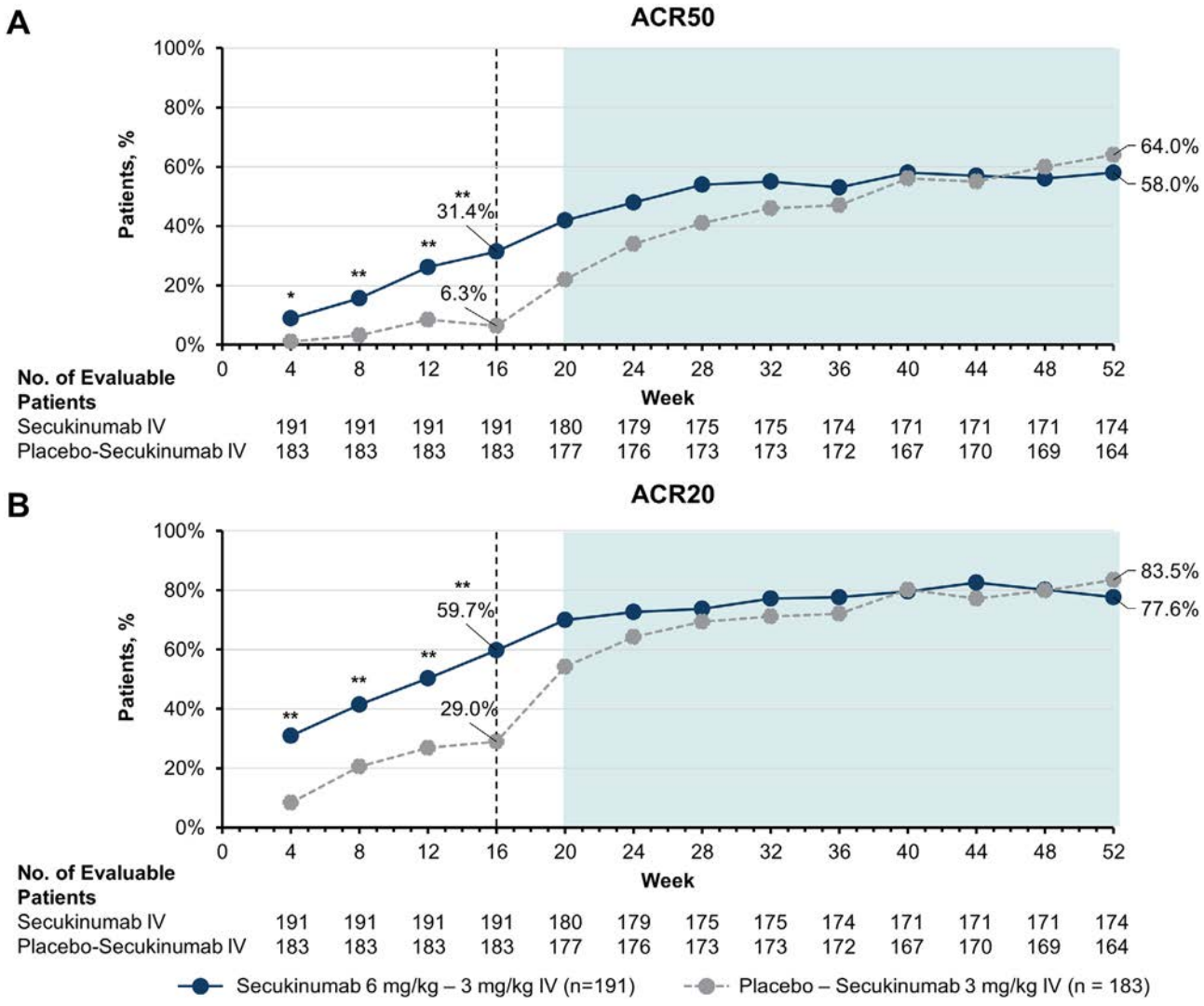


**Figure 2.** Proportion of patients with psoriatic arthritis who achieved (A) ACR50 or (B) ACR20 through week 16 (nonresponder imputation) and through week 52 (observed data). Unshaded area of the graph represents data reported using nonresponder imputation; the shaded area of the graph represents time points at which data are reported as observed. ACR20, 20% improvement in American College of Rheumatology response criteria; ACR50, 50% improvement in American College of Rheumatology response criteria; IV, intravenous; No., number. *$P < 0.0005$ versus placebo, **$P < 0.0001$ versus placebo. Color figure can be viewed in the online issue, which is available at http://onlinelibrary.wiley.com/doi/10.1002/art.42997/abstract.

placebo/IV secukinumab also had similar improvements from baseline to week 52 in all continuous efficacy measures.

Patients who received IV secukinumab had significantly greater achievement of ACR70 (15.7% vs 2.1%; $P < 0.0001$) and PASDAS-LDA (36.7% vs 11.1%; $P < 0.0001$) and improvements from baseline in PsA pain (LS mean [±SE], −24.2 [±1.9] vs −11.1 [±1.8]; $P < 0.0001$) than patients who received placebo at week 16. At week 52, patients who received IV secukinumab and placebo/IV secukinumab had similar achievement of ACR70 (42.0% vs 44.5%) and PASDAS-LDA (68.3% vs 68.8%) and similar improvements from baseline in PsA pain (LS mean [±SD], −35.7 [±27.1] vs −35.4 [±27.9]). Regardless of previous TNFi exposure, patients who received IV secukinumab had greater achievement of binary efficacy measures and greater improvements from baseline in continuous efficacy measures at week 16 than patients who received placebo (Supplementary Table 1). For patients in both treatment arms, receiving secukinumab generally showed comparable efficacy at week 52 across outcomes regardless of previous TNFi exposure (Supplementary Table 2), but there were some numerical differences in treatment responses. ACR50 and MDA rates were higher, and mNAPSI change from baseline to week 16 was greater with IV secukinumab treatment in patients who were TNFi-naive versus TNFi-inadequate responders. Within the group of patients who received IV secukinumab, patients who were TNFi naive had greater achievement of PASI90 than those who were TNFi-inadequate responders. Within the group of patients who received placebo/IV secukinumab, those who were TNFi naive had greater improvements in SF-36 PCS and achievement of enthesitis resolution than those who were TNFi-inadequate responders.

**Table 3.** Achievement of binary efficacy responses at week 52 and improvements in continuous disease measures from baseline to week 52 (observed data)*

| Efficacy measure[a] | IV secukinumab (n = 191) | Placebo/IV secukinumab (n = 190) |
|---|---|---|
| ACR50, n/m (%) | 101/174 (58.0) | 105/164 (64.0) |
| ACR20, n/m (%) | 135/174 (77.6) | 137/164 (83.5) |
| Minimal disease activity, n/m (%) | 96/177 (54.2) | 93/171[b] (54.4) |
| PASI90, n/m (%)[c] | 73/91 (80.2) | 78/100 (78.0) |
| PASDAS, LS mean change from baseline (±SD)[d] | −3.4 (±1.5) | −3.3 (±1.6) |
| HAQ-DI, LS mean change from baseline (±SD)[e] | −0.5 (±0.5) | −0.5 (±0.5) |
| SF-36 PCS, LS mean change from baseline (±SD)[f] | 9.0 (±8.0) | 8.4 (±8.9)[b] |
| FACIT-Fatigue, LS mean change from baseline (±SD)[g] | 9.1 (±11.2) | 8.8 (±11.6)[b] |
| mNAPSI, LS mean change from baseline (±SD)[h] | −16.0 (±17.7) | −14.5 (±17.6) |
| Resolution of dactylitis, n/m (%)[i] | 71/79 (89.9) | 54/62 (87.1) |
| Resolution of enthesitis, n/m (%)[j] | 90/116 (77.6) | 76/100 (76.0) |

* "n" indicates the number of patients who achieved each categorical response; "m" indicates the total number of patients with evaluable data. ACR20, 20% improvement in American College of Rheumatology response criteria; ACR50, 50% improvement in American College of Rheumatology response criteria; FACIT-Fatigue, Functional Assessment of Chronic Illness Therapy – Fatigue; HAQ-DI, Health Assessment Questionnaire–Disability Index; IV, intravenous; LS, least-squares; mNAPSI, modified Nail Psoriasis Severity Index; PASDAS, Psoriatic Arthritis Disease Activity Score; PASI90, 90% improvement in Psoriasis Area and Severity Index score; SF-36 PCS, 36-Item Short Form Health Survey physical component score.
[a] Efficacy measures are arranged according to the predefined hypothesis-testing hierarchy shown in Supplementary Figure 2.
[b] One patient completed their last physician visit within the week 52 analysis window but discontinued the study before week 52.
[c] Patients with psoriasis at baseline were evaluated.
[d] There were 163 evaluable patients who received IV secukinumab, and 156 patients who received placebo/IV secukinumab.
[e] There were 175 evaluable patients who received IV secukinumab, and 169 patients who received placebo/IV secukinumab.
[f] There were 171 evaluable patients who received IV secukinumab, and 172 patients who received placebo/IV secukinumab.
[g] There were 170 evaluable patients who received IV secukinumab, and 171 patients who received placebo/IV secukinumab.
[h] Patients with nail psoriasis at baseline were evaluated. There were 119 evaluable patients who received IV secukinumab, and 111 patients who received placebo/IV secukinumab.
[i] Patients with dactylitis at baseline were evaluated.
[j] Patients with enthesitis at baseline were evaluated.

**Safety.** During treatment period 1, TEAEs were reported in 37.7% and 38.4% of patients who received IV secukinumab and placebo, respectively (Table 4). The most commonly reported TEAEs up to week 16 were COVID-19, hypertension, increased aspartate aminotransferase and alanine aminotransferase, nausea, positive SARS-CoV-2 test, headache, arthralgia, and upper respiratory tract infection. Four patients (one who received IV secukinumab and three who received placebo) discontinued treatment due to a TEAE during treatment period 1. Through week 16, SAEs were reported in three patients who received IV secukinumab (one patient each with COVID-19, pyelonephritis, inadequate control of diabetes mellitus, and hypertension; one patient reported two SAEs) and four patients who received placebo (two patients with COVID-19 pneumonia and one patient each with cerebrovascular accident and transient ischemic attack).

Over the entire treatment period, 63.4% of patients who received any IV secukinumab reported TEAEs (Supplementary Table 3). The most commonly reported TEAEs were COVID-19, urinary tract infection, arthralgia, headache, hypertension, nasopharyngitis, increased alanine aminotransferase, and positive SARS-CoV-2 test. Through week 60, SAEs were reported in 5.9% of patients who received any IV secukinumab. Seven patients who received any IV secukinumab discontinued treatment due to a TEAE during the entire study period. Over the entire treatment period, four patients with candidiasis were reported among those who received any IV secukinumab. Two patients had oral candidiasis that was mild in severity; one of the patients' oral candidiasis was suspected to be related to the

**Table 4.** Safety through week 16 (placebo-controlled period)*

| Parameter | IV secukinumab (n = 191), n (%) | Placebo (n = 190), n (%) |
|---|---|---|
| TEAEs | 72 (37.7) | 73 (38.4) |
| Serious or other significant events | | |
| Nonfatal SAEs | 3 (1.6) | 4 (2.1) |
| Death[a] | 0 | 1 (0.5) |
| Discontinued treatment due to TEAEs | 1 (0.5) | 3 (1.6) |
| Most frequent TEAEs[b] | | |
| COVID-19 | 6 (3.1) | 7 (3.7) |
| Hypertension | 5 (2.6) | 1 (0.5) |
| Aspartate aminotransferase increased | 4 (2.1) | 2 (1.1) |
| Nausea | 4 (2.1) | 2 (1.1) |
| Positive SARS-CoV-2 test | 4 (2.1) | 1 (0.5) |
| Alanine aminotransferase increased | 2 (1.0) | 4 (2.1) |
| Headache | 2 (1.0) | 5 (2.6) |
| Arthralgia | 1 (0.5) | 4 (2.1) |
| Upper respiratory tract infection | 1 (0.5) | 6 (3.2) |

* A patient with multiple occurrences of a TEAE with one treatment is counted only once in the TEAE category for that treatment. IV, intravenous; SAE, serious adverse event; TEAE, treatment-emergent adverse event.
[a] One death due to cerebrovascular accident occurred in the group of patients who received placebo.
[b] TEAEs occurring in ≥2% of either group are listed by preferred term (Medical Dictionary for Regulatory Activities version 25.0) in descending order of frequency in the group of patients who received IV secukinumab.

secukinumab treatment and was resolved. The third patient's oral candidiasis that was moderate in severity was not suspected to be related to study treatment and was unresolved. One patient's vulvovaginal candidiasis that was moderate in severity was not suspected to be related to secukinumab treatment and was resolved. The determination of whether candidiasis was suspected to be related to study treatment was based on the treating physician's assessment. No patients were reported to have Crohn disease or ulcerative colitis. One patient who received placebo died due to cerebrovascular accident before week 16; no other deaths were reported. Over the entire treatment period, one patient who received any IV secukinumab experienced myocardial infarction.

## DISCUSSION

In this placebo-controlled phase 3 trial, receiving IV secukinumab improved the signs and symptoms of PsA through 52 weeks of treatment. Patients with PsA who received IV secukinumab had significantly greater improvements in disease activity, psoriasis, physical function, and QoL through week 16 than patients who received placebo. Patients who switched from placebo to IV secukinumab at week 16 experienced rapid and sustained improvements in these disease measures. Improvements in disease measures in patients who received any IV secukinumab were sustained or increased through week 52. Improvements were seen with secukinumab regardless of previous TNFi exposure. The safety profile of IV secukinumab observed through 52 weeks of treatment in the current study was consistent with previous reports on SC secukinumab in patients with PsA.[8–11]

The improvements in PsA disease control observed with IV secukinumab treatment in this study are consistent with results from previous phase 3 studies that investigated SC secukinumab treatment for patients with PsA.[8–11] IV and SC secukinumab administration were both effective in controlling disease activity, as measured by the proportions of patients achieving ACR responses and resolution of dactylitis and enthesitis. Furthermore, IV and SC secukinumab were both effective in improving health-related QoL and physical ability, as measured by improvements in HAQ-DI, SF-36 PCS, and FACIT-Fatigue scores. However, the proportions of patients who achieved MDA or PASI90 through week 52 with IV secukinumab were numerically higher than the proportions of patients who achieved MDA or PASI90 with SC secukinumab.[10,19–22]

IV secukinumab was generally well tolerated through the entire study period, consistent with the previously reported safety profile for SC secukinumab.[8,20] The incidence of treatment discontinuation due to TEAEs with IV secukinumab over the entire treatment period was consistent with that in previous reports on SC secukinumab through 52 weeks.[8,20] The FUTURE 1 study previously investigated the use of IV secukinumab in patients with PsA at a dose of 10 mg/kg administered at weeks 0, 2, and 4, followed by SC secukinumab (150 or 75 mg) every four weeks.[12] However, INVIGORATE-2 is the first study to investigate IV secukinumab administration over the entire 52-week treatment period in patients with active PsA.

Although many patients with PsA prefer oral and SC routes of drug administration,[23–25] a recent study found that 77% of patients with inflammatory diseases such as PsA who received IV biologics reported being very satisfied with their current IV medication.[26] Among patients who received IV biologics, ≥80% reported preferring IV to SC route of administration, commonly due to dislike of self-injections and needles, IV administration being done by a professional, staff interaction at the infusion site, and the ease of remembering doses with an appointment.[26] Therefore, the availability of IV secukinumab may be beneficial and would provide additional treatment options for these patients and their physicians. Additional treatment modalities could benefit specific patient populations, such as patients with obesity who are more likely to have higher disease activity[27] and may benefit from tighter control of weight-based treatment.

Some limitations of this study should be considered when interpreting the results reported here. INVIGORATE-2 did not

perform a head-to-head comparison between IV and SC routes of secukinumab administration. As such, comparisons of the relative efficacy of IV versus SC secukinumab should be interpreted with caution due to potential differences between patient populations. Evaluation of statistical significance using a predefined hypothesis-testing hierarchy, as done in this study, is influenced by the order of the endpoints in the testing strategy. However, all primary and secondary endpoints reached significance in this study, likely minimizing the possibility of bias. Because the number of patients who had an inadequate response to previous TNFi treatment was low in both the groups of patients who received IV secukinumab and placebo/IV secukinumab, the results of the subgroup analyses should be interpreted with caution. However, the finding that receiving IV secukinumab was effective regardless of previous TNFi exposure is consistent with previous results for SC secukinumab.[8–12] Further studies are needed to assess the efficacy of IV secukinumab in other clinical measures, such as radiographic progression; future subgroup analyses could identify specific patient populations who may receive the most benefit from IV secukinumab.

In conclusion, receiving IV secukinumab provided rapid and sustained improvements in disease signs and symptoms at week 16 and through 52 weeks of treatment in patients with active PsA. The safety profile of IV secukinumab was consistent with that previously reported for SC secukinumab, and no new safety signals were observed. Administration of IV secukinumab could provide rheumatologists additional treatment options to help address the individual treatment needs of patients with PsA.

## AUTHOR CONTRIBUTIONS

All authors were involved in drafting the article and revising it critically for important intellectual content, and all authors approved the final version to be published. Dr Kivitz had full access to all of the data in the study and takes responsibility for the integrity of the data and the accuracy of the data analysis.

**Study conception and design.** Whelan, Dumortier, Zhu, Martin, Pricop.
**Acquisition of data.** Whelan, Dumortier, Zhu, Martin, Pricop.
**Analysis and interpretation of data.** Kivitz, Sedova, Churchill, Kotha, Singhal, Torres, Valenzuela, Whelan, Dumortier, Zhu, Martin, Pricop.

## ROLE OF THE STUDY SPONSOR

This work was supported by Novartis Pharmaceuticals Corporation, East Hanover, NJ, USA. Novartis Pharmaceuticals Corporation had a role in the study design and in the collection, analysis, or interpretation of the data and the decision to submit the manuscript for publication. Medical writing support was provided by Ken Gresham, PhD, CMPP, of Nucleus Global, an Inizio Company, and was funded by Novartis Pharmaceuticals Corporation.

## REFERENCES

1. Ocampo DV, Gladman D. Psoriatic arthritis. F1000Res 2019;8:1665.
2. Azuaga AB, Ramírez J, Cañete JD. Psoriatic arthritis: pathogenesis and targeted therapies. Int J Mol Sci 2023;24:4901.
3. Gudu T, Gossec L. Quality of life in psoriatic arthritis. Expert Rev Clin Immunol 2018;14:405–417.
4. Lee S, Xie L, Wang Y, et al. Comorbidity and economic burden among moderate-to-severe psoriasis and/or psoriatic arthritis patients in the US Department of Defense population. J Med Econ 2018;21:564–570.
5. Kolbinger F, Di Padova F, Deodhar A, et al. Secukinumab for the treatment of psoriasis, psoriatic arthritis, and axial spondyloarthritis: physical and pharmacological properties underlie the observed clinical efficacy and safety. Pharmacol Ther 2022;229:107925.
6. Cosentyx® (Secukinumab) [prescribing information]. East Hanover, NJ: Novartis Pharmaceuticals Corporation, October 2023.
7. European Medicines Agency. Cosentyx: Summary of Product Characteristics. Novartis Europharm Limited. Accessed August 16, 2023. https://www.ema.europa.eu/en/documents/product-information/cosentyx-epar-product-information_en.pdf
8. McInnes IB, Mease PJ, Kirkham B, et al. Secukinumab, a human anti-interleukin-17a monoclonal antibody, in patients with psoriatic arthritis (future 2): a randomised, double-blind, placebo-controlled, phase 3 trial. Lancet 2015;386:1137–1146.
9. Nash P, Mease PJ, McInnes IB, et al. Efficacy and safety of secukinumab administration by autoinjector in patients with psoriatic arthritis: results from a randomized, placebo-controlled trial (FUTURE 3). Arthritis Res Ther 2018;20:47.
10. Kivitz AJ, Nash P, Tahir H, et al. Efficacy and safety of subcutaneous secukinumab 150 mg with or without loading regimen in psoriatic arthritis: results from the FUTURE 4 study. Rheumatol Ther 2019;6:393–407.
11. Mease P, van der Heijde D, Landewé R, et al. Secukinumab improves active psoriatic arthritis symptoms and inhibits radiographic progression: primary results from the randomised, double-blind, phase III FUTURE 5 study. Ann Rheum Dis 2018;77:890–897.
12. Mease PJ, McInnes IB, Kirkham B, et al. Secukinumab inhibition of interleukin-17a in patients with psoriatic arthritis. N Engl J Med 2015;373:1329–1339.
13. Ogdie A, Coates LC, Gladman DD. Treatment guidelines in psoriatic arthritis. Rheumatology (Oxford) 2020;59(Suppl 1):i37–i46.
14. Taylor W, Gladman D, Helliwell P, Marchesoni A, Mease P, Mielants H. CASPAR Study Group. Classification criteria for psoriatic arthritis: development of new criteria from a large international study. Arthritis Rheum. 2006;54(8):2665–2673. doi:10.1002/art.21972
15. Felson DT, Anderson JJ, Boers M, et al. The American College of Rheumatology preliminary core set of disease activity measures for rheumatoid arthritis clinical trials. The Committee on Outcome Measures in Rheumatoid Arthritis Clinical Trials. Arthritis Rheum. 1993;36(6):729–740. doi:10.1002/art.1780360601
16. American College of Rheumatology Committee to Reevaluate Improvement Criteria. A proposed revision to the ACR20: the hybrid measure of American College of Rheumatology response. Arthritis Rheum. 2007;57(2):193–202. doi:10.1002/art.22552. Erratum in: Arthritis Rheum. 2007 Dec 15;57(8):1574.
17. Coates LC, Fransen J, Helliwell PS. Defining minimal disease activity in psoriatic arthritis: a proposed objective target for treatment. Ann Rheum Dis 2010;69(1):48–53.
18. Bretz F, Maurer W, Brannath W, et al. A graphical approach to sequentially rejective multiple test procedures. Stat Med 2009;28(4):586–604.
19. Coates LC, Mease PJ, Gossec L, et al. Minimal disease activity among active psoriatic arthritis patients treated with secukinumab: 2-year results from a multicenter, randomized, double-blind, parallel-group, placebo-controlled phase III study. Arthritis Care Res (Hoboken) 2018;70:1529–1535.

20. van der Heijde D, Mease PJ, Landewé RB, et al. Secukinumab provides sustained low rates of radiographic progression in psoriatic arthritis: 52-week results from a phase 3 study, FUTURE 5. Rheumatology (Oxford) 2020;59:1325–1334.
21. McInnes IB, Behrens F, Mease PJ, et al. Secukinumab versus adalimumab for treatment of active psoriatic arthritis (EXCEED): a double-blind, parallel-group, randomised, active-controlled, phase 3b trial. Lancet 2020;395:1496–1505.
22. Nash P, Mease PJ, McInnes IB, et al. Efficacy and safety of secukinumab administration by autoinjector in patients with psoriatic arthritis: results from a randomized, placebo-controlled trial (future 3). Arthritis Res Ther 2018;20:47.
23. Aletaha D, Husni ME, Merola JF, et al. Treatment mode preferences in psoriatic arthritis: a qualitative multi-country study. Patient Prefer Adherence 2020;14:949–961.
24. Xu Y, Sudharshan L, Hsu MA, et al. Patient preferences associated with therapies for psoriatic arthritis: a conjoint analysis. Am Health Drug Benefits 2018;11:408–417.
25. Ogdie A, Myers K, Mansfield C, et al. Experiences and treatment preferences in patients with psoriatic arthritis: a cross-sectional study in the ArthritisPower registry. Rheumatol Ther 2022;9:735–751.
26. Bolge SC, Eldridge HM, Lofland JH, et al. Patient experience with intravenous biologic therapies for ankylosing spondylitis, Crohn's disease, psoriatic arthritis, psoriasis, rheumatoid arthritis, and ulcerative colitis. Patient Prefer Adherence 2017;11:661–669.
27. Højgaard P, Glintborg B, Kristensen LE, et al. The influence of obesity on response to tumour necrosis factor-α inhibitors in psoriatic arthritis: results from the DANBIO and ICEBIO registries. Rheumatology (Oxford) 2016;55:2191–2199.

American College of Rheumatology
Empowering Rheumatology Professionals

**Arthritis & Rheumatology**
Vol. 77, No. 2, February 2025, pp 180–189
DOI 10.1002/art.42987
© 2024 American College of Rheumatology

# Hypoxia Promotes the Expression of ADAM9 by Tubular Epithelial Cells, Which Enhances Transforming Growth Factor β1 Activation and Promotes Tissue Fibrosis in Patients With Lupus Nephritis

Masataka Umeda,[1] Kohei Karino,[2] Abhigyan Satyam,[2] Nobuya Yoshida,[2] Ryo Hisada,[2] Rhea Bhargava,[2] Theodoros Vichos,[2] Ana Laura Kunzler,[2] Takashi Igawa,[3] Kunihiro Ichinose,[4] Kenta Torigoe,[5] Tomoya Nishino,[5] Takahiro Maeda,[3] Caroline A. Owen,[6] Reza Abdi,[6] Atsushi Kawakami,[3] and George C. Tsokos[2]

**Objective.** Enhanced expression of transforming growth factor (TGF) β in the kidneys of patients with lupus nephritis (LN) can lead to progressive fibrosis, resulting in end-organ damage. ADAM9 activates TGFβ1 by cleaving the latency-associated peptide (LAP). We hypothesized that ADAM9 in the kidney may accelerate fibrogenesis by activating TGFβ1.

**Methods.** We assessed the expression of ADAM9 in the kidneys of mice and humans who were lupus prone. In vitro experiments were conducted using tubular epithelial cells (TECs) isolated from mice and explored the mechanisms responsible for the up-regulation of ADAM9 and the subsequent activation of TGFβ1. To assess the role of ADAM9 in the development of tubular-intestinal fibrosis in individuals with LN, we generated MRL/*lpr* mice who were *Adam9* deficient.

**Results.** ADAM9 was highly expressed in tubules from MRL/*lpr* mice. The transcription factor hypoxia-inducible factor–1α was found to promote the transcription of ADAM9 in TECs. TECs from mice who were *Adam9* deficient and exposed to the hypoxia mimetic agent dimethyloxalylglycine failed to cleave the LAP to produce bioactive TGFβ1 from latent TGFβ1. Coculture of TECs from mice who were *Adam9* deficient with fibroblasts in the presence of dimethyloxalylglycine and latent TGFβ1 produced decreased amounts of type I collagen and α–smooth muscle actin (SMA) by fibroblasts. MRL/*lpr* mice who were *Adam9* deficient showed reduced interstitial fibrosis. At the translational level, ADAM9 expression in tissues and urine of patients with LN was found to increase.

**Conclusion.** Hypoxia promotes the expression of ADAM9 by TECs, which is responsible for the development of interstitial fibrosis in patients with LN by enhancing the TGFβ1 activation, which promotes fibroblasts to produce collagen and α-SMA.

## INTRODUCTION

Systemic lupus erythematosus (SLE) is an autoimmune disorder that is characterized by dysfunction of various immune players, leading to inflammation in multiple organs.[1] Approximately 40% of patients with SLE have lupus nephritis (LN), and the estimated overall 10-year incidence of end-stage renal disease is reported to be 4%.[2] Factors outside the immune system, such as the increased expression of the calcium calmodulin kinase 4 in podocytes and the hypoxic environment in the kidney, are

Dr Umeda's work was supported by the Japanese Society for the Promotion of Science KAKENHI (grants 21K20905 and 22K16362). Dr Satyam's work was supported by the NIH (grant 1R21-AI-151367-01A1). Dr Yoshida's work was supported by the Gilead Sciences Research Scholars Program in Rheumatology. Dr Tsokos's work was supported by the NIH (grants R37-AI-49954 and P01-AI-179405).

[1]Masataka Umeda, MD, PhD: Beth Israel Deaconess Medical Center, Harvard Medical School, Boston, Massachusetts, and Nagasaki University Graduate School of Biomedical Sciences, Nagasaki, Japan; [2]Kohei Karino, MD, PhD, Abhigyan Satyam, PhD, Nobuya Yoshida, MD, PhD, Ryo Hisada, MD, PhD, Rhea Bhargava, MD, Theodoros Vichos, MD, Ana Laura Kunzler, MD, George C. Tsokos, MD: Beth Israel Deaconess Medical Center, Harvard Medical School, Boston, Massachusetts; [3]Takashi Igawa, MD, Takahiro Maeda, MD, PhD, Atsushi Kawakami, MD, PhD: Nagasaki University Graduate School of Biomedical Sciences, Nagasaki, Japan; [4]Kunihiro Ichinose, MD, PhD: Nagasaki University Graduate School of Biomedical Sciences, Nagasaki, and Shimane University Faculty of Medicine, Izumo, Japan; [5]Kenta Torigoe, MD, PhD, Tomoya Nishino, MD, PhD: Nagasaki University Hospital, Nagasaki, Japan; [6]Caroline A. Owen, MD, PhD, Reza Abdi, MD: Brigham and Women's Hospital, Harvard Medical School, Boston, Massachusetts.

Drs Umeda, Karino, and Satyam contributed equally to this work.

Additional supplementary information cited in this article can be found online in the Supporting Information section (http://onlinelibrary.wiley.com/doi/10.1002/art.42987).

Author disclosures and graphical abstract are available at https://onlinelibrary.wiley.com/doi/10.1002/art.42987.

Address correspondence via email to Masataka Umeda, MD, PhD, at masatakau0807@nagasaki-u.ac.jp; or to George C. Tsokos, MD, at gtsokos@bidmc.harvard.edu.

Submitted for publication November 27, 2022; accepted in revised form August 22, 2024.

known to contribute to the development of LN.[3–5] Increased levels of transforming growth factor (TGF) β1 in the kidneys of patients with LN can lead to dysregulated tissue repair, progressive fibrogenesis, and increased end-organ damage.[6]

Metalloproteinases act as sheddases to alter extracellular and cell surface molecules, including growth factors resulting in fibrogenesis.[7] It is noteworthy that ADAMs, a disintegrin and metalloproteinase, [Correction added on 17 December 2024, after first online publication: the preceding text has been corrected in this version.] are involved in fibrosis-associated pathways by proteolytic release of membrane-bound ligands and receptor ectodomains and the remodeling of the extracellular matrix.[8] ADAM9 is a transmembrane protein with a metalloproteinase domain responsible for its proteolytic activity. It has been linked with processes such as retinal neovascularization[9,10] and tumor progression.[11–13] ADAM9 shares an 82% similarity between mice and humans.[14] We previously reported that ADAM9, which is highly expressed in T helper (Th) 17 cells from patients with SLE, activates latent TGFβ1 to generate bioactive TGFβ1 by cleaving off the latency-associated peptide (LAP).[15] A previously conducted proteomics analysis showed increased ADAM9 levels in the urine from patients with LN.[16] ADAM9 is also known to be increased in the lungs of patients with chronic obstructive pulmonary disease, and mice who were *Adam9* deficient and exposed to cigarette smoke were protected from small airway fibrosis.[17] Based on these data, we hypothesized that ADAM9 enhances TGFβ1 activation and promotes tissue fibrosis in individuals with LN.

In this study, we demonstrate that ADAM9 is highly expressed in tubules in MRL/*lpr* mice and the tubules and urine of patients with LN. We show that the transcription factor hypoxia-inducible factor (HIF)-1α enhances the transcription of *ADAM9* in renal tubular epithelial cells (TECs), which in turn enhances the production of bioactive TGFβ1 from latent TGFβ1 and, through this, the production of type I collagen (COL1) and α–smooth muscle actin (SMA) by fibroblasts. MRL/*lpr* mice who were *Adam9* deficient showed less interstitial fibrosis. Collectively, our results show that hypoxia promotes the expression of ADAM9 by TECs, which contributes to the development of interstitial fibrosis in individuals with LN by bioactive TGFβ1 in renal fibroblasts.

## PATIENTS AND METHODS

**Human samples.** Several methods, including coculture of TECs and fibroblasts, immunofluorescence, histologic staining and analysis, enzyme-linked immunosorbent assay (ELISA), RNA isolation and quantitative polymerase chain reaction, Western blotting, flow cytometry, phosphorylated Sma- and Mad-related protein (SMAD)2/3 phospho-flow cytometry for fibroblasts cocultured with TECs, cleavage of LAP by murine primary TECs cultured in vitro, luciferase assays, and chromatin immunoprecipitation assays, are provided in the Supplementary Methods. Patients diagnosed with SLE according to the criteria established by the American College of Rheumatology[18] and healthy individuals were included in the study. Human renal biopsies were collected at the Universities of Nagasaki University, and the classification of LN was conducted by the International Society of Nephrology/Renal Pathology Society criteria.[19] Implantation biopsies from living kidney donors were used as healthy controls. The study protocol was approved by the institutional review boards of Beth Israel Deaconess Medical Center (BIDMC) and Nagasaki University (2006-P-0298 and 22051612, respectively), and informed consent was obtained from all participants. Research participant information is shown in Supplementary Tables 1 and 2.

**Mice.** Mice who were *Adam9*$^{-/-}$ in a pure C57BL/6 background were provided by Caroline Owen (Brigham and Women's Hospital).[20] C57BL6J mice were purchased from The Jackson Laboratory. Mice who were Adam9$^{-/-}$ were backcrossed into MRL/*lpr* mice for 11 generations to obtain MRL/*lpr* mice who were *Adam9*$^{-/-}$, and 11 generations of MRL/*lpr* mice who were *Adam9*$^{+/+}$ were used as mice with an MRL/*lpr* background who were ADAM9 sufficient (control group). All mice with an MRL/*lpr* background for experiments were females, and males were excluded. For the comparison between MRL/*lpr* mice who were *Adam9*$^{+/+}$ and MRL/*lpr* mice who were *Adam9*$^{-/-}$, the quantified intensity of the disease in tubulointerstitial areas was the primary endpoint. Animals were killed at 4 to 8 weeks of age for in vitro experiments and 16 weeks for in vivo experiments. Murine CD4$^+$ T cells were isolated using the mouse CD4$^+$ T Cell Isolation Kit (Miltenyi Biotec). All mice were kept in a pathogen-free animal facility at BIDMC, and all experiments were approved by the Institutional Animal Care and Use Committee of BIDMC. The experimental unit is a single animal. There are no excluded data points except for one missing serum sample from an MRL/*lpr* mouse who was *Adam9*$^{+/+}$ for analyzing the antibodies to double-stranded DNA (dsDNA). MU was aware of the group allocation at the different stages of the experiment.

**Renal epithelial cell and fibroblast enrichment and culture.** Mouse primary renal epithelial cells (TECs) were isolated and enriched as previously reported[21] with Renal Epithelial Cell Growth Medium 2 (PromoCell) at 37°C. After enrichment of TECs, all cultures were conducted with Renal Epithelial Cell Growth Medium-2 on cell-derived, extracellular matrix–coated 24-well plates.[22] Mouse primary renal fibroblasts were isolated as previously reported[23] and cultured in the medium containing Dulbecco's Modified Eagle Medium, 10% fetal bovine serum, and 1% penicillin–streptomycin. Dimethyloxalylglycine (DMOG; catalog 400091, EMD Millipore) was used as a hypoxia mimetic agent, and CAY10585 (Abcam) was used as an HIF-1α inhibitor. All experiments were conducted within the second or third passage of cell culture with 60% to 80% confluence.

**Statistical analyses.** Comparisons between two independent groups were conducted using an unpaired two-tailed

Student's *t*-test. For comparisons between two related groups, a paired *t*-test was used. When comparing more than two groups, we employed one-way analysis of variance followed by Tukey's post hoc tests for multiple comparisons. The sample sizes were determined based on our prior laboratory experience. All statistical analyses were conducted using GraphPad Prism 7.0 software (GraphPad Software). *P* less than 0.05 was considered statistically significant.

## RESULTS

**ADAM9 is expressed in tubules of the mice and patients who were lupus prone with LN.** To assess the expression of ADAM9 in individuals with LN, we first compared ADAM9 levels in kidney lysates of 16-week-old MRL/*lpr* mice and age- and sex-matched MPJ control mice and found that ADAM9 protein levels were higher in the kidney lysates of MRL/*lpr* mice compared to MPJ mice (Figure 1A). Immunofluorescence staining of kidney tissues revealed that ADAM9 was highly expressed in the tubules of MRL/*lpr* mice (Figure 1B), whereas the expression of ADAM9 in the glomeruli was relatively low (Supplementary Figure 1A). In parallel, we found that the ADAM9 expression was increased in the tubules of patients with LN compared to healthy controls (Figure 1C). Glomeruli from patients with LN also expressed low levels of ADAM9 (Supplementary Figure 1B). As mentioned above, a previous study reported that ADAM9 was enriched in the urine of patients with LN.[16] In agreement, using an ELISA, we found that the concentration of ADAM9, corrected to the concentration of urine creatinine, was increased in the urine from patients with LN compared to healthy controls (Figure 1D). We considered that the increased expression of ADAM9 in the tubules contributed to the pathogenesis of LN and planned experiments to determine why it is increased and whether its absence in mice who were lupus prone would mitigate disease severity.

**Hypoxia promotes the expression of ADAM9 in TECs.** Previously, we had shown that the transcription factor inducible cAMP early repressor (ICER), one of the splice variants of the transcription factor CREM, is predominantly expressed in $CD4^+$ T cells from MRL/*lpr* mice,[24] and that ICER induced the expression of ADAM9 in Th17 cells.[15] Unlike lysates from $CD4^+$ T cells, kidney lysates from 16-week-old MRL/*lpr* mice did not express any ICER/CREM, as assessed by Western blotting (Figure 2A). This result suggested that the expression of ADAM9 in TECs is controlled otherwise. Previous studies have shown that ADAM9 was induced by hypoxia in gastric cancer cells and esophageal squamous cell carcinoma.[25,26] In addition, HIF-1α is highly expressed in glomerular and tubulointerstitial areas of LN kidney tissues and that the expression levels correlated with the severity of kidney injury.[27] Because HIF-1α is a transcription factor and the putative hypoxia-response element (HRE) sequence RCGTG (in which R is A or G)[28] exists in the promoter region of the *ADAM9* gene, which is well conserved in both humans and mice, we hypothesized that HIF-1α promotes ADAM9 expression in TECs.

To assess this hypothesis, we isolated renal TECs from murine kidneys and incubated them with or without DMOG, a hypoxia mimetic agent, and analyzed the expressions of HIF-1α and ADAM9. ADAM9, along with HIF-1α expression, was induced upon exposure to DMOG in a dose-dependent manner (Figure 2B). Next, we used CAY10585, an inhibitor of HIF-1α gene transcriptional activity and accumulation, and found that it reduces the expression of ADAM9 in TECs (Figure 2C). These data show that hypoxia and HIF-1α are requisite for the expression of ADAM9 in TECs.

Next, we measured the messenger RNA levels of other members of the ADAM family in TECs cultured with or without DMOG. Besides ADAM9, we included ADAM10, -12, -17, and -19, which have been reported to be involved in various aspects of kidney function.[29–31] We found that ADAM9 was the only member of the ADAM family that displayed enhanced expression in the presence of DMOG (Figure 2D). In contrast, ADAM19 was significantly down-regulated upon incubation of TECs with DMOG. Previous studies have shown that hypoxia induces microRNA (miR)-153, which inhibits tumor growth and metastasis by targeting ADAM19.[32,33] Although we have not examined miR-153 in TECs, we speculate that the same mechanism is involved in the expression of ADAM19 in TECs under hypoxia conditions.

**HIF-1α binds to the *Adam9* promoter directly and increases its activity in TECs.** Next, we investigated whether HIF-1α promotes ADAM9 expression by binding directly to the HRE site defined by the Adam9 promoter. To this end, we constructed luciferase reporter constructs driven by either the complete or by a mutated HRE (Δ-118/-114) Adam9 promoter (Figure 3A). We observed that the reporter activity driven by the Adam9 promoter was reduced in TECs transfected with the mutated construct, compared to those with the full-length promoter, after treatment with DMOG (Figure 3B). Additionally, the presence of CAY10585, an HIF-1α inhibitor, decreased the Adam9 promoter activity in TECs, irrespective of whether they had been transfected with the full-length or the mutated reporter constructs (Figure 3B). To confirm that HIF-1α binds to the Adam9 promoter at the HRE site, TECs were treated with DMOG and subjected to chromatin immunoprecipitation assays. HIF-1α was found to accumulate specifically at the Adam9 promoter region containing the HRE, whereas minimal binding was observed at the intron 3 region of the adjacent Tm2d2 gene, which also has a putative HRE (Figure 3C). This experiment suggests selective binding of HIF-1α to the Adam9 promoter in TECs. These findings affirm that HIF-1α directly induces ADAM9 expression by binding to its promoter in TECs.

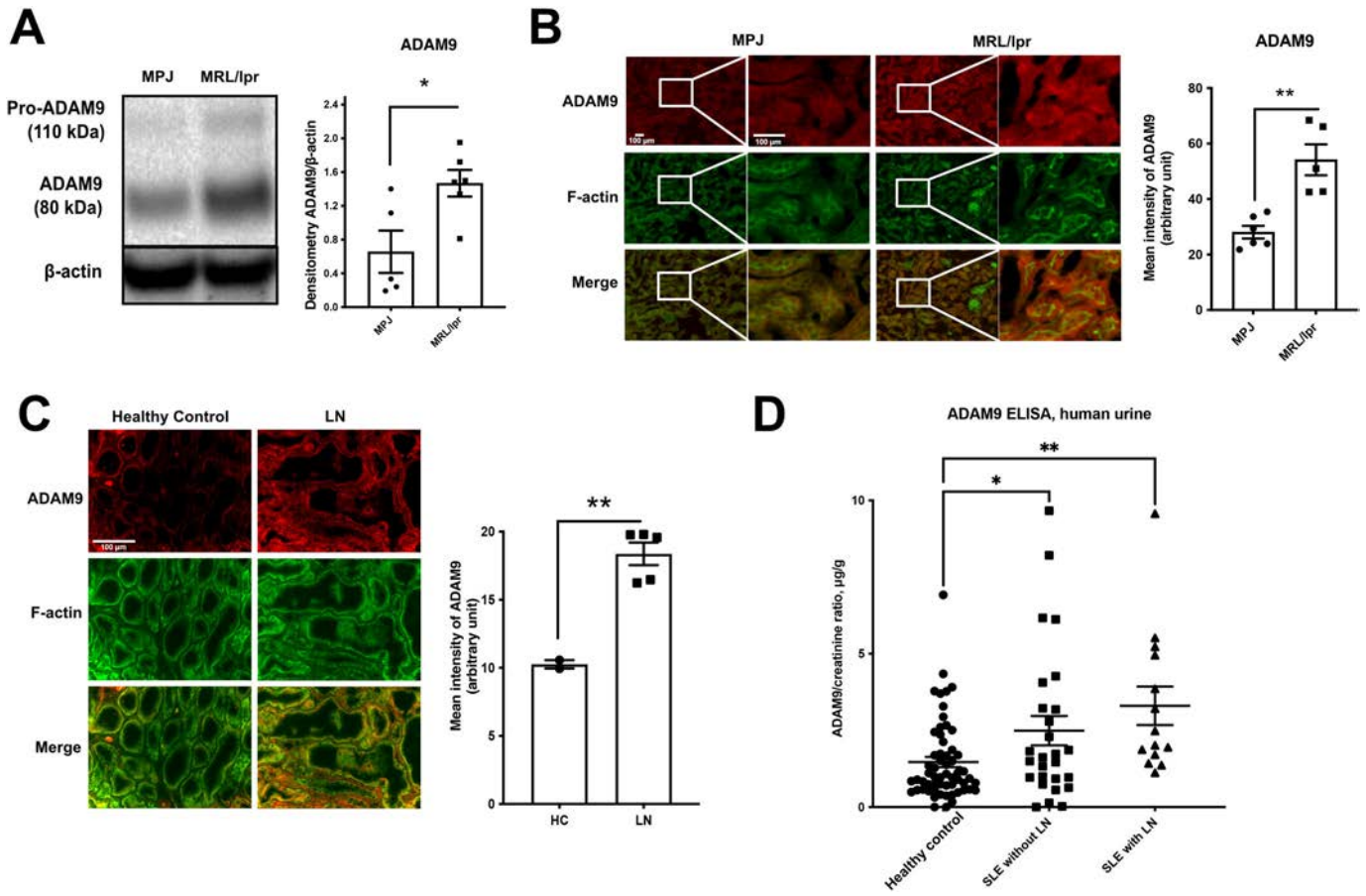


**Figure 1.** ADAM9 expression is increased in the tubules of mice and patients who were lupus prone with lupus nephritis (LN). (A) A representative Western blot of kidney lysates from 16-week-old MRL/*lpr* and MPJ mice blotted for pro-ADAM9, ADAM9 (active), and β-actin are shown (left). Cumulative densitometric readings of ADAM9 (active) and β-actin are shown (right; five MPJ mice and six MRL/*lpr* mice). *$P < 0.05$. (B) Representative immunofluorescent images for ADAM9 and F-actin in tissues from 16-week-old MRL/*lpr* and MPJ mice are shown in the left. Red and green color represents ADAM9 and F-actin, respectively (scale, 100 μm). The right panel shows quantified fluorescence intensity of ADAM9 (six MPJ mice and five MRL/*lpr* mice). **$P < 0.01$. (C) Representative images of immunofluorescence for ADAM9 and F-actin from healthy controls (HCs) and patients with histologic class IV LN are shown (left). Red and green color represents ADAM9 and F-actin, respectively (scale, 100 μm). The right panel shows the quantified fluorescence intensity of ADAM9 (two HCs and five individuals with LN). **$P < 0.01$. (D) The urine ADAM9 to creatine ratio from HCs, individuals with SLE without LN, and individuals with SLE with LN were analyzed by ELISA (59 HCs, 27 individuals with SLE without LN, and 14 individuals with SLE with LN). Mean ± SEM. **$P < 0.01$. ELISA, enzyme-linked immunosorbent assay; MPJ; MRL/*lpr*; SLE, systemic lupus erythematosus.

**TGFβ1 activation by ADAM9 in TECs activates fibroblasts.** TGFβ1 has a critical role in the development of fibrosis in LN by activating fibroblasts.[6] TGFβ1 is initially secreted in a latent complex form (latent TGFβ1), which consists of disulfide-linked homodimers complexed with the LAP, and LAP needs to be cleaved by metalloproteinases to generate active TGFβ.[34,35] Previously, we showed that LAP is a substrate of ADAM9 and ADAM9 expressed on Th17 cells can transform latent TGFβ1 into bioactive TGFβ1 by cleaving LAP.[15] To confirm the ability of ADAM9 to activate TGFβ1 in TECs, we assessed the enzymatic function of ADAM9 in a live-cell setting. We cultured TECs from mice who were *Adam9* sufficient or deficient with DMOG and latent TGFβ1 and found that LAP levels in the culture supernatants were decreased in TECs from mice who were *Adam9* sufficient compared with cells from mice who were *Adam9* deficient (Figure 4A). This result suggests that ADAM9 expressed in TECs activates TGFβ1 by cleaving LAP. Next, to assess the role of ADAM9 in the activation of fibroblasts, we cocultured TECs and fibroblasts using a Transwell assay. In the upper compartment, TECs from mice who were *Adam9* sufficient or deficient were cultured with latent TGFβ1 and DMOG. In the lower compartment, fibroblasts were obtained from mice who were *Adam9* deficient to eliminate the effect of ADAM9 expressed by fibroblasts (Figure 4B). After 24 hours of incubation, we measured the expression of α-SMA and COL1 in the fibroblasts as markers of their activation. Fibroblasts cultured with TECs from mice who were *Adam9* deficient displayed decreased expression of α-SMA and COL1 compared to fibroblasts cultured with TECs

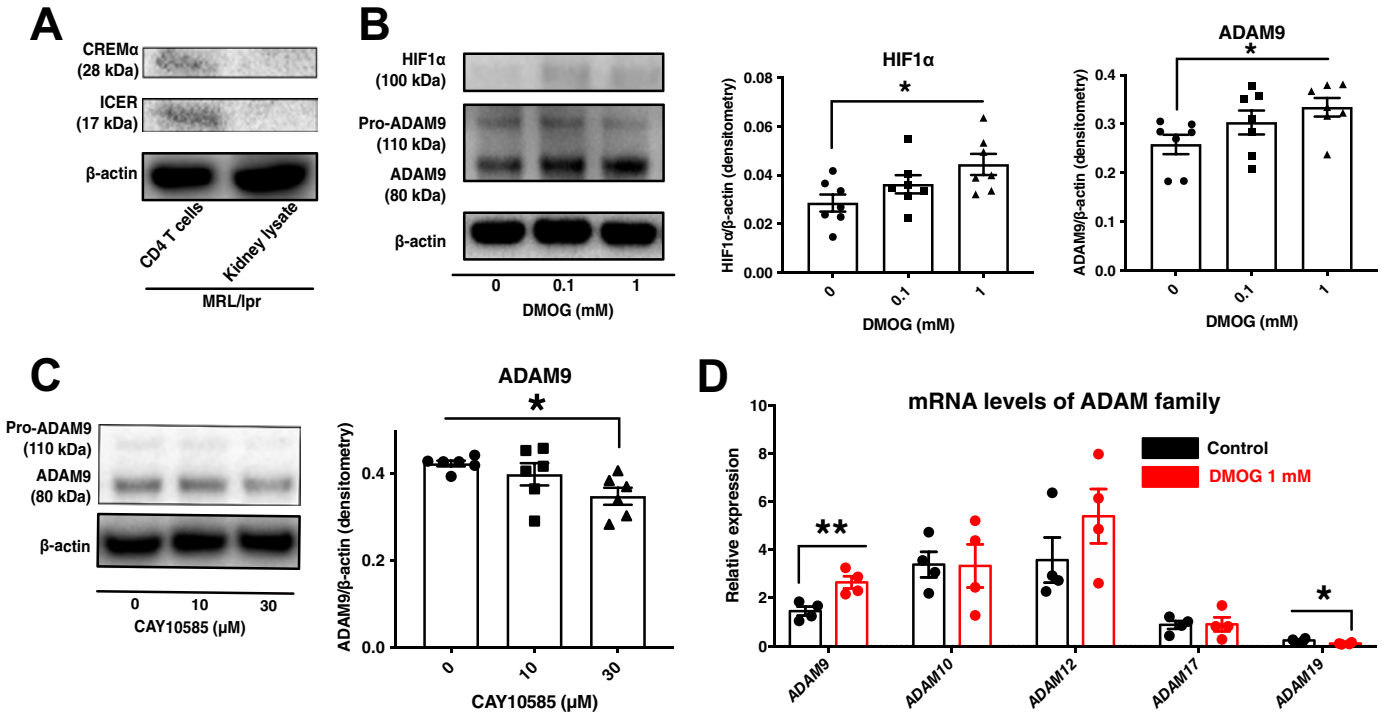


**Figure 2.** Hypoxia enhances ADAM9 expression in tubular epithelial cells (TECs). (A) Western blot of lysates of $CD4^+$ T cells and kidney tissue from 16-week-old of MRL/*lpr* mice for CREM and actin protein expression. (B) Enriched renal TECs from B6 mice were incubated with or without the hypoxia mimetic DMOG and protein expression of HIF-1α, pro-ADAM9, ADAM9, and β-actin at 24 hours was determined by Western blotting. A representative (of six) blot is shown (left), and cumulative densitometric readings of HIF-1α, ADAM9, and β-actin are shown (middle and right). *$P < 0.05$. (C) Enriched TECs from B6 mice were incubated with or without CAY10585, an inhibitor of HIF-1α, and protein expression of ADAM9, and β-actin at 24 hours were determined by Western blotting. A representative blot is shown (left) and cumulative densitometric readings of ADAM9, and β-actin are shown (right; n = 6). *$P < 0.05$. (D) mRNA expression (quantitative reverse transcriptase–polymerase chain reaction) of members of the ADAM family in TECs cultured for 24 hours with or without DMOG. Cumulative data are shown (n = 4). Mean ± SEM. *$P < 0.05$, **$P < 0.01$. DMOG, dimethyloxalylglycine; HIF, hypoxia-inducible factor; ICER, inducible cAMP early repressor; MRL/*lpr*; mRNA, messenger RNA.

from mice who were *Adam9* sufficient (Figure 4C). Next, to assess the involvement of TGFβ1 downstream signaling events, we examined the levels of phosphorylated SMAD2/3 in fibroblasts by flow cytometry. TGFβ1 binding to the TGFβ1 receptor elicits the phosphorylation of Ser465 and Ser467 of Smad2 and Ser423 and Ser425 of Smad3.[36,37] As shown in Figure 4D, the median fluorescence intensity of phosphorylated SMAD2/3 was diminished in fibroblasts cultured with TECs from mice who were *Adam9* deficient compared to fibroblasts cultured with TECs from mice who were *Adam9* sufficient. Collectively, we have confirmed that ADAM9 in TECs promotes the activation of fibroblasts through the activation of TGFβ1 and the subsequent phosphorylation of SMAD2/3.

**Deletion of *ADAM9* ameliorates LN.** Given that ADAM9 deficiency had impacted the activation of fibroblasts in vitro, we assessed the importance of ADAM9 in the pathogenesis of LN in vivo. To this end, we generated MRL/*lpr* mice who were *Adam9*$^{-/-}$, and when aged to 16 weeks of age, we studied them in parallel with their MRL/*lpr* controls who were *Adam9*$^{+/+}$. Histologic sections from kidneys of MRL/*lpr* mice who were *Adam9*$^{-/-}$ displayed significantly reduced tubular score compared to mice who were *Adam9* sufficient (Figure 5A). Sirius red staining also showed less interstitial fibrosis in MRL/*lpr* mice who were *Adam9*$^{-/-}$ (Supplementary Figure 2A). In addition, the glomerular score was significantly decreased in the mice who were *Adam9* deficient compared to the mice who were *Adam9* sufficient (Figure 5A). Although the mean values for urine albumin to creatinine ratio and serum levels of dsDNA were numerically lower in MRL/*lpr* mice who were *Adam9*$^{-/-}$, these values did not reach statistical significance (Supplementary Figure 2B and C). Flowcytometry analysis showed reduced number of kidney-infiltrating, IL-17A–producing T cells in MRL/*lpr* mice who were *Adam9*$^{-/-}$ compared with their controls (Supplementary Figure 2D and E). These results confirmed that ADAM9 deletion ameliorates LN.

## DISCUSSION

Damage to the renal tubules is one of the pivotal factors that dictate the prognosis in patients with LN. An international multicenter study showed that histologic tubular damage is an independent predictive factor of low glomerular filtration rates in

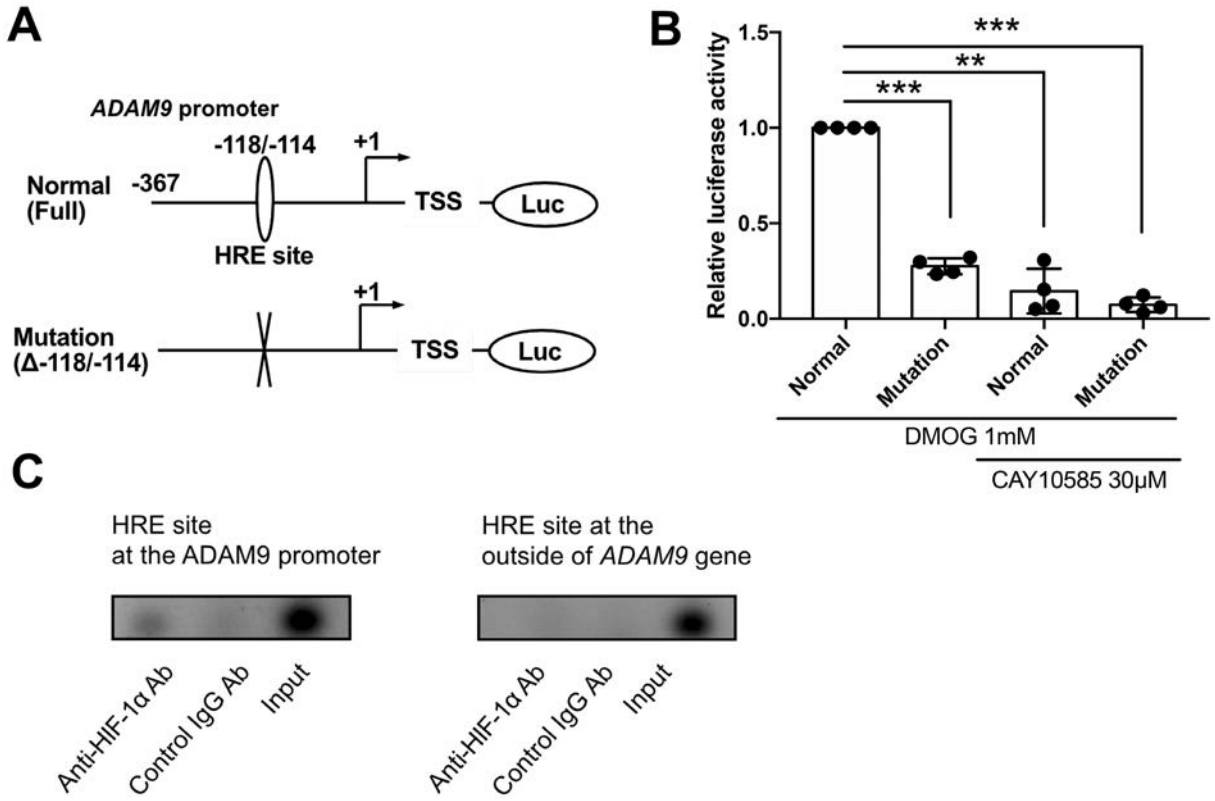


**Figure 3.** HIF-1α binds to the ADAM9 promoter directly and increases its activity in tubular epithelial cells (TECs). (A) Schematic representation of the reporter constructs. Numbers represent the position from the transcription start site (TSS) of the murine *Adam9* gene. (B) The full-length *Adam9* promoter region (full) or a version containing a mutated HRE binding site (Δ-118/-114) was transfected into TECs, then incubated in the presence of DMOG with or without CAY10585. Cells were harvested and lysed at 24 hours. The cumulative results of four independent experiments are shown. $^{**}P < 0.01$, $^{***}P < 0.001$. (C) TECs were incubated with 1 mM of DMOG, then harvested and lysed at 24 hours, and the binding of HIF-1α to the HRE site was assessed by chromatin immunoprecipitation assay. An HRE site at the intron 3 of the adjacent gene (Tm2d2) was used as a negative control. Bands were detected in agarose gels after polymerase chain reaction amplification. Representative blots from three experiments are shown. Mean ± SEM. DMOG, dimethyloxalylglycine; HIF, hypoxia-inducible factor; HRE, hypoxia-response element; Luc, luciferace.

patients with LN.[38] Also, tubular injury was shown to be a predictor of renal function outcome and to predict a doubling in serum creatinine levels, end-stage renal disease, and death independently of the histologic classification of LN.[39] In addition, tubular basement membrane immune complex deposition is associated with disease activity and progression of LN.[40] These reports direct attention to the study of mechanisms that are involved in the damage of kidney tubules.

In the present study, we identified that ADAM9 is expressed at increased levels in the tubules of kidneys from humans and mice with lupus and that the transcription factor HIF-1α increases the expression of ADAM9 directly at the transcriptional level. ADAM9 in TECs activates fibroblasts by generating bioactive TGFβ1, which activates fibroblasts to produce collagen. MRL/*lpr* mice who were *Adam9* deficient showed mitigated interstitial fibrosis (Figure 5B).

TGFβ1 plays a critical role in the progression of fibrosis not only in individuals with LN but also in individuals with various kidney diseases through its profibrotic function.[6,41,42] In addition, TGFβ1 is a multifunctional cytokine that skews naive $CD4^+$ T cells to Th17 cells as an immunomodulator in combination with IL-6,[43] whereas the combination of TGFβ1 and IL-2 directs polarization toward T regulatory cells.[44] Despite the involvement of TGFβ1 in the pathogenesis of various kidney diseases, the mechanism of TGFβ1 activation in the kidney has not been elucidated. Our study assigns to a proteinase, ADAM9, the role of generating bioactive TGFβ1 in the kidney.

Hypoxia and HIFs are determinants of fibrosis in carcinogenesis in several cancers by enhancing the production of profibrotic and fibrotic factors.[45–47] ADAM9 has been reported to be involved in tumor progression and is associated with poor prognosis.[11,12,48] Hypoxia in the kidney is associated with both acute kidney injury and chronic kidney disease, and hypoxia has been claimed to be the expressed pathophysiology.[49,50] Hypoxia in the tubulointerstitium of individuals with diseased kidneys is proposed as the final common pathway toward end-stage kidney disease.[51] ADAM9 expression has been linked to the release of proangiogenic factors, resulting in retinal neovascularization.[10]

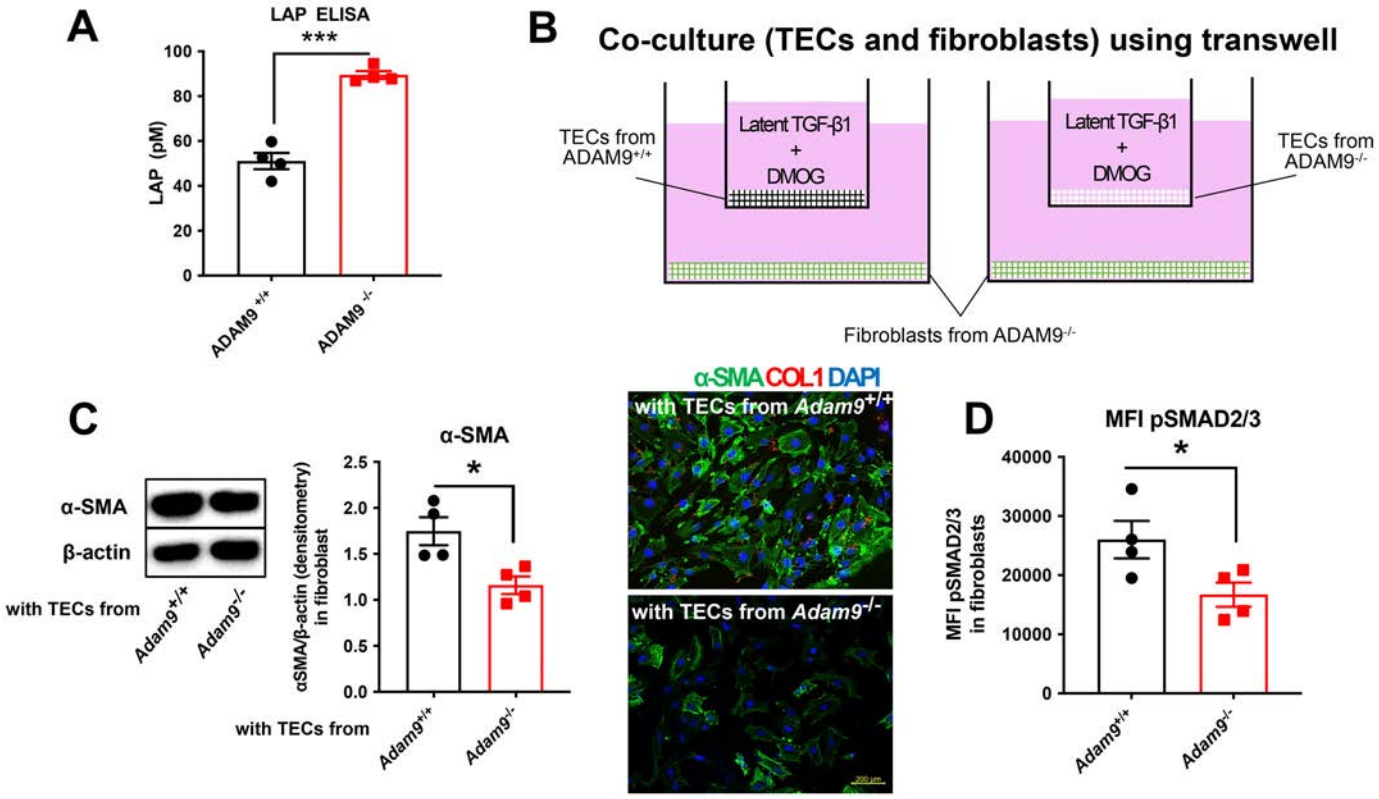


**Figure 4.** TECs from mice who were *Adam9* deficient show decreased ability in activating TGFβ1 and fibroblasts. (A) Enriched TECs from mice who were *Adam9* sufficient and *Adam9* deficient were incubated with DMOG (1 mM) and latent TGFβ1 (1.0 ng/mL) for 24 hours. Culture media were analyzed by ELISA to detect latency-associated peptide (LAP; n = 4). ***$P < 0.001$. (B) Schematic representation showing the coculture of TECs and fibroblasts. The upper compartment contained TECs from mice who were *Adam9* sufficient or deficient with 10 ng/100 μL of latent TGFβ1 and 1 mM of DMOG, and the lower compartment contained fibroblasts obtained from mice who were *Adam9* deficient. After 24 hours of incubation, fibroblasts in the lower compartment were analyzed. (C) A representative Western blot for α–smooth muscle actin (SMA) and β-actin expressions by fibroblasts cocultured with TECs from mice who were *Adam9* sufficient or deficient is shown (left), and cumulative densitometric readings of α-SMA and β-actin are shown (middle; n = 4). Representative immunofluorescence images of fibroblasts cocultured with TECs are shown (right). Green, red, or blue color represents α-SMA, type I collagen (COL1), or DAPI, respectively (scale, 200 μm). *$P < 0.05$. (D) After the coculture with TECs, fibroblasts were analyzed by flow cytometry to assess p-Smad2/3. The cumulative median fluorescence intensity (MFI) of p-SMAD2/3 is shown (n = 4). Mean ± SEM. *$P < 0.05$. DMOG, dimethyloxalylglycine; ELISA, enzyme-linked immunosorbent assay; SMAD, Sma- and Mad-related protein; TEC, tubular epithelial cell; TGF, transforming growth factor.

However, none of the previous reports has elucidated the precise mechanism whereby hypoxia enhances ADAM9 expression. The present study demonstrates that the transcription factor HIF-1α binds the *Adam9* promoter and enhances its expression in TECs. Taken together, we have shown that the HIF-1α/ADAM9/TGFβ1 is important in the pathogenesis of tissue fibrosis in LN.

There are several limitations in this study. First, we have not conducted experiments under actual hypoxia conditions. Instead of using a hypoxia incubator, all our experiments requiring hypoxia were conducted by using the hypoxia mimetic agent DMOG. Yet, the induction of HIF-1α by hypoxia mimetic agent is well established. Second, we used mice of MRL/*lpr* background who were ADAM9 germline deficient for the in vivo experiments. As we reported previously, ADAM9 is also important for the polarization of Th17 cells,[15] and germline deficiency of ADAM9 may affect the contribution of immune cells. Indeed, mice of MRL/*lpr* background who were *Adam9* deficient showed a decreased number of kidney-infiltrating, IL-17A–producing T cells. To further investigate the physiologic significance of ADAM9 in a TEC-specific manner, the use of TECs of conditional knockout mice with *Adam9* or bone marrow chimeras is required. Despite observing higher levels of ADAM9 levels in the urine of patients with SLE with LN compared to those without LN, this difference did not reach statistical significance. Previous reports have indicated that patients with SLE without clinical renal abnormalities can still exhibit kidney pathology.[52] This suggests that baseline renal abnormalities or hypoxia in individuals with SLE can influence ADAM9 concentrations in the urine of patients without clinical nephritis. Further investigation is needed to verify this hypothesis.

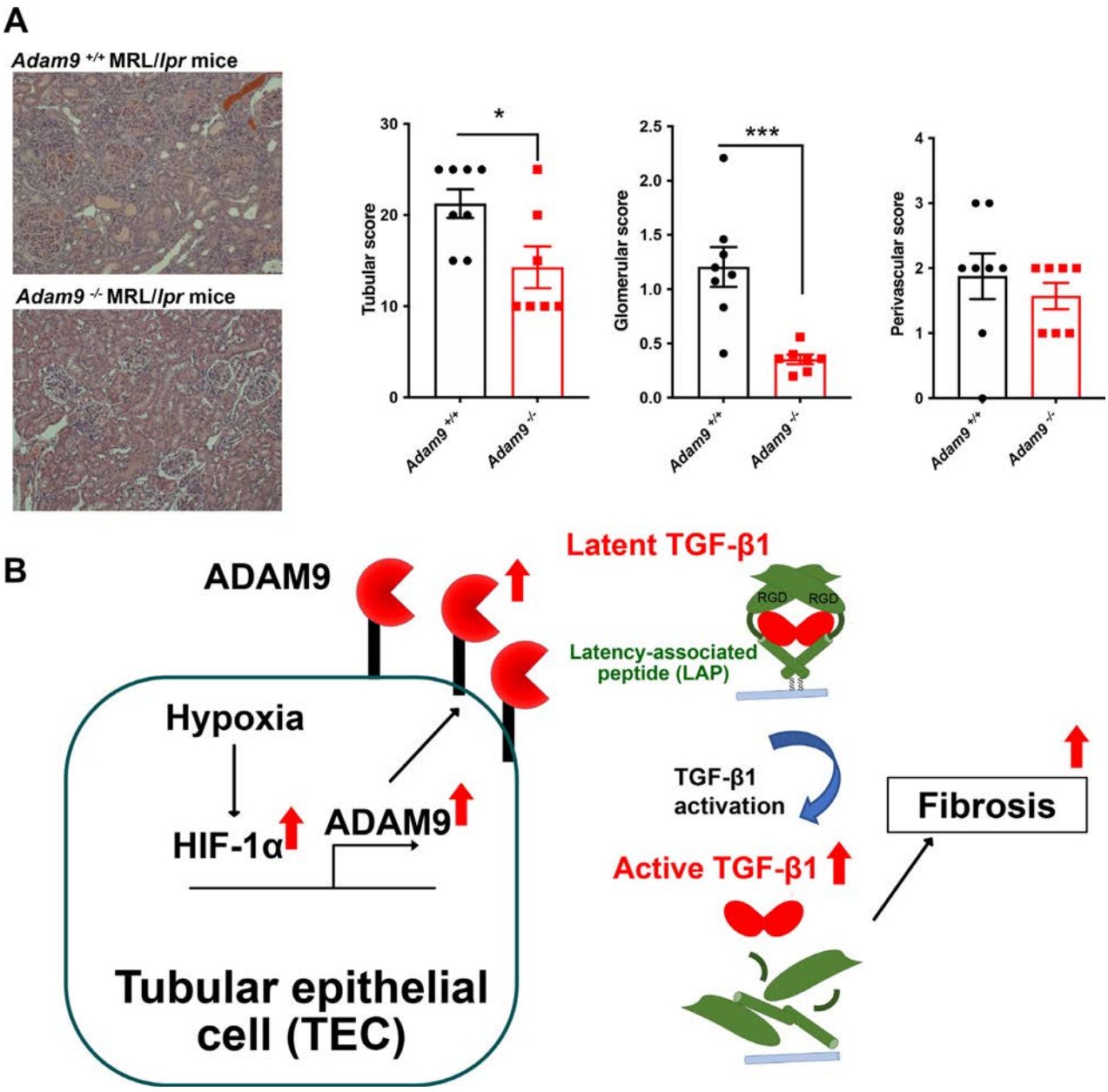


**Figure 5.** *Adam9* deficiency mitigates the severity of LN in MRL/*lpr* mice. (A) Mice from an MRL/*lpr* background who were *Adam9* sufficient and deficient were euthanized at the age of 16 weeks old. Representative images from hematoxylin and eosin–stained sections of kidneys are shown (scale, 100 μm). *$P < 0.05$, ***$P < 0.001$. (B) Cumulative kidney pathology scores are shown (8 mice who were *Adam9* sufficient mice, 7 mice who were *Adam9* deficient, and 15 total mice). Mean ± SEM. Proposed model depicting that hypoxia promotes the expression of ADAM9 by TECs, which enhances TGFβ1 activation and promotes tissue fibrosis in individuals with LN. HIF, hypoxia-inducible factor; LN, lupus nephritis; MRL/*lpr*; RGD, arginyl-glycyl-aspartic acid motif; TGF, transforming growth factor.

In sum, we have identified ADAM9 as a proteinase that enhances TGFβ1 activation in TECs, resulting in fibrosis through the activation of fibroblasts. Hypoxia and HIF-1α promote the expression of ADAM9 by binding to its promoter directly. Our findings uncover a novel mechanism involved in the pathogenesis of LN that is not directly mediated by the immune system. From the demonstrated importance of ADAM9 in the development of LN in mice and kidneys of patients with LN, we propose that ADAM9 inhibition may represent a novel therapeutic approach to mitigate kidney failure in patients with LN.

## AUTHOR CONTRIBUTIONS

All authors contributed to at least one of the following manuscript preparation roles: conceptualization AND/OR methodology, software, investigation, formal analysis, data curation, visualization, and validation

AND drafting or reviewing/editing the final draft. As corresponding authors, Drs Umeda and Tsokos confirm that all authors have provided the final approval of the version to be published, and take responsibility for the affirmations regarding article submission (eg, not under consideration by another journal), the integrity of the data presented, and the statements regarding compliance with institutional review board/Helsinki Declaration requirements.

## REFERENCES


1. Tsokos GC. Systemic lupus erythematosus. N Engl J Med 2011;365:2110–2121.
2. Hanly JG, O'Keeffe AG, Su L, et al. The frequency and outcome of lupus nephritis: results from an international inception cohort study. Rheumatology (Oxford) 2016;55:252–262.
3. Maeda K, Otomo K, Yoshida N, et al. CaMK4 compromises podocyte function in autoimmune and nonautoimmune kidney disease. J Clin Invest 2018;128:3445–3459.
4. Chen PM, Wilson PC, Shyer JA, et al. Kidney tissue hypoxia dictates T cell-mediated injury in murine lupus nephritis. Sci Transl Med 2020;12:eaay1620.
5. Ichinose K, Ushigusa T, Nishino A, et al. Lupus nephritis IgG induction of calcium/calmodulin-dependent protein kinase IV expression in podocytes and alteration of their function. Arthritis Rheumatol 2016;68:944–952.
6. Saxena V, Lienesch DW, Zhou M, et al. Dual roles of immunoregulatory cytokine TGF-beta in the pathogenesis of autoimmunity-mediated organ damage. J Immunol 2008;180:1903–1912.
7. Costanza B, Umelo IA, Bellier J, et al. Stromal modulators of TGF-β in cancer. J Clin Med 2017;6:7.
8. Schmidt-Arras D, Rose-John S. Regulation of fibrotic processes in the liver by ADAM proteases. Cells 2019;8:1226.
9. Parry DA, Toomes C, Bida L, et al. Loss of the metalloprotease ADAM9 leads to cone-rod dystrophy in humans and retinal degeneration in mice. Am J Hum Genet 2009;84:683–691.
10. Guaiquil V, Swendeman S, Yoshida T, et al. ADAM9 is involved in pathological retinal neovascularization. Mol Cell Biol 2009;29:2694–2703.
11. Grutzmann R, Luttges J, Sipos B, et al. ADAM9 expression in pancreatic cancer is associated with tumour type and is a prognostic factor in ductal adenocarcinoma. Br J Cancer 2004;90:1053–1058.
12. Fritzsche FR, Wassermann K, Jung M, et al. ADAM9 is highly expressed in renal cell cancer and is associated with tumour progression. BMC Cancer 2008;8:179.
13. Peduto L, Reuter VE, Shaffer DR, et al. Critical function for ADAM9 in mouse prostate cancer. Cancer Res 2005;65:9312–9319.
14. Weskamp G, Kratzschmar J, Reid MS, et al. MDC9, a widely expressed cellular disintegrin containing cytoplasmic SH3 ligand domains. J Cell Biol 1996;132:717–726.
15. Umeda M, Yoshida N, Hisada R, et al. ADAM9 enhances Th17 cell differentiation and autoimmunity by activating TGF-β1. Proc Natl Acad Sci U S A 2021;118:e2023230118.
16. Stanley S, Vanarsa K, Soliman S, et al. Comprehensive aptamer-based screening identifies a spectrum of urinary biomarkers of lupus nephritis across ethnicities. Nat Commun 2020;11:2197.
17. Wang X, Polverino F, Rojas-Quintero J, et al. A disintegrin and a metalloproteinase-9 (ADAM9): a novel proteinase culprit with multifarious contributions to COPD. Am J Respir Crit Care Med 2018;198:1500–1518.
18. Hochberg MC. Updating the American College of Rheumatology revised criteria for the classification of systemic lupus erythematosus. Arthritis Rheum 1997;40:1725.
19. Weening JJ, D'Agati VD, Schwartz MM, et al. The classification of glomerulonephritis in systemic lupus erythematosus revisited. Kidney Int 2004;65:521–530.
20. Weskamp G, Cai H, Brodie TA, et al. Mice lacking the metalloprotease-disintegrin MDC9 (ADAM9) have no evident major abnormalities during development or adult life. Mol Cell Biol 2002;22:1537–1544.
21. Ding W, Yousefi K, Shehadeh LA. Isolation, characterization, and high throughput extracellular flux analysis of mouse primary renal tubular epithelial cells. J Vis Exp 2018;(136):57718.
22. Satyam A, Tsokos MG, Tresback JS, et al. Cell-derived extracellular matrix-rich biomimetic substrate supports podocyte proliferation, differentiation, and maintenance of native phenotype. Adv Funct Mater 2020;30:1908752.
23. Grimwood L, Masterson R. Propagation and culture of renal fibroblasts. Methods Mol Biol 2009;466:25–37.
24. Yoshida N, Comte D, Mizui M, et al. ICER is requisite for Th17 differentiation. Nat Commun 2016;7:12993.
25. Kim JM, Jeung HC, Rha SY, et al. The effect of disintegrin-metalloproteinase ADAM9 in gastric cancer progression. Mol Cancer Ther 2014;13:3074–3085.
26. Lin YS, Kuo TT, Lo CC, et al. ADAM9 functions as a transcriptional regulator to drive angiogenesis in esophageal squamous cell carcinoma. Int J Biol Sci 2021;17:3898–3910.
27. Deng W, Ren Y, Feng X, et al. Hypoxia inducible factor-1 alpha promotes mesangial cell proliferation in lupus nephritis. Am J Nephrol 2014;40:507–515.
28. Wenger RH, Stiehl DP, Camenisch G. Integration of oxygen signaling at the consensus HRE. Sci STKE 2005;2005:re12.
29. Kato T, Hagiyama M, Ito A. Renal ADAM10 and 17: their physiological and medical meanings. Front Cell Dev Biol 2018;6:153.
30. Gao J, Yang D, Xu H, et al. ADAM metallopeptidase domain 12 overexpression correlates with prognosis and immune cell infiltration in clear cell renal cell carcinoma. Bioengineered 2022;13:2412–2429.
31. Melenhorst WB, van den Heuvel MC, Timmer A, et al. ADAM19 expression in human nephrogenesis and renal disease: associations with clinical and structural deterioration. Kidney Int 2006;70:1269–1278.
32. Liang H, Xiao J, Zhou Z, et al. Hypoxia induces miR-153 through the IRE1α-XBP1 pathway to fine tune the HIF1α/VEGFA axis in breast cancer angiogenesis. Oncogene 2018;37:1961–1975.
33. Wang X, Wang E, Cao J, et al. MiR-145 inhibits the epithelial-to-mesenchymal transition via targeting ADAM19 in human glioblastoma. Oncotarget 2017;8:92545–92554.
34. Annes JP, Munger JS, Rifkin DB. Making sense of latent TGFbeta activation. J Cell Sci 2003;116:217–224.
35. Travis MA, Sheppard D. TGF-beta activation and function in immunity. Annu Rev Immunol 2014;32:51–82.
36. Abdollah S, Macias-Silva M, Tsukazaki T, et al. TbetaRI phosphorylation of Smad2 on Ser465 and Ser467 is required for Smad2-Smad4 complex formation and signaling. J Biol Chem 1997;272:27678–27685.
37. Liu X, Sun Y, Constantinescu SN, et al. Transforming growth factor beta-induced phosphorylation of Smad3 is required for growth inhibition and transcriptional induction in epithelial cells. Proc Natl Acad Sci U S A 1997;94:10669–10674.
38. Pagni F, Galimberti S, Galbiati E, et al. Tubulointerstitial lesions in lupus nephritis: international multicentre study in a large cohort of patients with repeat biopsy. Nephrology (Carlton) 2016;21:35–45.
39. Obrisca B, Jurubita R, Andronesi A, et al. Histological predictors of renal outcome in lupus nephritis: the importance of tubulointerstitial lesions and scoring of glomerular lesions. Lupus 2018;27:1455–1463.

40. Wang H, Xu J, Zhang X, et al. Tubular basement membrane immune complex deposition is associated with activity and progression of lupus nephritis: a large multicenter Chinese study. Lupus 2018;27:545–555.
41. Border WA, Noble NA. Transforming growth factor beta in tissue fibrosis. N Engl J Med 1994;331:1286–1292.
42. Border WA, Noble NA, Yamamoto T, et al. Natural inhibitor of transforming growth factor-beta protects against scarring in experimental kidney disease. Nature 1992;360:361–364.
43. Bettelli E, Carrier Y, Gao W, et al. Reciprocal developmental pathways for the generation of pathogenic effector TH17 and regulatory T cells. Nature 2006;441:235–238.
44. Bommireddy R, Doetschman T. TGFbeta1 and Treg cells: alliance for tolerance. Trends Mol Med 2007;13:492–501.
45. Triantafyllou EA, Mylonis I, Simos G, et al. Hypoxia induces pro-fibrotic and fibrosis marker genes in hepatocellular carcinoma cells independently of inflammatory stimulation and the NF-κB pathway. Hypoxia (Auckl) 2019;7:87–91.
46. Roth KJ, Copple BL. Role of hypoxia-inducible factors in the development of liver fibrosis. Cell Mol Gastroenterol Hepatol 2015;1:589–597.
47. Gilkes DM, Semenza GL, Wirtz D. Hypoxia and the extracellular matrix: drivers of tumour metastasis. Nat Rev Cancer 2014;14:430–439.
48. Zubel A, Flechtenmacher C, Edler L, et al. Expression of ADAM9 in CIN3 lesions and squamous cell carcinomas of the cervix. Gynecol Oncol 2009;114:332–336.
49. Nangaku M, Rosenberger C, Heyman SN, et al. Regulation of hypoxia-inducible factor in kidney disease. Clin Exp Pharmacol Physiol 2013;40:148–157.
50. Mimura I, Nangaku M. The suffocating kidney: tubulointerstitial hypoxia in end-stage renal disease. Nat Rev Nephrol 2010;6:667–678.
51. Fine LG, Bandyopadhay D, Norman JT. Is there a common mechanism for the progression of different types of renal diseases other than proteinuria? Towards the unifying theme of chronic hypoxia. Kidney Int Suppl 2000;75:S22–S26.
52. O'Dell JR, Hays RC, Guggenheim SJ, et al. Systemic lupus erythematosus without clinical renal abnormalities: renal biopsy findings and clinical course. Ann Rheum Dis 1985;44:415–419.

**Arthritis & Rheumatology**
Vol. 77, No. 2, February 2025, pp 190–201
DOI 10.1002/art.42989
© 2024 EMD Serono. *Arthritis & Rheumatology* published by Wiley Periodicals LLC on behalf of American College of Rheumatology. This is an open access article under the terms of the Creative Commons Attribution-NonCommercial-NoDerivs License, which permits use and distribution in any medium, provided the original work is properly cited, the use is non-commercial and no modifications or adaptations are made.

American College of Rheumatology
*Empowering Rheumatology Professionals*

# TLR7/8 Activation in Immune Cells and Muscle by RNA-Containing Immune Complexes: Role in Inflammation and the Pathogenesis of Myositis

Yin Wu,[1] Aditee Deshpande,[1] Nicholas Geraci,[1] Petra Budde,[2] Vera Sellers,[1] Phanindra Velisetty,[1] Chia-Chi Sun,[1] Fatima Strand,[1] Carmina Bhavsar,[1] Timothy B. Niewold,[3] Mark A. Jensen,[4] Irina Kalatskaya,[1] Kavita Y. Sarin,[5] David Fiorentino,[5] and Andrew T. Bender[1]

**Objective.** Activation of endosomal toll-like receptors (TLRs) is one possible driver of inflammation in idiopathic inflammatory myopathies (IIM). We investigated the potential contribution of TLR7 and TLR8 to IIM pathogenesis.

**Methods.** Activation of TLR7/8 in healthy donor peripheral blood mononuclear cells (PBMCs) by immune complexes from patients with IIMs and lupus was tested. Autoantibody profiling of patient IgG samples was performed using a 1581 antigen array. TLR7 and/or TLR8 activation by RNA molecules associated with autoantibodies was assessed. Gene expression in human myoblasts and satellite cells following treatment with supernatants from TLR7/8-activated PBMCs was evaluated by NanoString. C57BL/6 mice were dosed intramuscularly with the TLR7/8 agonist R848 and single-cell RNA-sequencing was performed on the muscle to ascertain the cell types responding to TLR7/8 activation and the downstream effects.

**Results.** Overall, 69 patients with IIMs were included with representation of dermatomyositis, polymyositis, and inclusion body myositis subsets. Immune complexes from patients with IIMs, as well as autoantibody-associated RNAs histidyl-transfer RNA, Y1, Y4, and U1, activated PBMCs to produce interferon-α and IL-6 via TLR7/8. Several canonical (Ro60, Ro52, and HIST1H4A) and novel (IL-36RN) autoreactivities correlated highly with TLR7/8 activation. Supernatants from TLR7/8-activated PBMCs had a negative impact on human myoblasts and satellite cells. Endothelial cells were activated by R848 in mouse muscle in vivo in addition to immune cells such as monocytes and macrophages.

**Conclusion.** Our results suggest that patients with IIMs have autoantibodies in their blood causing TLR7/8 activation, which leads to inflammation in muscles with potential deleterious effects.

## INTRODUCTION

Idiopathic inflammatory myopathies (IIMs) comprise a group of disorders in which patients experience a variety of symptoms, most commonly muscle weakness.[1] IIM pathogenesis varies for each subtype, although inflammation is usually a key driver.[1] The type I interferon (IFN) pathway has been linked to the pathogenesis of the IIM subtypes dermatomyositis (DM) and polymyositis (PM).[2] Although elevation of IFN in the blood of patients with IIMs is well documented,[3] the causal pathway(s) leading to IFN production have not been conclusively elucidated. IFN elevation is also a hallmark of another autoimmune disease, systemic lupus erythematosus (SLE), and is linked with more active disease and severe manifestations, such as lupus nephritis (LN).[4] Activation of toll-like receptor (TLR) 7 and TLR8 has been linked to an increase in IFN in SLE.[5]

TLR7 and TLR8 are endosome-localized receptors that recognize single-stranded RNA.[6] TLR7 is expressed primarily in

Sponsored by EMD Serono, Billerica, Massachusetts (CrossRef Funder ID: 10.13039/100004755). The healthcare business of Merck KGaA, Darmstadt, Germany funded editorial support by Bioscript Group Ltd.

[1]Yin Wu, BS, Aditee Deshpande, MS (current address: Novo Nordisk, Lexington MA), Nicholas Geraci, PhD, Vera Sellers, PhD (current address: Novartis, Cambridge MA), Phanindra Velisetty, PhD (current address: UCB, Cambridge MA), Chia-Chi Sun, PhD, Fatima Strand, PhD, Carmina Bhavsar, MS, Irina Kalatskaya, PhD, Andrew T. Bender, PhD (current address: AbbVie, Worcester, Massachusetts): EMD Serono, Billerica, Massachusetts; [2]Petra Budde, PhD: Oncimmune Germany GmbH, Dortmund, Germany; [3]Timothy B. Niewold, MD: Hospital for Special Surgery, New York, New York; [4]Mark A. Jensen, PhD: Iterative Therapeutics, Chicago, Illinois; [5]Kavita Y. Sarin, MD, PhD, David Fiorentino, MD, PhD: Stanford University, Redwood City, California.

Additional supplementary information cited in this article can be found online in the Supporting Information section (http://onlinelibrary.wiley.com/doi/10.1002/art.42989).

Author disclosures are available at https://onlinelibrary.wiley.com/doi/10.1002/art.42989.

Address correspondence via email to Yin Wu at yin.wu@emdserono.com.

Submitted for publication April 11, 2024; accepted in revised form September 10, 2024.

[Correction added on 3 December 2024, after first online publication: Yin Wu has been designated as corresponding author and "health care" was corrected to "healthcare" throughout.]

monocytes, plasmacytoid dendritic cells (pDCs), and B cells. TLR8 has an overlapping but also distinct expression profile, as it is expressed in monocytes, myeloid DCs, and neutrophils.[7] Expression of TLRs in nonimmune cells is not well characterized. TLR7/8 normally respond to single-stranded viral RNA and function as part of antiviral defense, but aberrant activation by self RNA (such as Alu RNA, microRNA, and RNA associated with immune complexes) has been linked to autoimmunity development.[6] The NF-κB and IFN regulatory factor pathways are downstream of TLR7/8 activation and, depending on the cell type, lead to cell activation and the production of inflammatory cytokines and IFNs.[7,8] *TLR7/8* gain-of-function genetic variants have been associated with lupus development,[9,10] and *TLR7/8* inhibition[11–13] has had a therapeutic effect in several mouse models of lupus. In these studies, a link with autoantibodies, IFN, and disease development was made.

Several lines of evidence suggest that TLR7/8 activation may play a role in IIM pathogenesis. Autoantibodies associated with IIM may contain RNA that activates TLR7/8.[14] Activation via TLR7/8 produces IFN, which is likely relevant to IIMs for several reasons. Firstly, an elevated IFN gene signature (IFN-GS) has been observed in the skin, muscle, and blood of patients with DM and PM,[15] which correlated with the presence of autoantibodies against RNA-binding proteins in DM.[16,17] The combination of these factors is also seen in lupus associated with higher TLR7 activity.[18] Secondly, IFN levels correlate with disease severity highlighted by higher Cutaneous DM Disease Area and Severity Index scores.[17,19] And thirdly, changes in IFN and IL-6 correlated with changes in disease severity in DM.[20] Interestingly, plasma samples from patients with IIMs containing autoantibodies stimulated IFN production ex vivo in an RNA-dependent manner.[21] Animal experiments showed that various micro RNAs are TLR7 ligands, suggesting that TLR7 activation in muscle may contribute directly to IIM pathogenesis.[22] Finally, TLR7 activation in dying muscle cells in mice promoted antisynthetase autoantibody production and increased muscle inflammation.[23]

As increasing evidence suggests a role for TLR7/8 in autoimmune diseases, several TLR7/8 inhibitors have been developed, including enpatoran,[12,24] afimetoran,[13] E6742,[25] and MHV370.[11] Given the extensive evidence indicating that TLR7/8 contribute to the pathogenesis of lupus, TLR7/8 inhibitors are now in clinical trials for SLE and cutaneous lupus erythematosus. Based on similarities in the pathogenesis of lupus and IIM (especially DM), these compounds may also benefit patients with IIMs. Newer small-molecule TLR7/8 inhibitors are greatly improved compared with older oligonucleotide-based compounds, such as IMO-8400, which did not show clinical benefit in psoriasis[26] and DM,[27] possibly because of suboptimal pharmacokinetics and inadequate target coverage.

Gaining a better understanding of the role of TLR7/8 in driving IIM pathogenesis and the mechanisms involved may support testing this concept clinically. In this study, we evaluated whether TLR7/8 activation contributes to the pathogenesis of IIMs and whether enpatoran, a potent and selective TLR7/8 inhibitor,[12] may be an effective therapeutic strategy. Following the observation that patients with IIMs have RNA-containing immune complexes that activate TLR7/8 in their circulation, we investigated the effect of TLR7/8 activation on muscle cells. Overall, this work indicates that autoantibody-mediated TLR7/8 activation may contribute to inflammation in patients with IIMs.

## MATERIALS AND METHODS

**Blood sample collection.** All patients provided informed consent in accordance with institutional review board approval at each institution. Patients were selected for these studies who were representative of the different disease types. We aimed to include patients who were both IFN high and low as well as positive for different autoantibodies. Blood samples were collected from patients with LN, SLE, and DM at Massachusetts General Hospital, New York University Grossman School of Medicine, and Stanford University, respectively. In addition, Sanguine Biosciences collected samples from patients with confirmed diagnosis of inclusion body myositis (IBM), PM, and DM at various locations in the United States. Patient demographics and characteristics are shown in Supplementary Table 1. Each institution collected samples from healthy participants to serve as healthy controls. Blood plasma was isolated and frozen. Later, IgG was purified using protein A resin, and the protein concentration was determined.

**Autoantibody profiling.** Testing for myositis-specific autoantibodies was performed on samples from patients with DM as described previously.[28] Antigen specificities contained in purified IgG were determined by Oncimmune Germany GmbH (Dortmund, Germany) using the SeroTag technology, employing an array with 1581 human antigens coupled to Luminex beads.[29] Antigens with a low bead count were removed from the data set. Filtered raw mean fluorescence intensity[30] values were then Log2 transformed and median-centered for further analysis.

**Immune complex formation and peripheral blood mononuclear cell (PBMC) stimulation.** To generate necrotic cell lysates, human embryonic kidney 293 cells were suspended at a concentration of 50 $\times 10^6$ cells/mL in phosphate-buffered saline (PBS; Gibco, Grand Island, NY, USA). The cells were frozen at −80°C for 10 minutes followed by thawing at 37°C for four freeze/thaw cycles. The lysate was centrifuged at 400 × *g* for 5 minutes to separate nonlyzed cells, and the supernatant was collected as necrotic cell lysate.

PBMCs were isolated from leukopaks collected from healthy donors (New York Blood Center, New York, NY, USA) in sodium heparin tubes using Ficoll-Paque Plus (Cytiva Life Sciences, Uppsala, Sweden). The cells were plated in 96-well U-bottom plates

(4 ×$10^5$ cells/well) in RPMI 1640 Medium (Gibco) supplemented with 10% fetal bovine serum (FBS; Corning, Woodland, CA, USA). Before stimulation, PBMCs were pretreated with 1 μM of enpatoran[12] for 30 minutes. The necrotic cell lysate (10% vol/vol) and IgG (0.1 mg/mL) purified from patients' plasma were added to the PBMCs, which were incubated at 37°C for 24 hours. The supernatants were collected, and cytokine production was measured by AlphaLISA (PerkinElmer, Waltham, MA, USA).

**PBMC stimulation with RNA ligands.** PBMCs were plated in 96-well U-bottom plates (5 ×$10^5$ cells/well) in RPMI 1640 Medium supplemented with 10% FBS. RNA molecules were custom synthesized by Azenta Life Sciences (Chelmsford, MA, USA; Supplementary Table 2). Each RNA was reconstituted in deionized sterile water at 100 μg/mL, and 10 μL was added to 100 μL of LyoVec (InvivoGen, San Diego, CA, USA) at room temperature for 30 minutes. PBMCs were pretreated with 1 μM of enpatoran for 30 minutes at 37°C or left untreated, and the RNA-LyoVec complexes were added at a final RNA concentration of 1 μg/mL for 24 hours. The supernatants were collected, and cytokine production was measured using the MSD U-PLEX biomarker group (hu) assay.

**Stimulation of human myoblasts and satellite cells with treated PBMC supernatants.** PBMCs were plated in RPMI 1640 media supplemented with 10% FBS in 12-well plates (5 ×$10^6$ cells/well). The cells were left unstimulated or treated with 3 μM of the TLR7/8 agonist R848 (InvivoGen) at 37°C for 24 hours. Human skeletal myoblasts and satellite cells, purchased from Creative Bioarray (Shirley, NY, USA), were plated in 12-well plates (0.5 ×$10^6$ cells/mL) in SuperCult Skeletal Muscle Satellite Cell Medium (Creative Bioarray). After 24 hours, supernatants from the untreated and R848-stimulated PBMCs were added to the muscle cells (1 mL/well; total volume 2 mL) overnight at 37°C. Attached muscle cells were collected (by pipetting and with a cell scraper) and pelleted by centrifugation at 500 × *g* for 5 minutes. The supernatant was discarded, and the cells were resuspended in 500 μL of RLT Buffer and passed through QIAshredders (Qiagen, Germantown, MD, USA) by centrifugation for 2 minutes at 8,000 × *g*. RNA isolation was performed using the Qiagen miRNEasy Tissue/Cells Advanced Micro Kit according to the manufacturer's instructions.

**NanoString analysis.** Gene expression in purified RNA samples was analyzed by NanoString. For PBMC activation, a 46-gene custom panel with markers of inflammation was used. For muscle cell analysis, a custom 121-gene set containing markers of inflammation, muscle cell growth and health, and housekeeping genes was used (Supplementary File 1). A total of 500 ng of RNA per sample was run on the nCounter Pro Analysis System (NanoString, Seattle, WA, USA). The data were processed using nSolver (NanoString), and Log2 fold changes were calculated for each sample relative to cells treated with supernatants from control PBMCs.

**Mouse muscle isolation.** All animal studies were performed in accordance with the Guide for the Care and Use of Laboratory Animals and all local and national laws and regulations regarding animal care, using protocols approved by the local Institutional Animal Care and Use Committee. C57BL/6 female mice, age 8–12 weeks, were purchased from Charles River Laboratories (Wilmington, MA, USA). Mice were prepared for intramuscular injection by shaving the hind right thigh and anesthetized using isoflurane. The injection site was sterilized using isopropyl alcohol pads. R848 was injected directly into the tibialis anterior muscle in the right hind limb at a dose of 25 μg/animal in a volume of 50 μL. Control mice were injected with sterile PBS. Mice were euthanized 1.5 hours after injection by $CO_2$ inhalation, and the tibialis anterior muscle was collected in six-well plates containing Dulbecco's Modified Eagle Medium (Gibco) with 10% FBS. An early timepoint was chosen to assess the direct effects of TLR7/8 activation and minimize the secondary effects of cytokines produced after the initial TLR7/8 stimulation. No criteria for the inclusion/exclusion of mice were set, and none of the mice were excluded in the analysis. Further details for tissue processing for gene expression analysis are provided in the Supplementary Methods.

**Single-cell RNA-sequencing (scRNA-seq).** ScRNA-seq was performed using the 10X Genomics platform (10X Genomics, Pleasanton, CA, USA) as previously described.[31] Single-cell suspensions of mouse muscle cells were loaded onto the Chromium Controller (10X Genomics) with a target of 10,000 cells collected per sample and were captured and processed according to the manufacturer's instructions. Further details are provided in the Supplementary Methods.

**Data availability.** Any requests for additional data by qualified scientific and medical researchers for legitimate research purposes will be subject to the healthcare business of Merck KGaA, Darmstadt, Germany's Data Sharing Policy. All requests should be submitted in writing to the healthcare business of Merck KGaA, Darmstadt, Germany's data sharing portal (https://www.emdgroup.com/en/research/our-approach-to-research-and-development/healthcare/clinical-trials/commitment-responsible-data-sharing.html). When the healthcare business of Merck KGaA, Darmstadt, Germany, has a co-research, co-development, or co-marketing or co-promotion agreement, or when the product has been out-licensed, the responsibility for disclosure might be dependent on the agreement between parties. Under these circumstances, the healthcare business of Merck KGaA, Darmstadt, Germany, will endeavor to gain agreement to share data in response to requests. The single-cell data are openly available in GEO (accession number GSE272898).

## RESULTS

**Activation of TLR7/8 by patient-derived immune complexes.** Serum IgG isolated from 69 patients with IIMs as well as 14 patients with lupus and 18 healthy controls was combined with necrotic cell lysate to form immune complexes that were added to healthy donor PBMCs. IFN-α production was stimulated by immune complexes generated using IgG from five of the six patients with LN tested and two of the eight patients with SLE tested (Figure 1A). Two LN samples from blood collected at different timepoints were tested and showed nearly identical results, suggesting that the stimulatory IgG may be stable over time. In the IIM subsets, immune complexes from one patient with PM and a subset of patients with DM induced IFN-α activity, whereas immune complexes from patients with IBM did not. DM samples were grouped based on the presence of myositis-specific autoantibodies against Jo-1, EJ, TIF1-, NXP2, SAE, Mi-2, MDA5, and ZO. Only one DM sample was positive for SAE, whereas almost all (6 of 7) DM samples that stimulated IFN-α were positive for Jo-1 (Figure 1B). When the PBMCs were pretreated with enpatoran, IFN-α production was completely inhibited (Figure 1C), demonstrating that IFN-α production was mediated by TLR7/8 activation. IgG and necrotic cell lysate alone had no stimulatory activity (data not shown).

Gene expression analysis on the PBMC lysates showed that the samples that stimulated IFN-α protein also induced changes in gene expression, and the most prominent effect was the induction of IFN-stimulated genes (ISGs; Figure 2A). An IFN-GS, calculated based on ISG expression, was apparent in the patients also positive for protein induction (Figure 2B). Expression of various IFN-α isoforms (*IFNA4/7/10/17/21* and *IFNA1/13*) was also induced (Supplementary Figure 1A). Interestingly, only a modest induction of NF-κB cytokine genes, including *IL6*, *IL1B*, and *TNF* or the NF-κB activation markers *TNFAIP3* and *NFKBIA*, was observed in a limited number of patients (Figure 2A; Supplementary Figure 1B). This suggests that TLR7/8 activation induced by the immune complexes had a greater effect on the IFN regulatory factor pathway than the NF-κB pathway in this system.

**Autoantibody profiling.** IgG samples were profiled for autoantibodies using a high content array with 1581 antigens (Supplementary Figure 2). A Spearman correlation matrix analysis was performed in Spotfire using the results of the ex vivo IgG stimulation assay (Figures 1 and 2) and the autoantibody profiling data to identify reactivities that may be associated with TLR7/8 stimulation in the lupus (SLE/LN) or IIM (DM/PM) samples (the two disease types were evaluated separately). Reactivities were identified that strongly correlated with TLR7/8 activation (the top 10 hits are shown in Figure 3A and 3B). For SLE/LN samples, titers of several canonical autoantibodies, such as TROVE2 (Ro60), TRIM21 (Ro52), SSB (La), and HIST1H4A (histones),

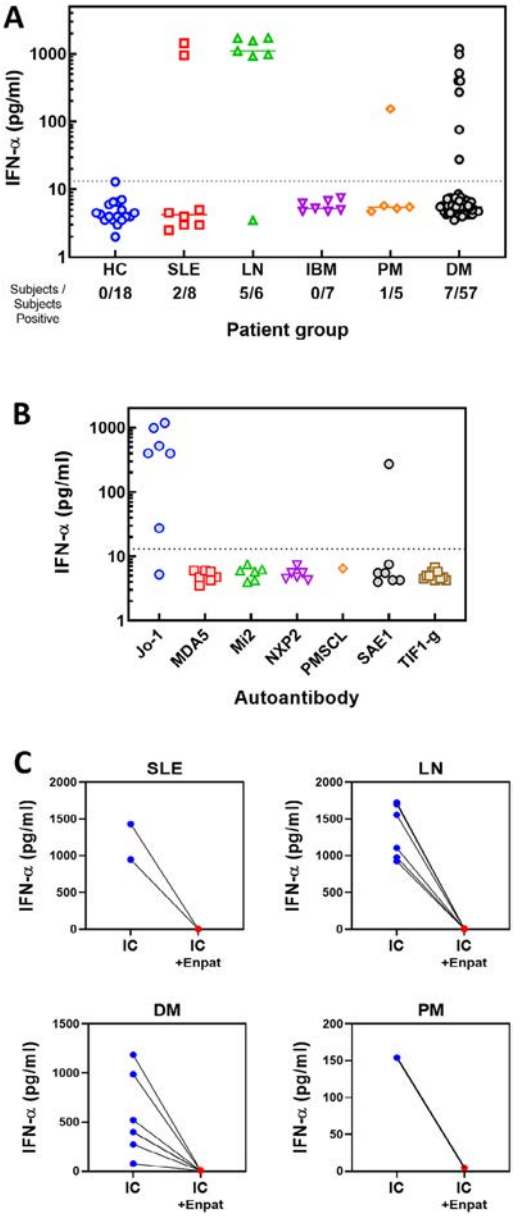


**Figure 1.** Toll-like receptor 7/8 activation in human PBMCs by patient-derived immune complexes. IgG was isolated from plasma samples from HCs and patients with SLE, LN, IBM, PM, and DM and combined with necrotic cell lysate to form immune complexes that were used to stimulate healthy donor PBMCs. (A) After 24 hours of treatment, supernatants were collected from the PBMCs, and IFN-α was measured by AlphaLISA. Means from 2–4 experiments for each IgG are shown and each symbol represents an IgG sample. (B) Samples from patients with DM were grouped based on myositis-specific autoantibody positivity. (C) For samples that had stimulating activity, the PBMCs were pretreated with enpatoran for 30 minutes before the immune complexes were added to the cells, and IFN-α was measured following 24 hours of treatment. All IgG samples were tested with 2–4 healthy donor PBMCs. DM, dermatomyositis; HC, healthy control; IBM, inclusion body myositis; IC, immune complex; IFN-α, interferon-α; LN, lupus nephritis; PBMC, peripheral blood mononuclear cell; PM, polymyositis; SLE, systemic lupus erythematosus. Color figure can be viewed in the online issue, which is available at http://onlinelibrary.wiley.com/doi/10.1002/art.42989/abstract.

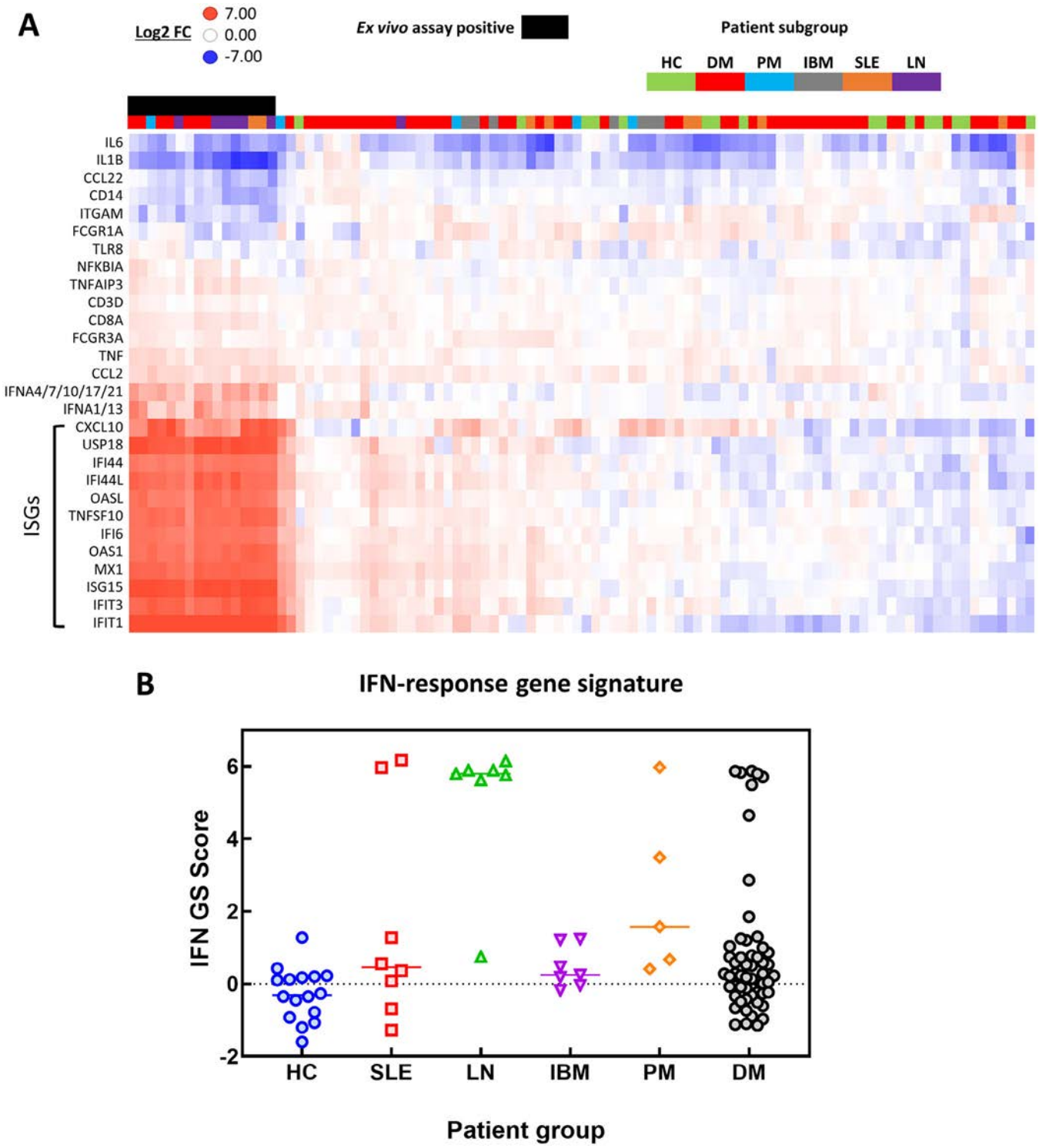


**Figure 2.** Gene expression changes induced by patient-derived immune complexes. IgG was isolated from plasma samples from HCs and patients with SLE, LN, IBM, PM, and DM and then combined with necrotic cell lysate to form immune complexes that were used to stimulate healthy donor PBMCs. After 24 hours of treatment, the cells were collected and analyzed by NanoString to measure changes in gene expression. (A) Heat map shows the Log2 FC compared with HC IgG samples. Each column represents a separate IgG sample, and the patient group is indicated by coloring. The samples that stimulated IFN-α protein production are indicated by black coloring. (B) An IFN-GS score was calculated using the ISGs indicated in the heat map and scores were plotted for each individual sample. Data are averaged from independent experiments run with two PBMC donors for each IgG sample. DM, dermatomyositis; FC, fold change; IFN-GS, interferon gene signature; HC, healthy control; IBM, inclusion body myositis; IFN-α, interferon-α; ISG, interferon-stimulated gene; LN, lupus nephritis; PBMC, peripheral blood mononuclear cell; PM, polymyositis; SLE, systemic lupus erythematosus; TNF, tumor necrosis factor.

A

**Lupus: SLE/LN**

| Reactivity | p-value | R |
|---|---|---|
| TROVE2 (SSA/Ro60) | 3.79E-05 | 0.68 |
| SSB (La) | 3.79E-05 | 0.68 |
| TRIM21 (SSA/Ro52) | 7.21E-05 | 0.66 |
| IL36RN | 9.78E-05 | 0.65 |
| HIST1H4A | 3.02E-04 | 0.61 |
| ZMYND8 | 3.92E-04 | 0.61 |
| CEP290 | 5.05E-04 | -0.60 |
| CENPJ | 6.45E-04 | 0.59 |
| ZDHHC16 | 1.03E-03 | -0.57 |
| FARSA | 1.03E-03 | 0.57 |

B

**IIM: DM/PM**

| Reactivity | p-value | R |
|---|---|---|
| TRIM21 (Ro52) | 5.73E-05 | 0.44 |
| IL36RN | 8.06E-05 | 0.43 |
| CENPJ | 8.77E-05 | 0.43 |
| HIST1H4A | 9.53E-05 | 0.43 |
| STAT2 | 1.44E-04 | 0.42 |
| HARS (Jo-1) | 3.94E-04 | 0.39 |
| ITGB7 | 5.28E-04 | 0.38 |
| S100A11 | 1.40E-03 | 0.36 |
| KRT8 | 1.94E-03 | 0.35 |
| IL4R | 2.50E-03 | 0.34 |

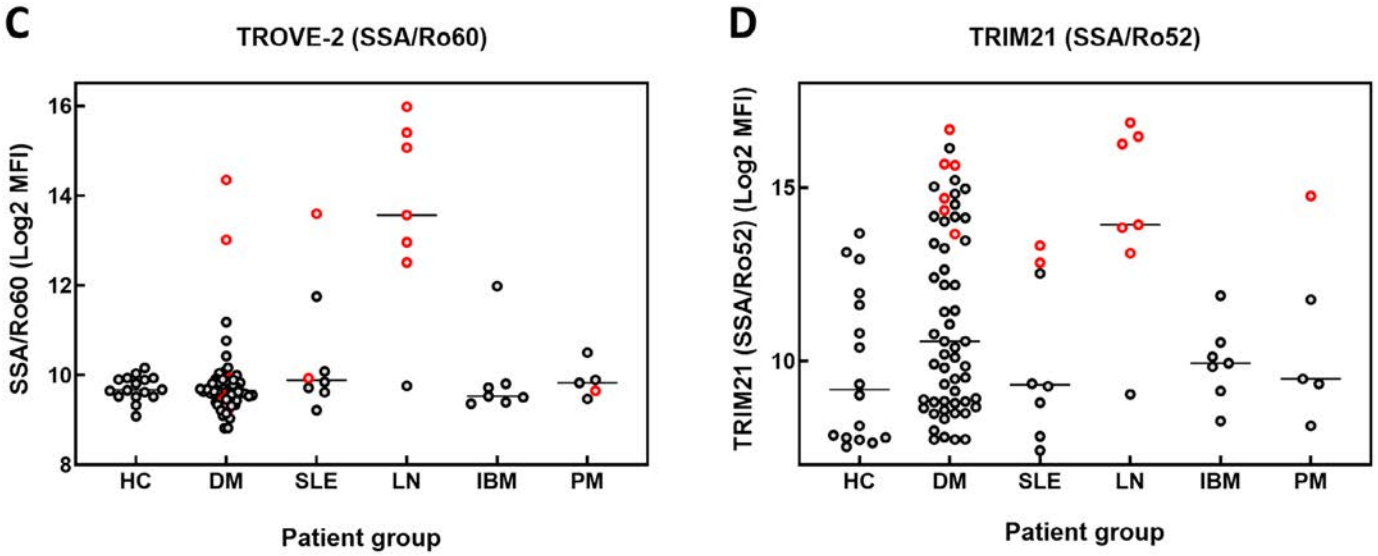


**Figure 3.** Autoantibodies associated with toll-like receptor 7/8 stimulation by immune complexes. (A) Autoreactivity of IgG from plasma samples from HCs and patients with SLE, LN, IBM, PM, and DM was profiled on a 1581-feature antigen array and correlation analysis was performed to identify the reactivities that correlated most highly with positivity in the ex vivo assay. The 10 reactivities that correlated most highly with the positivity of patients with (A) SLE/LN or (B) DM/PM are shown. (C and D) The top 2 reactivities that correlated most highly with stimulation of PBMCs are plotted by disease subgroup. The samples that were stimulatory in the PBMC assay for interferon-α production are shown in red. CENPJ, centromere protein J, DM, dermatomyositis; HC, healthy control; IBM, inclusion body myositis; LN, lupus nephritis; MFI, mean fluorescence intensity; PBMC, peripheral blood mononuclear cell; PM, polymyositis; SLE, systemic lupus erythematosus; TRIM21 or SSA/Ro52, tripartite motif-containing 21, TROVE2, or Ra/SSA TROVE domain family member 2.

correlated with IFN-α production in the ex vivo assay. For DM/PM samples, TRIM21 was also a top hit and additional other reactivities were common, such as CENPJ (centromere) and HIST1H4A. The presence of SSB was unique to the SLE/LN samples, whereas histidyl-transfer RNA (His-tRNA) synthetase (Jo-1) was only associated with IIMs. IL36RN, STAT2, and IL4R were unexpectedly associated to some degree with TLR7/8 stimulation. Expression levels of highly associated reactivities were evaluated by patient group to illustrate how expression correlates with ex vivo stimulation on an individual patient level (Figure 3C and D; Supplementary Figure 3A–3E). Notably, patients with DM who were Jo-1 positive and stimulatory in the ex vivo assay were also positive for TRIM21. No single reactivity was uniquely correlated with positivity in the ex vivo assay. Based on these results, it is likely that more than one reactivity activates TLR7/8.

**RNAs associated with immune complexes stimulate TLR7/8.** Several autoantibodies that were associated with TLR7/8 activation are known to react with RNA-binding proteins and, consequently, are likely to have RNA present in their immune complexes. Notable examples are Y4 and Y1 RNA with anti-

Ro60[32] and U1 RNA with anti-Smith and anti-RNP.[33] Other autoantibodies associated with myositis, such as Jo-1 and anti-SRP, also bind to proteins that have RNA ligands (Jo-1 binds to His-tRNA synthetase, and anti-SRP binds to SRP that has RNA as a component), and although they are pathogenic, it is unclear whether pathogenicity is via RNA.[34,35] We tested if RNA ligands from these autoantibodies can stimulate TLR7/8 and whether this can be inhibited by enpatoran.

PBMCs were treated with RNA molecules complexed with LyoVec in the presence or absence of enpatoran, and cytokine production was measured (Figure 4). Control PBMCs and PBMCs treated with LyoVec did not show any cytokine production, whereas R848 effectively induced cytokines, and this was inhibited by enpatoran. When His-tRNA, Y1, Y4, and U1 complexed with LyoVec were added to PBMCs, IFN-α2, IL-6, IL-1β, and IFN-γ were all induced (Figure 4). The induction of IFN-α2 by His-tRNA was effectively blocked by enpatoran, but this was less effective for Y4, U1, and Y1 (Figure 4A). Enpatoran effectively reduced the production of IL-6, IL-1β, and IFN-γ induced by all RNAs tested (Figure 4B–D). The pattern of cytokine induction was different for R848 and the natural RNA ligands. R848 induced IL-6 and IL-1β to greater degrees than the RNA ligands but IFN-α2 and IFN-γ less so. It is possible there are differences in the cell types activated or the ratio of TLR7 and TLR8 activated by different RNAs versus R848.

**Cell types activated in mouse muscle by TLR7/8 stimulation.** ScRNA-seq analysis of 11,450 cells from mouse muscle tissue sections following R848 injection identified 19 cell populations, including 4 fibroblast and 2 endothelial cell, 2 macrophage, and 2 T cell subpopulations (Figure 5A). To identify which cell populations were activated downstream of TLR7/8, IFN-GS and NF-κB-GS scores were calculated and heat maps generated (Figure 5B and 5C). There was a noticeable IFN response in most cell populations, with the greatest IFN-GS induction in neutrophils, endothelial cells, and macrophages, and some response in T cells (Figure 5B). However, IFN induction was not observed in any muscle cell type after R848 injection. The NF-κB-GS was expressed under basal conditions in many cell populations and was induced by R848 most in macrophages and neutrophils, with some increase also seen in endothelial cells (Figure 5C).

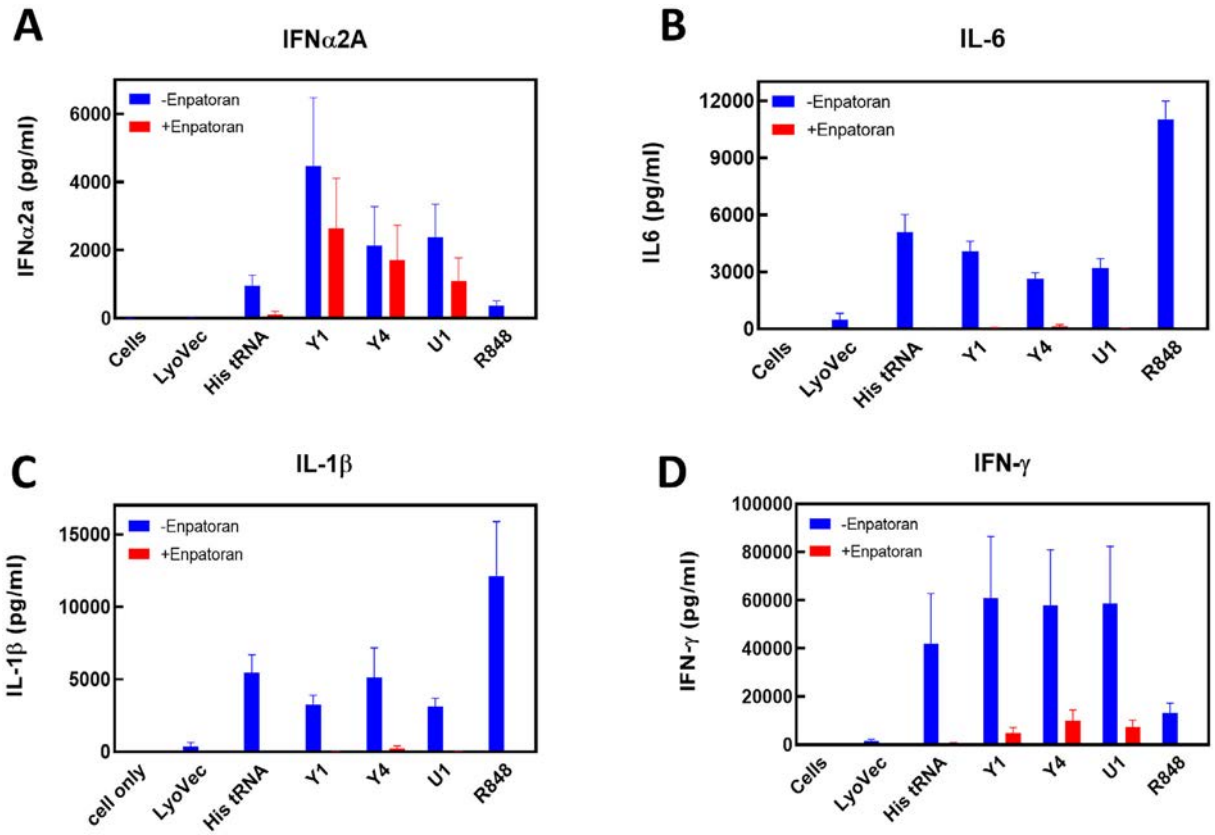


**Figure 4.** Immune complex–associated RNAs stimulate toll-like receptor 7/8. RNA molecules associated with various autoantibodies were synthesized in vitro. The RNAs were complexed with LyoVec and PBMCs were treated with 1 μg/mL of the RNA/LyoVec complexes. PBMCs were also pretreated with 1 μM enpatoran for 30 minutes before treatment with the complexes. After 24 hours, supernatants were collected and the production of (A) IFN-α2a, (B) IL-6, (C) IL-1β, and (D) IFN-γ was measured using an MSD U-PLEX biomarker group assay. Means and SE of the means plotted are shown. Data are from two independent experiments using four healthy donor PBMCs. His-tRNA, histidyl-transfer RNA; IFN-α2a, interferon-α2a; IFN-γ, interferon-γ; PBMC, peripheral blood mononuclear cell.

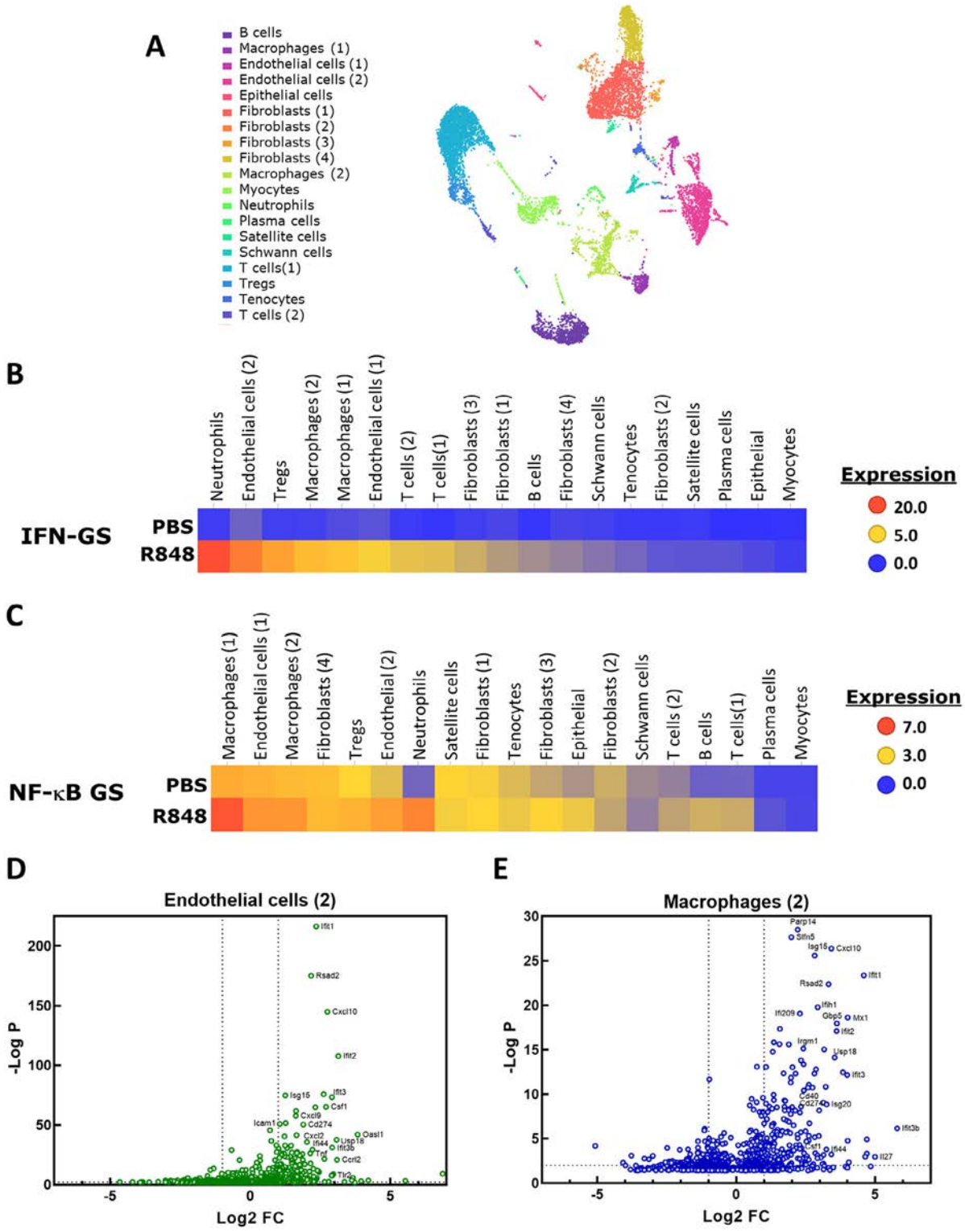


**Figure 5.** Cell types activated in mouse muscle by toll-like receptor 7/8 stimulation. Healthy C57BL/6 mice were injected intramuscularly with R848 or PBS. After 1.5 hours the muscle tissue was collected, and a single-cell suspension was made. The cells were analyzed by single-cell RNA-sequencing using the 10X Genomics platform. (A) Cell populations were identified and labeled on a uniform manifold approximation and projection. (B) An IFN-GS score was calculated for each cluster using a six-gene panel. (C) Similarly, an NF-κB-GS was calculated using a seven-gene panel. (D and E) Volcano plots were constructed to show genes that were differentially expressed after R848 treatment for both the (D) endothelial cells (2) cluster and (E) macrophages (2) cluster. Dotted lines show the Log2 FC and $P < 0.01$ cutoffs in the volcano plots. A combined data set was generated using cells from three separate experiments with eight mice per group. FC, fold change; IFN-GS, interferon gene signature; PBS, phosphate-buffered saline; Treg, regulatory T cell.

Volcano plots were generated to highlight the most significantly affected genes in two of the cell clusters with the greatest response to R848, endothelial cells (2) and macrophages (2). *ICAM1*, *TNF*, and *CSF1* (M-CSF) were notably increased in the endothelial cells, along with many IFN response genes, including *IFIT1*, *RSAD2*, and *CXCL10* (Figure 5D). Pathway analysis on the up-regulated genes showed that IFN signaling-related pathways and TLR-activation pathways were most affected, consistent with TLR7/8 activation (Supplementary Table 3). The macrophages also showed induction of IFN response genes as well as increased *CD40*, *CD247* (PD-L1), and *CSF1* (M-CSF) in response to R848 (Figure 5E). Pathway analysis of the genes up-regulated in macrophages also showed increased IFN activation and cytokine signaling (Supplementary Table 4). R848 dosing had no effect on IFN-GS or NF-κB-GS in the myocyte population (Figure 5B and 5C), and no other genes were found to be differentially expressed. The number of satellite cells and muscle stem cells was too low to reliably identify statistically significant gene changes.

**TLR7/8-stimulated PBMCs negatively impact human muscle stem cells.** To better understand the potential effects of TLR7/8 activation in the muscle of patients with IIMs, human myoblast and satellite cells were used to model muscle function and renewal. First, the expression of active TLR7/8 and response to TLR7/8 ligands was tested; no evidence was found that myoblast and satellite cells induce cytokine production in response to treatment with R848 or TLR7- and TLR8-specific ligands (data not shown). Next, to determine whether myoblasts and satellite cells are affected by immune cells activated by TLR7/8 stimulation, gene expression was evaluated following treatment with supernatants from PBMCs that had been stimulated overnight with R848. The induction of inflammatory gene expression, and a decrease in muscle cell marker expression, was observed (Figure 6A). The expression of cytokine genes *IL1B*, *IL6*, and *IL32* (Figure 6B), as well as chemokine genes *CCL2* and *CXCL3* and the growth factor *FGF2*, were increased in both cell types relative to the unstimulated control (Figure 6C). Decreased expression of muscle cell marker genes *MSTN*, *MYOD1*, and *MYF5* was observed, which was much more dramatic in myoblasts than satellite cells (Figure 6D).

## DISCUSSION

In this study, we identified lupus and IIM subtypes that are associated with type I IFN-stimulating autoantibodies and characterized the reactivities responsible for IFN activation mediated by TLR7/8 activation. These findings have clinical relevance because they suggest that TLR7/8 inhibitors such as enpatoran may reduce inflammation and the pathogenicity of autoantibodies in IIMs.

We show that robust production of IFN-α downstream of TLR7/8 stimulation ex vivo can be connected to clinical phenotypes of SLE, LN, and IIM patient subsets. Higher levels of autoantibodies, such as the ones associated with ex vivo stimulation, are also correlated with higher IFN (or IFN activity) in patients,[16,18] suggesting that immune complex stimulation of IFN in vivo may be occurring as it does ex vivo. Patients often have multiple autoreactivities, and determining which is responsible for TLR7/8 activation is difficult. Some of the reactivities that correlated highly with TLR7/8 activation, such as anti-Ro/SSA and anti-La/SSB, bind to proteins that may have associated RNA[32,36] and are good candidates as TLR7/8 activators. Others, such as anti-HIST1H4A and anti-CENPJ, have also been reported to have associated RNA.[37] It is less clear why anti-IL-36RN and anti-STAT2 correlate with ex vivo stimulation; there may be undiscovered synergies between these reactivities and other autoantibodies to drive stimulatory immune complex formation in vivo. In previous work, anti-MDA5 was highly associated with IFN stimulation[38] and higher IFN scores in patients with DM,[17] but despite MDA5 being an RNA-binding protein we did not observe a similar correlation. Interestingly, many of the reactivities associated with IFN stimulation were observed in both lupus and IIMs, suggesting common mechanisms of disease, although it is likely that disease-specific reactivities also activate TLR7/8, such as Jo-1.

Jo-1 correlated highly with TLR7/8 stimulation, which has been previously described.[21] We found that His-tRNA, which may exist in immune complexes with Jo-1,[39] could stimulate TLR7/8, strengthening the argument that Jo-1 could activate TLR7/8 in IIM. Anti–Jo-1 antibodies are highly associated with antisynthetase syndrome. Additionally, Y1 and Y4 RNA, which are associated with Ro/La, and U1 RNA, which is associated with U1-snRNP, were also found to activate TLR7/8, suggesting that Ro/La and U1-snRNP autoreactivities are TLR7/8 stimulators.

Several lines of evidence suggest that autoantibodies may contribute to disease in IIMs, and treatments that affect autoantibodies have shown some efficacy. Promising results were observed for rituximab in early IIM trials, although the primary endpoint of a Phase 3 trial was not met,[40] potentially owing to inadequate autoantibody reduction.[41] Intravenous Ig is approved for use in DM, and, although its mechanism of action is not well understood, it may reduce the activity of autoantibodies through saturation of Fc or FcRn receptors or reduce complement activation by immune complexes.[42] It is possible that TLR7/8 activation by Jo-1 in the antisynthetase patient subset of IIMs may be the mechanism by which some myositis-specific autoantibodies are pathogenic. Deposition of RNA-containing immune complexes in skin, muscle, and other immune tissues may activate TLR7/8 and trigger inflammatory cytokine production or B cell activation, with subsequent inflammation leading to tissue damage. TLR7/8 inhibitors such as enpatoran may block these processes.

Defining which cell types are stimulated by TLR7/8 activation may be important to understand IIM pathogenesis. In our studies, TLR7/8 activity was not observed in human myoblasts or satellite cells in vitro or mouse myocytes in vivo. It is possible that TLR7/8 expression is up-regulated in myositis muscle, as has been observed by Tournadre et al, and thus we did not observe TLR7/8 activity in our experiments with healthy samples.[43]

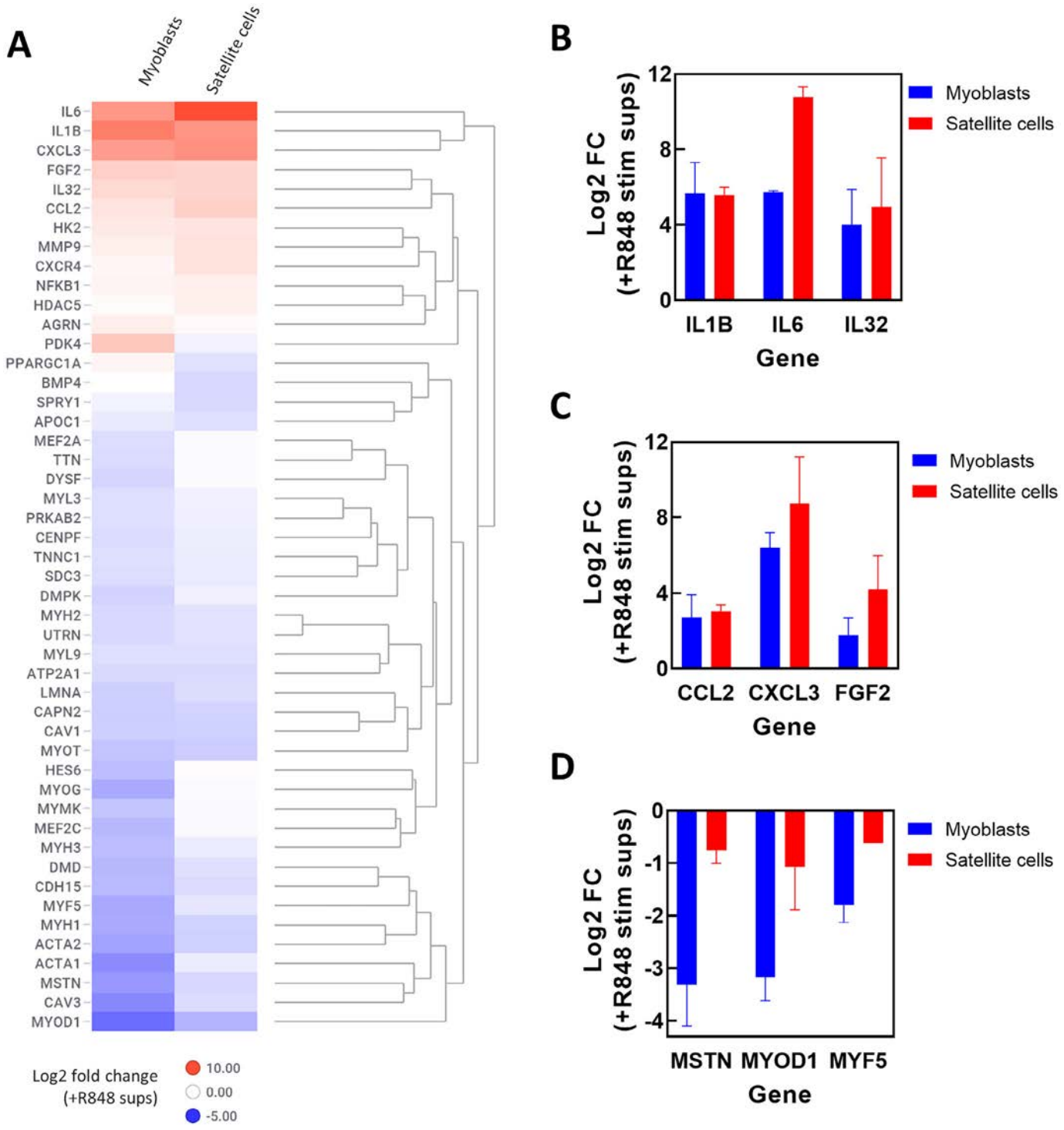


**Figure 6.** Supernatants from toll-like receptor 7/8–stimulated PBMCs negatively impact human muscle cells. Healthy donor PBMCs were stimulated with 3 μM R848 or left unstimulated for 24 hours and the supernatants were collected. Human myoblasts and satellite cells in culture were treated for 20 hours with the PBMC supernatants. After treatment, the myoblasts and satellite cells were collected, RNA was isolated, and NanoString gene expression analysis was performed. (A) Heat map shows Log2 FC calculated for the cells treated with supernatants from the R848-stimulated PBMCs relative to cells treated with supernatants from nonstimulated PBMCs. (B–D) Log2 FC for (B and C) selected inflammatory genes and (D) muscle cell markers are shown. Data are averaged from two independent experiments. CXCL, C-X-C motif chemokine ligand; FC, fold change; FGF2, fibroblast growth factor 2; MSTN, myostatin; MYF5, myogenic factor 5; MYOD1, myogenic differentiation 1; PBMC, peripheral blood mononuclear cell.

However, in our studies, human myoblasts and satellite cells were negatively impacted by products of immune cells stimulated by TLR7/8 activation. In vivo, after R848 injection into muscle, endothelial cells developed an inflammatory phenotype, as evidenced by the induction of mRNA for cytokines (eg, *TNF* and *CSF1*) and adhesion molecules (eg, *ICAM1*). It is not clear if the endothelial cells were stimulated directly by TLR7/8 activation or by cytokines produced from the primary activation of immune cells. Although IFN induction was not observed in any muscle cell type after R848 injection, induction of an IFN-GS was seen in most cell types. Because an elevated IFN-GS is observed in the blood of patients with DM and cutaneous lupus erythematosus, as well as unaffected skin biopsies from patients with SLE and patients with juvenile DM,[44] it is possible that locally produced IFN is responsible for both tissue and systemic inflammation. However, locally produced IFN was not observed in the scRNA-seq data, despite the IFN-GS, which may be due to the detection sensitivity of scRNA-seq or the distribution of R848 to distant sites that trigger systemic IFN, which then acts in the muscle. Additional ex vivo experiments in which muscle cells are treated directly with TLR7/8 agonists would remove the potentially confounding in vivo effects of cytokines produced at distant sites and may provide more insight into the TLR7/8-driven activation profile of muscle cells.

Based on our results, we hypothesize that TLR7/8 activation occurs in immune cells in patients with IIMs, and the products from those cells then negatively affect muscle stem cells (myoblasts and satellite cells), leading to decreased differentiation into myocytes and, ultimately, deficits in muscle function. Additionally, TLR7/8 activation leads to endothelial inflammation and dysfunction, which has pathogenic consequences in the muscle and skin of patients with IIMs.

The limitations of this study include the small sample size of the SLE, PM, and IBM subsets. Additionally, because of the limited amount of IgG isolated from patient samples, it was not possible to test specific autoantibodies for their ability to stimulate TLR7/8; correlation analyses were performed instead.

The treatment of IIMs remains challenging, and novel therapies are urgently needed. TLR7/8 inhibition is a novel approach that may provide efficacy by inhibiting aspects of both innate and adaptive immunity. The presence of circulating RNA-binding autoantibodies that stimulate TLR7/8 in IIMs suggests that some B cells are driven by TLR activation in vivo, as previously shown.[14] Suppressing TLR7/8 activation of B cells may be of benefit by dampening both autoantibody and immune complex formation and the subsequent TLR7/8 driven activation of myeloid cells that likely leads to inflammation and tissue damage. The reduction of autoreactive B cells using TLR7/8 inhibitors is a more targeted approach than B cell depletion or inhibition and may be advantageous because of reduced immunosuppressive risk. TLR7/8 inhibitors may also dampen innate immune processes by reducing IFN production from pDCs and cytokine production from other myeloid cells. Our data showing that enpatoran blocked pDC activation by immune complexes supports this possibility. Inhibition of resident myeloid cell activation with compounds such as enpatoran may prevent tissue destruction, as demonstrated in mouse lupus models where kidney dysfunction was prevented and reversed by enpatoran.[12] The efficacy of enpatoran in IIMs (DM/PM) is currently being evaluated in a Phase 2 trial (NEPTUNIA, NCT05650567). The results of this preclinical study provide important mechanistic insights supporting this approach.

## ACKNOWLEDGMENTS

The authors would like to recognize the contributions of the following individuals at Oncimmune for their work in autoantibody profiling: Hans-Dieter Zucht (data analysis and Luminex technology), Ann-Sophie Lindemann (data quality control and statistics), and Jana Gajewski (Luminex assay technology). The authors thank Jill Buyon, Peter Izmirly, and Michael Belmont from the New York University Grossman School of Medicine who helped identify patients with lupus who were recruited for this study. The authors also thank Ian Strohbehn, Meghan Sise, and Herbert Lin from Massachusetts General Hospital who provided samples from patients with lupus nephritis that were used in the study.

## AUTHOR CONTRIBUTIONS

All authors contributed to at least one of the following manuscript preparation roles: conceptualization AND/OR methodology, software, investigation, formal analysis, data curation, visualization, and validation AND drafting or reviewing/editing the final draft. As corresponding author, Ms Wu confirms that all authors have provided the final approval of the version to be published, and takes responsibility for the affirmations regarding article submission (eg, not under consideration by another journal), the integrity of the data presented, and the statements regarding compliance with institutional review board/Helsinki Declaration requirements.

## ROLE OF THE STUDY SPONSOR

EMD Serono was involved in the study design and the collection, analysis, and interpretation of the data. EMD Serono reviewed the manuscript and approved the final version. Samantha Lommano of Bioscript Group Ltd provided editorial support, funded by the healthcare business of Merck KGaA, Darmstadt, Germany.

## REFERENCES

1. Lundberg IE, Fujimoto M, Vencovsky J, et al. Idiopathic inflammatory myopathies. Nat Rev Dis Primers 2021;7(1):86.
2. Bolko L, Jiang W, Tawara N, et al. The role of interferons type I, II and III in myositis: a review. Brain Pathol 2021;31(3):e12955.
3. Gasparotto M, Franco C, Zanatta E, et al. The interferon in idiopathic inflammatory myopathies: different signatures and new therapeutic perspectives. A literature review. Autoimmun Rev 2023;22(6):103334.
4. Postal M, Vivaldo JF, Fernandez-Ruiz R, et al. Type I interferon in the pathogenesis of systemic lupus erythematosus. Curr Opin Immunol 2020;67:87–94.
5. Miyake K, Shibata T, Ohto U, et al. Mechanisms controlling nucleic acid-sensing toll-like receptors. Int Immunol 2018;30(2):43–51.
6. Miyake K, Shibata T, Ohto U, et al. Emerging roles of the processing of nucleic acids and toll-like receptors in innate immune responses to nucleic acids. J Leukoc Biol 2017;101(1):135–142.

7. Bender AT, Tzvetkov E, Pereira A, et al. TLR7 and TLR8 differentially activate the IRF and NF-κB pathways in specific cell types to promote inflammation. Immunohorizons 2020;4(2):93–107.
8. Gorden KB, Gorski KS, Gibson SJ, et al. Synthetic TLR agonists reveal functional differences between human TLR7 and TLR8. J Immunol 2005;174(3):1259–1268.
9. Lee YH, Choi SJ, Ji JD, et al. Association between toll-like receptor polymorphisms and systemic lupus erythematosus: a meta-analysis update. Lupus 2016;25(6):593–601.
10. Brown GJ, Cañete PF, Wang H, et al. TLR7 gain-of-function genetic variation causes human lupus. Nature 2022;605(7909):349–356.
11. Hawtin S, André C, Collignon-Zipfel G, et al. Preclinical characterization of the toll-like receptor 7/8 antagonist MHV370 for lupus therapy. Cell Rep Med 2023;4(5):101036.
12. Vlach J, Bender AT, Przetak M, et al. Discovery of M5049: a novel selective toll-like receptor 7/8 inhibitor for treatment of autoimmunity. J Pharmacol Exp Ther 2021;376(3):397–409.
13. Dudhgaonkar S, Rudra A, Ranade S, et al. Inhibition of toll-like receptor 7 (TLR7) with the potent and selective inhibitor of human TLR7 and TLR8 BMS-986256 provides robust efficacy in murine lupus models, reversing established disease. Arthritis Rheumatol 2021;73(suppl 9).
14. Green NM, Moody KS, Debatis M, et al. Activation of autoreactive B cells by endogenous TLR7 and TLR3 RNA ligands. J Biol Chem 2012;287(47):39789–39799.
15. Wong D, Kea B, Pesich R, et al. Interferon and biologic signatures in dermatomyositis skin: specificity and heterogeneity across diseases. PLoS One 2012;7(1):e29161.
16. Ekholm L, Vosslamber S, Tjärnlund A, et al. Autoantibody specificities and type I interferon pathway activation in idiopathic inflammatory myopathies. Scand J Immunol 2016;84(2):100–109.
17. Tabata MM, Hodgkinson LM, Wu TT, et al. The type I interferon signature reflects multiple phenotypic and activity measures in dermatomyositis. Arthritis Rheumatol 2023;75(10):1842–1849.
18. Wang T, Marken J, Chen J, et al. High *TLR7* expression drives the expansion of $CD19^{+}CD24^{hi}CD38^{hi}$ transitional B Cells and autoantibody production in SLE patients. Front Immunol 2019;10:1243.
19. Huard C, Gullà SV, Bennett DV, et al. Correlation of cutaneous disease activity with type 1 interferon gene signature and interferon β in dermatomyositis. Br J Dermatol 2017;176(5):1224–1230.
20. Reed AM, Peterson E, Bilgic H, et al. Changes in novel biomarkers of disease activity in juvenile and adult dermatomyositis are sensitive biomarkers of disease course. Arthritis Rheum 2012;64(12):4078–4086.
21. Eloranta ML, Barbasso Helmers S, Ulfgren AK, et al. A possible mechanism for endogenous activation of the type I interferon system in myositis patients with anti-Jo-1 or anti-Ro 52/anti-Ro 60 autoantibodies. Arthritis Rheum 2007;56(9):3112–3124.
22. Kinder TB, Heier CR, Tully CB, et al. Muscle weakness in myositis: microRNA-mediated dystrophin reduction in a myositis mouse model and human muscle biopsies. Arthritis Rheumatol 2020;72(7):1170–1183.
23. Sciorati C, Monno A, Doglio MG, et al. Exacerbation of murine experimental autoimmune myositis by toll-like receptor 7/8. Arthritis Rheumatol 2018;70(8):1276–1287.
24. Port A, Shaw JV, Klopp-Schulze L, et al. Phase 1 study in healthy participants of the safety, pharmacokinetics, and pharmacodynamics of enpatoran (M5049), a dual antagonist of toll-like receptors 7 and 8. Pharmacol Res Perspect 2021;9(5):e00842.
25. Yamakawa N, Tago F, Nakai K, et al. First-in-human study of the safety, tolerability, pharmacokinetics, and pharmacodynamics of E6742, a dual antagonist of toll-like receptors 7 and 8, in healthy volunteers. Clin Pharmacol Drug Dev 2023;12(4):363–375.
26. Balak DM, van Doorn MB, Arbeit RD, et al. IMO-8400, a toll-like receptor 7, 8, and 9 antagonist, demonstrates clinical activity in a phase 2a, randomized, placebo-controlled trial in patients with moderate-to-severe plaque psoriasis. Clin Immunol 2017;174:63–72.
27. Kim YJ, Schiopu E, Dankó K, et al. A phase 2, double-blinded, placebo-controlled trial of toll-like receptor 7/8/9 antagonist, IMO-8400, in dermatomyositis. J Am Acad Dermatol 2021;84(4):1160–1162.
28. Fiorentino DF, Gutierrez-Alamillo L, Hines D, et al. Distinct dermatomyositis populations are detected with different autoantibody assay platforms. Clin Exp Rheumatol 2019;37(6):1048–1051.
29. Budde P, Zucht HD, Vordenbäumen S, et al. Multiparametric detection of autoantibodies in systemic lupus erythematosus. Lupus 2016;25(8):812–822.
30. Fejtkova M, Sukova M, Hlozkova K, et al. TLR8/TLR7 dysregulation due to a novel TLR8 mutation causes severe autoimmune hemolytic anemia and autoinflammation in identical twins. Am J Hematol 2022;97(3):338–351.
31. Deshmukh A, Pereira A, Geraci N, et al. Preclinical evidence for the glucocorticoid-sparing potential of a dual toll-like receptor 7/8 inhibitor in autoimmune diseases. J Pharmacol Exp Ther 2024;388(3):751–764.
32. Boccitto M, Wolin SL. Ro60 and Y RNAs: structure, functions, and roles in autoimmunity. Crit Rev Biochem Mol Biol 2019;54(2):133–152.
33. Kattah NH, Kattah MG, Utz PJ. The U1-snRNP complex: structural properties relating to autoimmune pathogenesis in rheumatic diseases. Immunol Rev 2010;233(1):126–145.
34. Bergua C, Chiavelli H, Allenbach Y, et al. In vivo pathogenicity of IgG from patients with anti-SRP or anti-HMGCR autoantibodies in immune-mediated necrotising myopathy. Ann Rheum Dis 2019;78(1):131–139.
35. Galindo-Feria AS, Wang G, Lundberg IE. Autoantibodies: pathogenic or epiphenomenon. Best Pract Res Clin Rheumatol 2022;36(2):101767.
36. Vílchez-Oya F, Balastegui Martin H, García-Martínez E, et al. Not all autoantibodies are clinically relevant. Classic and novel autoantibodies in Sjögren's syndrome: a critical review. Front Immunol 2022;13:1003054.
37. Leclerc S, Kitagawa K. The role of human centromeric RNA in chromosome stability. Front Mol Biosci 2021;8:642732.
38. Wang K, Zhao J, Wu W, et al. RNA-containing immune complexes formed by anti-melanoma differentiation associated gene 5 autoantibody are potent inducers of IFN-α. Front Immunol 2021;12;743704.
39. Wilhelm SDP, Kenana R, Qiu Y, et al. Towards a cure for HARS disease. Genes (Basel) 2023;14(2):254.
40. Oddis CV, Reed AM, Aggarwal R, et al; RIM Study Group. Rituximab in the treatment of refractory adult and juvenile dermatomyositis and adult polymyositis: a randomized, placebo-phase trial. Arthritis Rheum 2013;65(2):314–324.
41. Aggarwal R, Oddis CV, Goudeau D, et al. Autoantibody levels in myositis patients correlate with clinical response during B cell depletion with rituximab. Rheumatology (Oxford) 2016;55(6):991–999.
42. Chaigne B, Mouthon L. Mechanisms of action of intravenous immunoglobulin. Transfus Apher Sci 2017;56(1):45–49.
43. Tournadre A, Lenief V, Miossec P. Expression of toll-like receptor 3 and toll-like receptor 7 in muscle is characteristic of inflammatory myopathy and is differentially regulated by Th1 and Th17 cytokines. Arthritis Rheum 2010;62(7):2144–2151.
44. Turnier JL, Kahlenberg JM. The role of cutaneous type I IFNs in autoimmune and autoinflammatory diseases. J Immunol 2020;205(11):2941–2950.

**Arthritis & Rheumatology**
Vol. 77, No. 2, February 2025, pp 202–211
DOI 10.1002/art.42986
© 2024 The Author(s). *Arthritis & Rheumatology* published by Wiley Periodicals LLC on behalf of American College of Rheumatology. This is an open access article under the terms of the Creative Commons Attribution License, which permits use, distribution and reproduction in any medium, provided the original work is properly cited.

American College of Rheumatology
*Empowering Rheumatology Professionals*

# Short-Term Risk of Cardiovascular Events in People Newly Diagnosed With Gout

Edoardo Cipolletta,[1] Georgina Nakafero,[2] Pascal Richette,[3] Anthony J. Avery,[2] Mamas A. Mamas,[4] Laila J. Tata,[2] and Abhishek Abhishek[2]

**Objective.** To investigate the temporal association between the first diagnosis of gout and cardiovascular events in the short term.

**Methods.** We performed a self-controlled case series analysis and a cohort study using data from linked primary care, hospitalization, and mortality records from the United Kingdom's Clinical Practice Research Database-GOLD. We included individuals with a new diagnosis of gout either in the primary care or secondary care between January 1, 1997 and December 31, 2020. The first consultation at which gout was diagnosed was the exposure of interest. The main outcome consisted of cardiovascular events (ie, a composite of fatal and nonfatal myocardial infarction, ischemic or hemorrhagic stroke, and transient ischemic attack).

**Results.** The 4,398 patients (66.9% male, mean age 74.6 years) had a cardiovascular event within at least two years of their first recorded diagnosis of gout. The incidence of cardiovascular events was significantly higher in the 30 days after the first diagnosis of gout compared to baseline (adjusted incidence rate ratio 1.55, 95% confidence interval [CI] 1.33–1.83). Among 76,440 patients (72.9% male, mean age 63.2 years) included in the cohort study, the incidence of cardiovascular events in the 30 days after the first gout diagnosis (31.2 events per 1,000 person-years, 95% CI 27.1–35.9) was significantly higher than in days 31 to 730 after gout diagnosis (21.6 events per 1,000 person-years, 95% CI 20.8–22.4) with a rate difference of −9.6 events per 1,000 person-years (95% CI −14.0 to −5.1).

**Conclusion.** Individuals had a short-term increased risk of cardiovascular events in the 30 days following the first consultation at which gout was diagnosed.

## INTRODUCTION

Gout affects 1.0% to 4.0% of adults in Western countries.[1] Traditionally viewed as a self-limiting form of arthritis, it is associated with cardiovascular comorbidities.[2] Hyperuricemia was long considered a potential reason for the excess cardiovascular burden in people with gout, but Mendelian randomization studies and the ALL-HEART study did not provide evidence about the causal role of hyperuricemia in the pathogenesis of cardiovascular comorbidities.[3,4] Thus, the potential mechanism linking gout and cardiovascular events may be related to systemic and vascular inflammation during gout flares.

Gout flares have been associated with a transient increase in the risk of cardiovascular events in two separate studies, one from the United Kingdom and another from Australia.[5,6] However, these studies either included people with long-standing gout[5] or people hospitalized for gout flare.[6] Their findings might be affected by survivor bias, potentially affecting the magnitude of the association. Additionally, there may be potential confounding effects from the regular prescription of nonsteroidal anti-inflammatory drugs (NSAIDs) or colchicine to either prevent or treat gout flares. This is an important issue because regular NSAID prescription is associated with an increased risk of cardiovascular events, whereas regular colchicine prescriptions may

Access to data from the Clinical Practice Research Datalink and the linked data from Hospital Episode Statistics and Office for National Statistics was funded by the University of Nottingham. The funders of this study had no role in the design and conduct of the study; collection, management, analysis, and interpretation of the data; preparation, review, or approval of the manuscript; and decision to submit the manuscript for publication.

[1]Edoardo Cipolletta, MD: University of Nottingham, Nottingham, United Kingdom, and Polytechnic University of Marche, Ancona, Italy; [2]Georgina Nakafero, PhD, Anthony J. Avery, DM, Laila J. Tata, PhD, Abhishek Abhishek, PhD: University of Nottingham, Nottingham, United Kingdom; [3]Pascal Richette, PhD: Hospital Lariboisière, INSERM U1132, Paris, France; [4]Mamas A. Mamas, PhD: Keele University, Keele, United Kingdom.

Drs Tata and Abhishek contributed equally to this work.

Additional supplementary information cited in this article can be found online in the Supporting Information section (https://acrjournals.onlinelibrary.wiley.com/doi/10.1002/art.42986).

Author disclosures are available at https://onlinelibrary.wiley.com/doi/10.1002/art.42986.

Address correspondence via email to Edoardo Cipolletta, MD, at edoardo.cipolletta@nottingham.ac.uk.

Submitted for publication April 9, 2024; accepted in revised form August 30, 2024.

prevent cardiovascular events.[7,8] Therefore, it is important to assess whether there is a transient increase in cardiovascular events following gout flares, occurring only in the initial period following gout diagnosis, at a time when there is no effect of survivor bias and minimal effect from long-term anti-inflammatory drug prescription. The presence of such an association would strongly support early proactive cardiovascular risk management in people newly diagnosed with gout. Currently, there is a discrepancy between international recommendations regarding the screening and the management of cardiovascular risk factors in those newly diagnosed with gout.[9–12] The British Society of Rheumatology[12] and the EULAR[10] guidelines suggest screening cardiovascular risk factors and cardiovascular comorbidities in all patients with gout and managing them appropriately. Conversely, the American College of Rheumatology[9] and the American College of Physicians[11] guidelines do not make any mention of that.

The main aim of this study was to assess whether there is a short-term increased risk of cardiovascular events in patients diagnosed with newly diagnosed gout. We also estimated the incidence of cardiovascular events in the first two years following the first gout diagnosis to provide absolute incidence rates. In this study, we used the same data source as our previously published study, but the data were restricted to the first recorded consultation for gout.[5]

## PATIENTS AND METHODS

**Study design and study period.** A self-controlled case series (SCCS) study evaluated the temporal association between the first diagnosis of gout (ie, typically a flare consultation at which gout could be diagnosed in primary care or secondary care) and cardiovascular events. In the SCCS study, eligible patients (ie, those with an exposure and an outcome) act as their own controls. Indeed, comparisons are made within individuals and not between them,[13] and fixed, time-invariant confounding is accounted for. A cohort study provided estimates of the incidence of cardiovascular events following the first consultation in which gout was diagnosed. The study period spanned from January 1, 1997 to December 31, 2020.

**Data source.** Linked primary care, hospitalization, and mortality data were extracted from the Clinical Practice Research Datalink (CPRD)-GOLD, Hospital Episode Statistics (HES), and Office for National Statistics (ONS) databases, respectively.[14] CPRD-GOLD contains anonymized patient data on sociodemographic and lifestyle factors, prescriptions, diagnoses, and test results originating during routine care from more than 18 million individuals in England.[14]

**Source population.** Patients were newly diagnosed with gout at 18 years or older who contributed research-quality data to CPRD-GOLD, with their primary care records linked to HES and ONS datasets. To minimize the risk of including prevalent gout cases as incident,[15] we included patients with a new diagnosis of gout at least two years after their registration at the current practice, without prior prescriptions of urate-lowering therapy in primary care or prior hospitalization for gout in which gout was not the primary reason for hospitalization. Patients whose first primary care record of gout indicated prevalent gout (eg, history of gout, gout monitoring, etc) were also excluded.

**Exposures.** We used two definitions to identify the first recorded diagnosis of gout:

- Definition 1 (broad): first primary care consultation or hospitalization with gout as the first discharge diagnosis. Flares are by far the most common presentation of gout,[1] and therefore, any first record of a new diagnosis of gout can be reasonably considered as a proxy for the first gout flare, which required contact with the health care system.
- Definition 2 (strict): first primary consultation for gout with either NSAID, colchicine, or glucocorticoid prescription on the same date, a first primary care consultation for gout indicating gout flare care, or hospitalization with gout as the first discharge diagnosis.[5,16–18]

The broad definition allowed us to capture all consultations at which gout was first diagnosed, whereas the strict definition was used to assess the validity of the findings.[19–21]

**Outcomes.** The primary outcome was the first cardiovascular event after the study entry defined as acute myocardial infarction, stroke (ischemic or hemorrhagic), or transient ischemic attack. Secondary outcomes assessed separately were acute myocardial infarction, cerebrovascular events (ie, stroke [ischemic or hemorrhagic] or transient ischemic attack), and any cardiovascular event requiring hospitalization or leading to death. Events were ascertained using primary care, hospitalization, and mortality records, as linkage across all data sources has been shown to improve outcome ascertainment.[22–24] The date of the cardiovascular event was the earliest of the above dates.

**Study population.** To measure the incidence of cardiovascular events following the first gout diagnosis, two separate cohorts were formed using definitions 1 and 2, respectively. Patients were followed up from their first gout diagnosis to the earliest date of last data collection from the practice, transfer out of practice, end of the study period, up to two years after the first gout diagnosis, cardiovascular event, or death.

For the SCCS analyses, only patients who experienced a cardiovascular event in the patients' available registration time up to two years before or up to two years after the first gout diagnosis were included. Two separate SCCS study datasets were

formed using exposure definitions 1 and 2, respectively. The exposed period extended up to 120 days after the first gout diagnosis. The baseline period extended up to 730 days before the first gout diagnosis and 615 days after the end of the exposed period (Figure 1). The SCCS study period was censored at the earliest date of study end, transfer out, date of last data collection from the general practice, a subsequent gout flare, or death. Because gout flares typically last for less than two weeks, we considered subsequent gout flares to be present if there was a primary care consultation for gout accompanied by an anti-inflammatory drug prescription on the same date, primary care consultation for gout at which a Read code for gout flare was recorded, or hospitalization with gout as the primary diagnosis that occurred more than 14 days after the first gout diagnosis.[5,18]

**Statistical analysis.** The incidence (with 95% confidence interval [CI]) of cardiovascular events per 1,000 person-years was calculated on days 1 to 30, 31 to 120, 121 to 730, and 31 to 730 following the first gout diagnosis. Risk differences were calculated for each stratum using days 1 to 30 as the reference category.

In the SCCS analysis, incidence rates and rate difference per 1,000 person-days and adjusted incidence rate ratios (aIRRs) with 95% CIs were calculated for each stratum of the exposed period (0–30, 31–60, and 61–120 days) compared with the baseline.[13] We adjusted the SCCS for seasons to account for the seasonal trend of gout flares and cardiovascular events,[25,26] and age (one-year bands) to account for the increasing incidence of gout and cardiovascular events with age.[20] Sample size estimation is presented in Supplementary Material S1.

The SCCS assumptions could be violated by outcomes that increase mortality rates in the short term or when the outcome of interest influences the likelihood of exposure.[27,28] To evaluate if event-dependent exposure could be an issue for the SCCS analyses, we plotted the number of outcomes by time before or after gout diagnosis using both exposure definitions. We did not observe a decrease in the occurrence of outcomes in the 30 days immediately before gout diagnosis (Supplementary Material S2). Therefore, an induction period (ie, a period preceding the exposure that was considered separate from the baseline period to minimize potential confounding) was not added to the main analysis.

To assess if event-dependent observation periods could be an issue for the analyses, we plotted a histogram of the time from the outcome to the actual end of observation in patients who were censored and uncensored using both exposure definitions. A spike close to zero is apparent in the censored data histograms (Supplementary Material S2). This finding indicates the presence of event-dependent observation periods (censoring on the date of death because of outcome), which we tested further with sensitivity analyses. We performed the following sensitivity analyses:

- used the planned end of observation (eg, 730 days after the first consultation for gout) as the actual end of observation for each case who died of the cardiovascular event and for those who were censored on the date of the next flare[28];
- excluded patients with fatal cardiovascular events[27];
- divided the exposure period into shorter intervals;
- included an induction period immediately before the exposure period;
- reduced the baseline period to up to 365 days before and 365 days after the end of the 120-day exposed period to reduce the potential impact of time-varying confounders;
- excluded patients with a cardiovascular event on the same date as the first gout diagnosis;
- excluded people with a prescription for NSAIDs, colchicine, or glucocorticoids in the 60 days before first consultation for gout;
- and included only patients with latest serum urate levels >480 μmol/L to increase the confidence in gout diagnosis. To be considered, serum urate must have been measured within five years of the first recorded gout consultation (ie,

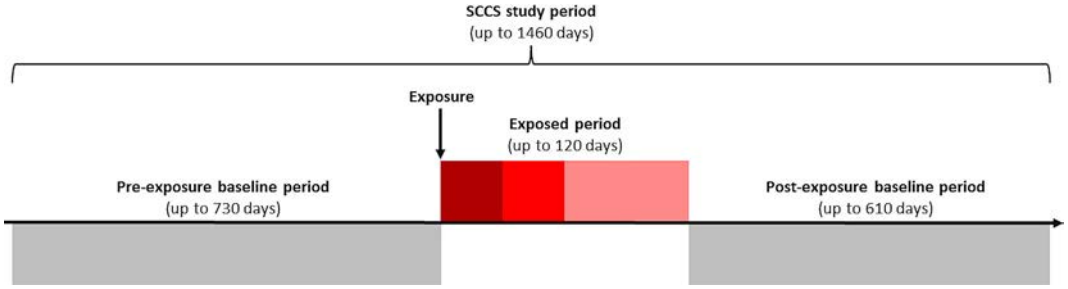


**Figure 1.** Schematic representation of the SCCS study design. The exposed period (in shades of red) was defined as the period following the exposure. It started on the date of the first gout diagnosis. It ended at the earliest of 120 days after the first gout diagnosis, study end, transfer out, date of last data collection from the general practice, a subsequent gout flare, or death. The baseline period (in gray) consisted of pre-exposure and post-exposure periods. The pre-exposure baseline period (up to 730 days) started at 730 days before the first gout diagnosis. It ended on the day before the first gout diagnosis. The postexposure baseline period (up to 610 days) started on the day after the end of the exposed period. It ended at the earliest date of study end, transfer out, date of last data collection from the general practice, a subsequent gout flare, death, or 610 days after the end of the exposed period. SCCS, self-controlled case series.

gout diagnosis). Serum urate measured on the same date as the first recorded gout diagnosis was included because gout flare only reduces serum urate,[29] and if the serum urate was >480 µmol/L if the measurement was taken on the date of gout flare, it would have been even higher if tested after gout flare resolution.[29]

We also performed stratified analyses according to age (≤70 years old vs >70 years old), sex, prescriptions for anti-inflammatory drugs (ie, colchicine, glucocorticoids, and NSAIDs) on the date of the first gout diagnosis or within a week after the first gout diagnosis, and hospitalization for gout on the same date as the first gout diagnosis. We evaluated the presence of interactions in these subgroups. We also conducted stratified analyses according to comorbidities (ie, chronic kidney disease, heart failure, diabetes mellitus, and hypertension) and diuretic prescription (ie, below the median and above the median number of prescriptions) to account for the potential confounding effect of these variables in the association between gout diagnosis and cardiovascular events.

To detect unmeasured or unmeasurable sources of bias (eg, the health care–seeking behavior bias), we conducted a negative control analysis[30] with the first consultation for cataract as the outcome. Negative controls in epidemiologic studies are similar to negative controls in laboratory experiments or a placebo treatment group in a randomized controlled trial.[30] If an association is observed between the exposure and the negative control outcome that is impossible by the hypothesized mechanism, this suggests that the study is biased.[30]

First-ever consultation for cataract was our negative control outcome because there is no plausible biologic relationship between gout and the development of cataract. Patients newly diagnosed with gout were included in the SCCS analysis if they also consulted for cataract the for the first time in the 730 days before or after the first gout diagnosis. Similarly, patients diagnosed with gout for the first time were included in the cohort study if they also consulted for cataract for the first time in the 730 days after the first gout diagnosis.

**Ethics, reporting, and patient and public involvement.** This study was approved by CPRD Research Data Governance (protocol 20_000233). This manuscript followed the STrengthening the Reporting of OBservational studies in Epidemiology (STROBE) guidelines.[31] Code lists are provided in Supplementary Material S3. Patient organizations (the UK Gout Society) will be involved in the dissemination plans.

**Data availability.** This study used data from the CPRD. These data were provided under a license that does not permit data sharing with third parties. They can be obtained from CPRD.

## RESULTS

**Temporal association between first recorded gout diagnosis and cardiovascular events in the cohort studies.** The 76,440 patients newly diagnosed with gout were included in cohort 1 (Figure 2, Table 1). Among them, 2,956

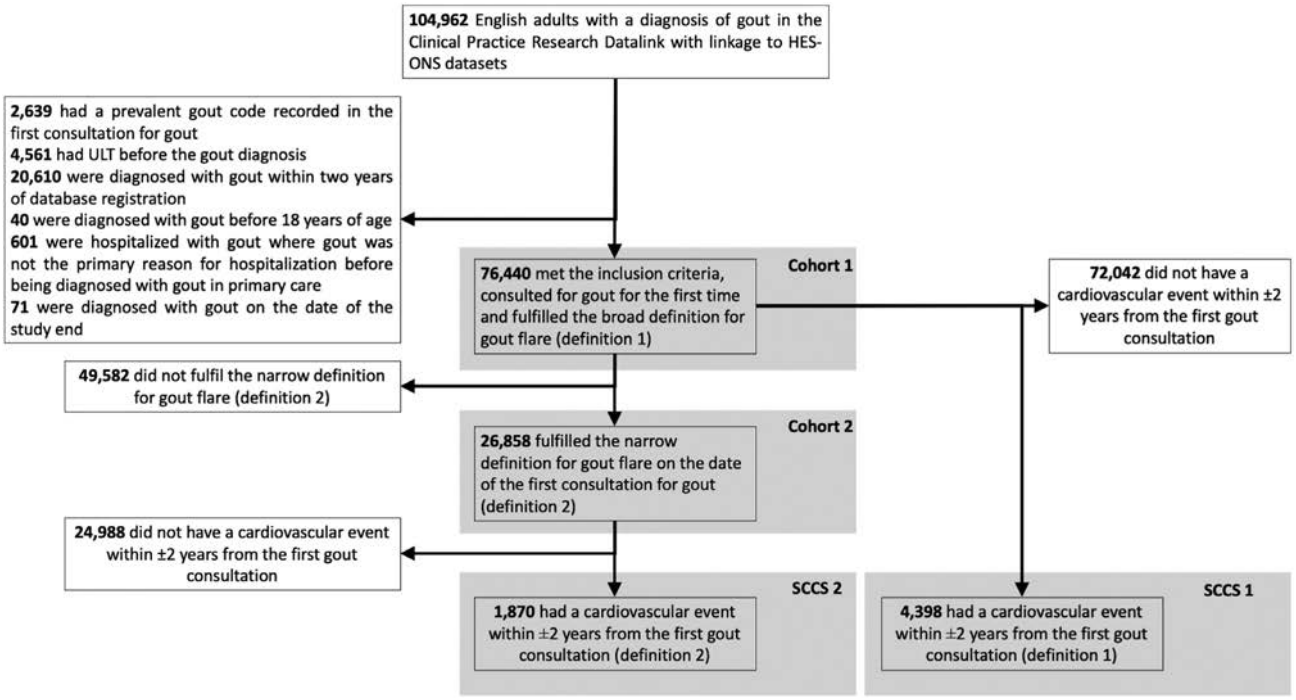


**Figure 2.** Flow diagram for patient selection. HES, Hospital Episode Statistics; ONS, Office for National Statistics; SCCS, self-controlled case series; ULT, urate-lowering therapy.

**Table 1.** Baseline clinical and demographic data of patients with gout included in the study*

| Patient data | Cohort 1[a] (n = 76,440) | Cohort 2[b] (n = 26,858) | SCCS 1[c] (n = 4,398) | SCCS 2[d] (n = 1,870) |
|---|---|---|---|---|
| Age, mean (SD), y | 63.2 (15.4) | 64.8 (15.2) | 74.6 (11.5) | 75.2 (11.0) |
| Female, n (%) | 20,674 (27.1) | 7,506 (28.0) | 1,456 (33.1) | 609 (32.4) |
| Alcohol use | | | | |
| Nondrinker, n (%) | 8,630 (11.3) | 3,175 (11.8) | 715 (16.3) | 305 (16.3) |
| Past drinker, n (%) | 1,437 (1.9) | 582 (2.2) | 130 (3.0) | 58 (3.1) |
| Current drinker, n (%) | 57,092 (74.7) | 20,145 (75.0) | 3,098 (70.4) | 1,327 (71.0) |
| Missing data, n (%) | 9,281 (12.1) | 2,956 (11.0) | 455 (10.4) | 181 (9.7) |
| Body mass index, mean (SD) | 28.9 (5.1) | 31.0 (7.7) | 28.3 (5.0) | 28.2 (4.9) |
| Missing data, n (%) | 10,027 (13.1) | 3,181 (11.8) | 506 (11.5) | 199 (10.6) |
| Smoking habit | | | | |
| Nonsmoker, n (%) | 37,834 (49.5) | 12,990 (48.4) | 1,985 (45.1) | 847 (45.3) |
| Past smoker, n (%) | 24,789 (32.4) | 9,274 (34.5) | 1,772 (40.3) | 760 (40.6) |
| Current smoker, n (%) | 10,102 (13.2) | 3,478 (13.0) | 477 (10.9) | 199 (10.6) |
| Missing data, n (%) | 3,715 (4.9) | 1,116 (4.1) | 164 (3.7) | 65 (3.5) |
| 2019 English Index of Multiple Deprivation, mean (SD) | 3.0 (2.0–4.0) | 3.0 (2.0–4.0) | 3.0 (2.0–4.0) | 3.0 (2.0–4.0) |
| Missing data, n (%) | 8,188 (10.7) | 2,455 (9.1) | 104 (3.4) | 42 (2.2) |
| Subcutaneous tophi, n (%) | 361 (0.5) | 12 (0.1) | 37 (0.8) | 5 (0.3) |
| Recent prior prescription for NSAIDs[e], n (%) | 5,507 (7.2) | 711 (2.6) | 286 (6.5) | 56 (3.0) |
| Recent prior prescription for glucocorticoids[e], n (%) | 2,106 (2.8) | 752 (2.8) | 208 (4.7) | 78 (4.2) |
| Recent prior prescription for colchicine[e], n (%) | 1,451 (1.9) | 190 (0.7) | 106 (2.4) | 33 (0.7) |
| Prescription for NSAIDs on the date of the first gout consultation, n (%) | 16,018 (21.0) | 14,404 (39.5) | 804 (18.3) | 734 (39.3) |
| Prescription for colchicine on the date of the first gout consultation, n (%) | 11,815 (15.5) | 10,616 (53.6) | 915 (20.8) | 816 (43.6) |
| Hospitalization for gout on the date of the first gout consultation, n (%) | 612 (0.8) | 612 (2.3) | 146 (3.3) | 146 (7.8) |
| Prescription for glucocorticoids on the date of the first gout consultation, n (%) | 1,313 (1.7) | 1,196 (4.5) | 136 (3.1) | 126 (6.7) |
| Charlson Comorbidity Index, median (IQR) | 1.0 (0.0–2.0) | 1.0 (0.0–2.0) | 2.0 (1.0–4.0) | 3.0 (1.0–4.0) |
| Number of hospitalizations for any cause in the previous year, median (IQR, maximum) | 0.0 (0.0–0.0, 3.0) | 0.0 (0.0–0.0, 3.0) | 0.0 (0.0–1.0, 3.0) | 0.0 (0.0–2.0, 3.0) |
| Number of primary care consultations for any cause in the previous year, median (IQR) | 80 (5.0–15.0) | 9.0 (6.0–17.0) | 15.0 (10.0–23.0) | 17.0 (11.0–25.0) |
| ESC high/very high cardiovascular risk category,[46] n (%) | 29,754 (38.9) | 11,522 (42.9) | 3,707 (84.3) | 1,609 (86.0) |
| History of acute coronary syndrome or stroke before the study start, n (%) | 10,193 (13.3) | 4,023 (15.0) | 1,480 (33.7) | 627 (33.5) |
| Peripheral artery disease, n (%) | 3,934 (5.1) | 1,593 (5.9) | 643 (14.6) | 283 (15.1) |
| Chronic kidney disease (stage III–V), n (%) | 10,823 (14.2) | 4,498 (16.7) | 1,230 (28.0) | 562 (30.1) |
| Chronic kidney disease (stage IV–V), n (%) | 1,650 (2.2) | 660 (2.5) | 224 (5.1) | 96 (5.1) |
| Diabetes mellitus, n (%) | 8,490 (11.1) | 3,396 (12.6) | 314 (7.1) | 391 (20.9) |
| Diabetes mellitus with target organ damage[f], n (%) | 2,619 (3.4) | 1,075 (4.0) | 866 (19.7) | 152 (8.1) |
| Atrial fibrillation, n (%) | 7,159 (9.4) | 3,011 (11.2) | 944 (21.5) | 424 (22.7) |
| Hypercholesterolemia, n (%) | 12,346 (16.2) | 4,615 (17.2) | 1,069 (24.3) | 481 (25.7) |
| Arterial hypertension, n (%) | 36,459 (47.7) | 13,505 (50.3) | 2,912 (66.2) | 1,240 (66.3) |
| Recent prior prescription for statins[e], n (%) | 19,444 (25.4) | 7,701 (28.7) | 2,186 (49.7) | 984 (52.6) |
| Recent prior prescription for antihypertensive drugs[e], n (%) | 34,003 (44.5) | 12,950 (48.2) | 3,111 (70.7) | 1,374 (73.5) |
| Recent prior prescription for diuretics[e], n (%) | 25,779 (33.7) | 9,599 (35.7) | 2,492 (56.7) | 1,060 (56.7) |
| Recent prior prescription for antiplatelet agents[e], n (%) | 14,307 (18.7) | 5,655 (21.1) | 2,268 (51.6) | 1,001 (53.5) |

* ESC, European Society of Cardiology; IQR, interquartile range; NSAID, nonsteroidal anti-inflammatory drug; SCCS: self-controlled case series.
[a] Cohort 1 included people who met the inclusion criteria (ie, age ≥18 years old, availability of research-quality data, two years of gout-free registration at the current general practice, no previous hospitalizations for gout, prescriptions of urate-lowering therapy, or mention of codes indicating prevalent gout [ie, history of gout] before or on gout diagnosis date).
[b] Cohort 2 included people who met the inclusion criteria and were diagnosed with gout using the strict exposure definition.
[c] SCCS 1 included people from cohort 1 who experienced at least one cardiovascular event at least two years from gout diagnosis.
[d] SCCS 2 included people from cohort 2 who experienced at least one cardiovascular event at least two years from gout diagnosis.
[e] A recent prior prescription was defined as a prescription of any length issued in the 60 days before the first gout diagnosis.
[f] Target organ damage was defined according to ESC guidelines.[46]

(3.9%) experienced at least one cardiovascular event within the next two years. The incidence of first cardiovascular event, myocardial infarction, and cerebrovascular events was 22.1 (95% CI 21.3–22.9), 9.4 (95% CI 8.9–9.9), and 13.0 (95% CI 12.4–13.6) per 1,000 person-years, respectively (Table 2). There were 1,123 (4.2%) cardiovascular events in two years after gout

**Table 2.** Incidence rate of cardiovascular events on days 1 to 30, 31 to 120, and 121 to 730 after first gout diagnosis*

| Days after the first gout diagnosis | Number of cardiovascular events | Person-time at risk (y) | Incidence rate per 1,000 patient-years at risk (95% CI) | Rate difference per 1,000 patient-years at risk (95% CI) |
|---|---|---|---|---|
| Patients who met the inclusion criteria were diagnosed with gout using the broad exposure definition (definition 1) (n = 76,440) | | | | |
| 1–30 | 195 | 6,252.2 | 31.2 (27.1–35.9) | Reference |
| 31–120 | 426 | 18,367.8 | 23.2 (21.1–25.5) | −8.0 (−12.8 to −3.2) |
| 121–730 | 2,335 | 109,399.6 | 21.3 (20.5–22.2) | −9.9 (−14.2 to −5.5) |
| 31–730 | 2,761 | 127,767.4 | 21.6 (20.8–22.4) | −9.6 (−14.0 to −5.1) |
| Patients who met the inclusion criteria were diagnosed using the strict exposure definition (definition 2) (n = 26,858) | | | | |
| 1–30 | 66 | 2,195.8 | 30.1 (23.6–38.3) | Reference |
| 31–120 | 176 | 6,439.4 | 27.3 (23.6–31.7) | −2.7 (−10.9 to 5.4) |
| 121–730 | 881 | 38,029.0 | 23.2 (21.7–24.7) | −6.9 (−14.3 to 0.5) |
| 31–730 | 1,057 | 44,468.4 | 23.8 (22.4–25.2) | −6.3 (−13.3 to 1.1) |

* CI, confidence interval.

diagnosis among the 26,858 patients newly diagnosed with gout, meeting the strict definition. The incidence of cardiovascular events was comparable with those in cohort 1 (Table 2).

The incidence of cardiovascular events was significantly higher in the first 30 days after the first gout diagnosis compared with their incidence in days 121 to 730 in cohort 1 (31.2 [95% CI 27.1–35.9] vs 21.3 in [95% CI 20.5–22.2] events/1,000 person-years) with a rate difference of –9.9 (95% CI –14.2 to –5.5) events per 1,000 person-years. The difference was only numerically higher in cohort 2 (30.1 [95% CI 23.6–38.3] vs 23.2 [95% CI

| Gout flare exposure window, days after the first flare consultation | Events | Person-days | Event rates per 1,000 person-days (95%CI) | Crude rate difference per 1,000 person-days (95%CI) | Adjusted IRR (95%CI) |
|---|---|---|---|---|---|
| **Main analysis [N=4,398]** | | | | | |
| 0-30 | 161 | 129,604 | 1.15 (0.89-1.48) | 0.48 (0.29-0.67) | 1.55 (1.33-1.83) |
| 31-60 | 110 | 126,514 | 0.84 (0.63-1.13) | 0.11 (-0.06 to 0.27) | 1.11 (0.92-1.24) |
| 61-120 | 206 | 245,184 | 0.86 (0.70-1.07) | 0.08 (-0.04 to 0.21) | 1.09 (0.94-1.25) |
| Baseline period | 3,921 | 5,141,844 | 0.77 (0.72-0.83) | Reference | Reference |
| **Considering stroke as the outcome [N=1,951]** | | | | | |
| 0-30 | 63 | 57,239 | 1.10 (0.86-1.42) | 0.32 (0.05-0.79) | 1.33 (1.03-1.71) |
| 31-60 | 47 | 55,448 | 0.85 (0.63-1.13) | 0.07 (-0.18 to 0.31) | 1.06 (0.79-1.42) |
| 61-120 | 100 | 106,721 | 0.94 (0.77-1.15) | 0.16 (-0.03 to 0.35) | 1.20 (0.97-1.46) |
| Baseline period | 1,741 | 2,237,761 | 0.78 (0.73-0.83) | Reference | Reference |
| **Considering myocardial infarction as the outcome [N=2,469]** | | | | | |
| 0-30 | 100 | 73,025 | 1.37 (1.12-1.67) | 0.62 (0.35-0.89) | 1.76 (1.44-2.15) |
| 31-60 | 63 | 71,726 | 0.88 (0.68-1.13) | 0.13 (-0.09 to 0.35) | 1.14 (0.89-1.47) |
| 61-120 | 111 | 139,695 | 0.79 (0.66-0.96) | 0.05 (-0.11 to 0.20) | 1.04 (0.85-1.26) |
| Baseline period | 2,195 | 2,929,274 | 0.75 (0.71-0.80) | Reference | Reference |
| **Considering cardiovascular events requiring hospitalisation or leading to death as the outcome [N=2,095]** | | | | | |
| 0-30 | 78 | 61,775 | 1.21 (0.85-1.71) | 0.49 (0.21 to 0.77) | 1.58 (1.26-1.98) |
| 31-60 | 53 | 60,056 | 0.79 (0.51-1.22) | 0.11 (-0.13 to 0.35) | 1.11 (0.85-1.46) |
| 61-120 | 120 | 115,492 | 0.80 (0.59-1.10) | 0.27 (0.08 to 0.46) | 1.26 (1.08-1.56) |
| Baseline period | 1,844 | 2,388,087 | 0.79 (0.72-0.87) | Reference | Reference |

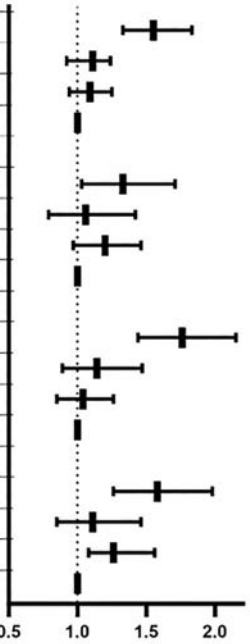


**Figure 3.** Cardiovascular events associated with first recorded diagnosis of gout in either the primary or hospitalized because of gout. The number of patients included in each analysis is reported in square brackets. The analyses were adjusted for age and calendar season. The baseline interval consisted of a pre-exposure period of up to 730 days before the first consultation for gout and a postexposure period of up to 610 days after the exposed period at most. IRR, incidence rate ratio; CI, confidence interval.

21.7–24.7] events per 1,000 person-years, respectively) with a rate difference of –6.9 (95% CI –14.5 to 0.5) events per 1,000 person-years (Table 2).

**Temporal association between first recorded gout diagnosis and cardiovascular events using the broad definition (definition 1).** The 4,398 patients with a cardiovascular event within 730 days before or after gout diagnosis were included (Table 1). There were 477 and 3,921 cardiovascular events in exposed and baseline periods, respectively (aIRR 1.20, 95% CI 1.12–1.36).

The incidence of cardiovascular events was significantly higher in the 30 days following the first gout diagnosis. Compared with the baseline period, the aIRRs for days 0 to 30, 31 to 60, and 61 to 120 of the exposed period were 1.55 (95% CI 1.33–1.83), 1.11 (95% CI 0.92–1.34), and 1.09 (95% CI 0.94–1.25), respectively (Figure 3).

**Temporal association between the first gout diagnosis and cardiovascular events using the strict definition (definition 2).** The 1,870 patients with a cardiovascular event within 730 days before or after gout diagnosis were included in this analysis (Table 1). There were 197 and 1,673 cardiovascular events in exposed and baseline periods, respectively (aIRR 1.17, 95% CI 1.01–1.36).

The incidence of cardiovascular events was significantly higher in the 30 days following the first gout diagnosis compared with the baseline period. Compared with the baseline period, the aIRRs for days 0 to 30, 31 to 60, and 61 to 120 of the exposed period were 1.40 (95% CI 1.09–1.80), 1.06 (95% CI 0.78–1.42), and 1.10 (95% CI 0.89–1.36), respectively (Figure 4).

**Sensitivity analyses.** The results of the sensitivity analyses were consistent with the main analysis (Figures 2 and 3; Supplementary Materials S4, S5, S6, and S7). The greatest relative increase was observed in the first 15 days after the first gout diagnosis (definition 1 aIRR 1.70, 95% CI 1.38–2.10; definition 2 aIRR 1.52, 95% CI 1.10–2.11). Furthermore, the temporal association was still present when we considered cardiovascular events requiring hospitalization or leading to death as the outcome (definition 1 aIRR 1.58, 95% CI 1.26–1.98; definition 2 aIRR 1.48, 95% CI 1.05–2.11) and when we excluded people with previous cardiovascular events (definition 1 aIRR 1.53, 95% CI 1.26–1.87; definition 2 aIRR 1.39, 95% CI 1.01–1.90).

There was no evidence for a statistically significant interaction between the age group and the first gout diagnosis on the

| Gout flare exposure window, days after the first flare consultation | Events | Person-days | Event rates per 1,000 person-days (95%CI) | Crude rate difference per 1,000 person-days (95%CI) | Adjusted IRR (95%CI) |
|---|---|---|---|---|---|
| **Main analysis [N=1,870]** | | | | | |
| 0-30 | 63 | 54,879 | 1.15 (0.89-1.48) | 0.38 (0.09-0.66) | 1.40 (1.09-1.80) |
| 31-60 | 45 | 53,392 | 0.84 (0.63-1.13) | 0.07 (-0.18 to 0.32) | 1.06 (0.78-1.42) |
| 61-120 | 89 | 103,375 | 0.86 (0.70-1.07) | 0.09 (-0.09 to 0.27) | 1.10 (0.89-1.36) |
| Baseline period | 1,673 | 2,167,797 | 0.77 (0.72-0.83) | Reference | Reference |
| **Considering stroke as the outcome [N=886]** | | | | | |
| 0-30 | 29 | 28,228 | 1.03 (0.71-1.49) | 0.32 (-0.06 to 0.69) | 1.30 (0.89-1.90) |
| 31-60 | 24 | 27,372 | 0.88 (0.58-1.32) | 0.16 (-0.19 to 0.52) | 1.16 (0.77-1.75) |
| 61-120 | 44 | 52,642 | 0.87 (0.62-1.13) | 0.16 (-0.10 to 0.42) | 1.11 (0.81-1.52) |
| Baseline period | 789 | 1,108,324 | 0.71 (0.64-0.79) | Reference | Reference |
| **Considering myocardial infarction as the outcome [N=1,073]** | | | | | |
| 0-30 | 40 | 33,361 | 1.20 (0.87-1.65) | 0.48 (0.10-0.85) | 1.60 (1.16-2.19) |
| 31-60 | 25 | 32,670 | 0.77 (0.51-1.14) | 0.04 (-0.26 to 0.35) | 1.03 (0.69-1.53) |
| 61-120 | 46 | 63,587 | 0.72 (0.54-0.97) | 0.00 (-0.21 to 0.21) | 0.97 (0.72-1.31) |
| Baseline period | 962 | 1,330,606 | 0.72 (0.66-0.79) | Reference | Reference |
| **Considering cardiovascular events requiring hospitalisation or leading to death as the outcome [N=929]** | | | | | |
| 0-30 | 33 | 27,301 | 1.21 (0.85-1.71) | 0.42 (0.01 to 0.83) | 1.48 (1.05-2.11) |
| 31-60 | 21 | 26,512 | 0.79 (0.51-1.22) | 0.00 (-0.34 to 0.34) | 0.98 (0.63-1.51) |
| 61-120 | 41 | 51,100 | 0.80 (0.59-1.10) | 0.01 (-0.24 to 0.26) | 0.97 (0.70-1.34) |
| Baseline period | 834 | 1,053,229 | 0.79 (0.72-0.87) | Reference | Reference |

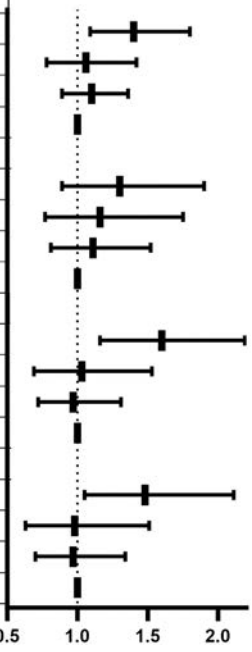


**Figure 4.** Cardiovascular events associated with the first recorded diagnosis of gout and either prescribed an anti-inflammatory drug on the same date or hospitalized because of gout. The number of patients included in each analysis is reported in square brackets. The analyses were adjusted for age and calendar season. The baseline interval consisted of a pre-exposure period of up to 730 days before the first consultation for gout and a postexposure period of up to 610 days after the exposed period at most. IRR, incidence rate ratio; CI, confidence interval.

occurrence of cardiovascular events ($p_{interaction}$ = 0.14 and 0.27 for definitions 1 and 2, respectively). Women had a significantly greater increase in the risk of cardiovascular events after a new gout diagnosis than men when using a broad definition ($p_{interaction}$ = 0.03 for definition 1) but not when using a strict definition ($p_{interaction}$ = 0.12 for definition 2) (Supplementary Materials S5 and S7).

Results were also consistent in the stratified analyses according to comorbidities (ie, chronic kidney disease, heart failure, diabetes mellitus, and hypertension) and diuretic prescription. Although not statistically significant, the association between the first gout diagnosis and cardiovascular events was weaker in people prescribed colchicine (prescribed on the same date as the first gout diagnosis: aIRR 0.84, 95% CI 0.53–1.33; and prescribed within one week after the first gout diagnosis: aIRR 1.17, 95% CI 0.80–1.71) compared to people prescribed NSAIDs (prescribed on the same date as the first gout diagnosis: aIRR 1.39, 95% CI 0.93–2.06; prescribed within one week after the first gout diagnosis: aIRR 1.48, 95% CI 1.02–2.16) (Supplementary Material S7).

**Negative control outcome.** In both SCCS analyses, the first consultation at which gout was diagnosed was not temporally associated with the first consultation for cataract (Supplementary Materials S8 and S9). Similarly, the incidence rates of the first-ever consultation for cataract did not significantly vary between the first 30 days after the first consultation at which gout was diagnosed and days 31 to 730 in the cohort studies (Supplementary Material S10).

## DISCUSSION

We evaluated the temporal association between the first consultation at which gout was diagnosed and cardiovascular events. Using a large nationwide dataset incorporating primary care, hospitalization, and mortality records, we observed the first consultation at which gout was diagnosed to be temporally associated with a transient increase in cardiovascular events in the subsequent 30 days regardless of the definition used. Confidence in our findings was increased by the fact that the greatest relative increase was observed in the first 15 days after the first diagnosis and that the temporal association was still present when we considered hard outcomes such as cardiovascular events requiring hospitalization or leading to death. The cohort studies, including all eligible patients and showing significantly higher incidence rates of cardiovascular events in the first 30 days after the first consultation at which gout was diagnosed, were consistent with the SCCS analyses.

Previous cohort studies have shown increased cardiovascular morbidity after gout diagnosis but have not focused on early gout nor the temporal association between first gout diagnosis, which could be first gout flare consultation, and cardiovascular events.[32,33] Among people newly diagnosed with gout, the incidence of cardiovascular events within the subsequent 30 days was significantly higher than within the next two years in the present study. It was also higher than previous studies in which a longer follow-up period after gout diagnosis was considered.[32,33]

The incidence of cardiovascular events in the 30 days after the first gout diagnosis in our study was comparable to those reported in studies examining the short-term risk of cardiovascular events following respiratory infections.[34] Like respiratory infections, the potential mechanism underpinning the higher incidence of cardiovascular events immediately after the first gout diagnosis may be related to atherothrombosis, platelet activation, endothelial dysfunction, and biomechanical stress triggered by systemic and vascular inflammation during gout flares.[35] Several mediators such as interleukin-1beta, interleukin-6, and tumor necrosis factor superfamily 14 are elevated during gout flares and have been shown to promote both cardiovascular events[36,39,40] and local and systemic inflammation.[41] Further proof of their role comes from the observation that the inhibition of interleukin-1beta by canakinumab and inhibition of inflammasome assembly by colchicine prevents cardiovascular events in populations without gout.[36–38]

In a previous study that included people with long-standing gout, we reported that gout flares were associated with a transient increase in cardiovascular events.[5] Lopez et al observed that the first-ever hospital admission for gout flare was associated with an increased risk of major acute cardiovascular events (ie, acute coronary syndrome, stroke, heart failure, or cardiovascular death) in the 30 days following the hospital discharge in an Australian population of 941 patients with gout.[6] However, the generalizability of the latter study was limited by hospital-based recruitment. Those who may seek hospital admission for gout flare may either have severe and/or refractory gout flare and comorbidities that make it difficult for them to be managed in primary care. Moreover, neither of these two studies assessed risk following the first gout diagnosis. In the present study, we also used two definitions to ascertain the first gout diagnosis. The broad definition allowed us to capture all the consultations at which gout was diagnosed in primary care and secondary care. Because flares are by far the most common presentation of gout,[1] we speculated that any first record of gout can be reasonably considered as a proxy for the first gout flare requiring contact with the health care system. The strict definition enabled us to establish the internal validity of the association because it captured all the consultations at which the first gout flare was recorded in primary care and secondary care.

Although not statistically significant, women had a higher incidence rate of cardiovascular events after the diagnosis of gout compared to men. This finding is in line with a recently published paper[2] in which the excess risk of a broad range of cardiovascular diseases in gout was greater in women than men. This could be related to the older age and the higher burden of cardiovascular comorbidities, such as obesity, dyslipidemia, chronic kidney disease, diabetes mellitus, and heart failure.[42]

The main strength of this study is the use of SCCS design that allows us to examine the association between a transient exposure and an outcome of interest automatically accounting for fixed covariates. As recommended, we checked the validity of the assumptions. We extracted data from a high-quality, nationwide, general population–based electronic health record database containing both primary care, secondary care, and mortality data, allowing us to capture all outcomes. We also estimate the absolute incidence of cardiovascular events in people with a new diagnosis of gout, showing a similar temporal trend. Thus, our results are generalizable. Also, the use of routinely collected data allowed us to minimize the risk of recall bias. Selection bias was minimized by universal access to health care for all UK residents free at the point of use. The lack of a temporal association with a negative control outcome supports a low risk of unmeasured and unmeasurable bias, such as the health care-seeking behavior bias.

We must acknowledge some limitations. The first is the uncertainty regarding the onset of gout symptoms. We used the date of the contact with the health care system on which a gout diagnosis was made as the exposure date. We believe that it is a reasonable proxy, especially in the context of gout flares in which symptoms usually peak within 12 to 24 hours of onset. We could not be sure about the fact that the first gout diagnosis is the consultation for the first-ever gout flare experienced by the patient. However, gout flare has typical characteristics, and it is likely that most patients in this study were consulting for gout flare for the first time.[43]

Although we performed sensitivity, stratified, and negative control analyses, another limitation is that the risk of residual unmeasured time-varying confounding could not be completely ruled out. However, results of the analyses stratified on the major cardiovascular risk factors for gout flares (ie, chronic kidney disease, diabetes mellitus, arterial hypertension, heart failure, and prescription of diuretics) were consistent with the main analysis. Third, we did not conduct an adjudication of cardiovascular outcomes. However, these outcomes have been widely adopted in previous research.[23,24] Fourth, these results might apply only to gout flares that are of sufficient severity to require contact with the health care system. Fifth, the available sample size limited our ability to draw any definite conclusion on the comparative impact of different anti-inflammatory medications prescribed to treat gout flares. Nevertheless, patients who received a prescription for colchicine had a nonsignificant decrease in the incidence of cardiovascular events in the first 30 days compared to those prescribed with NSAIDs or glucocorticoids. Sixth, we cannot exclude that a proportion of patients with gout can be misdiagnosed with other crystal arthropathies, osteoarthritis, or other chronic inflammatory arthritis. However, previous validation studies have shown that a primary care diagnosis of gout has a positive predictive value of 90%.[44,45] Furthermore, the association was still significant when we considered those with serum urate levels ≥480 μmol/L. Seventh, the prevalence of tophaceous gout was relatively low. This may be related to the fact that the study population consisted of people with early gout. However, it is possible that the low prevalence was because of a poor recording of subcutaneous tophi in primary care. Finally, our dataset did not include data about consultations for gout in accident and emergency departments that did not require overnight admission to the hospital. Although such patients may have more severe gout flares than those who only consulted their general practitioner, they would have a less severe gout flare and fewer comorbidities than those requiring overnight hospital admission; we do not believe that their exclusion biases the observed association.

The first gout diagnosis was associated with an increased risk of cardiovascular events in the short term. Inflammation during the first gout flare is the most plausible explanation for this association. These findings support the need for cardiovascular risk management from the time of first gout consultation.

## AUTHOR CONTRIBUTIONS

All authors contributed to at least one of the following manuscript preparation roles: conceptualization AND/OR methodology, software, investigation, formal analysis, data curation, visualization, and validation AND drafting or reviewing/editing the final draft. As corresponding author, Dr Cipolletta confirms that all authors have provided the final approval of the version to be published, and takes responsibility for the affirmations regarding article submission (eg, not under consideration by another journal), the integrity of the data presented, and the statements regarding compliance with institutional review board/Helsinki Declaration requirements.

## REFERENCES

1. Dalbeth N, Gosling AL, Gaffo A, et al. Gout. Lancet 2021;397(10287):1843–1855.
2. Ferguson LD, Molenberghs G, Verbeke G, et al. Gout and incidence of 12 cardiovascular diseases: a case-control study including 152 663 individuals with gout and 709 981 matched controls. Lancet Rheumatol 2024;6(3):e156–e167.
3. Li X, Meng X, Timofeeva M, et al. Serum uric acid levels and multiple health outcomes: umbrella review of evidence from observational studies, randomised controlled trials, and Mendelian randomisation studies. BMJ 2017;357:j2376.
4. Mackenzie IS, Hawkey CJ, Ford I, et al. Allopurinol versus usual care in UK patients with ischaemic heart disease (ALL-HEART): a multicentre, prospective, randomised, open-label, blinded-endpoint trial. Lancet 2022;400(10359):1195–1205.
5. Cipolletta E, Tata LJ, Nakafero G, et al. Association between gout flare and subsequent cardiovascular events among patients with gout. JAMA 2022;328(5):440–450.
6. Lopez D, Dwivedi G, Nossent J, et al. Risk of major adverse cardiovascular event following incident hospitalization for acute gout: a Western Australian population-level linked data study. ACR Open Rheumatol 2023;5(6):298–304.
7. Trelle S, Reichenbach S, Wandel S, et al. Cardiovascular safety of non-steroidal anti-inflammatory drugs: network meta-analysis. BMJ 2011;342(7789):154.

8. Pascart T, Robinet P, Ottaviani S, et al. Evaluating the safety and short-term equivalence of colchicine versus prednisone in older patients with acute calcium pyrophosphate crystal arthritis (COLCHICORT): an open-label, multicentre, randomised trial. Lancet Rheumatol 2023;5(9):e523–e531.
9. FitzGerald JD, Dalbeth N, Mikuls T, et al. 2020 American College of Rheumatology guideline for the management of gout. Arthritis Care Res (Hoboken) 2020;72(6):744–760.
10. Richette P, Doherty M, Pascual E, et al. 2016 updated EULAR evidence-based recommendations for the management of gout. Ann Rheum Dis 2017;76(1):29–42.
11. Qaseem A, Harris RP, Forciea MA, et al. Management of acute and recurrent gout: a clinical practice guideline from the American College of Physicians. Ann Intern Med 2017;166(1):58–68.
12. Hui M, Carr A, Cameron S, et al. The British Society for Rheumatology Guideline for the management of gout. Rheumatology (Oxford) 2017; 56(7):1056–1059.
13. Whitaker H, Farrington C, Spiessens B, et al. Tutorial in biostatistics: the self-controlled case series method. Stat Med 2006;25(10):1768–1797.
14. Herrett E, Gallagher AM, Bhaskaran K, et al. Data resource profile: Clinical Practice Research Datalink (CPRD). Int J Epidemiol 2015; 44(3):827–836.
15. Kuo CF, Grainge MJ, Mallen C, et al. Rising burden of gout in the UK but continuing suboptimal management: a nationwide population study. Ann Rheum Dis 2015;74(4):661–667.
16. McCormick N, Yokose C, Challener GJ, et al. Serum urate and recurrent gout. JAMA 2024;331(5):417–424.
17. Joshi AD, McCormick N, Yokose C, et al. Prediagnostic glycoprotein acetyl levels and incident and recurrent flare risk accounting for serum urate levels: a population-based, prospective study and Mendelian randomization analysis. Arthritis Rheumatol 2023;75(9):1648–1657.
18. Cipolletta E, Tata LJ, Nakafero G, et al. Risk of venous thromboembolism with gout flares. Arthritis Rheumatol 2023;75(9):1638–1647.
19. Zheng C, Rashid N, Wu YL, et al. Using natural language processing and machine learning to identify gout flares from electronic clinical notes. Arthritis Care Res (Hoboken) 2014;66(11):1740–1748.
20. Rothenbacher D, Primatesta P, Ferreira A, et al. Frequency and risk factors of gout flares in a large population-based cohort of incident gout. Rheumatology (Oxford) 2011;50(5):973–981.
21. MacFarlane LA, Liu CC, Solomon DH, et al. Validation of claims-based algorithms for gout flares. Pharmacoepidemiol Drug Saf 2016;25(7): 820–826.
22. Adnet F, Renault R, Jabre P, et al. Incidence of acute myocardial infarction resulting in sudden death outside the hospital. Emerg Med J 2011;28(10):884–886.
23. Morgan A, Sinnott S, Smeeth L, et al. Concordance in the recording of stroke across UK primary and secondary care datasets: a population-based cohort study. BJGP Open 2021;5(2):1–11.
24. Herrett E, Shah AD, Boggon R, et al. Completeness and diagnostic validity of recording acute myocardial infarction events in primary care, hospital care, disease registry, and national mortality records: cohort study. Br Med J 2013;346(7909):f2350.
25. Choi HJ, Moon KW, Kim HO, et al. Seasonal variations and associated factors of gout attacks: a prospective multicenter study in Korea. J Korean Med Sci. 2020;35(20):e133.
26. Stewart S, Keates AK, Redfern A, et al. Seasonal variations in cardiovascular disease. Nat Rev 2017;14(11):654–664.
27. Whitaker HJ, Ghebremichael-Weldeselassie Y, Douglas IJ, et al. Investigating the assumptions of the self-controlled case series method. Stat Med 2018;37(4):643–658.
28. Ghebremichael-Weldeselassie Y, Jabagi MJ, Botton J, et al. A modified self-controlled case series method for event-dependent exposures and high event-related mortality, with application to COVID-19 vaccine safety. Stat Med 2022;41(10):1735.
29. Urano W, Associate R, Yamanaka H, et al. The inflammatory process in the mechanism of decreased serum uric acid concentrations during acute gouty arthritis. J Rheumatol 2002;29(9):1950–1953.
30. Arnold BF, Ercumen A. Negative control outcomes: a tool to detect bias in randomized trials. JAMA 2016;316(24):2597.
31. von Elm E, Altman DG, Egger M, et al. Strengthening the reporting of observational studies in epidemiology (STROBE) statement: guidelines for reporting observational studies. BMJ 2007;335(7624): 806–808.
32. Clarson L, Hider S, Belcher J, et al. Increased risk of vascular disease associated with gout: a retrospective, matched cohort study in the UK clinical practice research datalink. Ann Rheum Dis 2015;74(4): 642–647.
33. Colantonio LD, Saag KG, Singh JA, et al. Gout is associated with an increased risk for incident heart failure among older adults: The REasons for Geographic and Racial Differences in Stroke (REGARDS) cohort study. Arthritis Res Ther 2020;22(1):1–13.
34. Sipilä PN, Lindbohm JV, Batty GD, et al. Severe infection and risk of cardiovascular disease: a multicohort study. Circulation 2023; 147(21):1582–1593.
35. Willerson JT, Ridker PM. Inflammation as a cardiovascular risk factor. Circulation 2004;109(21 Suppl 1):II2–10.
36. Ridker PM, Everett BM, Thuren T, et al. Antiinflammatory therapy with canakinumab for atherosclerotic disease. N Engl J Med 2017; 377(12):1119–1131.
37. Tardif JC, Kouz S, Waters DD, et al. Efficacy and safety of low-dose colchicine after myocardial infarction. N Engl J Med 2019;381(26): 2497–2505.
38. Nidorf SM, Fiolet ATL, Mosterd A, et al. Colchicine in patients with chronic coronary disease. N Engl J Med 2020;383(19):1838–1847.
39. Koenig W, Sager HB. Inflammation and cardiovascular disease: new epidemiologic data and their potential implications for anti-cytokine therapy. Eur J Prev Cardiol 2023;30(16):1728–1730.
40. Hsu CY, Tseng WK, Wu YW, et al. Circulating TNFSF14 (tumor necrosis factor superfamily 14) predicts clinical outcome in patients with stable coronary artery disease. Arterioscler Thromb Vasc Biol. 2019; 39(6):1240–1252.
41. Ea HK, Kischkel B, Chirayath TW, et al. Systemic inflammatory cytokine profiles in patients with gout during flare, intercritical and treat-to-target phases: TNFSF14 as new biomarker. Ann Rheum Dis 2024;83(7):945–956.
42. Rodríguez-Sosa E, De Miguel E, Borrás F, et al. Filling gaps in female gout: a cross-sectional study of comorbidities in 192 037 hospitalised patients. RMD Open 2023;9(2):e003191.
43. Stewart S, Guillen AG, Taylor WJ, et al. The experience of a gout flare: a meta-synthesis of qualitative studies. Semin Arthritis Rheum 2020; 50(4):805–811.
44. Watson L, Muller S, Roddy E. Primary care diagnosis of gout compared to a primary care diagnostic rule for gout and to classification criteria. J Rheumatol 2019;46(11):1542.
45. Meier CR, Jick H. Omeprazole, other antiulcer drugs and newly diagnosed gout. Br J Clin Pharmacol 1997;44(2):175–178.
46. Visseren FLJ, Mach F, Smulders YM, et al. 2021 ESC guidelines on cardiovascular disease prevention in clinical practice. Eur Heart J 2021;42(34):3227–3337.

**Arthritis & Rheumatology**
Vol. 77, No. 2, February 2025, pp 212–225
DOI 10.1002/art.42988
© 2024 The Author(s). *Arthritis & Rheumatology* published by Wiley Periodicals LLC on behalf of American College of Rheumatology. This is an open access article under the terms of the Creative Commons Attribution-NonCommercial License, which permits use, distribution and reproduction in any medium, provided the original work is properly cited and is not used for commercial purposes.

American College of Rheumatology
Empowering Rheumatology Professionals

# Unraveling the Genetics of Shared Clinical and Serological Manifestations in Patients With Systemic Inflammatory Autoimmune Diseases

Matteo Bianchi,[1] Sergey V. Kozyrev,[1] Antonella Notarnicola,[2] Johanna K. Sandling,[1] Mats Pettersson,[1] Dag Leonard,[1] Christopher Sjöwall,[3] Iva Gunnarsson,[4] Solbritt Rantapää-Dahlqvist,[5] Anders A. Bengtsson,[6] Andreas Jönsen,[6] Elisabet Svenungsson,[4] Helena Enocsson,[3] Marika Kvarnström,[4] Helena Forsblad-d'Elia,[7] Sara Magnusson Bucher,[8] Katrine B. Norheim,[9] Eva Baecklund,[1] Roland Jonsson,[10] Daniel Hammenfors,[11] Per Eriksson,[3] Thomas Mandl,[12] Roald Omdal,[13] Leonid Padyukov,[4] Helena Andersson,[14] Øyvind Molberg,[14] Louise Pyndt Diederichsen,[15] Ann-Christine Syvänen,[1] Marie Wahren-Herlenius,[16] Gunnel Nordmark,[1] Ingrid E. Lundberg,[4] Lars Rönnblom,[1] and Kerstin Lindblad-Toh,[17] with the DISSECT consortium and the ImmunoArray consortium

**Objective.** Systemic inflammatory autoimmune diseases (SIADs) such as systemic lupus erythematosus (SLE), primary Sjögren disease (pSS), and idiopathic inflammatory myopathies (myositis) are complex conditions characterized by shared circulating autoantibodies and clinical manifestations, including skin rashes, among others. This study was aimed at elucidating the genetics underlying these common features.

**Methods.** We performed targeted DNA sequencing of coding and regulatory regions from approximately 1,900 immune-related genes in a large cohort of 2,292 well-characterized Scandinavian patients with SIADs with SLE, pSS, and myositis as well as 1,252 controls. A gene-based functionally weighted genetic score for aggregate testing of all genetic variants, including rare variants, was complemented by in silico functional analyses and in vitro reporter experiments.

**Results.** Case–control association analysis detected known and potentially novel genetic loci in agreement with previous genetic and transcriptomics findings linked to the SIAD autoimmune background. Intriguingly, case–case comparisons between patient subgroups with and without specific autoantibodies revealed that the subgroups defined by antinuclear antibodies and anti–double-stranded DNA antibodies have unique genetic profiles reflecting their heterogeneity. When focusing on clinical features, we overall showed that dual-specificity phosphatase 1 (*DUSP1*) protective genetic variants lead to increased gene expression and potentially to anti-inflammatory effects on the SIAD-associated skin phenotype. This is consistent with recent genetic findings on eczema and with the previously reported down-regulation of the MAPK signaling-related gene *DUSP1* in other skin disorders.

**Conclusion.** Together, this suggests common molecular mechanisms potentially underlying overlapping clinical manifestations shared among different disorders and informs clinical heterogeneity, which could be translated to improve disease diagnostic and treatment, also in more generalized disease frameworks.

## INTRODUCTION

Systemic inflammatory autoimmune diseases (SIADs) such as systemic lupus erythematosus (SLE), primary Sjögren disease (pSS), and idiopathic inflammatory myopathies (myositis) are chronic heterogeneous rare conditions in which inflammation and the primary pathogenic events can be restricted to different organ systems and co-occur with specific

Supported by the Swedish Research Council for Medicine and Health (grants Dnr 2018-02399, 2018-02535, and 2016-01254), the Swedish Rheumatism Association, King Gustav V's 80-year Foundation, the Swedish Society of Medicine, the Ingegerd Johansson Donation, the Swedish Heart Lung Foundation, The Swedish Cancer Society, the Knut and Alice Wallenberg Foundation, the Norwegian Research Council, and the Torsten Söderberg Foundation. ALF funding was received from Stockholm County, KID funding was received from the Karolinska Institutet, and a Wallenberg Scholar Award as well as a Distinguished Professor award were given to Dr Lindblad-Toh.

[1]Matteo Bianchi, PhD, Sergey V. Kozyrev, PhD, Johanna K. Sandling, PhD, Mats Pettersson, PhD, Dag Leonard, MD, PhD, Eva Baecklund, MD, PhD, Ann-Christine Syvänen, PhD, Gunnel Nordmark, MD, PhD, Lars Rönnblom, MD, PhD: Uppsala University, Uppsala, Sweden; [2]Antonella Notarnicola, MD, PhD: Karolinska University Hospital, Stockholm, Sweden; [3]Christopher Sjöwall, MD, PhD, Helena Enocsson, PhD, Per Eriksson, MD, PhD: Linköping

serological profiles.[1–3] Patients with SIADs show remarkable similarities, such as overexpression of type I interferon (IFN)–regulated genes (ie, IFN signature), identical circulating autoantibodies mainly targeting nuclear antigens (eg, antinuclear antibodies [ANA], SSA-Ro, SSB-La), and analogous clinical manifestations and comorbidities, including skin rashes, arthritis, different types of malignancies, and renal and lung involvement, which develop regardless of the primary disease diagnosis.[4] In addition, a number of shared genetic loci encompassing genes involved in innate and adaptive immune responses have been identified as disease risk factors, thus overall highlighting a partially shared genetic etiology in patients with SIADs.[5–8]

The genetic background of patients with SIADs has been primarily explored via genome-wide association and targeted genotyping studies, as well as meta-analyses, unraveling disease associations mainly driven by common genetic variation.[5,6,8] Conversely, the contribution of the full spectrum of genetic variation has not been comprehensively evaluated in patients with SIADs, especially when considering their shared serological and clinical features. For this purpose, the detection of those genetic variants rarer in the population is required, as well as large and inclusive datasets in which different patient cohorts are combined.[9] This has to be ideally complemented by the implementation of algorithms testing the cumulative effect of different genetic variants, especially of those in the lower range of allele frequency in sizable genetic regions.[10] In fact, it has been shown that multiple causal variants underlie genetic associations in complex diseases[11] and that rare variants also contribute to disease heritability.[12] Using next-generation targeted DNA sequencing of regulatory and coding regions in a large cross-disease sample cohort including Scandinavian patients with SLE, pSS, and myositis as well as healthy controls, the objective of the present study was to examine the contribution of the whole spectrum of genetic variants in defining the genetic background underlying these patients with SIADs and potentially also their secondary shared serological and clinical manifestations, thus allowing the identification of genetic profiles conceivably relevant for patient stratification in the clinic.

## PATIENTS AND METHODS

For detailed materials and methods description, see Supplementary Materials and Methods. Members of the DISSECT and ImmunoArray consortia can be found in Appendixes A and B, respectively.

**Study participants.** The study cohort consisted of healthy controls as well as patients diagnosed with SLE, pSS, and myositis, from whom blood specimens and detailed clinical and serological information were collected at Scandinavian rheumatology clinics (ie, Sweden, Denmark, and Norway) in compliance with individual consent and regional ethical permits. Patient characteristics, as well as their clinical and serological profiles, have been previously described in details.[13–15] Serological and clinical patient subgroups were defined based on the occurrence of the same circulating autoantibodies in the former and to inclusively combine clinical manifestations and comorbidities into collective features related to the same organ/tissue or comprising the same diagnosis in the latter (Table 1).

**Targeted DNA sequencing and bioinformatics analysis.** A comprehensive description of the capture array design and implementation, as well as the targeted sequencing of the samples included in this study, has been previously provided.[13–16] Briefly, the targeted array included 1,853 genes involved in immune function, inflammation, and autoimmunity for which both coding and potentially regulatory regions were captured. After mapping the sequencing reads to the human GRCh37 reference genome and initial data quality control (QC), variant discovery, and joint genotyping of the whole study cohort of patients and healthy controls was performed under the GATK Best Practices framework (GATK version 3.3.0), followed by variant and individual QC, including relatedness, population stratification, and ancestry assessment.

University, Linköping, Sweden; [4]Iva Gunnarsson, MD, PhD, Elisabet Svenungsson, MD, PhD, Marika Kvarnström, MD, PhD, Leonid Padyukov, MD, PhD, Ingrid E. Lundberg, MD, PhD: Karolinska Institutet and Karolinska University Hospital, Stockholm, Sweden; [5]Solbritt Rantapää-Dahlqvist, MD, PhD: Umeå University, Umeå, Sweden; [6]Anders A. Bengtsson, MD, PhD, Andreas Jönsen, MD, PhD: Lund University and Skåne University Hospital, Lund, Sweden; [7]Helena Forsblad-d'Elia, MD, PhD: University of Gothenburg, Gothenburg, Sweden; [8]Sara Magnusson Bucher, MD: Örebro University, Örebro, Sweden; [9]Katrine B. Norheim, MD, PhD: Stavanger University Hospital, Stavanger, Norway; [10]Roland Jonsson, DMD, PhD; University of Bergen, Bergen, Norway; [11]Daniel Hammenfors, MD; Haukeland University Hospital, Bergen, Norway; [12]Thomas Mandl, MD, PhD; Lund University, Sweden; [13]Roald Omdal, MD, PHD; Stavanger University Hospital, Stavanger, Norway, and University of Bergen, Bergen, Norway; [14]Helena Andersson, MD, PhD, Øyvind Molberg, MD, PhD: Oslo University Hospital, Oslo, Norway; [15]Louise Pyndt Diederichsen, MD, PhD: Odense University Hospital, Odense, Denmark, and Copenhagen University Hospital, Rigshospitalet, Copenhagen, Denmark; [16]Marie Wahren-Herlenius, MD, PhD: Karolinska Institutet, Karolinska University Hospital, Stockholm, Sweden, and Broegelmann Research Laboratory, University of Bergen, Bergen, Norway; [17]Kerstin Lindblad-Toh, PhD: Uppsala University, Uppsala, Sweden, and Broad Institute of Massachusetts Institute of Technology and Harvard, Cambridge, Massachusetts.

Additional Supplementary information cited in this article can be found online in the Supporting Information section (http://onlinelibrary.wiley.com/doi/10.1002/art.42988).

Author disclosures are available at https://onlinelibrary.wiley.com/doi/10.1002/art.42988.

Address correspondence via email to Matteo Bianchi, PhD, at matteo.bianchi@imbim.uu.se; or to Kerstin Lindblad-Toh, PhD, at kersli@broadinstitute.org.

Submitted for publication January 13, 2024; accepted in revised form September 3, 2024.

**Single-marker and gene-based aggregate association analyses.** Logistic regression was implemented in PLINK version 1.90 to perform single-marker case–control analysis of common single-nucleotide variants (SNVs; minor allele frequency [MAF] ≥ 0.01) comparing all patients with SIADs with all control individuals. Gene-based aggregate association testing of all SNVs, including rare variants, was performed using a method that was inspired by the simplest type of genetic burden test, which sums up all detected mutations in each individual.[17] In our study, we assigned a genetic score (GS) to each individual and gene. For every SNV, the corresponding Combined Annotation Dependent Depletion (CADD) score[18] was multiplied by the number of variant (ie, alternate) alleles in each individual. The sum of all products of all SNVs for each gene and for each individual was then defined as the GS. The differential distribution of GSs between patients with SIADs and the control group, as well as their statistical significance, was tested using logistic regression in R. GS-based aggregate testing was also extended to the serological and clinical patient subgroups via case–control analysis and case–case analysis. In order to provide additional support to our GS-based approach, the results for the analysis contrasting all patients with SIADs and controls were also evaluated in comparison to those generated by the optimized sequence kernel association test (SKAT-O). In addition to including sex as a covariate based on its well-established status of risk factor for SIADs, all association analyses and models included the four most significant population principal components (PCs) as covariates. Four PCs significantly capture the intrinsic variation present in our cohort, which subsequently results in a system with homogenous structure and without any apparent stratification, cluster, or batch effect (Supplementary Figure 1). Statistical significance was evaluated after Bonferroni and Benjamini and Hochberg (false discovery rate [FDR]) correction ($\alpha = 0.05$).

**In silico variant functional annotation and reporter assays for dual-specificity phosphatase 1 genetic variants.** Using publicly available databases, catalogs, and computational tools, we prioritized genes of interest and in silico functionally annotated SNVs. For dual-specificity phosphatase 1 (*DUSP1*), reporter constructs were generated for SNVs or haplotypes as described by Roy et al[19] (Supplementary Data 1), transfected in HeLa cells and analyzed by quantitative real-time polymerase chain reaction (qRT-PCR) or the dual-luciferase reporter assay. Experiments were repeated three times with five replicates for each construct, and statistical analyses were performed with unpaired Student's *t*-test and one-way analysis of variance. The endogenous *DUSP1* gene expression was analyzed by qRT-PCR after stimulation of HeLa cells with prednisolone.

All participants provided informed consent to participate in the study, and the study was approved by the regional ethics board in Uppsala (Dnr 2015/450 and 2016/155). Sequencing and genotype data at the individual level are not publicly available due to them containing information that could compromise research participant privacy and consent. However, they are available from the corresponding author upon reasonable request and on a collaborative basis, protecting the participants' personal information. The bioinformatics scripts used to perform all the analyses described in this study are available at https://github.com/teone182/Dissect_CrossDisease.

## RESULTS

The primary dataset with a total of 2,292 Scandinavian patients with SIADs with SLE (n = 935), pSS (n = 906), and myositis (n = 451), as well as 1,252 control individuals, was characterized by call rates >98% and included 400,491 SNVs. Of these, 294,001 were rare variants (MAF < 0.01).

**Cross-disease single-variant and gene-based aggregate association analysis.** To test whether we could detect novel SIAD risk loci, we performed both single-variant association analysis and gene-based aggregate association testing. Comparing all patients with SIADs and the control individuals using 106,490 common markers, single-variant analysis confirmed the major histocompatibility complex (MHC), *IRF5*, and *NCF2* loci as key players in systemic inflammatory autoimmunity. The strongest association was observed for an upstream variant of *HLA-DRB1* (rs7775984-G, adjusted $P = 2.92 \times 10^{-48}$; odds ratio [OR] 3.5, 95% confidence interval [CI] 3.0–4.1; Supplementary Figures 2 and 3; Supplementary Tables 1 and 2).

We further extended the comparison of the patient and control groups by implementing gene-based aggregate testing (results summarized in Supplementary Table 3). When comparing all patients (n = 2,292) and the control individuals (n = 1,252), the GS-based aggregate analysis identified Bonferroni-significant associations mainly in the MHC region (20 genes, top hits *C2*, *HLA-C*, *MSH5*, *TNXB*, Bonferroni $P < 3.59 \times 10^{-13}$). The other non-MHC significant aggregate associations hit *IRF5* (Bonferroni $P = 4.94 \times 10^{-6}$) and *YDJC* (Bonferroni $P = 0.029$), both known as SIAD-associated genes, as well as the novel *MAP3K6*, *SLC5A6*, and *CGREF1* (Bonferroni $P = 0.0051$, 0.011, and 0.037, respectively). At the FDR statistical threshold, several non-MHC genes showed aggregate associations, including those previously implicated in SIAD *PHRF1* (FDR $P = 0.0048$), *ETS1* (FDR $P = 0.0052$), and *UBE2L3* (FDR $P = 0.031$), as well as the novel *MX1* (FDR $P = 0.049$).

Our GS-based analysis detected both previously known and novel potential loci, thus confirming the validity of the test and its noteworthy performance. The comparison of the results obtained for all the genes analyzed with the GS-based method and SKAT-O indicated a marked correlation (Spearman rho 0.53, $P < 2.2 \times 10^{-16}$; Supplementary Figure 4). Out of the 1,795 genes tested, 2.6% (n = 46) and 3.4% (n = 61) were FDR significant in the GS and SKAT-O analysis (Supplementary Tables 3 and 4), respectively, with 35 showing overlap. Among these 35 overlapping genes, 12 were non-MHC genes. When only the set of 46 FDR-significant genes in the GS-

**Table 1.** Basic characteristics of the study participants*

| | SLE | pSS | Myositis | Control | Total |
|---|---|---|---|---|---|
| Individuals | 935 | 906 | 451 | 1,252 | 3,544 |
| Females, n (%) | 806 (86) | 845 (93) | 300 (67) | 1,080 (86) | – |
| Mean age at diagnosis (min to max), y | 39 (3–85) | 47 (14–90) | 51 (7–88) | NA | – |
| Mean age (min to max), y | NA | NA | NA | 54 (19–88) | – |
| Origin, n (%) | | | | | |
| Sweden | 935 (100) | 687 (76) | 256 (57) | 1,043 (83) | 2,921 |
| Denmark | 0 (0) | 0 (0) | 68 (15) | 0 (0) | 68 |
| Norway | 0 (0) | 219 (24) | 127 (28) | 209 (17) | 555 |
| Serological subgroup, n (%) | | | | | |
| ANA[a] | 920 (98) | 681 (75) | 178 (39) | ND | 1,779 |
| dsDNA[b] | 438 (47) | 29 (3) | ND | ND | 467 |
| SSA | 343 (37) | 644 (71) | 120 (27) | ND | 1,107 |
| Ro52 | 244 (26) | 155 (17) | 101 (22) | ND | 500 |
| Ro60 | 313 (33) | 273 (30) | 27 (6) | ND | 613 |
| SSB | 200 (21) | 388 (43) | 11 (2) | ND | 599 |
| RNP | 177 (19) | 43 (5) | 21 (5) | ND | 241 |
| RF | 125 (13) | 297 (33) | 10 (2) | ND | 432 |
| SM[c] | 92 (10) | 9 (1) | 1 (0) | ND | 102 |
| Clinical subgroup, n (%) | | | | | |
| Arthritis[d] | 732 (78) | 168 (19) | 153 (34) | NA | 1,053 |
| Cancer[e] | 77 (8) | 41 (5) | 91 (20) | NA | 209 |
| Cardiac involvement[f] | 176 (19) | 0 (0) | 57 (13) | NA | 233 |
| Hematologic disorder[g] | 600 (64) | 341 (38) | 0 (0) | NA | 941 |
| Lung involvement[h] | 23 (2) | 41 (5) | 183 (41) | NA | 247 |
| Raynaud phenomenon | 153 (16) | 253 (28) | 124 (27) | NA | 530 |
| Renal disorder[i] | 331 (35) | 19 (2) | 0 (0) | NA | 350 |
| Skin involvement[j] | 794 (85) | 94 (10) | 208 (46) | NA | 1,096 |

* Percentages were calculated on the total number of patients with each of the three diseases considered (ie, SLE, pSS, and myositis) and the control group. ACR, American College of Rheumatology; ANA, antinuclear antibodies; dsDNA, double-stranded DNA; max, maximum; min, minimum; NA, not applicable; ND, not determined; pSS, primary Sjögren disease; RF, rheumatoid factor; SIAD, systemic inflammatory autoimmune disease; SLE, systemic lupus erythematosus; SM, Smith.
[a] ANA positivity refers to the ACR-11[52,53] classification criterion for patients with SLE.
[b] dsDNA positivity refers to the ACR-10B[52,53] classification criterion for patients with SLE.
[c] SM positivity refers to the ACR-10C[52,53] classification criterion for patients with SLE.
[d] Arthritis positivity refers to the ACR-5[52,53] classification criterion for patients with SLE.
[e] Cancer included any malignancy or lymphoma in patients with SLE, lymphoma in patients with pSS, and any malignancy in patients with myositis. A total of 41% of these patients developed the malignancy after SIAD diagnosis, 21% before SIAD diagnosis, and 38% were lacking data.
[f] Cardiac involvement included pericarditis (ACR-6B)[52,53] or myocardial infarction in patients with SLE, any heart dysfunction due to myositis in patients with myositis.
[g] Hematologic disorder included hematologic disorder (ACR-9)[52,53] in patients with SLE and anemia, leucopenia, lymphopenia, or thrombocytopenia in patients with pSS.
[h] Lung involvement included interstitial lung disease in patients with SLE, pSS, and myositis.
[i] Renal disorder included lupus nephritis (ACR-7)[52,53] in patients with SLE and interstitial nephritis in patients with pSS.
[j] Skin involvement included malar rash (ACR-1)[52,53], discoid rash (ACR-2)[52,53], photosensitivity (ACR-3)[52,53], oral ulcer (ACR-4)[52,53], or alopecia in patients with SLE; dermal vasculitis in patients with pSS; and heliotrope rash, Gottron papules or sign, erythroderma, periungual erythema, mechanics hands, calcinosis, ulceration, or vasculitis in patients with myositis.

based analysis was considered, the GS- and SKAT-O–derived *P* values had a substantially stronger correlation (Spearman rho 0.69, $P < 4.34 \times 10^{-9}$; Supplementary Figure 5). Overall, this suggests that the two methods appear to be equivalent in terms of association outcomes. However, we note that in the context of our study, the GS-based approach might compare favorably with SKAT-O in interpretation and translational potential, providing additional information on the size and direction of effect for each tested gene in relation to any phenotype or set of individuals considered.

**Aggregate testing of the cross-SIADs major serological patient subgroups.** Because a hallmark of SLE, pSS, and myositis is represented by shared circulating autoantibodies directed against nuclear antigens and immunoglobulins, we extended the GS-based test to those subsets of patients presenting with a specific autoantibody regardless of their primary SIAD (Table 1; Figure 1). GS-based case–control aggregate analysis of the major serological subgroups with SIADs mainly revealed strong Bonferroni-significant associations with MHC genes (Figure 2; Supplementary Tables 5 and 6). To more accurately dissect the genetic background underlying the occurrence of shared autoantibodies, we sought to control for the contribution of generalized SIAD genetic components, among which the MHC locus represents the strongest factor. For each defined

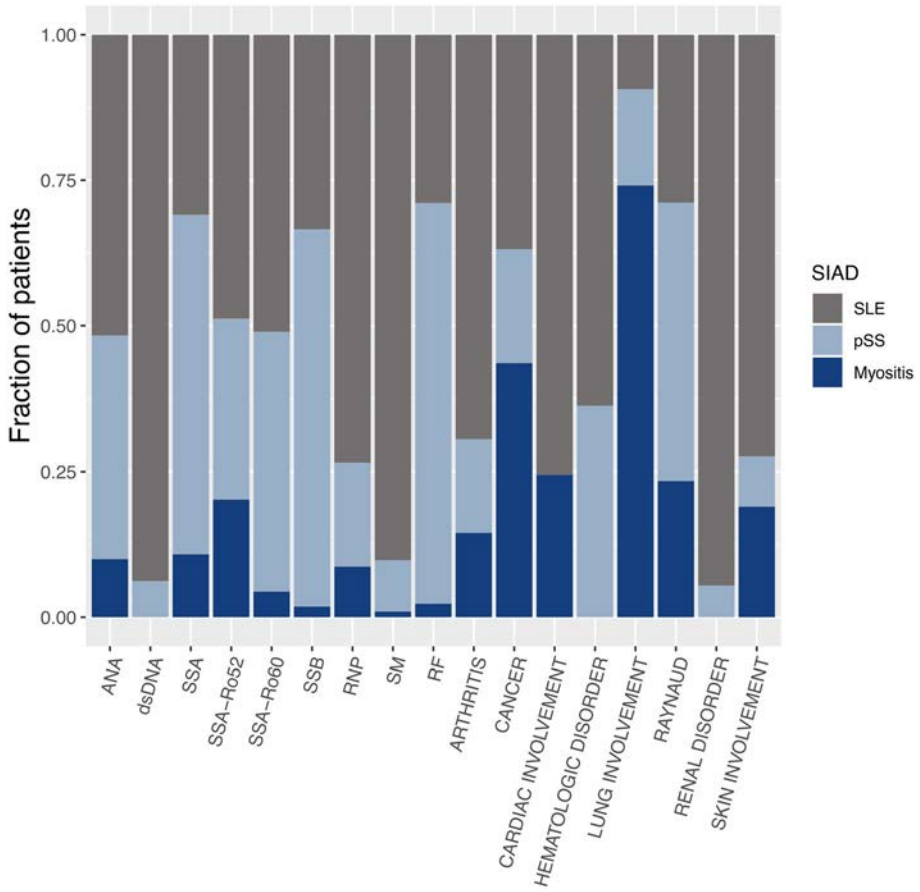


**Figure 1.** Bar plot showing the stratification of the different serological and clinical patient subgroups defined by the occurrence of autoantibodies and clinical features shared among patients with SIADs. Every subgroup is further categorized based on the prevalence of patients with SLE, pSS, or myositis. For additional numerical information, see Table 1 and Supplementary Table 1. ANA, antinuclear antibodies; dsDNA, double-stranded DNA; pSS, primary Sjögren disease; RF, rheumatoid factor; SIAD, systemic inflammatory autoimmune disease; SLE, systemic lupus erythematosus; SM, Smith.

serological subgroup, we therefore performed GS-based case–case aggregate association analysis by contrasting patients who were autoantibody positive against those who were autoantibody negative (Figure 2; Supplementary Tables 5 and 6). Although the RF, SSA, SSA-Ro52, SSA-Ro60, and SSB subgroups showed Bonferroni-corrected significant associations with the MHC region and no associations outside this locus, the subgroup of patients who were double-stranded DNA (dsDNA) positive displayed the opposite pattern, with a few associations emerging only in non-MHC genes (eight genes, top hit *RXRA*, Bonferroni $P = 7.39 \times 10^{-5}$). Interestingly, the association signals for the subgroup of patients who were ANA positive were weak and approximately in the same range of magnitude as in both MHC and non-MHC genes (median Bonferroni $P = 0.011$ and 0.0063, respectively), with *ISG15* (Bonferroni $P = 0.0063$) being the only gene detected outside MHC (Figure 2). Finally, no association with either MHC or non-MHC genes was detected in the subgroup of patients who were RNP and SM positive, presumably due to their small sample size (Figure 2).

**Characterization of clinical features shared among patients with SIADs.** To better understand the etiology of those clinical manifestations and comorbidities shared among SIADs, we performed the same GS-based case–control and case–case aggregate association analyses but this time focused on those subsets of patients presenting with aggregate clinical conditions regardless of their primary SIAD diagnosis (Figure 1; Table 1; Supplementary Tables 7 and 8). Besides a few weak associations with non-MHC genes, GS-based case–control analysis revealed pervasive associations with the MHC region (Figure 3), reflecting the typical immunogenetic background of such disorders. In contrast, case–case analysis completely abolished MHC associations and detected genetic signals exclusively located in non-MHC loci. Apart from a few potentially pleiotropic genes associated with more than one aggregate clinical and/or serological feature across the case–control and/or case–case analyses (ie, *CEP131*, *COL61A*, *CXCL5*, *GNA13*, *IL17REL*, *ISG15*, *JUN*, *LSP1*, *PRM3*, *RXRA*, *TH*, and *TOGARAM2*), the case–case analysis also

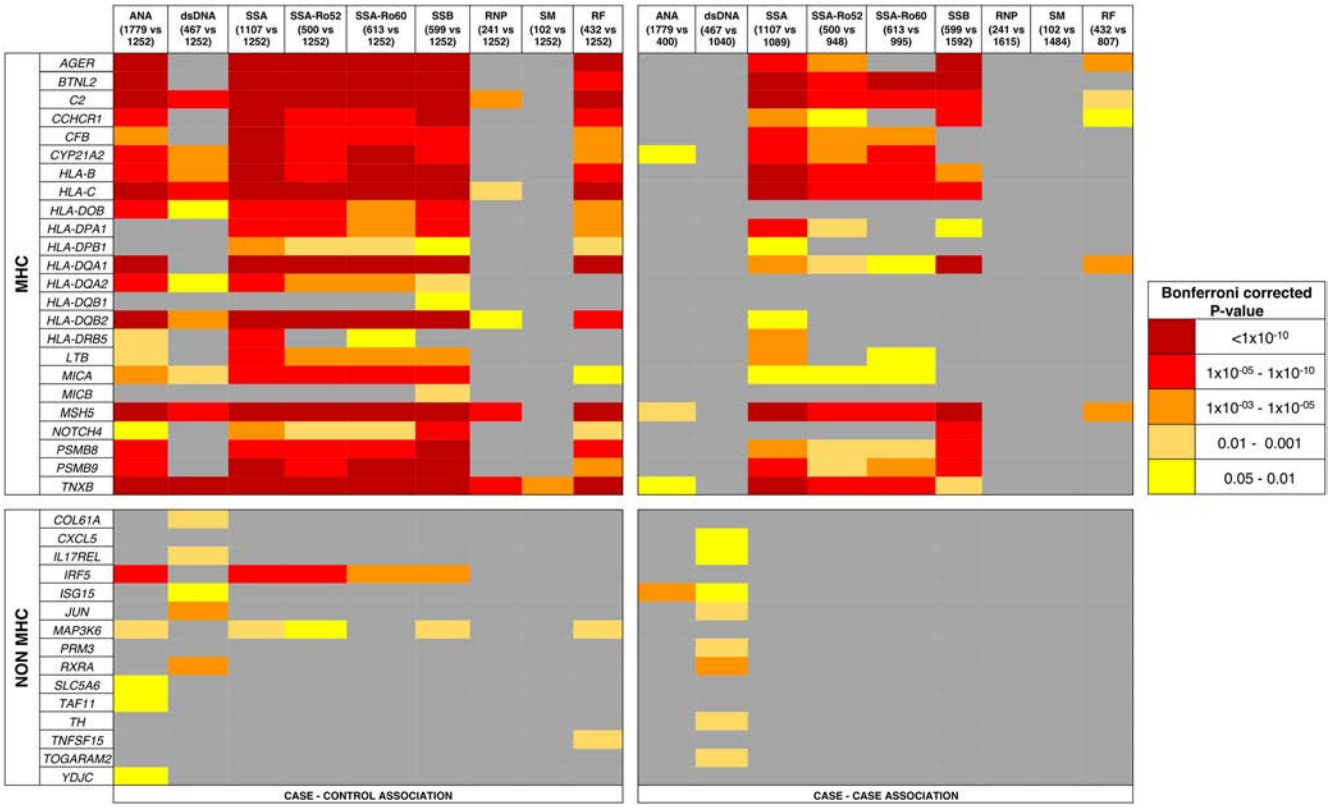


**Figure 2.** Heatmap showing the results of the genetic score–based aggregate case–control and case–case association testing for the subgroups of patients with SIAD defined based on the presence of shared autoantibodies. For each autoantibody indicated at the top, the results of the case–control analysis derive from the contrast between the patients with SIADs who were autoantibody positive and the control individuals, whereas the results of the case–case analysis derive from the contrast between the patients with SIADs who were autoantibody positive and those who were autoantibody negative (patients with missing data were not considered in the analysis). The number of samples of each group contrasted is shown under the autoantibody at the top. The results are further categorized into those pertaining genes located in the MHC locus and those located outside this region. The Bonferroni-corrected *P* values were obtained after correcting the association raw *P* values from the logistic regression model for the 1,795 genes tested. ANA, antinuclear antibody; dsDNA, double-stranded DNA; MHC, major histocompatibility complex; RF, rheumatoid factor; SIAD, systemic inflammatory autoimmune disease; SM, Smith.

highlighted genetic signals that were exclusively associated to unique subsets of patients with a particular clinical aggregate subphenotype (ie, signals not detected in additional aggregate clinical and/or serological subgroups in any of the case–control and case–case comparisons). This potentially indicates genetic contributions restricted to the clinically defined patient subgroups, as well as presumably independent on the genetic background of patients with SIADs (Figure 3). Protein kinase C zeta (*PRKCZ*; Bonferroni $P = 0.015$) and transcription factor 7 (*TCF7*) (Bonferroni $P = 0.0020$) were detected as uniquely associated with arthritis and cancer, respectively. After examining patients with SIADs with skin involvement in contrast to those without such manifestation, exclusive associations were detected in three genes (top hit *DUSP1*, Bonferroni $P = 0.00022$; *CDKN2A*, Bonferroni $P = 0.0076$; *BRDT*, Bonferroni $P = 0.035$). The analysis considering patients with cardiac or lung involvement, Raynaud phenomenon, and renal disorder did not show any aggregate significant associations.

**The gene *DUSP1* as a candidate for protection against skin lesions.** Although the detected case–case aggregate associations reflected functionally weighted burdens of all variants in the considered gene spaces, we investigated whether we could further pinpoint genes and variants of particular interest in the context of the etiology of each clinical subphenotype. To overcome the inherent difficulties linked to the prospective interpretation of pleiotropy and to pragmatically prioritize candidate genes and variants, we focused on *DUSP1*, which was the strongest genetic signal exclusively associated to a unique clinical subphenotype (ie, skin involvement) in the case–case analyses, despite *PRKCZ* and *TCF7* being also uniquely associated with arthritis and cancer, respectively. *DUSP1* emerged as the most remarkable candidate for further in-depth analysis given that (i) it has recently been implicated in another skin-related disease—eczema,[20] (ii) the genetic variation pattern and the protective genetic effect against the SIAD-associated clinical skin phenotype observed in our study (OR 0.53, 95% CI 0.42–0.68; Supplementary Table 8) are consistent with the results by Grosche et al,[20]

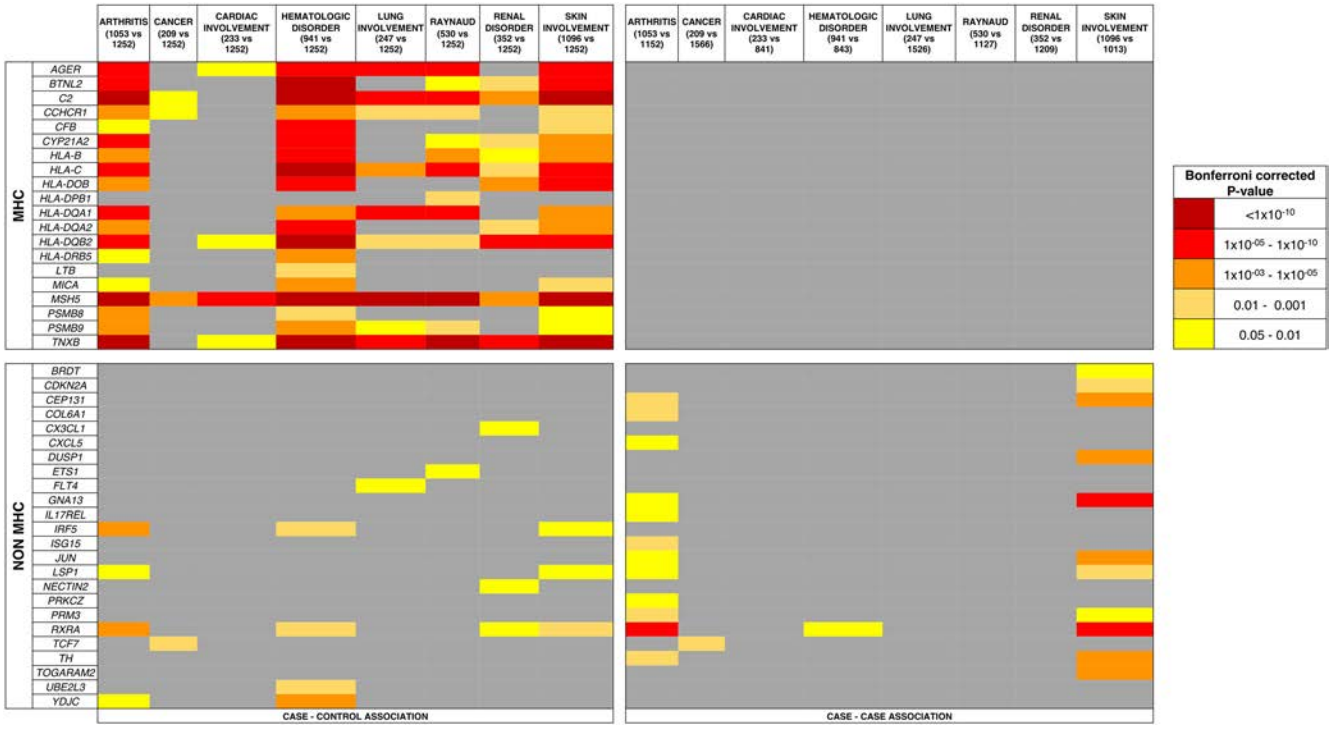


**Figure 3.** Heatmap showing the results of the genetic score–based aggregate case–control and case–case association testing for the subgroups of patients with SIAD defined based on the presence of shared clinical manifestations and comorbidities. For each clinical feature indicated at the top, the results of the case–control analysis derive from the contrast between the patients with SIADs who were positive for the feature and the control individuals, whereas the results of the case–case analysis derive from the contrast between the patients with SIADs who were positive and negative for the feature (patients with missing data are not considered in the analysis). The number of samples of each group contrasted is shown under the feature at the top. The results are further categorized into those pertaining genes located in the MHC locus and those located outside this region. The Bonferroni-corrected *P* values were obtained after correcting the association raw *P* values from the logistic regression model for the 1,795 genes tested. MHC, major histocompatibility complex; SIAD, systemic inflammatory autoimmune disease.

and (iii) the *DUSP1* SNVs detected in our study (n = 32) overlap with predicted or experimentally validated regulatory elements as well as with evolutionary constrained positions, thus indicating a likely functional role (Figures 4A–C and 5; Supplementary Tables 9 and 10). Of these 32 variants, 12 showed a protective genetic effect, 12 a risk effect, and 8 showed neutrality (Figure 4B). Furthermore, haplotype analysis identified a presumably protective haplotype block spanning the entire *DUSP1* gene (Supplementary Figure 6).

**Confirmation of the regulatory function of *DUSP1* variants.** To experimentally evaluate the regulatory potential of the 32 *DUSP1* variants detected in this study, we generated 49 reporter constructs carrying haplotypes identified in the patients and constituting 18 test regions in total (Figure 4D and E) and assessed them in HeLa cells normally expressing *DUSP1* (Supplementary Figure 7). We examined the expression levels of the reporters in unstimulated cells and cells stimulated with prednisolone, known to up-regulate *DUSP1*.[21] For all variants, except for those immediately downstream of the *DUSP1* 3'UTR (3'UTR-SNVs, region 5; Supplementary Figure 8; Supplementary Table 11), we observed a substantial up-regulation of the reporters' transcription compared to the control, indicating strong enhancer potential of all regions in HeLa cells (Supplementary Figure 9; Supplementary Table 11), thereby confirming their regulatory potential suggested by the in silico functional annotations. Notably, treatment with prednisolone resulted in either negative or neutral effect on the transcription levels of the majority of the reporter regions compared to the unstimulated conditions (Supplementary Figures 10 and 11; Supplementary Table 11).

A total of 11 of the 18 tested enhancer regions (61%) showed statistically significant differences in expression levels between allelic or haplotypic constructs in unstimulated cells. The effect alleles of regions 2 and 9 increased transcription of the reporter, whereas those of regions 4, 6, 10, 11, and 14 led to down-regulation. Three regions (ie, 15, 16, and 17) with haplotypes harboring two or more variants showed a complex outcome in which some effect alleles were associated with expression up-regulation and some others with down-regulation. Despite not reaching statistical significance, the effect alleles of regions 1, 3, 8, 12, and 13 led to stable expression up-regulation. Finally, regions 7 and 18 overlap with SINE and Alu repeat elements, respectively, and consistently did not show allelic differences in expression levels.

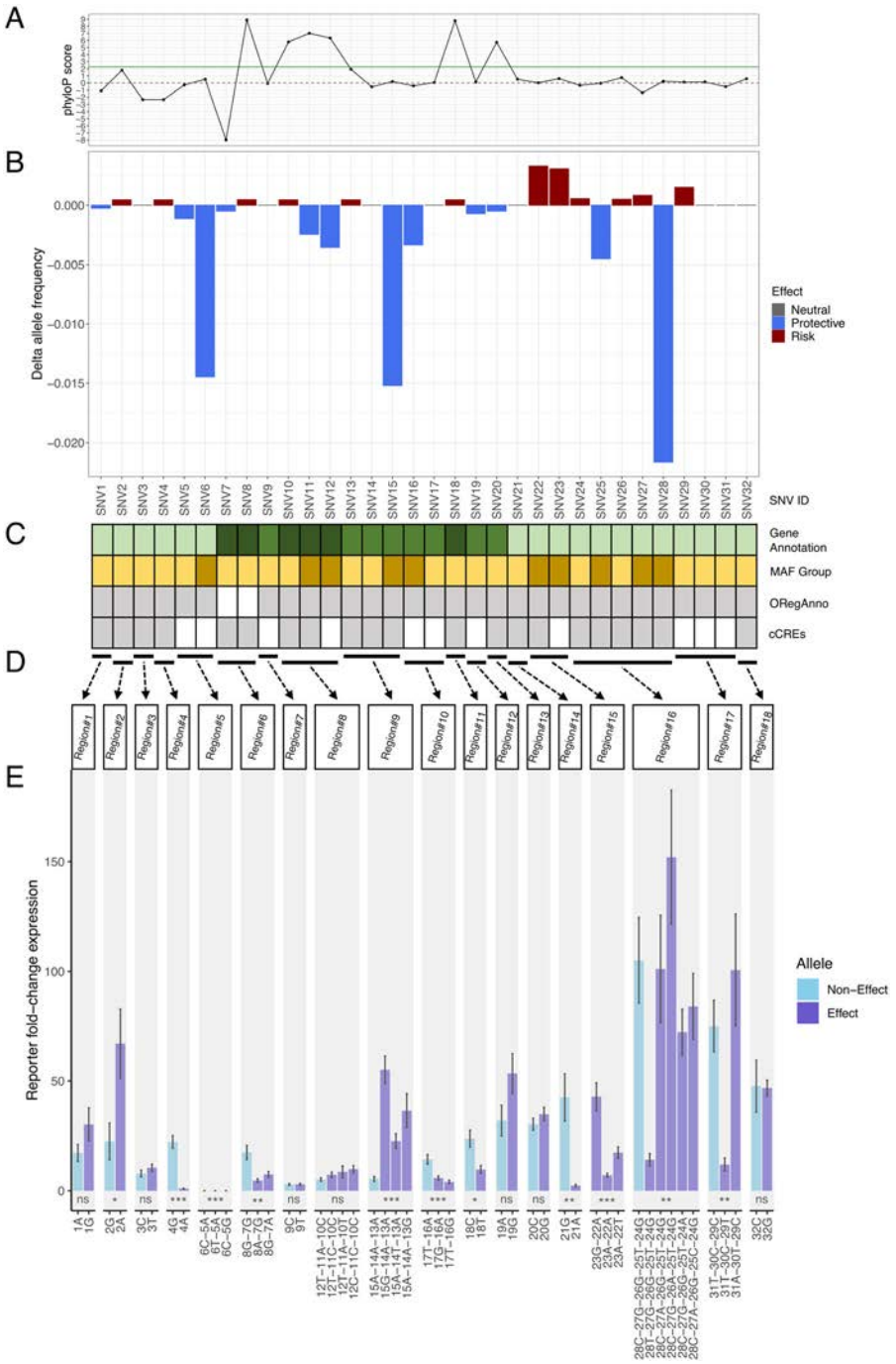


**Figure 4.** Genetic effects, in silico annotations, and reporter assay results for each *DUSP1* variant detected in our study. (A) Zoonomia Project evolutionary constraint metric.[26] (B) Delta allele frequency obtained as the minor (ie, effect) allele frequency difference between the patients with systemic inflammatory autoimmune diseases with and without skin involvement. (C) "Gene annotation": regional annotation (pale green, upstream/downstream; green, intronic; dark green, exonic); "MAF group": brown, common; yellow, rare; and "ORegAnno" and "cCREs": gray, overlap with ORegAnno/ENCODE cCREs; white, no overlap. (D) The *DUSP1* variants included in each of 18 enhancer regions tested with reporter assay are depicted with horizontal black lines and connected with dashed arrows to the corresponding region. (E) Expression levels of all 49 reporter allelic constructs constituting the 18 total tested enhancer regions. Reporter constructs are shown on the x-axis and identified as SNV ID (only numerical) and allele for single-variant construct or multiple SNV IDs (only numerical) and alleles for haplotype constructs. Alleles and construct orientation refer to the negative strand and are relative to the transcription start site, respectively. Noneffect and effect alleles refer to the major and minor alleles, respectively. For details, see Supplementary Materials and Methods. Unpaired Student's *t*-test and one-way analysis of variance were used for single-variant and haplotype constructs, respectively. $^{*}P < 0.05$, $^{**}P < 0.01$, $^{***}P < 0.001$. cCRE, candidate cis-regulatory element; *DUSP1*, dual-specificity phosphatase 1; ENCODE, Encyclopedia of DNA Elements; ID, identifier; MAF, minor allele frequency; ns, nonsignificant; ORegAnno, Open Regulatory Annotation database; SNV, single-nucleotide variant.

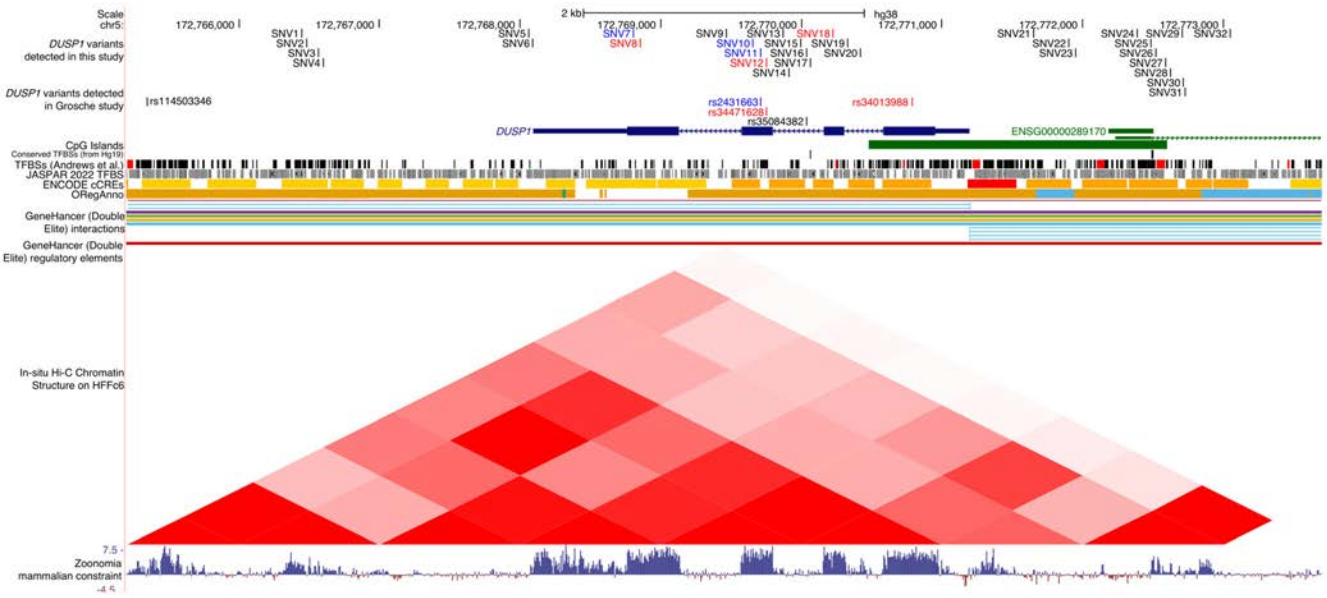


**Figure 5.** UCSC Genome Browser view (Hg38) of the *DUSP1* locus. *DUSP1* variants were detected and tested in this study ("*DUSP1* variants detected in this study"). Nonsynonymous and synonymous variants are indicated in red and blue, respectively. The same color labels apply for the *DUSP1* variants detected in the study by Grosche et al[20] ("*DUSP1* variants detected in Grosche study"). "Conserved TFBS (from Hg19)" are conserved TFBSs lifted over to GRCh38. "TFBSs (Andrews et al)" are TFBSs sourced from the Zoonomia project[21]. CTCF TFBSs are colored in red. "JASPAR 2022 TFBSs" are experimentally defined TFBSs for eukaryotes. "ENCODE cCREs" are ENCODE Registry of cCREs in the human genome. "ORegAnno" is the open regulatory region associated with active gene expression. "GeneHancer (double elite) interactions" are highly filtered interactions between regulatory elements and genes. The light blue interactions are associations between *DUSP1* and cis-regulatory elements. "GeneHancer (double elite) regulatory elements" are highly filtered regulatory elements. "In situ Hi-C chromatin structure on HFFc6" is a zoomed-in heatmap of chromatin folding data from in situ HFFc6 cell lines. "Zoonomia mammalian constraint" consists of mammalian evolutionary constraint phyloP scores (Christmas et al[21]). cCRE, candidate cis-regulatory element; e; ENCODE, Encyclopedia of DNA Elements; ORegAnno, Open Regulatory Annotation database; SNV, single-nucleotide variant; TFBS, transcription factor binding site.

**Bridging *DUSP1* genetic variation and reporters' transcriptional activity.** Having available genetic and transcriptional activity data on *DUSP1* variants and the corresponding reporter regions, respectively, we further sought to explore their potential functional links. Considering the known anti-inflammatory effect of *DUSP1* overexpression,[22–26] we reasoned that genetic variants with a protective effect on skin involvement would theoretically enhance *DUSP1* expression in the tested enhancer regions, whereas those categorized as risk variants would consequently down-regulate *DUSP1* gene expression. When comparing the genetic variant effect (in the case of a haplotypic construct, the variant with the greatest genetic effect was used as index) and the corresponding reporter allelic effect (ie, direction of *DUSP1* expression), we observed positive correlation in 11 regions (61%), including two protective exonic variants—SNV11 (rs2431663) and SNV12 (rs34471628)—identified previously[20] (Figure 4E; Supplementary Tables 11 and 12). Differently from the highly protective genetic effect of SNV15 correlating well with the statistically significant increase of reporter expression of the corresponding region 9, SNV28 in region 16 showed the greatest protective genetic effect but was individually associated to a decreased expression of the reporter. Region 16 showed the most complex effect on transcription, with variable levels of expression depending on the tested haplotype. Interestingly, in foreskin fibroblast cells, this region appeared to be located in a separate topologically associated domain (TAD) comprising regions 14 to 18 (ie, from SNV21 to SNV32) and distinct from the one overlapping the locus extending from region 1 to region 13 (ie, from SNV1 to SNV20; Figure 5). The former also overlaps with several flanking CCCTC-binding factor (CTCF) binding sites as well as different GeneHancer interaction domains (Figure 5). Although SNV8 (region 6) was not an index variant in our analysis, this SNV and SNV18 (region 11) are evolutionarily constrained[21] nonsynonymous risk variants and were also consistently associated to a marked down-regulation of the corresponding reporter's expression.

## DISCUSSION

Here, we exploited the power of next-generation sequencing coupled with a large and detailed collection of the clinical and serological data from patients with SIADs to investigate how genetic variation from the full allele frequency spectrum contributes to disease susceptibility and shared subphenotypes.

Although to a different extent and significance level, the single-variant and gene-based case–control association design contrasting all patients with SIADs and healthy individuals largely replicated known associations with shared loci controlling antigen processing and presentation (MHC), type I IFN– and proinflammatory cytokine gene–related signaling (*IRF5*, *UBE2L3/YDJC*, *PHRF1*, *SH2B3*), lymphocytes functional differentiation (*ETS1*), and reactive oxygen species metabolism (*NCF2*), all in the context of perturbed innate and adaptive immune response background typical of SIADs. Among the potentially novel loci identified via gene-based analysis, *MAP3K6*, *CGREF1*, and *MX1* are related to the type I IFN pathway activation,[27–29] supporting a role in the pathophysiology of this pathway in all three SIADs. Although the type I IFN–mediated immune response has been widely observed and convincingly demonstrated at the transcriptomic level,[30–32] these results further support a multilevel genetic dysregulation of this pathway in the three SIADs in our study.

Consistent with previous research indicating strong associations between *HLA* alleles and the occurrence of nuclear autoantibodies in patients with SLE, pSS, and myositis,[33–36] our study indicated the MHC as the major susceptibility locus associated with autoantibody positivity. Differently from the subgroup of patients who were SSA/SSB positive in whom MHC appeared as the key and strongest genetic locus associated with both generalized autoimmune predisposition (ie, from case–control analysis) and specific autoantibody positivity (ie, from case–case analysis), the subgroups of patients who were ANA positive and dsDNA positive showed distinct association profiles in which MHC associations were weakened and abolished in the corresponding case–case analysis, respectively. The molecular heterogeneity of ANA together with the small sample size of the subset of patients who were ANA negative might explain the weak and diluted MHC associations in the case–case analysis of this serological subgroup. Outside the MHC locus, the case–case analysis identified an association with *ISG15*, a key IFN-stimulated gene, with the IFN signature previously linked to ANA positivity in individuals lacking an SIAD diagnosis.[37] In agreement with previous research in patients with SLE,[38] heterogeneity of MHC associations might also explain the lack of statistically significant signals within this locus when comparing the subgroups of patients who were dsDNA positive (dominated by patients with SLE) and those who were dsDNA negative. However, several statistically significant associations were detected outside the MHC region. From these observations, it is tempting to speculate that the production of dsDNA autoantibodies in patients with SIADs could at least in part be linked to environmental factors, such as previous bacterial infections, exerting their disease-triggering effects across a range of genetic susceptibility backgrounds. It has been demonstrated that antibodies targeting the highly immunogenic bacterial Z-DNA cross-react with self B-DNA, present in the serum.[39]

Demonstrating the likely independence of the signals from the shared SIAD autoimmune background, the absence of associations with the MHC locus from the comparison between patients with and without clinical subphenotypes suggested the possibility to pinpoint genetic factors and genes related to processes exclusively associated with each clinical subgroup of patients with SIADs. *PRKCZ*, exclusively associated with arthritis in the present study, has been implicated in patients with rheumatoid arthritis.[40,41] *TCF7*, here uniquely linked to cancer, encodes TCF1, a key molecular player in different types of malignancies.[42–45]

Finally, the strongest exclusive association was between *DUSP1* and skin involvement. Besides negatively regulating proinflammatory and T cell–mediated immune responses,[46,47] this gene has recently been described as having a protective effect against eczema in a meta-analysis of approximately 20,000 patients and 380,000 controls from 21 different populations.[20] Consistently, here, we detected a gene-based aggregate negative association between *DUSP1* and skin manifestations in patients with SIADs. Using reporter assays, we confirmed that *DUSP1* variants were indeed functional and exerted cis-regulatory effects on gene expression.

Moreover, we found that the majority of the variants comply with the hypothesis that protective and risk variants would be linked to *DUSP1* higher and lower expression, respectively. Strikingly, two variants identified also in the study by Grosche et al[20] (ie, SNV11 and SNV12) followed our hypothesis, together with two evolutionary constrained nonsynonymous risk variants, one of which (ie, SNV8; p.Val338Met) introduces a predicted detrimental change at the end of the highly conserved C-terminal protein tyrosine phosphatase domain of DUSP1.[48] A mismatch between a specific genetic effect and reporter expression observed for some of the variants might be partly due to the disruption of the optimal local architecture of the cis-regulatory sequence in short but variant-rich cloned DNA fragments. This is presumably the case of the variant with the greatest protective effect (ie, SNV28) and its corresponding reporter region that is characterized by an extremely complex expression pattern. In this region, cell-type specific alternative regulation and functional rewiring mechanisms could also underlie such discrepancies, as suggested by the presence of distinct TADs, CTCF-binding sites, and different functional interaction domains.

In our study, we did not detect any notable induction of the reporters' expression upon prednisolone treatment despite the two-fold up-regulation of *DUSP1* in HeLa cells. This might be due to the lack of high-affinity glucocorticoid-response elements (GREs) for direct binding of glucocorticoid receptors in the cloned fragments or, alternatively, the GRE cell–specific mode of action.[26] Besides cross-replicating each other, the independently identified associations of *DUSP1* with SIAD-associated skin phenotype and eczema suggest the implication of this gene in skin lesions, regardless of the primary disease etiology. This is also confirmed by other reports describing *DUSP1* down-regulation in lesional psoriatic skin compared to paired nonlesional psoriatic

skin[24] and in dermal mesenchymal stem cells from patients with psoriasis compared to healthy controls[23] as well as the correlation between *DUSP1* overexpression and protection against inflammatory skin fibrosis in a mouse model with scleroderma[25] and better overall survival in skin cutaneous melanoma.[49] Intriguingly, a recent machine learning analysis of gene expression from patients with cutaneous SLE, psoriasis, eczema, and systemic sclerosis revealed that skin biopsies from all these conditions displayed, compared to controls, shared features positively correlated with their characteristic inflammatory processes.[50] Consequently, the hypothesis of *DUSP1* high expression as having a generalized protective effect against nonspecific skin conditions seems plausible.

In the context of our study, the known association of *DUSP1* with C-reactive protein (CRP) levels is of note. The supplementary analysis of a subset of our cohort of patients with SIADs indicated genetically supported higher levels of CRP in patients without skin phenotype. Additionally, this showed consistency with the substantial contribution of type I IFN activation to skin clinical manifestations, which is also accompanied by a decrease in CRP levels (for details, see Supplementary Figure 12).[51]

Despite overall replicating the *DUSP1* findings of a previous independent megastudy[20] and therefore demonstrating the validity of our analysis, the present work is primarily limited by the lack of a direct replication cohort. However, our cohort represents, to the best of our knowledge, the largest and most unique resource combination of patients with SLE, pSS, and myositis and homogenously integration of coding and regulatory genetic variation from the full spectrum of allele frequency. Nonetheless, further research is warranted to validate these results in larger and more diverse cohorts and to explore the functional significance of the identified genetic variants in disease pathogenesis, as well as the shared and unique features of patients with SIADs. Moreover, we acknowledge that the *DUSP1* findings should be functionally validated with reporter assays in additional and more relevant in vitro models, such as skin-derived cell lines. At the same time, it is worth considering that such experiments might also be hampered by inherent technical difficulties (eg, cells refractory to transfection and/or exogenous reporter expression). In this study, discovery power might also be limited by the intrinsic design of our targeted array and GS-based method, which assays only a fraction of the genome and assumes the same variant direction of effect, respectively.

In summary, we detected known and potentially novel genetic loci associated with patients with SIADs that are congruent with previous genetic and transcriptomics analyses of such disorders. In parallel, we delineated unified and differential genetic signatures and profiles associated with subsets of patients with SIADs with shared serological and clinical features. This might partially explain the clinical heterogeneity found in patients who fulfilled the same disease classification criteria, thus being relevant for their molecular stratification. Moreover, in keeping with previous findings on other skin disorders, we highlighted a potentially functional role of *DUSP1* genetic variants in the context of SIAD-related cutaneous manifestations. Together, this suggests that common molecular mechanisms may underlie pathogenic conditions that are shared among different inflammatory disorders, which could possibly be translated to effectively improve treatment, also in more generalized disease frameworks.

## ACKNOWLEDGMENTS

We would like to thank all patients and control individuals taking part in this study for making this research possible. We thank Michael Dong for providing the Zoonomia phyloP and PhastCons evolutionary constraint scores. We also thank Gregory Andrews for providing the transcription factor binding sites dataset generated as part of the Zoonomia project. DNA sequencing and genotyping was performed at the SNP&SEQ Technology Platform in Uppsala. The facility is part of the National Genomics Infrastructure Sweden and Science for Life Laboratory. Computations were performed on resources provided by the Swedish National Infrastructure for Computing through Uppsala Multidisciplinary Center for Advanced Computational Science under projects SNIC SENS 2017142 and 2017107.

## AUTHOR CONTRIBUTIONS

All authors contributed to at least one of the following manuscript preparation roles: conceptualization AND/OR methodology, software, investigation, formal analysis, data curation, visualization, and validation AND drafting or reviewing/editing the final draft. As corresponding author, Dr Bianchi confirms that all authors have provided the final approval of the version to be published, and takes responsibility for the affirmations regarding article submission (eg, not under consideration by another journal), the integrity of the data presented, and the statements regarding compliance with institutional review board/Helsinki Declaration requirements.

## REFERENCES

1. Bengtsson AA, Ronnblom L. Systemic lupus erythematosus: still a challenge for physicians. J Intern Med 2017;281(1):52–64.
2. Dalakas MC. Inflammatory muscle diseases. N Engl J Med 2015; 372(18):1734–1747.
3. Mariette X, Criswell LA. Primary Sjogren's syndrome. N Engl J Med 2018;378(10):931–939.
4. Moutsopoulos HM. Autoimmune rheumatic diseases: one or many diseases? J Transl Autoimmun 2021;4:100129.
5. Acosta-Herrera M, Kerick M, Gonzalez-Serna D, et al; Myositis Genetics Consortium; Scleroderma Genetics Consortium. Genome-wide meta-analysis reveals shared new loci in systemic seropositive rheumatic diseases. Ann Rheum Dis 2019;78(3):311–319.
6. Langefeld CD, Ainsworth HC, Cunninghame Graham DS, et al. Transancestral mapping and genetic load in systemic lupus erythematosus. Nat Commun 2017;8:16021.
7. Lessard CJ, Li H, Adrianto I, et al. Variants at multiple loci implicated in both innate and adaptive immune responses are associated with Sjogren's syndrome. Nat Genet 2013;45(11):1284–1292.
8. Rothwell S, Cooper RG, Lundberg IE, et al. Dense genotyping of immune-related loci in idiopathic inflammatory myopathies confirms HLA alleles as the strongest genetic risk factor and suggests different genetic background for major clinical subgroups. Ann Rheum Dis 2016;75(8):1558–1566.

9. Kilpinen H, Barrett JC. How next-generation sequencing is transforming complex disease genetics. Trends Genet 2013;29(1):23–30.
10. Lee S, Abecasis GR, Boehnke M, et al. Rare-variant association analysis: study designs and statistical tests. Am J Hum Genet 2014;95(1): 5–23.
11. Abell NS, DeGorter MK, Gloudemans MJ, et al. Multiple causal variants underlie genetic associations in humans. Science 2022; 375(6586):1247–1254.
12. Zuk O, Schaffner SF, Samocha K, et al. Searching for missing heritability: designing rare variant association studies. Proc Natl Acad Sci U S A 2014;111(4):E455–E464.
13. Bianchi M, Kozyrev SV, Notarnicola A, et al. Contribution of rare genetic variation to disease susceptibility in a large Scandinavian myositis cohort. Arthritis Rheumatol 2022;74(2):342–352.
14. Sandling JK, Pucholt P, Hultin Rosenberg L, et al. Molecular pathways in patients with systemic lupus erythematosus revealed by gene-centred DNA sequencing. Ann Rheum Dis 2021;80(1):109–117.
15. Thorlacius GE, Hultin-Rosenberg L, Sandling JK, et al. Genetic and clinical basis for two distinct subtypes of primary Sjogren's syndrome. Rheumatology (Oxford) 2021;60(2):837–848.
16. Eriksson D, Bianchi M, Landegren N, et al. Extended exome sequencing identifies BACH2 as a novel major risk locus for Addison's disease. J Intern Med 2016;280(6):595–608.
17. Morgenthaler S, Thilly WG. A strategy to discover genes that carry multi-allelic or mono-allelic risk for common diseases: a cohort allelic sums test (CAST). Mutat Res 2007;615(1–2):28–56.
18. Rentzsch P, Witten D, Cooper GM, et al. CADD: predicting the deleteriousness of variants throughout the human genome. Nucleic Acids Res 2019;47(D1):D886–D894.
19. Roy A, Sakthikumar S, Kozyrev SV, et al. Using evolutionary constraint to define novel candidate driver genes in medulloblastoma. Proc Natl Acad Sci U S A 2023;120(33):e2300984120.
20. Grosche S, Marenholz I, Esparza-Gordillo J, et al. Rare variant analysis in eczema identifies exonic variants in DUSP1, NOTCH4 and SLC9A4. Nat Commun 2021;12(1):6618.
21. Christmas MJ, Kaplow IM, Genereux DP, et al. Evolutionary constraint and innovation across hundreds of placental mammals. Science 2023;380(6643):eabn3943.
22. Abraham SM, Lawrence T, Kleiman A, et al. Antiinflammatory effects of dexamethasone are partly dependent on induction of dual specificity phosphatase 1. J Exp Med 2006;203(8):1883–1889.
23. Chang WJ, Niu XP, Hou RX, et al. LITAF, HHEX, and DUSP1 expression in mesenchymal stem cells from patients with psoriasis. Genet Mol Res 2015;14(4):15793–15801.
24. Kjellerup RB, Johansen C, Kragballe K, et al. The expression of dual-specificity phosphatase 1 mRNA is downregulated in lesional psoriatic skin. Br J Dermatol 2013;168(2):339–345.
25. Scotece M, Hamalainen M, Leppanen T, et al. MKP-1 deficiency exacerbates skin fibrosis in a mouse model of scleroderma. Int J Mol Sci 2023;24(5):4668.
26. Vockley CM, D'Ippolito AM, McDowell IC, et al. Direct GR binding sites potentiate clusters of TF binding across the human genome. Cell 2016;166(5):1269–1281.e19.
27. Haller O, Kochs G. Human MxA protein: an interferon-induced dynamin-like GTPase with broad antiviral activity. J Interferon Cytokine Res 2011;31(1):79–87.
28. Hou P, Yang K, Jia P, et al. A novel selective autophagy receptor, CCDC50, delivers K63 polyubiquitination-activated RIG-I/MDA5 for degradation during viral infection. Cell Res 2021;31(1):62–79.
29. Kim N, Kukkonen S, Del Pilar Martinez-Viedma M, et al. Tat engagement of p38 MAP kinase and IRF7 pathways leads to activation of interferon-stimulated genes in antigen-presenting cells. Blood 2013; 121(20):4090–4100.
30. Bave U, Nordmark G, Lovgren T, et al. Activation of the type I interferon system in primary Sjogren's syndrome: a possible etiopathogenic mechanism. Arthritis Rheum 2005;52(4):1185–1195.
31. Crow MK, Kirou KA, Wohlgemuth J. Microarray analysis of interferon-regulated genes in SLE. Autoimmunity. 2003;36(8):481–490.
32. Pinal-Fernandez I, Casal-Dominguez M, Derfoul A, et al. Identification of distinctive interferon gene signatures in different types of myositis. Neurology 2019;93(12):e1193–e1204.
33. Gottenberg JE, Busson M, Loiseau P, et al. In primary Sjogren's syndrome, HLA class II is associated exclusively with autoantibody production and spreading of the autoimmune response. Arthritis Rheum 2003;48(8):2240–2245.
34. Leclair V, Galindo-Feria AS, Rothwell S, et al. Distinct HLA associations with autoantibody-defined subgroups in idiopathic inflammatory myopathies. EBioMedicine 2023;96:104804.
35. Morris DL, Fernando MM, Taylor KE, et al. MHC associations with clinical and autoantibody manifestations in European SLE. Genes Immun 2014;15(4):210–217.
36. O'Hanlon TP, Carrick DM, Targoff IN, et al. Immunogenetic risk and protective factors for the idiopathic inflammatory myopathies: distinct HLA-A, -B, -Cw, -DRB1, and -DQA1 allelic profiles distinguish European American patients with different myositis autoantibodies. Medicine (Baltimore) 2006;85(2):111–127.
37. Wither J, Johnson SR, Liu T, et al. Presence of an interferon signature in individuals who are anti-nuclear antibody positive lacking a systemic autoimmune rheumatic disease diagnosis. Arthritis Res Ther 2017; 19(1):41.
38. Chung SA, Taylor KE, Graham RR, et al. Differential genetic associations for systemic lupus erythematosus based on anti-dsDNA autoantibody production. PLoS Genet 2011;7(3):e1001323.
39. Spencer DM, Svenungsson E, Gunnarsson I, et al. The expression of antibodies to Z-DNA in the blood of patients with systemic lupus erythematosus: relationship to autoantibodies to B-DNA. Clin Immunol 2023;255:109763.
40. Nakano K, Whitaker JW, Boyle DL, et al. DNA methylome signature in rheumatoid arthritis. Ann Rheum Dis 2013;72(1):110–117.
41. Webster AP, Plant D, Ecker S, et al. Increased DNA methylation variability in rheumatoid arthritis-discordant monozygotic twins. Genome Med 2018;10(1):64.
42. Jeannet G, Boudousquie C, Gardiol N, et al. Essential role of the Wnt pathway effector Tcf-1 for the establishment of functional CD8 T cell memory. Proc Natl Acad Sci U S A 2010;107(21):9777–9782.
43. Osman A, Yan B, Li Y, et al. TCF-1 controls T(reg) cell functions that regulate inflammation, CD8(+) T cell cytotoxicity and severity of colon cancer. Nat Immunol 2021;22(9):1152–1162.
44. Sade-Feldman M, Yizhak K, Bjorgaard SL, et al. Defining T cell states associated with response to checkpoint immunotherapy in melanoma. Cell 2018;175(4):998–1013.e20.
45. Zhang J, Lyu T, Cao Y, et al. Role of TCF-1 in differentiation, exhaustion, and memory of CD8(+) T cells: a review. FASEB J 2021;35(5): e21549.
46. Chuang HC, Tan TH. MAP4K family kinases and DUSP family phosphatases in T-cell signaling and systemic lupus erythematosus. Cells 2019;8(11):1433.
47. Jeffrey KL, Camps M, Rommel C, et al. Targeting dual-specificity phosphatases: manipulating MAP kinase signalling and immune responses. Nat Rev Drug Discov 2007;6(5):391–403.
48. Camps M, Nichols A, Arkinstall S. Dual specificity phosphatases: a gene family for control of MAP kinase function. FASEB J 2000;14(1): 6–16.
49. Singh MK, Altameemi S, Lares M, et al. Role of dual specificity phosphatases (DUSPs) in melanoma cellular plasticity and drug resistance. Sci Rep 2022;12(1):14395.

50. Martinez BA, Shrotri S, Kingsmore KM, et al. Machine learning reveals distinct gene signature profiles in lesional and nonlesional regions of inflammatory skin diseases. Sci Adv 2022;8(17):eabn4776.
51. Enocsson H, Karlsson J, Li HY, et al. The complex role of C-reactive protein in systemic lupus erythematosus. J Clin Med 2021;10(24): 5837.
52. Hochberg MC. Updating the American College of Rheumatology revised criteria for the classification of systemic lupus erythematosus. *Arthritis Rheum*. 1997;40(9):1725.
53. Tan EM, Cohen AS, Fries JF, Masi AT, McShane DJ, Rothfield NF, et al. The 1982 revised criteria for the classification of systemic lupus erythematosus. *Arthritis Rheum*. 1982;25(11):1271-1277.

## APPENDIX A: DISSECT CONSORTIUM

Members of the DISSECT Consortium are as follows: Lars Rönnblom (Department of Medical Sciences, Rheumatology, Uppsala University, Uppsala, Sweden), Kerstin Lindblad-Toh (Science for Life Laboratory, Department of Medical Biochemistry and Microbiology, Uppsala University, Uppsala, Sweden; Broad Institute of MIT and Harvard, Cambridge, Massachusetts), Marie Wahren-Herlenius (Division of Rheumatology, Department of Medicine, Solna, Karolinska Institutet, Solna, Sweden; Karolinska University Hospital, Stockholm, Sweden; Broegelmann Research Laboratory, Department of Clinical Science, University of Bergen, Bergen, Norway), Gunnel Nordmark (Department of Medical Sciences, Rheumatology, Uppsala University, Uppsala, Sweden), Ingrid E. Lundberg (Division of Rheumatology, Department of Medicine, Solna, Karolinska Institutet, Solna, Sweden; Department of Gastro, Dermatology and Rheumatology, Karolinska University Hospital, Stockholm, Sweden), Ann-Christine Syvänen (Department of Medical Sciences, Molecular Medicine and Science for Life Laboratory, Uppsala University, Uppsala, Sweden), Johanna K. Sandling (Department of Medical Sciences, Rheumatology, Uppsala University, Uppsala, Sweden), Mateo Bianchi (Science for Life Laboratory, Department of Medical Biochemistry and Microbiology, Uppsala University, Uppsala, Sweden), Pascal Pucholt (Department of Medical Sciences, Rheumatology, Uppsala University, Uppsala, Sweden), Sergey V. Kozyrev (Science for Life Laboratory, Department of Medical Biochemistry and Microbiology, Uppsala University, Uppsala, Sweden), Maija-Leena Eloranta (Department of Medical Sciences, Rheumatology, Uppsala University, Uppsala, Sweden), Dag Leonard (Department of Medical Sciences, Rheumatology, Uppsala University, Uppsala, Sweden), Andreas Jönsen (Department of Clinical Sciences Lund, Rheumatology, Lund University, Skåne University Hospital, Lund, Sweden), Anders A. Bengtsson (Department of Clinical Sciences Lund, Rheumatology, Lund University, Skåne University Hospital, Lund, Sweden), Iva Gunnarsson (Division of Rheumatology, Department of Medicine, Solna, Karolinska Institutet, Solna, Sweden; Karolinska University Hospital, Stockholm, Sweden), Elisabet Svenungsson (Division of Rheumatology, Department of Medicine, Solna, Karolinska Institutet, Solna, Sweden; Karolinska University Hospital, Stockholm, Sweden), Leonid Padyukov (Division of Rheumatology, Department of Medicine, Solna, Karolinska Institutet, Solna, Sweden; Karolinska University Hospital, Stockholm, Sweden), Solbritt Rantapää-Dahlqvist (Department of Public Health and Clinical Medicine/Rheumatology, Umeå University, Umeå, Sweden), Christopher Sjöwall (Division of Inflammation and Infection, Department of Biomedical and Clinical Sciences, Linköping University, Linköping, Sweden), Helena Enocsson (Division of Inflammation and Infection, Department of Biomedical and Clinical Sciences, Linköping University, Linköping, Sweden), Roland Jonsson (Broegelmann Research Laboratory, Department of Clinical Science, University of Bergen, Bergen, Norway), Roald Omdal (Clinical Immunology Unit, Department of Internal Medicine, Stavanger University Hospital, Stavanger, Norway; Broegelmann Research Laboratory, Department of Clinical Science, University of Bergen, Bergen, Norway), Daniel Hammenfors (Department of Rheumatology, Haukeland University Hospital, Bergen, Norway), Elke Theander (Department of Rheumatology, Skåne University Hospital Malmö/Lund University, Lund, Sweden), Eva Baecklund (Division of Rheumatology, Department of Medical Sciences, Uppsala University, Uppsala, Sweden), Gudny Ella Thorlacius (Division of Rheumatology, Department of Medicine, Solna, Karolinska Institutet, Solna, Sweden; Karolinska University Hospital, Stockholm, Sweden), Helena Forsblad-d'Elia (Department of Rheumatology and Inflammation Research, Sahlgrenska Academy at University of Gothenburg, Gothenburg, Sweden), Johan G. Brun (Department of Rheumatology, Haukeland University Hospital, University of Bergen, Bergen, Norway), Juliana Imgenberg-Kreuz (Department of Medical Sciences, Rheumatology, Uppsala University, Uppsala, Sweden), Karl A. Brokstad (Broegelmann Research Laboratory, Department of Clinical Science, University of Bergen, Bergen, Norway), Kathrine Skarstein (The Gade Laboratory for Pathology, Department of Clinical Medicine, University of Bergen, Bergen, Norway), Katrine Brække Norheim (Department of Rheumatology, Stavanger University Hospital, Stavanger, Norway; Institute of Clinical Science, University of Bergen, Bergen, Norway), Lilian Vasaitis (Division of Rheumatology, Department of Medical Sciences, Uppsala University, Uppsala, Sweden), Malin V. Jonsson (Section for Oral and Maxillofacial Radiology, Department of Clinical Dentistry, University of Bergen, Bergen, Norway), Marika Kvarnström (Division of Rheumatology, Department of Medicine, Solna, Karolinska Institutet, Solna, Sweden; Karolinska University Hospital, Stockholm, Sweden; Academic Specialist Center, Center for Rheumatology, Stockholm Health Services, Region Stockholm, Stockholm, Sweden), Per Eriksson (Division of Inflammation and Infection, Department of Biomedical and Clinical Sciences, Linköping University, Linköping, Sweden), Sara Magnusson Bucher (Department of Rheumatology, Faculty of Medicine and Health, Örebro University, Örebro, Sweden), Silke Appel (Broegelmann Research Laboratory, Department of Clinical Science, University of Bergen, Bergen, Norway), Svein Joar Johnsen (Department of Rheumatology, Stavanger University Hospital, Stavanger, Norway), Thomas Mandl (Division of Rheumatology, Department of Clinical Sciences, Lund University, Malmö, Sweden), Lara Adnan Aqrawi (Department of Oral Surgery and Oral Medicine, Institute of Clinical Odontology, University of Oslo, Oslo, Norway; Department of Health Sciences, Kristiania University College, Oslo, Norway), Janicke Liaaen Jensen (Department of Oral Surgery and Oral Medicine, Institute of Clinical Odontology, University of Oslo, Oslo, Norway), Øyvind Palm (Department of Rheumatology, Oslo University Hospital, Oslo, Norway), Albin Björk (Division of Rheumatology, Department of Medicine, Solna, Karolinska Institutet, Solna, Sweden; Karolinska University Hospital, Stockholm, Sweden), Marie Fischer (Division of Rheumatology, Department of Medicine, Solna, Karolinska Institutet, Solna, Sweden; Karolinska University Hospital, Stockholm, Sweden), Antonella Notarnicola (Division of Rheumatology, Department of Medicine, Solna, Karolinska Institutet, Solna, Sweden; Department of Gastro, Dermatology and Rheumatology, Karolinska University Hospital, Stockholm, Sweden), Anna Tjärnlund (Karolinska Institutet and Karolinska University Hospital, Stockholm, Sweden), Maryam Dastmalchi (Karolinska Institutet and Karolinska University Hospital, Stockholm, Sweden), Louise Pyndt Diederichsen (Department of Rheumatology, Odense University Hospital, Odense, Denmark; Center for Rheumatology and Spine Diseases, Copenhagen University Hospital, Rigshospitalet, Copenhagen, Denmark), Maria Lidén, (Department of Medical Sciences, Rheumatology, Uppsala University, Uppsala, Sweden), Øyvind Molberg (Department of Rheumatology, Oslo University Hospital, Oslo, Norway; Institute of Clinical Medicine, University of Oslo, Oslo, Norway), Thomas Skogh (Division of Inflammation and Infection, Department of Biomedical and Clinical Sciences, Linköping University, Linköping, Sweden), Awat Jalal (Rheumatology Clinic, Örebro University Hospital, Örebro, Sweden), Balsam Hanna (Department of

Rheumatology, Sahlgrenska University Hospital, Gothenburg, Sweden), Helena Hellström (Department of Rheumatology, Falun, Sweden), Tomas Husmark (Department of Rheumatology, Falun, Sweden), Åsa Häggström (Division of Rheumatology, Department of Medicine, Kalmar Hospital, Kalmar, Sweden), Anna Svärd (Department of Rheumatology, Falun, Sweden; Center for Clinical Research Dalarna, Uppsala University, Uppsala, Sweden), Jennifer Meadows (Science for Life Laboratory, Department of Medical Biochemistry and Microbiology, Uppsala University, Uppsala, Sweden), Jessika Nordin (Science for Life Laboratory, Department of Medical Biochemistry and Microbiology, Uppsala University, Uppsala, Sweden), Fabiana H. G. Farias (Science for Life Laboratory, Department of Medical Biochemistry and Microbiology, Uppsala University, Uppsala, Sweden; Department of Psychiatry, Washington University, St. Louis, Missouri), Johanna Dahlqvist (Department of Medical Sciences, Uppsala University, Uppsala, Sweden; Science for Life Laboratory, Department of Medical Biochemistry and Microbiology, Uppsala University, Uppsala, Sweden), Argyri Mathioudaki (Science for Life Laboratory, Department of Medical Biochemistry and Microbiology, Uppsala University, Uppsala, Sweden), and Daniel Eriksson (Department of Medicine, Solna, Karolinska Institutet, Solna, Sweden; Department of Endocrinology, Metabolism and Diabetes, Karolinska University Hospital, Stockholm, Sweden).

## APPENDIX B: IMMUNOARRAY CONSORTIUM

Members of the ImmunoArray Consortium are as follows: Kerstin Lindblad-Toh (Science for Life Laboratory, Department of Medical Biochemistry and Microbiology, Uppsala University, Uppsala, Sweden; Broad Institute of MIT and Harvard, Cambridge, Massachusetts), Gerli Rosengren Pielberg (Science for Life Laboratory, Department of Medical Biochemistry and Microbiology, Uppsala University, Uppsala, Sweden), Anna Lobell (Office for Medicine and Pharmacy, Uppsala University, Uppsala, Sweden), Åsa Karlsson (Science for Life Laboratory, Department of Medical Biochemistry and Microbiology, Uppsala University, Uppsala, Sweden), Eva Murén (Science for Life Laboratory, Department of Medical Biochemistry and Microbiology, Uppsala University, Uppsala, Sweden), Göran Andersson (Department of Animal Breeding and Genetics, Swedish University of Agricultural Sciences, Uppsala, Sweden), Kerstin M. Ahlgren (Department of Surgical Sciences, Uppsala University, Uppsala, Sweden), Lars Rönnblom (Division of Rheumatology, Department of Medical Sciences, Uppsala University, Uppsala, Sweden), Maija-Leena Eloranta (Division of Rheumatology, Department of Medical Sciences, Uppsala University, Uppsala, Sweden), Nils Landegren (Department of Medical Biochemistry and Microbiology, Uppsala University, Uppsala, Sweden; Centre for Molecular Medicine, Department of Medicine, Solna, Karolinska Institute, Solna, Sweden), Olle Kämpe (Center for Molecular Medicine, Department of Medicine, Solna, Karolinska Institutet, Stockholm, Sweden; Department of Endocrinology, Metabolism and Diabetes, Karolinska University Hospital, Stockholm, Sweden; Science for Life Laboratory, Department of Medical Sciences, Uppsala University, Uppsala, Sweden; K.G. Jebsen Center for Autoimmune Diseases, University of Bergen, Norway), and Peter Söderkvist (Division of Cell Biology, Department of Biomedical and Clinical Sciences, Linköping University, Linköping, Sweden).

**Arthritis & Rheumatology**
Vol. 77, No. 2, February 2025, pp 226–238
DOI 10.1002/art.42985
© 2024 The Author(s). *Arthritis & Rheumatology* published by Wiley Periodicals LLC on behalf of American College of Rheumatology. This is an open access article under the terms of the Creative Commons Attribution-NonCommercial-NoDerivs License, which permits use and distribution in any medium, provided the original work is properly cited, the use is non-commercial and no modifications or adaptations are made.

American College of Rheumatology
*Empowering Rheumatology Professionals*

# Emapalumab Treatment in Patients With Rheumatologic Disease–Associated Hemophagocytic Lymphohistiocytosis in the United States: A Retrospective Medical Chart Review Study

Shanmuganathan Chandrakasan,[1] Carl E. Allen,[2] Deepika Bhatla,[3] John Carter,[4] May Chien,[5] Robert Cooper,[6] Lauren Draper,[3] Olive S. Eckstein,[2] Rabi Hanna,[7] J. Allyson Hays,[8] Michelle L. Hermiston,[9] Ashley P. Hinson,[10] Patricia M. Hobday,[11] Michael S. Isakoff,[12] Michael B. Jordan,[13] Jennifer W. Leiding,[14] Renee Modica,[15] Taizo A. Nakano,[16] Abiola Oladapo,[17] Sachit A. Patel,[18] Priti Pednekar,[19] Mona Riskalla,[11] Susmita N. Sarangi,[20] Prakash Satwani,[21] Anand Tandra,[22] Kelly J. Walkovich,[23] John D. Yee,[17] Adi Zoref-Lorenz,[24] and Edward M. Behrens,[25] on behalf of the REAL-HLH investigators

**Objective.** Rheumatologic disease–associated hemophagocytic lymphohistiocytosis (HLH), a rare, life-threatening, systemic hyperinflammatory syndrome, occurs as a complication of underlying rheumatologic disease. Real-world evidence is lacking on emapalumab, a fully human monoclonal antibody that neutralizes the proinflammatory cytokine interferon-γ, approved for treating patients with primary HLH.

**Methods.** REAL-HLH, a retrospective medical chart review study conducted across 33 US hospitals, assessed real-world treatment patterns and outcomes in patients with HLH treated with one or more dose of emapalumab between November 20, 2018, and October 31, 2021. Data are presented for the subset of patients with rheumatologic disease–associated HLH.

**Results.** Fifteen of 105 patients (14.3%) had rheumatologic disease–associated HLH. Of these, nine (60.0%) had systemic juvenile idiopathic arthritis, and one (6.7%) had adult-onset Still disease. Median (range) age at HLH diagnosis was 5 (0.9–39) years. Most patients (9 of 15; 60.0%) initiated emapalumab in an intensive care unit. Emapalumab was most frequently initiated for treating refractory or recurrent (10 of 15; 66.7%) disease. Most patients received HLH-related therapies before (10 of 15; 66.7%) and concurrently with (15 of 15; 100.0%) emapalumab. Emapalumab-containing regimens stabilized or achieved physician-determined normalization of most laboratory parameters, including absolute neutrophil count and absolute lymphocyte count (13 of 14; 92.9%), chemokine ligand 9 (9 of 11; 81.8%), and platelets and alanine transaminase (11 of 14; 78.6%), and reduced glucocorticoid dose by 80%. Overall survival and 12-month survival probability from emapalumab initiation were 86.7%.

**Conclusion.** Emapalumab-containing regimens stabilized or normalized most key laboratory parameters, reduced glucocorticoid dose, and were associated with low disease-related mortality, thereby demonstrating potential benefits in patients with rheumatologic disease–associated HLH.

Supported by Sobi, Inc.
[1]Shanmuganathan Chandrakasan, MD: Aflac Cancer and Blood Disorders Center, Children's Healthcare of Atlanta, Emory University, Atlanta, Georgia; [2]Carl E. Allen, MD, PhD, Olive S. Eckstein, MD: Baylor College of Medicine, Houston, Texas; [3]Deepika Bhatla, MD, Lauren Draper, MD (current address: Akron Children's Hospital, Akron, Ohio): Saint Louis University, Saint Louis, Missouri; [4]John Carter, MD, PhD: Oregon Health and Science University, Portland; [5]May Chien, MD: Lucile Packard Children's Hospital at Stanford University, Palo Alto, California; [6]Robert Cooper, MD: Bellflower Medical Center, Bellflower, California; [7]Rabi Hanna, MD: Cleveland Clinic Children's Hospital, Cleveland, Ohio; [8]J. Allyson Hays, MD: Children's Mercy Hospital, Kansas City, Missouri; [9]Michelle L. Hermiston, MD, PhD: University of California, San Francisco; [10]Ashley P. Hinson, MD: Atrium Health Levine Children's Hospital, Charlotte, North Carolina; [11]Patricia M. Hobday, MD, Mona Riskalla, MD: University of Minnesota Medical School, Minneapolis; [12]Michael S. Isakoff, MD: Connecticut Children's Medical Center, Hartford; [13]Michael B. Jordan, MD: Cincinnati Children's Hospital Medical Center and University of Cincinnati College of Medicine, Cincinnati, Ohio; [14]Jennifer W. Leiding, MD: Johns Hopkins University, Baltimore, Maryland, and Johns Hopkins All Children's Hospital, St. Petersburg, Florida; [15]Renee Modica, MD: University of Florida Health Shands Children's Hospital, Gainesville; [16]Taizo A. Nakano, MD: Children's Hospital Colorado, Aurora; [17]Abiola Oladapo, PhD, John D. Yee, MD, MPH (current address: Apnimed, Cambridge, Massachusetts): Sobi, Inc., Waltham, Massachusetts; [18]Sachit A. Patel, MD: University of Nebraska Medical Center, Omaha; [19]Priti Pednekar, PhD (current address: Astellas

## INTRODUCTION

Macrophage activation syndrome (MAS), a form of secondary hemophagocytic lymphohistiocytosis (sHLH), is an acute, life-threatening condition of extreme systemic hyperinflammation that develops as a complication of systemic juvenile idiopathic arthritis (sJIA), adult-onset Still disease (AOSD), systemic lupus erythematosus, and less commonly, in the setting of other autoimmune or autoinflammatory disorders.[1–6] Rheumatologists have traditionally used MAS to describe sHLH associated with rheumatologic disease ("rheumatologic disease–associated HLH"); however, efforts to refine and unify the nomenclature are underway.[3]

Clinical and laboratory abnormalities of rheumatologic disease–associated HLH may include high nonremitting fever, hepatosplenomegaly, cytopenias, coagulopathy, central nervous system abnormalities, elevated liver enzymes, and hemophagocytosis, which reflect the uncontrolled, dysregulated immune activation that drives pathogenesis.[2,5,7–12] Hyperferritinemia (typically >10,000 ng/mL) and elevated soluble interleukin-2 receptor α (sCD25) are prominent features of macrophage and T cell activation, respectively.[1,2,4,12–14] Rheumatologic disease–associated HLH and active rheumatologic disease can concurrently occur, and considerable overlap between their clinical features can significantly delay diagnosis.[9,11] Because the HLH 2004 diagnostic criteria are not sufficiently sensitive in the context of MAS, the 2016 American College of Rheumatology (ACR) MAS classification criteria and the 2019 MAS/sJIA score were specifically developed to classify and distinguish rheumatologic disease–associated HLH complicating sJIA from an sJIA flare and systemic infection.[12,15,16]

Untreated rheumatologic disease–associated HLH can rapidly progress to multiorgan failure and death and is associated with substantial mortality rates (8%–30%).[2,4,8,9,11,17,18] Currently, there is a paucity of clinical trials and US Food and Drug Administration–approved therapies specifically for rheumatologic disease–associated HLH.[19,20] Indeed, there is significant overlap between the immunosuppressive treatment of rheumatologic disease–associated HLH and the underlying rheumatologic disease, and treatment is based on clinical experience.[14,21,22] Rheumatologic disease–associated HLH is currently managed with high-dose or pulse corticosteroids (glucocorticoids) and, if inadequate, with cyclosporine or targeted therapies such as anakinra (interleukin [IL]-1 blockade).[4,18,20,23–25] Long-term treatment with glucocorticoids is associated with toxicity, susceptibility to secondary infections, weight gain, diabetes mellitus, hypertension, and an increased risk of developing glucocorticoid-refractory disease.[2] Some targeted therapies including IL-6 blockers (eg, tocilizumab) are prescribed with caution because they may mask the clinical symptoms of sJIA/MAS.[26,27]

Overactivation and expansion of T lymphocytes and macrophages in rheumatologic disease–associated HLH yields abnormally high levels of proinflammatory cytokines, such as interferon-γ (IFNγ), leading to pathologic inflammation.[2,5,7–10,28] IFNγ affects innate and adaptive immunity and is a key mediator of systemic hyperinflammation in HLH and rheumatologic disease–associated HLH. Serum IFNγ levels are significantly elevated in these syndromes and correlate with clinical presentation.[29] Notably, levels of IFNγ and its inducible chemokine ligand 9 (CXCL9) were significantly higher in patients with rheumatologic disease–associated HLH than in patients with active sJIA without HLH and returned to normal after HLH resolution, suggesting that IFNγ may be a viable target for controlling pathologic hyperinflammation.[3,6,30]

Emapalumab is a fully human IgG1 monoclonal antibody that binds to and neutralizes the biologic activity of IFNγ.[31] It was approved for primary HLH (pHLH) in the United States in November 2018 and remains the only approved treatment for adult and pediatric patients with pHLH with refractory, recurrent, or progressive disease or intolerance with conventional HLH therapy.[32] Off-label prescribing of emapalumab has been reported in patients with sHLH associated with various conditions.[33–36] In a single-arm, open-label, phase 2 trial, emapalumab achieved MAS remission in almost all patients with MAS complicating sJIA/AOSD.[23]

Unlike randomized clinical trials conducted in controlled settings and selective populations, real-world studies provide valuable evidence on drug prescribing, effectiveness, and safety in routine clinical practice.[37] The REAL-HLH study was conducted to assess real-world treatment patterns and outcomes among patients with HLH treated with emapalumab in the United States (for a list of REAL-HLH study investigators and sites, see Appendix A). In this report, results on patients with rheumatologic disease–associated HLH, including the subset with sJIA/AOSD, treated with emapalumab are presented.

## MATERIALS AND METHODS

**Study design.** This was a retrospective medical chart review study conducted across 33 US hospitals between November 20, 2018, and December 31, 2021. Patients treated

Pharma Inc., Northbrook, Illinois): PRECISIONheor, Bethesda, Maryland; [20]Susmita N. Sarangi, MD: Medstar Georgetown University Hospital, Washington, DC; [21]Prakash Satwani, MD: NewYork-Presbyterian Columbia University Irving Medical Center, New York City; [22]Anand Tandra, MD: Franciscan Health, Indianapolis, Indiana; [23]Kelly J. Walkovich, MD: University of Michigan Medical School, Ann Arbor; [24]Adi Zoref-Lorenz, MD: Cincinnati Children's Hospital Medical Center, Cincinnati, Ohio, and Tel Aviv University School of Medicine, Tel Aviv, Israel; [25]Edward M. Behrens, MD: Children's Hospital of Philadelphia, Philadelphia, Pennsylvania.

Additional supplementary information cited in this article can be found online in the Supporting Information section (http://onlinelibrary.wiley.com/doi/10.1002/art.42985).

Author disclosures are available at https://onlinelibrary.wiley.com/doi/10.1002/art.42985.

Address correspondence via email to Edward M. Behrens, MD, at behrens@chop.edu.

Submitted for publication April 3, 2024; accepted in revised form August 20, 2024.

with one or more dose of emapalumab between November 20, 2018, and October 31, 2021 (patient identification period), in routine clinical practice were identified, and their chart data were abstracted. Patient records were analyzed from the time of emapalumab initiation (index date) to the end of the study (December 31, 2021), end of data availability, or death, whichever occurred first. The protocol and data collection forms were reviewed by the Western Institutional Review-Copernicus Group Institutional Review Board (IRB) and local IRBs, where required. There was no direct patient involvement in the study and anonymized data collection was conducted in compliance with US Health Insurance Portability and Accountability Act policies.

**Patients.** Patients were classified as presenting with sHLH if they were treated for HLH but did not meet the pHLH classification criteria, defined as fulfillment of at least one of the following criteria (without evidence of underlying malignancy, rheumatologic, or metabolic disease): (1) identification of a known genetic mutation associated with pHLH (biallelic mutation/compound heterozygosity for *PRF1*, *UNC13D*, *STX11*, *STXBP2*, *RAB27A*, *LYST*, or *AP3B1*, or a monoallelic mutation for *SH2D1A*, or *XIAP*); (2) meeting at least five of the eight HLH-2004 criteria; or (3) having a family history of HLH.[15,38] A multispecialty panel of experts adjudicated the classification of patients who were diagnosed by their physician with pHLH but did not meet the classification criteria and those with a physician diagnosis of sHLH but who met the pHLH classification criteria.

This report focuses on the subset of patients with sHLH and physician-reported underlying rheumatologic disease (rheumatologic disease–associated HLH), including patients with sJIA/AOSD. All patients with a physician diagnosis of sJIA or AOSD at the time of HLH diagnosis with available data were evaluated to determine whether they met the ACR 2016 MAS criteria.[12]

**Outcomes and assessments.** The primary objective of the REAL-HLH study was to describe emapalumab treatment patterns (time to initiation of emapalumab from HLH diagnosis, treatment duration, dosing patterns, and reasons for initiating emapalumab) among patients with HLH treated with emapalumab. The reasons for initiating emapalumab included to treat progressive (worsening), relapsed/recurrent (reoccurrence after improvement), or refractory (unresponsive to treatment) disease. HLH-related therapies that were administered before or concurrently with emapalumab were also analyzed.

Secondary objectives included patient demographics, clinical characteristics, and treatment outcomes. Treatment outcomes assessed were change in glucocorticoid dosing over time, the proportion of patients who achieved or maintained normal (stabilized) laboratory parameters at any time during treatment as determined by the treating physician and based on defined laboratory criteria (ie, reversed ACR 2016 MAS criteria), and time to first normalization of laboratory parameters. The proportion of patients with abnormal laboratory values was based on data availability at time closest to emapalumab initiation. The proportion of patients achieving normalization or stabilization of laboratory parameters was based on data availability for those patients at that time and was determined only for parameters for which data were available for ≥50% of patients. For ferritin, clinically acceptable reductions, defined as <2000 ng/mL or ≥80% reduction from the value at the index date, were also evaluated.[32] Other outcomes included proportion of patients considered for and who received hematopoietic stem cell transplantation (HSCT) and overall and 12-month survival from emapalumab initiation. The reasons for patients not receiving transplant and causes of death were evaluated.

**Statistical analysis.** Because this was not a statistical hypothesis-driven study, power calculation was not necessary for sample size estimation. The sample size was determined by chart availability for eligible patients at the participating treatment centers. Continuous variables were summarized using means, SDs, medians, and interquartile ranges. Categoric variables were summarized using counts and percentages. Kaplan-Meier curves were used to evaluate time-to-event analyses, with a two-sided 95% confidence interval for survival estimates.

## RESULTS

**Demographics and clinical characteristics.** A total of 105 patients were enrolled in the REAL-HLH study; 98 (93.3%) were reportedly treated for HLH. The median (range) number of patients per site was 2 (1–15). Overall, 51 of 105 patients (48.6%) did not meet the criteria for pHLH and were categorized as presenting with sHLH (Supplementary Table 1). Based on the underlying disease, these patients (n = 51) were further classified into three categories: rheumatologic disease–associated HLH (n = 15), malignancy-associated HLH (n = 17), or "others" (n = 19; patients with miscellaneous underlying diseases and/or HLH triggers that could not be categorized as rheumatologic or malignant disease; Supplementary Figure 1).

Most patients (10 of 15; 66.7%) with rheumatologic disease–associated HLH (n = 15) had either sJIA (n = 9) or AOSD (n = 1; Table 1). In the remaining patients, HLH was associated with underlying rheumatoid arthritis (n = 1), systemic lupus erythematosus (n = 1), juvenile idiopathic arthritis (n = 1), diffuse myositis (n = 1), and *NLRC4* mutation (n = 1). Most patients were female (11 of 15; 73.3%), and the median (range) age at HLH diagnosis was 5.0 (0.9–39) years (Table 1). Most patients were children <12 years of age (n = 11) with a median (range) age at HLH diagnosis of 2.0 (0.9–10) years. The remaining patients were adults (n = 4) with a median (range) age at diagnosis of 24.5 (22–39) years.

For the subset of patients with sJIA/AOSD, the median (range) age at HLH diagnosis was 2.5 (1.0–22) years (Table 1). The patient with AOSD was 22 years of age. A majority (7 of 10; 70%) of patients with sJIA/AOSD met the 2016 ACR MAS classification criteria.[12]

**Table 1.** Demographics and clinical characteristics of patients with rheumatologic disease–associated HLH (n = 15) and the subset of patients with sJIA/AOSD (n = 10)*

| Parameter | Patients with rheumatologic disease–associated HLH (n = 15) | | Patients with rheumatologic disease–associated HLH, stratified by age (n = 15) | |
|---|---|---|---|---|
| | All patients (n = 15) | sJIA/AOSD (n = 10) | Children (<12 y),[a] (n = 11) | Adolescents and adults (≥12 y),[a] (n = 4) |
| Age at HLH diagnosis, median (range), y | 5.0 (0.9–39) | 2.5 (1.0–22.0)[b] | 2.0 (0.9–10.0) | 24.5 (22–39) |
| Female sex, n/N (%) | 11/15 (73.3) | 8/10 (80.0) | 8/11 (72.7) | 3/4 (75.0) |
| White American race, n/N (%) | 7/15 (46.7) | 6/10 (60.0) | 7/11 (63.3) | 0/4 (0.0) |
| Infection at HLH diagnosis, n/N (%) | 5/15 (33.3) | 3/10 (30.0) | 3/11 (27.3) | 2/4 (50.0) |
| Viral | 4/5 (80.0) | 3/3 (100.0) | 2/3 (66.7) | 2/2 (100.0) |
| Bacterial | 1/5 (20.0) | 0/3 (0.0) | 0/3 (0.0) | 1/2 (50.0) |
| CNS involvement at HLH diagnosis, n/N (%) | 1/15 (6.7) | 0/10 (0.0) | 1/11 (9.1) | 0/4 (0.0) |
| Age at initiation of emapalumab, median (range), y | 5.0 (0.9–39) | 2.5 (1.0–22.0) | 2.0 (1.0–10.0) | 24.5 (22.0–39.0) |
| Initiated emapalumab in an ICU, n/N (%) | 9/15 (60.0) | 6/10 (60.0) | 7/11 (63.3) | 2/4 (50.0) |
| Received supportive care at initiation of emapalumab, n/N (%) | 7/15 (46.7) | 6/10 (60.0) | 6/11 (54.5) | 1/4 (25.0) |
| Ventilator | 3/7 (42.9) | 3/6 (50.0) | 3/6 (50.0) | 0/1 (0.0) |
| Dialysis | 1/7 (14.3) | 1/6 (16.7) | 1/6 (16.7) | 0/1 (0.0) |
| Pressors | 0/7 (0.0) | 0/6 (0.0) | 0/6 (0.0) | 0/1 (0.0) |
| Extracorporeal membrane oxygenation | 0/7 (0.0) | 0/6 (0.0) | 0/6 (0.0) | 0/1 (0.0) |
| Other[c] | 4/7 (57.1) | 3/6 (50.0) | 3/6 (50.0) | 1/1 (100.0) |
| Abnormal laboratory markers or cytokine levels,[d] n/N, (%) | | | | |
| Ferritin, >684 ng/mL | 12/14 (85.7) | 8/9 (88.9) | 8/10 (80.0) | 4/4 (100.0) |
| Platelet count, ≤181 × $10^9$ cells/L | 9/15 (60.0) | 6/10 (60.0) | 5/11 (45.5) | 4/4 (100.0) |
| Alanine transaminase, >36 U/L | 11/15 (73.3) | 7/10 (70.0) | 7/11 (63.3) | 4/4 (100.0) |
| Fibrinogen levels, ≤360 mg/dL | 12/14 (85.7) | 8/10 (80.0) | 10/11 (90.9) | 2/3 (66.7) |
| Absolute neutrophil count, ≤3.7 × $10^9$ cells/L | 4/14 (28.6) | 3/10 (30.0) | 2/11 (18.2) | 2/3 (66.7) |
| sCD25[e] | 6/8 (75.0) | 5/5 (100.0) | 5/6 (83.3) | 1/2 (50.0) |
| Absolute lymphocyte count[e] | 6/14 (42.9) | 4/10 (40.0) | 4/11 (36.4) | 2/3 (66.7) |
| CXCL9[e] | 4/5 (80.0) | 3/4 (75.0) | 3/4 (75.0) | 1/1 (100.0) |

* AOSD, adult-onset Still disease; CNS, central nervous system; CXCL9, chemokine ligand 9; HLH, hemophagocytic lymphohistiocytosis; ICU, intensive care unit; sCD25, soluble interleukin-2 receptor alpha (IL-2Rα); sJIA, systemic juvenile idiopathic arthritis.

[a] Patients were classified as children (<12 years) and adolescents and adults (≥12 years) based on age at time of emapalumab initiation.

[b] The patient with AOSD was 22 years of age at diagnosis.

[c] High-flow nasal cannula; tunneled percutaneous catheter; nasogastric/orogastric tube insertion; bilevel positive airway pressure; continuous positive airway pressure.

[d] Based on defined criteria, and based on the most recent laboratory values closest to or at emapalumab initiation.

[e] Based on physician report.

Five of 15 patients (33.3%) with rheumatologic disease–associated HLH and 3 of 10 (30%) in the subset with sJIA/AOSD presented with infections at diagnosis; viral infections were the most common (Table 1; Supplementary Table 2). Overall, 60% of all patients (overall rheumatologic disease–associated HLH: 9 of 15; sJIA/AOSD: 6 of 10) were critically ill and received emapalumab in an intensive care unit (Table 1). Most patients had abnormal laboratory parameters (Table 1) before initiating emapalumab. Demographics, clinical characteristics, treatment patterns, and outcomes for patients classified as "others" are presented in Supplementary Material (Supplementary Tables 3–6; Supplementary Figures 2–5).

**Treatment patterns.** Emapalumab was most frequently initiated for treating refractory disease (5 of 15; 33.3%) and recurrent disease (5 of 15; 33.3%) across all patients with rheumatologic disease–associated HLH and in the subset with sJIA/AOSD (refractory disease: 4 of 10; 40%; recurrent disease: 3 of 10; 30%). Emapalumab was initiated to treat progressive disease in 4 of 15 patients (26.7%) with rheumatologic disease–associated HLH, including 2 of 10 patients (20%) in the subset with sJIA/AOSD. No specific reason was provided for one patient other than treatment of HLH secondary to MAS.

Almost two-thirds of all the patients (all rheumatologic disease–associated HLH: 10 of 15 [66.7%]; sJIA/AOSD: 6 of 10 [60%]) received HLH-related therapies before emapalumab initiation (Table 2). All patients (15 of 15, 100%) concurrently received emapalumab with HLH-related therapies. Glucocorticoids (100%) and anakinra (60%) were the most frequently used HLH-related therapies administered before or concurrently with emapalumab. The median (range) dose of glucocorticoids given before and concurrently with emapalumab was 3.6 (0.3–28.7) mg/kg per day and 1.9 (0.4–5.2) mg/kg per day, respectively, in patients with rheumatologic disease–associated HLH and 3.8 (2.8–28.7) mg/kg per day and 2.0 (0.6–5.2) mg/kg per day, respectively, in the subset of patients with sJIA/AOSD. The median (range) dose of anakinra given before and concurrently with emapalumab was 4.3 (3.2–6.7) mg/kg per day and 6.7 (2.7–13.2) mg/kg per day, respectively, in patients with rheumatologic disease–associated HLH and 5.0 (4.3–6.7) mg/kg per day and 7.4 (2.7–13.2) mg/kg per day, respectively, in the subset with sJIA/AOSD.

Median (range) time from HLH diagnosis to emapalumab initiation and overall treatment duration was 21.0 (1–988) days and 63 (3–397) days, respectively, for all patients with rheumatologic

**Table 2.** HLH-related therapies used before or concurrently with emapalumab treatment*

| Parameter | Rheumatologic disease–associated HLH (N = 15) | |
|---|---|---|
| | All patients (N = 15) | Patients with sJIA/AOSD (n = 10) |
| Received other HLH-related therapies before emapalumab, n/N (%) | 10/15 (66.7) | 6/10 (60.0) |
| Glucocorticoids | 10/10 (100.0) | 6/6 (100.0) |
| Anakinra | 6/10 (60.0)[a,c] | 4/6 (66.7)[b,c] |
| Etoposide | 3/10 (30.0) | 3/6 (50.0) |
| Cyclosporine | 2/10 (20.0) | 1/6 (16.7) |
| Ruxolitinib | 1/10 (10.0) | - |
| Rituximab | 1/10 (10.0) | - |
| Canakinumab | 1/10 (10.0) | 1/6 (16.7) |
| Received other HLH-related therapies concurrently with emapalumab, n/N (%) | 15/15 (100.0) | 10/10 (100.0) |
| Glucocorticoids | 15/15 (100.0) | 10/10 (100.0) |
| Anakinra[d] | 9/15 (60.0)[e] | 7/10 (70.0)[f] |
| Etoposide | 2/15 (13.3) | 1/10 (10.0) |
| Cyclosporine | 2/15 (13.3) | 1/10 (10.0) |
| Ruxolitinib | 2/15 (13.3) | - |
| Immunoglobulins | 1/15 (6.7) | 1/10 (10.0) |
| Others | 3/15 (20.0) | 2/10 (20.0) |

* AOSD, adult-onset Still disease; HLH, hemophagocytic lymphohistiocytosis; sJIA, systemic juvenile idiopathic arthritis.
[a] Median (range) dose of anakinra given before emapalumab in patients with rheumatologic disease–associated HLH (N = 5): 4.3 (3.2–6.7) mg/kg per day.
[b] Median (range) dose of anakinra given before emapalumab in patients with sJIA/AOSD (n = 3): 5.0 (4.3–6.7) mg/kg per day.
[c] One additional patient received anakinra before emapalumab but not within the 7-day period before emapalumab initiation.
[d] Patients received anakinra within 7 days of initiating emapalumab at a median (range) dose of 4.3 (3.2–6.7) mg/kg per day subcutaneously or 4.6 (4.2–5.0) mg/kg per day intravenously.
[e] Median (range) dose of anakinra given concurrently with emapalumab in patients with rheumatologic disease–associated HLH (n = 9): 6.7 (2.7–13.2) mg/kg per day.
[f] Median (range) dose of anakinra given concurrently with emapalumab in patients with sJIA/AOSD (n = 7): 7.4 (2.7–13.2) mg/kg per day.

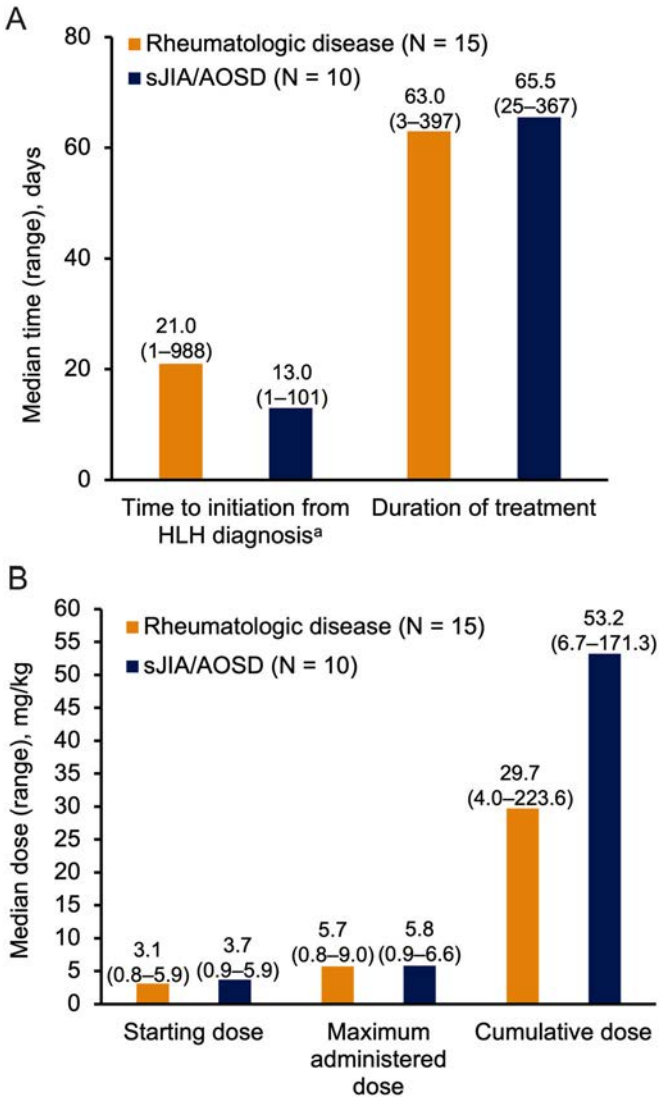


**Figure 1.** Emapalumab treatment patterns in patients with rheumatologic disease–associated HLH (n = 15) and the subset of patients with sJIA/AOSD (n = 10). (A) Time to emapalumab initiation from HLH diagnosis and duration of treatment with emapalumab. (B) Emapalumab dosing. [a]Date of diagnosis was missing for one patient. AOSD, adult-onset Still disease; HLH, hemophagocytic lymphohistiocytosis; sJIA, systemic juvenile idiopathic arthritis.

disease–associated HLH and 13.0 (1–101) days and 65.5 (25–367) days, respectively, for the subset with sJIA/AOSD (Figure 1A). The median (range) emapalumab starting, maximum administered single, and cumulative doses in all patients with rheumatologic disease–associated HLH were 3.1 (0.8–5.9) mg/kg, 5.7 (0.8–9.0) mg/kg, and 29.7 (4.0–223.6) mg/kg, respectively (Figure 1B). The median (range) emapalumab starting, maximum administered single, and cumulative doses in the subset of patients with sJIA/AOSD were 3.7 (0.9–5.9) mg/kg, 5.8 (0.9–6.6) mg/kg, and 53.2 (6.7–171.3) mg/kg, respectively (Figure 1B). The median (range) number of administered emapalumab doses was 15 (2–44) for all patients with rheumatologic disease–associated HLH and 15.5 (2–35) for the subset with sJIA/AOSD.

**Treatment outcomes.** Median values for key laboratory parameters (based on the 2016 ACR MAS criteria) at time closest to or at emapalumab initiation, including ferritin (rheumatologic disease–associated HLH: 6,743.5 ng/mL, sJIA/AOSD: 6,032.0 ng/mL), platelet count (rheumatologic disease–associated HLH: 109.0 × $10^9$ cells/L, sJIA/AOSD: 138.0 × $10^9$ cells/L), and fibrinogen (rheumatologic disease–associated HLH: 156.0 mg/dL, sJIA/AOSD: 211.5 mg/dL), indicated severe rheumatologic disease–associated HLH (Table 3). Median CXCL9 levels were 12,260 pg/mL for patients with rheumatologic disease–associated HLH and 22,792.2 pg/mL for the subset with sJIA/AOSD. Most laboratory parameters improved from time closest to emapalumab initiation up to week 8 of emapalumab treatment (Table 3).

*Physician-determined normalization or stabilization of laboratory parameters.* Following treatment with emapalumab-containing regimens, most key laboratory parameters achieved physician-determined normalization or remained stable in most patients with rheumatologic disease–associated HLH and in the subset with sJIA/AOSD. The proportion of patients with rheumatologic disease–associated HLH who achieved or maintained physician-determined normal values for each laboratory parameter at any time during treatment was 13 of 14 (92.9%) for absolute neutrophil count (ANC) and absolute lymphocyte count (ALC); 9 of 11 (81.8%) for CXCL9; 11 of 14 (78.6%) for platelets and alanine transaminase (ALT); 9 of 13 (69.2%) for fibrinogen; and 6 of 9 (66.7%) for sCD25 (Figure 2A; Supplementary Table 7). Similarly, in the subset with sJIA/AOSD, physician-determined normalization or stabilization was achieved in 9 of 10 patients (90.0%) for ANC and ALC; 8 of 10 (80%) for platelets and ALT; 6 of 8 (75%) for CXCL9; 4 of 6 (66.7%) for sCD25; and 6 of 10 (60%) for fibrinogen (Figure 2B; Supplementary Table 7).

Ferritin normalized in 6 of 14 patients (42.9%) with rheumatologic disease–associated HLH and in 5 of 10 patients (50%) with sJIA/AOSD (Figure 2A and B; Supplementary Table 7). The proportion of patients who achieved clinically acceptable reductions in ferritin (<2,000 ng/mL or ≥80% reduction from the value at the index date, whichever was lower) increased from 42.9% to 92.9% for all patients with rheumatologic disease–associated HLH and from 50.0% to 100.0% in the subset with sJIA/AOSD. In both groups, median (range) number of laboratory parameters that normalized was 6 (0–8).

Median time to physician-determined first normalization of laboratory parameters ranged from 7 days (ANC) to 38.5 days (ferritin) in all patients with rheumatologic disease–associated HLH (Figure 2A; Supplementary Table 7) and 7 days (ANC and ALC) to 51 days (sCD25) in the subset with sJIA/AOSD (Figure 2B; Supplementary Table 7). The median (range) time to first normalization of CXCL9 was 32 (5–129) days in patients with rheumatologic disease–

**Table 3.** Changes in laboratory parameter values from emapalumab initiation up to week 8 of emapalumab treatment in patients with rheumatologic disease–associated HLH (N = 15) and the subset of patients with sJIA/AOSD (n = 10)*

| Parameter | Baseline[a] | Week 2 | Week 4 | Week 8 |
|---|---|---|---|---|
| Patients with rheumatologic disease–associated HLH (N = 15) | | | | |
| Absolute neutrophil count × $10^9$ cells/L | | | | |
| n | 14 | 13 | 12 | 7 |
| Median (range) | 5.4 (0.1–47.3) | 4.2 (0–25.6) | 12.5 (1.6–35.0) | 6.9 (4.4–11.7) |
| Absolute lymphocyte count × $10^9$ cells/L | | | | |
| n | 14 | 13 | 12 | 7 |
| Median (range) | 1.3 (0.1–8.3) | 1.0 (0.2–4.2) | 1.6 (0.0–6.2) | 1.9 (1.5–6.8) |
| CXCL9, pg/mL | | | | |
| n | 5 | 7 | 5 | 3 |
| Median (range) | 12,260 (468.6–80,295) | 739 (108–16,202) | 367 (163–751) | 52 (24.5–59) |
| Alanine transaminase, U/L | | | | |
| n | 15 | 11 | 10 | 8 |
| Median (range) | 77 (18–1,082) | 83 (19–444) | 37 (21–353) | 47 (16–101) |
| Platelet count × $10^9$cells/L | | | | |
| n | 15 | 13 | 12 | 8 |
| Median (range) | 109 (0–506) | 115 (0.1–494) | 277.5 (0.5–779) | 215.5 (0.2–527) |
| Fibrinogen, mg/dL | | | | |
| n | 14 | 10 | 7 | 4 |
| Median (range) | 156 (20–856) | 299.5 (125–771) | 272 (0–379) | 351 (239–427) |
| sCD25, U/mL | | | | |
| n | 8 | 6 | 4 | 1 |
| Median (range) | 665.7 (0.6[b]–4,288) | 2,709.7 (220.7–9,302) | 1,626.6 (101.3–4,005) | 12,390 |
| Ferritin, ng/mL | | | | |
| n | 14 | 13 | 12 | 9 |
| Median (range) | 6,743.5 (411–81,393) | 2,080 (156–8,943) | 1,607 (28.4–5,685) | 387 (10–1,221) |
| Patients with sJIA/AOSD (N = 10) | | | | |
| Absolute neutrophil count × $10^9$ cells/L | | | | |
| n | 10 | 10 | 9 | 4 |
| Median (range) | 7.6 (2–47.3) | 5.8 (0–25.6) | 14.7 (1.6–35) | 10.1 (6.6–11.7) |
| Absolute lymphocyte count × $10^9$ cells/L | | | | |
| n | 10 | 10 | 9 | 4 |
| Median (range) | 1.3 (0.1–8.3) | 1.2 (0.2–4.2) | 1.5 (0–3) | 1.8 (1.5–2.5) |
| CXCL9, pg/mL | | | | |
| n | 4 | 5 | 4 | 2 |
| Median (range) | 22,792.2 (468.6–80,295) | 739 (311–16,202) | 481.5 (175–751) | 41.8 (24.5–59) |
| Alanine transaminase, U/L | | | | |
| n | 10 | 8 | 8 | 6 |
| Median (range) | 123 (18–1,082) | 77 (19–338) | 37 (21–353) | 59 (23–101) |
| Platelet count × $10^9$ cells/L | | | | |
| n | 10 | 10 | 9 | 5 |
| Median (range) | 138 (32–506) | 169 (39–494) | 290 (65–779) | 227 (25–428) |
| Fibrinogen, mg/dL | | | | |
| n | 10 | 8 | 6 | 3 |
| Median (range) | 211.5 (20–856) | 365.5 (125–771) | 287.5 (156–379) | 296 (239–406) |
| sCD25, U/mL | | | | |
| n | 5 | 4 | 3 | 1 |
| Median (range) | 683.4 (262–2,571) | 4,736.2 (244.1–9,302) | 3,068 (101.3–4,005) | 12,390 |
| Ferritin, ng/mL | | | | |
| n | 9 | 10 | 9 | 6 |
| Median (range) | 6,032 (591–81,393) | 1,572 (156–6,680) | 1,750 (28.4–5,685) | 357.9 (18–1,221) |

* AOSD, adult-onset Still disease; CXCL9, chemokine ligand 9; HLH, hemophagocytic lymphohistiocytosis; sCD25, soluble interleukin-2 receptor alpha (IL-2Rα); sJIA, systemic juvenile idiopathic arthritis.
[a] Based on the most recent laboratory values closest to or at emapalumab initiation.
[b] 5 pg/mL converted to U/mL by multiplying by 0.113.

associated HLH and 32 (5–39) days in the subset with sJIA/AOSD (Figure 2A and B; Supplementary Table 7).

*Normalization or stabilization of laboratory parameters per defined laboratory criteria.* Emapalumab-containing regimens also normalized laboratory parameters based on defined laboratory criteria in all patients at any time during treatment.[12] Most patients with rheumatologic disease–associated HLH achieved normal platelet counts (>181 × $10^9$ cells/L; 13/14 [92.9%]) and ANC (>3.7 × $10^9$ cells/L; 13/14 [92.9%]), ALT (<36 U/L; 11/14 [78.6%]), and ferritin levels (<684 ng/mL; 10/14 [71.4%], Figure 2C; Supplementary Table 7). All patients achieved normal fibrinogen levels (>360 mg/dL). All patients with sJIA/AOSD

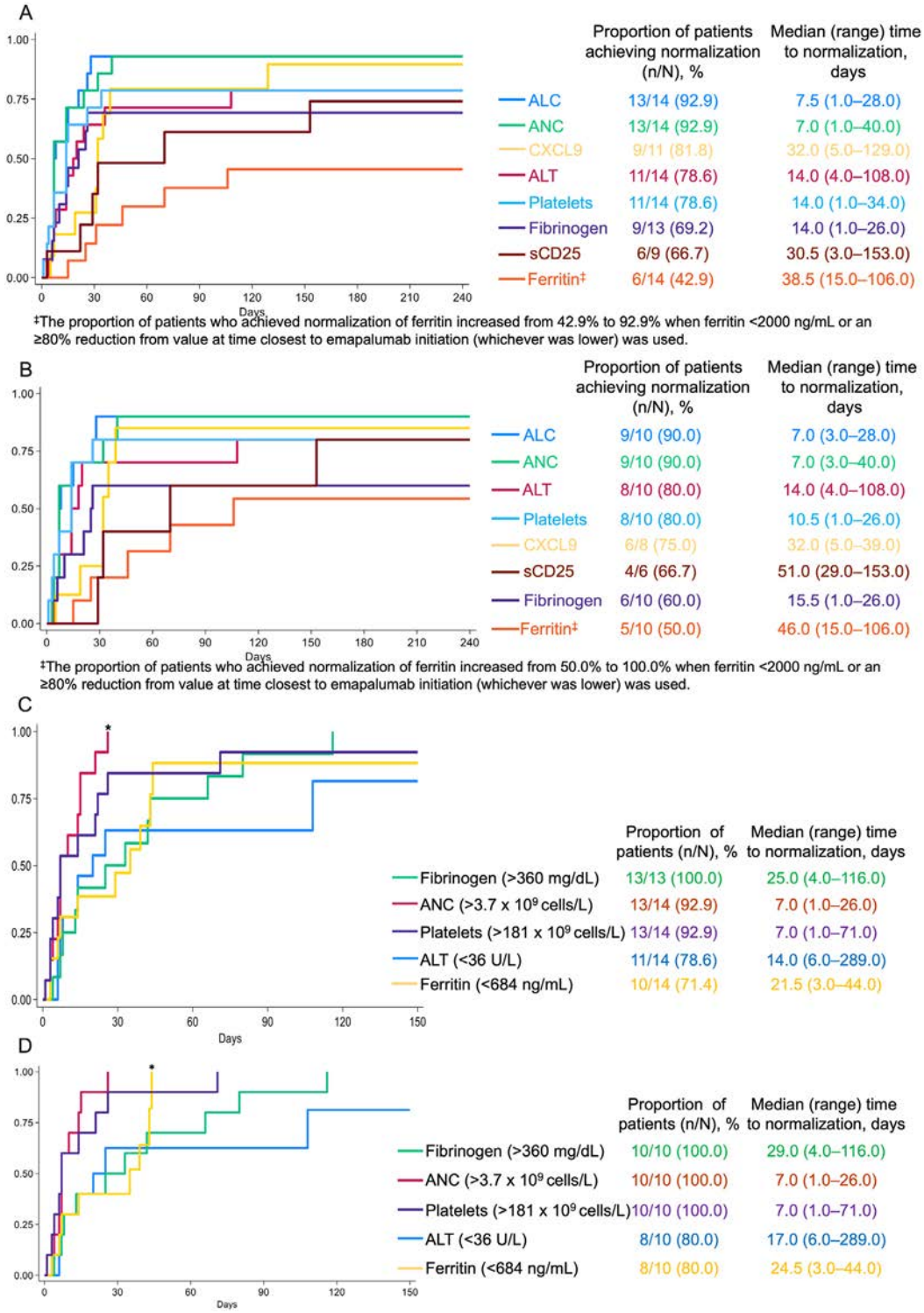


**Figure 2.** Time to first normalization of laboratory parameters based on physician's assessment[a] or defined laboratory value criteria[12] in patients with rheumatologic disease–associated HLH (N = 15) and the subset of patients with sJIA/AOSD (N = 10). Time to first normalization of laboratory parameters based on physician's assessment in (A) patients with rheumatologic disease–associated HLH (N = 15) and (B) patients with sJIA/AOSD (N = 10). Time to achieving defined laboratory parameters in (C) patients with rheumatologic disease–associated HLH (N = 15) and (D) patients with sJIA/AOSD (N = 10). [a]Normalization of laboratory and biomarker values were based on physician report. *Last time point when data were available. ALC, absolute lymphocyte count; ALT, alanine transaminase; ANC, absolute neutrophil count; AOSD, adult-onset Still disease; CXCL9, chemokine ligand 9; HLH, hemophagocytic lymphohistiocytosis; sCD25, soluble interleukin-2 receptor α; sJIA, systemic juvenile idiopathic arthritis.

achieved normal platelet counts, ANC levels, and fibrinogen levels, and 80% achieved normal ferritin and ALT levels (Figure 2D; Supplementary Table 7). Median time to normalization of laboratory parameters based on defined laboratory criteria ranged from 7 days (ANC, platelets) for all patients to 25 days for patients with rheumatologic disease–associated HLH and 29 days in patients with sJIA/AOSD, both for fibrinogen (Figure 2C and D; Supplementary Table 7).

*Change in average daily glucocorticoid dose.* For patients with rheumatologic disease–associated HLH, the median average daily glucocorticoid dose reduced from 3.6 mg/kg prednisone equivalent during the week preceding emapalumab initiation (n = 7) to 0.7 mg/kg during week 8 (n = 6) of emapalumab treatment (80.6% reduction; Figure 3A; Supplementary Table 8). In the subset of patients with sJIA/AOSD, the median average daily glucocorticoid dose reduced from 3.8 mg/kg prednisone equivalent during the week preceding emapalumab initiation (n = 3) to 1.3 mg/kg during week 8 (n = 4) of receiving emapalumab treatment (65.8% reduction; Figure 3B; Supplementary Table 8).

*HSCT in patients with recurrent, refractory, or progressive disease.* Due to the recurrent/refractory nature of HLH in this population, 7 of 15 patients (46.7%) with rheumatologic disease–associated HLH and 4 of 10 patients (40.0%) in the subset with sJIA/AOSD were considered for transplant (Figure 3C). Of these, two of seven patients (28.6%) with rheumatologic disease–associated HLH and one of four patients (25%) in the subset with sJIA/AOSD received HSCT. Five patients were considered for transplant but did not receive it because of an attempt to first control MAS before proceeding with transplant (n = 1), family refused transplant against medical advice (n = 1), the patient did not have genetic predisposition for HLH (n = 1), a final diagnosis of *NLRC4* mutation expressed in nonhematopoietic tissues (n = 1), and disease was controlled and transplant deferred (n = 1).

*Overall survival.* At the end of follow-up, 13 of 15 patients were alive (overall survival: 86.7%). The median (range) duration of follow-up was 397 (6–900) days for all patients with rheumatologic disease–associated HLH and 387.5 (29–900) days in the subset with sJIA/AOSD. The 12-month survival probability from emapalumab initiation was 86.7% among all patients with rheumatologic disease–associated HLH and 90.0% in the subset with sJIA/AOSD (Figure 3D).

**Causes of death.** Two deaths were reported. One patient with sJIA showed improvement in HLH; however, the patient had worsening disseminated viremia and eventually died due to uncontrolled viremia. Death was reported as unrelated to emapalumab or HLH. The second patient had rheumatoid arthritis and was reported as unresponsive to emapalumab. Death was attributed to HLH but deemed unrelated to emapalumab treatment.

## DISCUSSION

The REAL-HLH study was a retrospective medical chart review that described demographics, clinical characteristics, and real-world treatment patterns and outcomes in patients with HLH treated with emapalumab in the United States. In this report, results are presented for patients with rheumatologic disease–associated HLH and the subset of patients with sJIA/AOSD.

The overall patient population was racially diverse, approximately 73% were female, and 66.7% had sJIA/AOSD, the most commonly occurring rheumatologic conditions associated with HLH.[8,9,11,19,39] Approximately one-third of patients presented with infections at diagnosis; most infections were caused by viruses. Similarly, in a retrospective review of pediatric patients with rheumatologic disease–associated HLH, 11 of 24 cases were triggered by infections; 9 were viral.[9]

Differentiating between sepsis, HLH, rheumatologic disease–associated HLH, and a flare-up of underlying rheumatologic disease is important, especially when the latter two present concurrently, because this influences treatment choice.[11] In this study, 70% of patients with sJIA/AOSD met the 2016 ACR MAS classification criteria for identifying MAS complicating sJIA in pediatric patients.[12] In three patients, previous treatment with IL-1 or IL-6 inhibitors may have masked MAS features and precluded them from meeting the MAS criteria when this MAS episode occurred.[40]

Emapalumab was most frequently initiated for treating refractory and recurrent disease. Most patients received HLH-related therapies before (>50%) and concurrently with (100%) emapalumab, consistent with its indication as a second-line therapy in patients with pHLH. Glucocorticoids and anakinra were most frequently used. Consistent with these results, retrospective studies showed that rheumatologic disease–associated HLH was most frequently treated with pulse therapy with high-dose glucocorticoids (intravenous methylprednisolone or oral prednisolone), cyclosporine, or anakinra.[8,11,19,20] Standard (≤4 mg/kg per day) or high (>7.5 mg/kg per day) doses of anakinra were prescribed, similar to those in a single-arm, open-label, prospective trial of emapalumab in patients with rheumatologic disease–associated HLH complicating sJIA/AOSD with inadequate response to high-dose glucocorticoids. Anakinra presumably prevented sJIA flares and, therefore, may have accounted for why treatment with anakinra was continued.[23]

The median (range) emapalumab starting dose in the subset of patients with sJIA/AOSD was lower and the treatment duration was longer than those in the open-label, prospective trial of emapalumab in patients with rheumatologic disease–associated HLH and underlying sJIA/AOSD (3.7 [0.9–5.9] vs 6 mg/kg and 65.5 [25–367] vs 27 [7–39] days, respectively). These results underscore the unmet need for optimization of emapalumab dose and dosing frequency based on prospective trials and clinical evidence.[23]

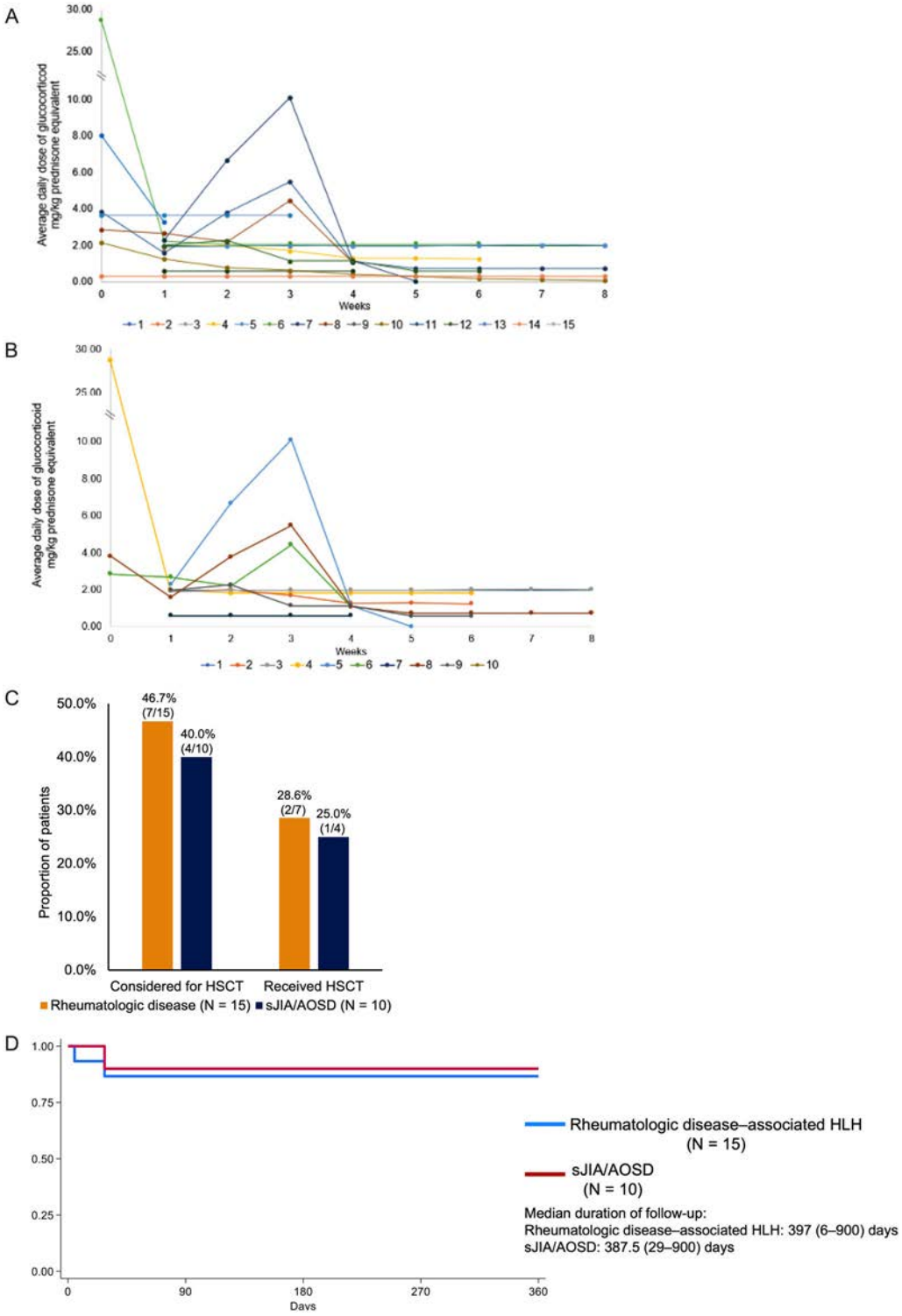


**Figure 3.** Treatment outcomes with HLH-related therapies including emapalumab in patients with rheumatologic disease–associated HLH (N = 15) and the subset of patients with sJIA/AOSD (N = 10). Change in average daily glucocorticoid dose (glucocorticoid tapering) from the week preceding emapalumab initiation up to week 8 of emapalumab treatment in (A) patients with rheumatologic disease–associated HLH (N = 15) and (B) patients with sJIA/AOSD (N = 10). Average daily dose of glucocorticoid (mg/kg prednisone equivalent) is shown starting from the week preceding emapalumab treatment (week 0, day –6 to day 0), followed by week 1 (day 1 to day 7), week 2 (day 8 to day 14), week 3 (day 15 to day 21), up to week 8 (day 50 to day 56) from emapalumab initiation. One patient received prior glucocorticoid treatment but not during the week preceding emapalumab treatment. (C) HSCT in patients with refractory/recurrent disease. (D) Overall survival from time of emapalumab initiation. One patient did not receive glucocorticoid treatment during the first 8 weeks of treatment with emapalumab. AOSD, adult-onset Still disease; HLH, hemophagocytic lymphohistiocytosis; HSCT, hematopoietic stem cell transplantation; sJIA, systemic juvenile idiopathic arthritis.

Abnormal laboratory values at the time closest to or at emapalumab initiation were consistent with those reported for rheumatologic disease–associated HLH in other retrospective case series and underscore MAS severity in this population.[8,11,19,39] Emapalumab-containing treatment regimens stabilized or achieved physician-determined normalization of key laboratory parameters in most patients with rheumatologic disease–associated HLH and in the subset with sJIA/AOSD. Ferritin levels markedly decreased in most patients; reductions of ≥50% are associated with decreased mortality.[14,41] Decrease in CXCL9 levels from the week preceding emapalumab initiation to week 8 of treatment may indicate emapalumab-mediated neutralization of IFNγ and control of life-threatening acute hyperinflammation. Most laboratory parameters also normalized per defined laboratory criteria, indicating control of rheumatologic disease–associated HLH activity. Similarly, in several retrospective studies, patients with rheumatologic disease–associated HLH treated with high-dose corticosteroids, cyclosporine, anakinra, or ruxolitinib showed improvements in laboratory parameters such as ferritin, fibrinogen, aspartate aminotransferase, and platelet count, and normalization of clinical signs, indicating MAS remission.[9,20,42,43] In a single-arm prospective trial, emapalumab normalized all laboratory parameters and neutralized IFNγ, thereby achieving MAS remission in 13 of 14 patients (93%) with sJIA/AOSD. Remission was maintained in 10 patients at the end of long-term follow-up.[23] Taken together, these results underscore the critical need for early initiation of effective treatment to control hyperinflammation and improve treatment outcomes in this high-risk population.[3,14]

Reductions in glucocorticoid dose were observed as early as week 4. The median average daily glucocorticoid dose reduced from the week preceding emapalumab initiation to week 8 of emapalumab treatment by 80% (from 3.6 to 0.7 mg/kg) in patients with rheumatologic disease–associated HLH and by 65% (from 3.8 to 1.3 mg/kg) in the subset with sJIA/AOSD, suggesting that emapalumab may enable early glucocorticoid tapering and thereby contribute to reducing drug-related toxicity in this population. These results are consistent with the approximately 96% reduction in median average daily glucocorticoid dose observed with emapalumab in a single-arm, prospective trial in patients with rheumatologic disease–associated HLH complicating sJIA/AOSD with inadequate response to high-dose glucocorticoids.[23]

Although HSCT is uncommon in patients with rheumatologic disease–associated HLH, a high proportion of patients in this study were considered for HSCT, possibly due to the recurrent/refractory nature of HLH, which required treatment escalation.[1] Following treatment with emapalumab-containing regimens, ≥25% of patients considered for HSCT received it.

This population consisted of patients with refractory/recurrent disease at high risk of mortality; however, there were only two deaths (overall survival: 86.7%). One death was attributed to uncontrolled viremia deemed unrelated to emapalumab or HLH. However, as emapalumab may increase the risk of viral or bacterial infections favored by IFNγ neutralization, the possible relationship between the viremia-related death and emapalumab treatment cannot be ruled out. The 12-month survival probability from emapalumab initiation was 86.7% in patients with rheumatologic disease–associated HLH and 90.0% in the subset with sJIA/AOSD. Retrospective studies have also demonstrated good prognosis in patients with rheumatologic disease–associated HLH with mortality rates ranging from 8.3% to 28.6%.[8,9,19,44]

As with all retrospective studies, limitations include missing or incomplete chart data required for analyses (eg, all prior treatments and laboratory parameter values at time closest to emapalumab initiation and during treatment for each patient may not be uniformly available across study sites). This may have precluded the assessment of "treatment response" and may affect the strength of the results. Safety data were not collected because the study did not have safety-related endpoints. Certain laboratory parameters lacked a standard definition of normal values, which may lead to variability in the results. Because patients received HLH-related therapies concurrently with emapalumab, the results from this study cannot be attributed exclusively to emapalumab. Given the rarity of HLH, the number of patients with rheumatologic disease–associated HLH was small, which limited the types of analyses that could be performed. The study may be inherently biased toward patients with a poor prognosis, as emapalumab is indicated as second-line treatment for pHLH and not currently approved in rheumatologic disease–associated HLH. Finally, the results of this study may not be generalizable beyond the study population.

There are no established recommendations for managing refractory rheumatologic disease–associated HLH. Although anecdotal evidence showed increased remission or survival with anakinra, other therapies (intravenous immunoglobulin, tocilizumab, JAK/STAT inhibitors, and etoposide) have had variable success and have not been prospectively evaluated.[4,14,18,23,41,45] Furthermore, targeted therapies require dose optimization, often to prevent triggering of MAS. Etoposide, considered only for treating refractory disease or central nervous system involvement, may be associated with myelosuppression and risk of secondary infections and malignancies.[2,5,14,45] In this study, emapalumab-containing regimens normalized rheumatologic disease–associated laboratory parameters, substantially reduced glucocorticoid dose, and were associated with low mortality, consistent with the findings of the open-label, prospective trial that evaluated emapalumab in patients with sJIA/AOSD.[23]

In conclusion, this retrospective chart review study reported real-world treatment patterns and outcomes in patients with rheumatologic disease–associated HLH, including a subset of patients with sJIA/AOSD, treated with emapalumab in the United States. Emapalumab-containing treatment regimens

achieved protocol criteria-based stabilization or normalization of most laboratory parameters in most patients and enabled glucocorticoid tapering. Overall survival and 12-month survival probability from emapalumab initiation were high. These data further establish the role of emapalumab in the neutralization of IFNγ and control of pathologic hyperinflammation, which may eventually enable HLH resolution. A phase 3 clinical trial of emapalumab in patients with sHLH/MAS and underlying rheumatologic disease is ongoing (NCT05001737).

## ACKNOWLEDGMENTS

Special thanks to Corey Best and Michael Marrone (Sobi, Inc.), Nicole Bariahtaris, Katie Everson, and Sajjad Raza (PRECISIONheor) for their assistance in coordination with and data collection from study sites. The authors thank the patients and their caregivers, investigators, and the REAL-HLH research team for their contributions.

## AUTHOR CONTRIBUTIONS

All authors contributed to at least one of the following manuscript preparation roles: conceptualization AND/OR methodology, software, investigation, formal analysis, data curation, visualization, and validation AND drafting or reviewing/editing the final draft. As corresponding author, Dr Behrens confirms that all authors have provided the final approval of the version to be published, and takes responsibility for the affirmations regarding article submission (eg, not under consideration by another journal), the integrity of the data presented, and the statements regarding compliance with institutional review board/Helsinki Declaration requirements.

## ROLE OF THE STUDY SPONSOR

In collaboration with the Study Steering Committee, Sobi, Inc. participated in the study design, collection, and analysis of the data. Sobi authors, along with all other authors, participated in reviewing, revising, and the decision to submit the manuscript for publication. Publication of this article was not contingent upon approval by Sobi, Inc. Medical writing assistance was provided by Aparna Nori, PhD, CMPP, of rareLife solutions, and funded by Sobi, Inc.

## ADDITIONAL DISCLOSURES

Author Oladapo is an employee of Sobi, Inc. Author Yee was an employee of Sobi, Inc. when the study was conducted. Author Pednekar was an employee of PRECISIONheor, which provided consultancy services to Sobi, Inc. when the study was conducted.

## REFERENCES

1. Schram AM, Berliner N. How I treat hemophagocytic lymphohistiocytosis in the adult patient. Blood 2015;125(19):2908–2914.
2. Cron RQ, Goyal G, Chatham WW. Cytokine storm syndrome. Annu Rev Med 2023;74(1):321–337.
3. Grom AA, Horne A, De Benedetti F. Macrophage activation syndrome in the era of biologic therapy. Nat Rev Rheumatol 2016;12(5):259–268.
4. Canna SW, Behrens EM. Making sense of the cytokine storm: a conceptual framework for understanding, diagnosing, and treating hemophagocytic syndromes. Pediatr Clin North Am 2012;59(2):329–344.
5. Allen CE, McClain KL. Pathophysiology and epidemiology of hemophagocytic lymphohistiocytosis. Hematology (Am Soc Hematol Educ Program) 2015;2015(1):177–182.
6. Bracaglia C, de Graaf K, Pires Marafon D, et al. Elevated circulating levels of interferon-γ and interferon-γ-induced chemokines characterise patients with macrophage activation syndrome complicating systemic juvenile idiopathic arthritis. Ann Rheum Dis 2017;76(1):166–172.
7. Grom AA, Ilowite NT, Pascual V, et al; Paediatric Rheumatology International Trials Organisation and the Pediatric Rheumatology Collaborative Study Group. Rate and clinical presentation of macrophage activation syndrome in patients with systemic juvenile idiopathic arthritis treated with canakinumab. Arthritis Rheumatol 2016;68(1):218–228.
8. Sawhney S, Woo P, Murray KJ. Macrophage activation syndrome: a potentially fatal complication of rheumatic disorders. Arch Dis Child 2001;85(5):421–426.
9. Stéphan JL, Koné-Paut I, Galambrun C, et al. Reactive haemophagocytic syndrome in children with inflammatory disorders. A retrospective study of 24 patients. Rheumatology (Oxford) 2001;40(11):1285–1292.
10. Janka GE, Lehmberg K. Hemophagocytic syndromes–an update. Blood Rev 2014;28(4):135–142.
11. Lenert A, Yao Q. Macrophage activation syndrome complicating adult onset Still's disease: a single center case series and comparison with literature. Semin Arthritis Rheum 2016;45(6):711–716.
12. Ravelli A, Minoia F, Davì S, et al; Paediatric Rheumatology International Trials Organisation; Childhood Arthritis and Rheumatology Research Alliance; Pediatric Rheumatology Collaborative Study Group; Histiocyte Society. 2016 classification criteria for macrophage activation syndrome complicating systemic juvenile idiopathic arthritis: a European League Against Rheumatism/American College of Rheumatology/Paediatric Rheumatology International Trials Organisation Collaborative Initiative. Arthritis Rheumatol 2016;68(3):566–576.
13. Behrens EM, Beukelman T, Paessler M, et al. Occult macrophage activation syndrome in patients with systemic juvenile idiopathic arthritis. J Rheumatol 2007;34(5):1133–1138.
14. Carter SJ, Tattersall RS, Ramanan AV. Macrophage activation syndrome in adults: recent advances in pathophysiology, diagnosis and treatment. Rheumatology (Oxford) 2019;58(1):5–17.
15. Henter JI, Horne A, Aricó M, et al. HLH-2004: diagnostic and therapeutic guidelines for hemophagocytic lymphohistiocytosis. Pediatr Blood Cancer 2007;48(2):124–131.
16. Minoia F, Bovis F, Davì S, et al; Pediatric Rheumatology International Trials Organization, the Childhood Arthritis & Rheumatology Research Alliance, the Pediatric Rheumatology Collaborative Study Group and the Histiocyte Society. Development and initial validation of the MS score for diagnosis of macrophage activation syndrome in systemic juvenile idiopathic arthritis. Ann Rheum Dis 2019;78(10):1357–1362.
17. Simonini G, Pagnini I, Innocenti L, et al. Macrophage activation syndrome/hemophagocytic lymphohistiocytosis and Kawasaki disease. Pediatr Blood Cancer 2010;55(3):592.
18. Shakoory B, Geerlinks A, Wilejto M, et al. The 2022 EULAR/ACR points to consider at the early stages of diagnosis and management of suspected haemophagocytic lymphohistiocytosis/macrophage activation syndrome (HLH/MAS). Arthritis Rheumatol 2023;75(10):1714–1732.
19. Gilboa M, Bornstein G, Ben-Zvi I, et al. Macrophage activation syndrome complicating rheumatic diseases in adults: case-based review. Rheumatol Int 2020;40(4):663–669.
20. Sönmez HE, Demir S, Bilginer Y, et al. Anakinra treatment in macrophage activation syndrome: a single center experience and systemic review of literature. Clin Rheumatol 2018;37(12):3329–3335.

21. Ravelli A, Davì S, Minoia F, et al. Macrophage activation syndrome. Hematol Oncol Clin North Am 2015;29(5):927–941.
22. Ramos-Casals M, Brito-Zerón P, López-Guillermo A, et al. Adult haemophagocytic syndrome. Lancet 2014;383(9927):1503–1516.
23. De Benedetti F, Grom AA, Brogan PA, et al. Efficacy and safety of emapalumab in macrophage activation syndrome. Ann Rheum Dis 2023;82(6):857–865.
24. Durand M, Troyanov Y, Laflamme P, et al. Macrophage activation syndrome treated with anakinra. J Rheumatol 2010;37(4):879–880.
25. La Rosée P, Horne A, Hines M, et al. Recommendations for the management of hemophagocytic lymphohistiocytosis in adults. Blood 2019;133(23):2465–2477.
26. De Benedetti F, Brunner HI, Ruperto N, et al; PRINTO; PRCSG. Randomized trial of tocilizumab in systemic juvenile idiopathic arthritis. N Engl J Med 2012;367(25):2385–2395.
27. Shimizu M, Nakagishi Y, Kasai K, et al. Tocilizumab masks the clinical symptoms of systemic juvenile idiopathic arthritis-associated macrophage activation syndrome: the diagnostic significance of interleukin-18 and interleukin-6. Cytokine 2012;58(2):287–294.
28. Janka GE. Familial and acquired hemophagocytic lymphohistiocytosis. Annu Rev Med 2012;63(1):233–246.
29. De Benedetti F, Prencipe G, Bracaglia C, et al. Targeting interferon-γ in hyperinflammation: opportunities and challenges. Nat Rev Rheumatol 2021;17(11):678–691.
30. Put K, Avau A, Brisse E, et al. Cytokines in systemic juvenile idiopathic arthritis and haemophagocytic lymphohistiocytosis: tipping the balance between interleukin-18 and interferon-γ. Rheumatology (Oxford) 2015;54(8):1507–1517.
31. Hatterer E, Richard F, Malinge P, et al. P156 investigating the novel mechanism of action for NI-0501, a human interferon gamma monoclonal antibody. Cytokine 2012;59(3):570.
32. Locatelli F, Jordan MB, Allen C, et al. Emapalumab in children with primary hemophagocytic lymphohistiocytosis. N Engl J Med 2020; 382(19):1811–1822.
33. Lam MT, Coppola S, Krumbach OHF, et al. A novel disorder involving dyshematopoiesis, inflammation, and HLH due to aberrant CDC42 function. J Exp Med 2019;216(12):2778–2799.
34. Lounder DT, Bin Q, de Min C, et al. Treatment of refractory hemophagocytic lymphohistiocytosis with emapalumab despite severe concurrent infections. Blood Adv 2019;3(1):47–50.
35. Bracaglia C, Insalaco A, Marucci G, et al. Therapeutic interferon gamma neutralization with emapalumab in patients with NRLC4- and CDC42-associated diseases characterized by recurrent and severe hemophagocytic lymphohistiocytosis. Arthritis Rheumatol 2020;72(suppl 4).
36. De Benedetti F, Brogan P, Bracaglia C, et al. OP0290 emapalumab (anti-interferon-gamma monoclonal antibody) in patients with macrophage activation syndrome (MAS) complicating systemic juvenile idiopathic arthritis (SJIA). Ann Rheum Dis 2020;79(suppl 1):180.
37. Dang A. Real-world evidence: a primer. Pharmaceut Med 2023;37(1): 25–36.
38. Jordan MB, Allen CE, Greenberg J, et al. Challenges in the diagnosis of hemophagocytic lymphohistiocytosis: recommendations from the North American Consortium for Histiocytosis (NACHO). Pediatr Blood Cancer 2019;66(11):e27929.
39. Yildiz H, Castanares-Zapatero D, d'Abadie P, et al. Hemophagocytic lymphohistiocytosis in adults: a retrospective study in a Belgian teaching hospital. Int J Gen Med 2022;15:8111–8120.
40. Schulert GS, Minoia F, Bohnsack J, et al. Effect of biologic therapy on clinical and laboratory features of macrophage activation syndrome associated with systemic juvenile idiopathic arthritis. Arthritis Care Res (Hoboken) 2018;70(3):409–419.
41. Eloseily EM, Weiser P, Crayne CB, et al. Benefit of anakinra in treating pediatric secondary hemophagocytic lymphohistiocytosis. Arthritis Rheumatol 2020;72(2):326–334.
42. Phadke O, Rouster-Stevens K, Giannopoulos H, et al. Intravenous administration of anakinra in children with macrophage activation syndrome. Pediatr Rheumatol Online J 2021;19(1):98.
43. Wang H, Gu J, Liang X, et al. Low dose ruxolitinib plus HLH-94 protocol: a potential choice for secondary HLH. Semin Hematol 2020; 57(1):26–30.
44. Naymagon L. Anakinra for the treatment of adult secondary HLH: a retrospective experience. Int J Hematol 2022;116(6):947–955.
45. Ehl S, Astigarraga I, von Bahr Greenwood T, et al. Recommendations for the use of etoposide-based therapy and bone marrow transplantation for the treatment of HLH: consensus statements by the HLH steering committee of the Histiocyte Society. J Allergy Clin Immunol Pract 2018;6(5):1508–1517.

## APPENDIX A: REAL-HLH STUDY INVESTIGATORS AND PARTICIPATING SITES

The study investigators and participating sites for the REAL-HLH study are as follows: Ann & Lurie Children's Hospital of Chicago: Joanna Weinstein; Atrium Health, Levine Children's Hospital: Ashley P. Hinson; Baylor College of Medicine, Texas Children's Cancer and Hematology Centers: Carl E. Allen, Olive S. Eckstein, and Nitya Gulati; Children's Healthcare of Atlanta, Emory University: Shanmuganathan Chandrakasan; Children's of Alabama, University of Alabama at Birmingham: Hilary Haines; Children's Hospital Colorado: Taizo A. Nakano; Children's Hospital & Medical Center, University of Nebraska Medical Center: Sachit A. Patel; Children's Hospital of Philadelphia: Edward M. Behrens; Providence Sacred Heart Medical Center and Children's Hospital: Stefanos Intzes; Children's Mercy Hospital: J. Allyson Hays; Children's National Medical Center: Blachy Dávila Saldaña; Cincinnati Children's Hospital Medical Center: Michael B. Jordan and Adi Zoref-Lorenz; Cleveland Clinic Children's Hospital: Rabi Hanna; Connecticut Children's Medical Center: Michael S. Isakoff; Cook Children's Medical Center: Anish K. Ray; Duke University Medical Center: Jennifer A. Rothman; Franciscan Health Hospital: Anand Tandra; Kaiser Permanente Los Angeles Medical Center: Robert Cooper; Johns Hopkins University: Jennifer W. Leiding; Lucile Packard Children's Hospital, Stanford: May Chien; Medstar Georgetown University Hospital: Susmita N. Sarangi; Methodist Hospital, San Antonio: Vinod K. Gidvani-Diaz; NewYork-Presbyterian Hospital: Prakash Satwani; Oregon Health and Science University: John Carter; Phoenix Children's Hospital: Michael Henry; Rady Children's Hospital, San Diego: Nicholas Gloude; Saint Louis Children's Hospital, Washington University: Sima Bhatt; Saint Louis University School of Medicine: Deepika Bhatla and Lauren Draper; Children's Hospital, University of California, Davis: Arun Panigrahi; University of California, San Francisco Medical Center: Michelle L. Hermiston; University of Florida Health, Gainesville Shands Children's Hospital: Renee Modica; University of Minnesota Medical Center: Mona Riskalla and Patricia Hobday; University of Oklahoma Health Sciences Center: Ashley Baker; Virginia Commonwealth University Medical Center: Brant Ward.

**Arthritis & Rheumatology**
Vol. 77, No. 2, February 2025, pp 239–240
© 2024 American College of Rheumatology

American College of Rheumatology
Empowering Rheumatology Professionals

**LETTER**

DOI 10.1002/art.42995

## Strength Training is Associated With Less Knee Osteoarthritis: Data From the Osteoarthritis Initiative: Comment on the Article by Lo et al

*To the Editor*,

Strength training is an effective strategy for improving muscle function and biomechanical control with the goal of reducing the risk of joint injury and increasing functional capacity.[1] However, there is still some controversy and uncertainty in the scientific community regarding its long-term effects on knee health, particularly in relation to osteoarthritis (OA). Much of the current literature is based on limited samples or specific populations, such as competitive athletes, so its broad applicability and veracity need to be more fully explored.[2]

It was with great interest that we read a recent paper by Lo et al that examined the relationship between strength training history and knee health using data from the OA Initiative.[3] In this retrospective analysis, the researchers examined the effect of frequency and intensity of strength training on knee pain, radiographic OA, and symptomatic OA over the lifetime of the participants. The study used sophisticated statistical analysis methods, such as regression analysis and dose-response assessment, to gain insight into the potential effects of strength training on knee health at different ages. This study adds important new perspectives and empirical evidence to the current literature on the effects of strength training on knee health. The results showed that a history of strength training was associated with a reduced risk of knee pain, radiographic OA, and symptomatic OA, with particularly significant effects among those who participated in high-intensity and long-term strength training. These findings not only support the promotion of strength training as a knee-protective strategy, but also provide a theoretical basis for the design of future interventions and prevention strategies.

We must point out limitations in the text to better refine this important piece of research. First, the specific grouping rules for the low, middle, and high quartiles of strength training were not detailed in the text, and these groupings were based on participant recall data. However, it may be difficult for participants to accurately recall and report the number and frequency of strength training sessions they performed at different ages; thus, these recall data may be inconsistent and biased, resulting in compromised grouping accuracy. Second, only a few baseline covariates, including age, sex, body mass index, and previous knee injury, are mentioned in the text, but there seems to be a high probability that this will cause the results to be influenced by other confounding factors. Factors that influence the symptoms and progression of knee osteoarthritis are diverse and commonly include nutritional status, economic conditions, medication use, activity level, smoking, alcohol consumption, and pre-existing comorbidities such as rheumatoid arthritis, diabetes, and depression.[4] Therefore, moderating only a limited number of covariates is not sufficient. Furthermore, the benefit of vigorous exercise may be seen in the results at the margin of statistical difference, and this apparently significant benefit may be lost if more covariates are moderated. Finally, we suggest that more subgroup analyses to explore the sensitivity of populations in different age groups and genders and even races to different strength exercises could further add depth to the article.

In conclusion, although this study demonstrates the beneficial effects of strength training on knee health, there are limitations as described that require further consideration. Future studies should further confirm the benefits of strength training on knee health through a more rigorous methodologic design.

*Author disclosures are available at https://onlinelibrary.wiley.com/doi/10.1002/art.42995.*

Yuncheng Bai, MD
Ge Wang, MB
wangge66_ynkh@hotmail.com
*The First People's Hospital of Yunnan Province,*
*Affiliated Hospital of Kunming University of Science and Technology and Kunming University of Science and Technology*
*Kunming, China*
Yang Wu, MD
*Huashan Hospital*
*Fudan University*
*Shanghai, China*

1. Erickson LN, Lucas KCH, Davis KA, et al. Effect of blood flow restriction training on quadriceps muscle strength, morphology, physiology, and knee biomechanics before and after anterior cruciate ligament reconstruction: protocol for a randomized clinical trial. Phys Ther 2019;99(8):1010–1019.
2. Arnold A, Thigpen CA, Beattie PF, et al. Overuse physeal injuries in youth athletes. Sports Health 2017;9(2):139–147.
3. Lo GH, Richard MJ, McAlindon TE, et al. Strength training is associated with less knee osteoarthritis: data from the Osteoarthritis Initiative. Arthritis Rheumatol 2024;76(3):377–383.
4. Kong L, Wang L, Meng F, et al. Association between smoking and risk of knee osteoarthritis: a systematic review and meta-analysis. Osteoarthritis Cartilage 2017;25(6):809–816.

DOI 10.1002/art.42994

## Reply

*To the Editor*,

We thank Bai and colleagues for commenting on our study.[1] We would like to address each point raised systematically.

The first point raised was that the groupings of low, middle, and high tertiles of strength training were not detailed in the text. We would point out that, under the subheading "Historical Physical Activity," we carefully described the definitions used to generate tertiles of strength training:

> "For each period, they answered additional questions regarding the number of years, months per year, and times per month they engaged in their top three activities. Estimates for the number of times the participants engaged in an activity were based on those answers, which were used to divide participants into low, middle, and high tertiles of participation in strength training. The tertile groupings were used to provide dose–response evaluations of strength training with the outcomes of interest."[2]

These definitions were indeed based on patient recall, but because we examined strength training over a lifetime, this is the most efficient method to ascertain this information. Prospective methods would require 50 years or more of observation, which is impractical. So, although retrospective data ascertainment is not ideal, it offers an otherwise impossible look at the relationships.

The second point was a concern that only a few baseline covariates were included in our adjusted models, increasing the chance that other confounding factors may influence the results. Bai and colleagues advocated that factors that influence the symptoms and progression of knee osteoarthritis (OA) should also be included. There must be strong consideration for the causal pathway when deciding which variables should enter a model because inclusion of intermediate variables in a model generally results in a bias toward the null.[3] If factors are on the causal pathway between strength training and knee OA, then they should not be included in the adjusted models. If we included all the additional variables recommended, this would result in an overadjustment, ie, an "excessive number of variables or parameters, uninformed by substantive knowledge (eg, lacking coherence with biologic, clinical, epidemiological, or social knowledge). It can obscure a true effect or create an apparent effect when none exists."[4]

The final point raised was that "more subgroup analyses to explore the sensitivity of populations in different age groups and genders and even races to different strength exercises could further add depth to the article." Although we agree that additional evaluation of the relationship between strength training and knee OA would be interesting, this exceeds the scope of this paper.

Thank you for the opportunity to address the concerns raised about our study. Although we agree that future studies need to confirm the benefits of strength training on knee health, we assert that our publication has been performed rigorously and provides an important first step to better understand this relationship.

*Author disclosures are available at https://onlinelibrary.wiley.com/doi/10.1002/art.42994.*

Grace H. Lo, MD, MSc
ghlo@bcm.edu
*Michael E. DeBakey VA Medical Center, Baylor College of Medicine*
*Houston, Texas*
Jeffrey B. Driban, PhD
*University of Massachusetts Chan Medical School*
*Worcester*

1. Bai Y, Wang G, Wu Y. Strength training is associated with less knee osteoarthritis: data from the Osteoarthritis Initiative: comment on the article by Lo et al. Arthritis Rheumatol 2025;77(2):239–240.
2. Lo GH, Richard MJ, McAlindon TE, et al. Strength training is associated with less knee osteoarthritis: data from the Osteoarthritis Initiative. Arthritis Rheumatol 2024;76(3):377–383.
3. Rothman K, Greenland S. Modern Epidemiology. 2nd ed. Lippincott-Raven; 1998.
4. Breslow N. Design and analysis of case-control studies. Annu Rev Public Health 1982;3:29–54.